The Dissertation Committee for Xiaolong Shen Certifies that this is the approved version of the following dissertation:

Developing Models for the Assessment and the Design of the In situ Remediation of Contaminated Sediments

Committee:

Isaac Sanchez, Supervisor

Danny Reible, Co-Supervisor

Roger Bonnecaze

Benny Freeman

Lynn Katz

Howard Liljestrand

Developing Models for the Assessment and the Design of the In situ Remediation of Contaminated Sediments

by

Xiaolong Shen, B.S.Chem.E; M.S.E

Dissertation

Presented to the Faculty of the Graduate School of

The University of Texas at Austin

in Partial Fulfillment

of the Requirements

for the Degree of

Doctor of Philosophy

The University of Texas at Austin

May 2017

Dedication

To my parents

Acknowledgements

I would like to firstly thank my advisor Dr. Reible for his guidance, encouragement and support over the past years. I would like to thank Dr. Sanchez for helping me continue to pursue my Ph.D. in UT. My immense gratitude goes to the rest of my committee; Dr. Bonnecaze, Dr. Freeman, Dr. Katz and Dr. Liljestrand for their guidance and advices on my research and dissertation.

There are many others without whose help I would never get to the current stage; Dave for leading me into the world of numerical simulation and coding, Magdalena and Songjing for guidance on passive sampling, Jim and Tea for teaching me voltammetry, Xin for helps on the CapSim model, Ariette, Courtney, Paul and Wardah for providing great helps on other lab issue.

I would like to thank my friends at UT and TTU. It would not been such a great time without you.

Developing Models for the Assessment and the Design of the In situ Remediation of Contaminated Sediments

Xiaolong Shen, Ph.D.

The University of Texas at Austin, 2017

Supervisor: Isaac Sanchez

Co-Supervisor: Danny Reible

The sediments in natural environment serve as sinks for contaminants from historical release, particularly hydrophobic organic compounds (HOC) and heavy metals. In-situ remediation, including monitored natural recovery (MNR), in-situ treatment (e.g. sorbing amendment) and in-situ capping, is one of the few alternative economically viable options with a proven record of success for sediment remediation. Modeling is often used to compare in-situ remedial approaches and design a system of meeting long term remedial goals.

The fate and transport of contaminants in a remediation system is commonly modeled using a generalized advection-dispersion-reaction equation with potentially different physical and chemical properties in each layer. An analytical solution was developed with computational efficiency and unconditional stability for the multi-layered

transport problem with linear processes and was shown to be more convenient for sensitivity analyses and parameter estimation and implement.

A numerical model, CapSim, has been developed to model the transport and fate under more general conditions. Several important processes in sediment environments, such as nonlinear and kinetically limited sorption, steady and periodic advection, bioturbation, consolidation and deposition, are incorporated in the model. The current model also allows description of multiplied coupled chemical reactions. It builds on a simpler numerical model of Lampert (2009). It allows assessment of the transport and fate of chemicals under the most important dynamic sediment processes.

Performance reference compounds (PRC) are often used to support passive sampling as a means of monitoring sediment processes and in situ remedial processes. An analytical solution was developed for modeling the release of PRC and uptake of target compounds in cylindrical passive sampling system.

In the presence of nonlinear sorbents such as activated carbon, the interpretation and application of PRCs is more difficult. The fate and transport model CapSim was used to simulate the behavior of PRCs and target compounds in a passive sampling system with activated carbon. The impacts from the non-linear sorption of the compounds in activated carbon as well as the competitive sorption between an isotope-labeled PRC and the non-labeled compound are discussed.

Table of Contents

List of Tables xiii

List of Figures xv

Chapter 1 Introduction 1

1.1 Background and problem statements 1

1.2 Research objectives and dissertation structure 3

1.3 Reference 4

Chapter 2 Literature Review 5

2.1 Sediment contamination 5

2.1.1 Sediment 5

2.1.1.1 Polycyclic Aromatic Hydrocarbons (PAH) 5

2.1.1.2 Polychlorinated Biphenyls (PCBs) 6

2.1.1.3 Mercury 8

2.2 Contaminated Sediment Remediation 9

2.2.1 Monitored Natural Recovery 10

2.2.2 Dredging 11

2.2.3 In-situ Remediation 12

2.3 Models for In-situ Remediation 14

2.3.1 Sorption 17

2.3.1.1 Equilibrium Sorption isotherms 17

2.3.1.2 Sorption kinetics 22

2.3.2 Bioturbation 24
2.3.3 Hydrodynamic dispersion 25
2.3.4 Tortuosity 26
2.3.5 1-D fate and transport models in porous media 27
2.3.6 Analytical models and solutions 28
2.3.6.1 Single layer system 29
2.3.6.2 Multi-layered system 29
2.4 Monitoring performance of capping 30
2.5 Summary 35
2.6 Reference 35
Chapter 3 An analytical solution for one–dimensional advective–dispersive solute equation in multilayered finite porous media 49
3.1 Introduction 50
3.2 Problem statement 51
3.3 Analytical solution 54
3.3.1 Non–dimensionalization and homogenization 54
3.3.2 Steady–state and transient solution 56
3.4 Verification 60
3.5 Discussion 66
3.5.1 Existence of hyperbolic eigenfunctions 66
3.5.2 Comparison with the existing analytical solution and numerical solution . 73
3.5.3 Solution limits 76

3.5.4 CapAn 77
3.6 Conclusions 77
3.7 References 78
Chapter 4 CapSim – a numerical modeling tool for evaluation of capping of contaminated sediment and sediment remedial design 80
4.1 Introduction 80
4.2 Modeling approach 83
4.2.1 Conceptual model 83
4.2.2 Mass conservative equations and auxiliary conditions 86
4.2.2.1 Mass conservative equations 86
4.2.2.2 Boundary conditions 91
4.2.2.3 Initial conditions 94
4.2.3 Numerical solutions 94
4.2.3.1 Discretization 95
4.2.3.2 Finite difference equation 96
4.2.3.3 Deposition and oscillated advection 97
4.2.4 Model structure 98
4.3 Model verification and application 99
4.3.1 Mercury and methylmercury 100
4.3.2 Phenanthrene 103
4.4 Discussion 107
4.4.1 Modeling activated carbon rework by bioturbation 107

4.4.2 Modeling multi-compartment kinetic sorptions 112
4.4.3 Modeling the breakthrough of in-situ remediation 113
4.5 Conclusions 116
4.6 References 116
Chapter 5 An Analytical Model for the Fate and Transport of Compounds in a Cylindrical PDMS Passive Samplers 122
5.1 Introduction 122
5.2 Modeling approaches 125
5.2.1 Existing 1-D rectangular model 125
5.2.2 1-D cylindrical model 128
5.3 Results and discussions 133
5.3.1 Solution verification 133
5.3.2 Comparing the cylindrical solution versus rectangular solution 134
5.3.3 Calibration of PRCs 139
5.4 Conclusions 144
5.5 References 145
Chapter 6 Modeling the Impacts from Non-linear Sorption to the Behavior of PRCs and Target Compounds in Passive Sampler Systems 149
6.1 Introduction 149
6.2 Model description 151
6.2.1 1-D fate and transport model in activated carbon amendment caps 152
6.2.2 Competitive sorption between PRC and target compounds 153

6.3 Results and discussion 155
6.3.1 Sorption model without competitive sorption 155
6.3.2 Sorption model with competitive sorption 160
6.4 Conclusions 161
6.5 References 162
Chapter 7 Conclusions and Recommendations 164
7.1 Research Objectives 164
7.2 Research Conclusions 165
7.2.1 Analytical solution and CapAn 165
7.2.2 CapSim 166
7.2.3 Analytical solution for cylindrical PDMS fiber 166
7.2.4 Modeling the impacts from non-linear sorption to the symmetric behavior of PRCs and target compounds in Passive sampling system 167
7.3 Recommendation for future work 168
Appendix A. Example of the eigenvalues and coefficients evaluation 170
Appendix B. VBA codes of CapAn 176
Appendix C. Matlab code for PRC calibration using the cylindrical solution 201
References 203

List of Tables

Table 2.1: A summary of literatures that reported experimentally measured Freundlich isotherm coefficients for HOCs sorption in activated carbon 20

Table 2.2: A summary of literatures that reported experimentally measured Freundlich isotherm coefficients for HOCs sorption in black carbon 20

Table 3.1: The three types of boundary conditions applied in the problem 53

Table 3.2: Dimensionless inhomogeneous boundary conditions 56

Table 3.3: Coefficients in elements of the linear system 57

Table 3.4: Coefficients in eigenfunctions of various boundary conditions 59

Table 3.5: Layer properties in the example of five-layer sand-clay-sand-clay-sand system 61

Table 3.6: Layer properties in the example comparing a mixed and thin layer sorbent layer 64

Table 3.7: Dimensionless solute concentration in a two-layer porous medium and mean differences with the reference (Ref) approach of numerical Laplace inversion approach of Leij and Genuchten (1995) 75

Table 3.8: Comparison of solute concentration with separated thin sorbent layers (a) and mixed sorbent layers (b) by the analytical solution and numerical solution with equivalent computation expense (NME). Both are referenced to a high spatial and time resolution numerical simulation with high computational expense (Ref, Lampert and Reible [2014]) 76

Table 4.1: Summary of fate and transport processes for various forms of contaminants. 85

Table 4.2: Constitutional equations for the parameters and coefficients in the conservation equation 89

Table 4.3: Summary of the properties in the mercury and phenanthrene example 101
Table 5.1: Characteristic length (30 days) of selected PAH and PCBs in a given sediment 129
Table 5.2: The dimensionless coefficients ξ and time τ for selected PAH and PCBs in passive sampling system with various PDMS fibers 138
Table 5.3: Comparison of the predicted fss using the rectangular and cylindrical solution with 2 PRCs 142
Table 6.1: Summary of properties and parameters in the passive sampling system with activated carbon amendments 156

List of Figures

Figure 2.1: Selected Remedial Technologies included in USEPA Records of Decision . 10

Figure 2.2: Illustration of cap components of a conventional armored sand cap (Palermo and Reible, 2007) 15

Figure 2.3: Comparison of experimental data and simulation results using (a) 1st order model and (b) 1-D diffusion model with external resistance for PCB uptake kinetics of PE in quiescent sediment. The values are shown as the PE concentration at each contact time relative to the equilibrium PE concentration determined in the slurry phase experiments (CPE(t)/CPE,eq). The experimental data are shown as means (symbols) with standard deviations (bars). (Choi et al., 2016)..... 34

Figure 3.1: Concentration as a function of distance at various times in a five layer case (results coincide with the results of Liu, 1998) 62

Figure 3.2: Porous media systems consisting of multiple individual homogeneous layers: (1) contaminated sediment capped with separated sand and sorbent layers; (2) contaminated sediment capped with mixing sand and sorbent layer 63

Figure 3.3: Comparison of the solute concentration profiles with mixing sorbent layers or separated thin sorbent layers. Analytical solution (solid and dashed lines) and the numerical solution (circles, triangles and crosses) solved by the numerical method from Reible and Lampert (2014)..... 65

Figure 3.4: Three types of eigenvectors and their correspondent eigenvalue range..... 67

Figure 3.5: The boundary function f1 and f2 versus eigenvalue β shown in equation (20)..... 70

Figure 3.6: Bounding Peclet number and ratio of retardation factors for existence of hyperbolic eigenfunctions in a two layer problem 71
Figure 3.7: Existence condition for hyperbolic–trigonometric eigenvectors with parameters given by Li and Cleall (2011) 73
Figure 4.1: Averaging output results in given time period in cases with a growing deposition layer or oscillated advection flow 98
Figure 4.2: Programming Structure of the CapSim 3 model 99
Figure 4.3: Comparison of porewater concentration depth profiles of MeHg simulated by CapSim(solid lines) and Comsol (dots, crosses and triangles)..... 102
Figure 4.4: Sensitivity analysis on the impacts of the tidal advection flow with various maximum Darcy velocity to the flux of the methylmercury at the top of the capping layer..... 102
Figure 4.5: Comparison of porewater concentration depth profiles of phenanthrene simulated by CapSim (solid lines) and Comsol (dots, crosses and triangles) 105
Figure 4.6: Sensitivity analysis on the impacts of (a) the deposition rate, (b) the kinetic sorption rate and (c) the bioturbation layer thickness, to the flux of the methylmercury at the top of the capping layer 107
Figure 4.7: The tracer-particle density profiles simulated by CapSim with the solid particle biodiffusion coefficient fitted to the observation from Roche et al. (2016)..... 109
Figure 4.8: The activated carbon fraction distribution profile simulated by CapSim with the solid particle biodiffusion coefficient fitted to the measurements from Lin et al. (2014)..... 110

Figure 4.9: Illustration of the impacts from the bioturbation-caused migration of activated carbon to the behavior of DDT in the underlying sediment: (a) porewater concentration depth profile simulated by CapSim for activated carbon capping system without or with bioturbation case; (b) PE uptake concentration for non-bioturbation case (solid line) and bioturbation case (broken line) from Lin et al (2014)..... 111
Figure 4.10: The 1,2,3,4-tetrachlorobenze concentration profile simulated by CapSim with the kinetic coefficients fitted to the batch sorption experimental results from Wu and Gschwend (1986). 113
Figure 4.11: The relationship between sorption characteristic time to porewater residence time in a layer to contaminant migration time relative to the assumption of equilibrium sorption (0 sorption time) 115
Figure 5.1: Sketch of the cross-section of passive sampler in sediment system 130
Figure 5.2: Illustration of the relative errors of fss calculated by the asymptotic approximate analytical solution (5.25) comparing to the numerical results for system with various value of coefficient ξ..... 134
Figure 5.3: Comparison of fss calculated by analytical solution in rectangular coordinate (blue lines) and cylindrical coordinate (red lines), and simulated numerically by CapSim (dots) for a passive sampling system with various coefficient ξ..... 137
Figure 5.4: Illustration of predicting fss of target compounds, PCB2(upper triangles), PCB101(lower triangles) and PCB209(crosses) from the PRCs fss (red dots) using the rectangular solution or the cylindrical solutions. 141
Figure 5.5: Estimated values of RDs for six PRCs from the rectangular and cylindrical solution 143

Figure 5.6: Comparison of 30-day fss of 88 target PCB congeners predicted by the rectangular and cylindrical solution using RD values estimated from calibration equation in Figure 5.5 144
Figure 6.1: Comparison of the fss of PRCs and target compounds with various initial concentrations 158
Figure 6.2: The dependency of the fss ratio on the initial concentration ratio between PRCs and target compounds with various sorption isotherm in activated carbon 159
Figure 6.3: Comparison of the fss of isotope-labeled PRCs and target compounds with various initial concentrations 161

Chapter 1 Introduction

1.1 BACKGROUND AND PROBLEM STATEMENTS

Prior to 1950, industry, mining, agriculture and other anthropogenic activities released substantial wastes directly to the natural environment with minimal treatment. The decades of the 1960s and 1970s reflected an awakening of environmental consciousness and improvements in waste management. Public recognition of the environmental problems of surface water drove the passage of regulations to limit effluent releases. These actions led to a significant improvement in the quality of our surface water. However, the earlier unlimited release of the contaminants to the water bodies resulted in an accumulation of pollutants in the underlying sediments, and they were a 'sink' for persistent hydrophobic organic contaminants and heavy metals. After removal of the effluent releases, the sediments that once served as sinks have now become long-term sources of exposure and risk to the water bodies.

U.S.EPA (1998) estimated that approximately 10 percent of the subaqueous sediment (1.2 billion cubic yards in total volume) in the United States is sufficiently contaminated with toxic pollutants to pose potential risks to fish and threaten humans and other wildlife through the food chain. A subsequent assessment in 2004 revealed that 33.4 percent of the Environmental Monitoring and Assessment Program (EMAP) sediment sampling stations were classified as Tier I which is defined as "associated adverse effects on aquatic life or human health are probable". Thus, contaminated

subaqueous sediments remain serious environmental challenges on both the national and global levels.

Three traditional approaches are often applied to reduce or eliminate the release of contaminants from sediment to overlying water. The least invasive approach is monitored natural attenuation, often through deposition and burial of contaminated sediments by cleaner sediments, but it is often ineffective for highly persistent sediment contaminants or in environments where sediment deposition is limited. The most invasive approach, dredging, the removal and disposal of the sediments, is a potentially effective remedial strategy, but is characterized by high cost and its effectiveness can be limited due to resuspension and subsequent deposition of contaminants leaving to residual contamination that remains after dredging. In-situ management approaches such as capping or in-situ treatment are potentially more cost-efficient and often involve little disturbance of the sediment contaminants and can effectively isolate or reduce the bioavailability of the sediment contaminants. In-situ treatment involves mixing of amendments, typically sorbents such as activated carbon, into the sediment to reduce contaminant availability and mobility. In-situ capping, referring placement of a clean layer of sediments or sands on top of the contaminated sediment, eliminates or reduces the release rates of contaminants by physically separating the contaminated sediments from overlying water bodies.

Effective in-situ remedial design requires the evaluation of the attenuation of contaminant risks associated with the remedial approach. This is largely related to being able to predict the near-surface concentrations and flux of contaminants under various

remedial scenarios. To achieve this goal, several analytical tools have been developed (Palermo et al., 1998, or Lampert and Reible, 2009). These simple analytical tools, however, do not allow incorporation of many critical processes in sediment environment, such as bioturbation and deposition.

1.2 RESEARCH OBJECTIVES AND DISSERTATION STRUCTURE

This research is dedicated to developed innovative modeling tools in helping the understanding the transport and fate of the contaminants in the sediments, capping materials, and the passive samplers. Chapter 2 present a literature review of the previous modeling work on contaminated sediment assessment and remediation. Chapter 3 to 6 addresses the following objectives.

- An analytical model, CapAn, has been developed based on an innovative analytical solution for fate and transport of solutes in multi-layered porous media (Chapter 3)
- A numerical model, CapSim, has been developed to model the transport and fate under more general conditions. Several important processes in sediment environments, such as nonlinear and kinetically limited sorption, steady and periodic advection, bioturbation, consolidation and deposition, are incorporated in the model. The current model also allows description of multiplied coupled chemical reactions. It builds on a simpler numerical model

of Lambert (2009). It allows assessment of the transport and fate of chemicals under most the important dynamic sediment processes. (Chapter 4)

- Performance reference compounds (PRC) are often used to support passive sampling as a means of monitoring sediment processes and in situ remedial processes. An analytical solution was developed for modeling the release of PRC and uptake of target compounds in the cylindrical passive sampling system. (Chapter 5)
- In the presence of nonlinear sorbents such as activated carbon, the interpretation and application of PRCs are more difficult. The fate and transport model CapSim was used to simulate the behavior of PRCs and target compounds in a passive sampling system with activated carbon. The impacts from the non-linear sorption of the compounds in activated carbon as well as the competitive sorption between an isotope-labeled PRC and the non-labeled compound are discussed. (Chapter 6)
- Chapter 7 summarizes conclusions of the research presented in the previous chapters and make recommendations for future work

1.3 REFERENCE

USEPA. 1998. National Conference on Management and Treatment of Contaminated Sediments. EPA-625-R-98-001. USEPA, Cincinnati, OH, USA.

Lampert, D. J. and D. Reible (2009). "An analytical modeling approach for evaluation of capping of contaminated sediments." Soil and Sediment Contamination 18(4): 470-488.

Palermo, M. R. (1998). "Design considerations for in-situ capping of contaminated sediments." Water Science and Technology 37(6-7): 315-321.

Chapter 2 Literature Review

2.1 SEDIMENT CONTAMINATION

2.1.1 Sediment

Sediment is solid matter that accumulates at the bottom of water bodies. Many sediments simply represent the accumulation of soils that has eroded from the terrestrial surface.

Sediment contaminants

Sediments contain a variety of hydrophobic contaminants that preferentially accumulate in sediments including polycyclic aromatic hydrocarbons (PAHs), polychlorinated biphenyls (PCBs), and metals, each of which will be described separately.

2.1.1.1 Polycyclic Aromatic Hydrocarbons (PAH)

PAHs constitute a group of priority pollutants which are produced in high amounts by natural and anthropogenic sources. In the natural environment, PAHs are generated primarily by three processes: (a) diagenesis of organic material, (b) combustion of organic material, and (c) biogenesis. Anthropogenic sources are generally considered the dominant source of PAHs observed in the environment (Sims and Overcash, 1983). Of the anthropogenic sources, combustion is thought to account for over 90% the environmental concentrations of PAHs (Howsam and Jones, 1998).

Andelman and Suess (1970) provide a comprehensive overview of the literature on PAH pollution. In summary, PAHs were discharged in industrial and municipal

effluents as well as through atmospheric deposition. The hydrophobicity of a chemical is an important property that determines its affinity to solid particles, mobility in pore space and bioavailability for benthic organisms (Mackay et al., 1998). The hydrophobicity for PAHs and other HOCs are commonly characterized by the octanol-water partitioning coefficient K_{ow}, which varies from $10^{3.17}$ for the lightest PAH, naphthalene, to $10^{7.85}$ for benzo[a]pyrene. Karcher (1988) summarized a full set of the experimental values of K_{ow} for PAHs.

The hydrophobicity of organic compounds is also related to their sorption onto sediment organic matter, typically characterized by the organic carbon based partitioning coefficient defined by

$$K_{oc} = \frac{W_s}{f_{oc} C_w}$$

Where W is the sorbed concentration on soils or sediments, C_w is the concentration of the compound in adjacent water and f_{oc} is the fraction organic carbon of the soil or sediment. K_{oc} is a compound specific property and is typically similar in magnitude to K_{ow} (e.g. $K_{oc} \sim 0.21 K_{ow}$ by Karickhoff (1981)). Thus K_{ow} or K_{oc} define the tendency for a compound to partition to the organic matter in the soil or sediment and the sorbed amount can be estimated from concentration in the adjacent water (e.g. interstitial or porewater), the fraction organic carbon and K_{oc}.

2.1.1.2 Polychlorinated Biphenyls (PCBs)

PCBs are a class of organic compounds consisting of two fused biphenyl rings with various degrees of chlorination (one to ten atoms). Theoretically, there are 209

different congeners according to different arrangements of chlorine atoms on the two-phenyl rings.

PCBs were produced in the United States from 1929 to 1977 for a number of industrial applications due to their low reactivity and high stability. PCBs were firstly noted as a contaminant in 1966 and were then found to strongly biaccumulate in marine organisms (Jensen, 1972). After extensive research on accumulation and toxicity of PCBs, the U.S. government essentially banned the production and use of PCBs under the Toxic Substances Control Act in 1976.

Shiaris and Sayler (1982) studied biological degradation of PCBs by freshwater microorganisms, but found that only the lower chlorinated compounds could be degraded aerobically. Bedard et al. (1987) shows that more highly chlorinated PCBs can be degraded anaerobically by reductive dechlorination to lower chlorinated compounds that can be subsequently be degraded aerobically. Thus the authors suggested a two-stage process for PCB decay. In general, however, PCB degradation is slow and limited to monochlorinated biphenyl. Complete dechlorination to biphenyl is not generally observed and thus PCBs are a persistent organic contaminant in sediments.

Similar to PAHs, the K_{ow} or the Koc largely determine the sorption behavior of PCBs onto sediments. The most commonly used reference for K_{ow} values is Hawker and Connell (1988), which is predicted using the relative retention time in reverse-phase high-performance liquid chromatography (RP-HPLC) and thin layer chromatrography (RP-TLC).

2.1.1.3 Mercury

Mercury (Hg) is a toxic element that is widely distributed in the environment largely because of anthropogenic activities (Fitzgerald et al. 1998). The biogeochemistry of Hg in the aquatic environment is complex. Hg compounds can be associated with other species including natural organic matter, inorganic and organic sulfides, transported between sediment and water phase, transformed to other species including methyl mercury, which can be taken up by organisms or lost to the atmosphere. The toxicological and ecological effect of Hg strongly depends on its chemical form (Clarkson 1998). The major form of Hg that is toxic is methyl mercury (MeHg), (Morel et al. 1998; Kraepiel et al. 2003) which accumulates in fish and lead to exposure to humans through the food chain. (Kudo and Miyahara, 1991) Therefore, the speciation of Hg, especially the proportion of MeHg, is critical to understanding the exposure of Hg to humans and other upper food chain organisms.

The transformation between Hg and MeHg involves complex biogeochemistry. In most freshwater and coastal aquatic systems, the MeHg is produced primarily by anaerobic bacteria living in anoxic zones like sediment. Demethylation often occurs more slowly than peak methylation rates and thus demethylation is often neglected in the underlying sediments although it can be important in the surficial oxic environment (Bessinger et al. 2012).

As stated above, MeHg is mainly generated in the anoxic sediment layer that is not directly exposed to the water body. Therefore, a comprehensive analysis on the exposure risk of Hg needs to consider the transport efficiency of MeHg through the aerobic layer to

the overlying water as well. A recent study by Bessinger et al. (2012), modeled the fate and transport of Hg in a cap. The model included a particular set of equilibrium and kinetic biogeochemical reactions. The model did not consider the impact of the cap on the biogeochemical environment nor the potential effects of other dynamic phenomena.

A variety of other metals is also important in sediments including Cd, Pb, Zn, Cu and Ni. These metals often form metal sulfides in an anoxic sediment environment and their potential negative consequences are reduced due to the low biological availability and mobility of these sulfides. These species are not considered herein, although the model CapSim could be used to simulate their transport and transformation.

2.2 CONTAMINATED SEDIMENT REMEDIATION

Remediation of contaminated sediments remains a technological challenge due to both the large volume of contaminated sediments and the limited options that can be applied. According to EPA's "Contaminated Sediment Remediation Guidance for Hazardous Waste Sites" (U.S.EPA, 2005), the current mature and available management strategies are monitored natural recovery (MNR), in-situ management through capping or active amendment treatment and dredging followed by disposal in a landfill. At some sites, one of the three remediation approaches may serve as the primary approach for remediation, while at other sites, they may be combined together to enhance the remediation performance. Figure 2.1 illustrates the records of decision made by EPA in selecting remedial design methods. Since 2005, there has been an obvious growth of sites remediated with multiple approaches including dredging, capping and MNR.

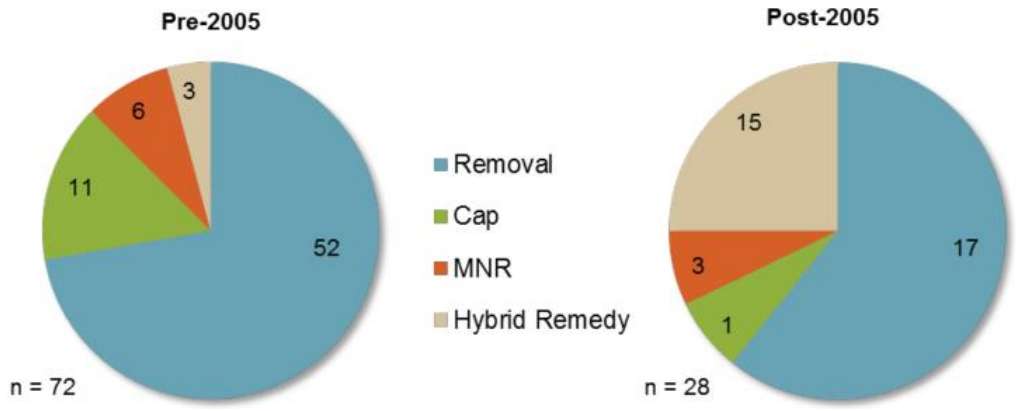

Figure 2.1: Selected Remedial Technologies included in USEPA Records of Decision (Mohan et al. 2016)

2.2.1 Monitored Natural Recovery

MNR involves leaving contaminated sediments in place and allowing ongoing aquatic sedimentary and biological processes to contain destroy or otherwise reduce the bioavailability of the contaminants in order to protect receptors (NRC, 1997; EPA, 2005). The natural processes that act to reduce human health and ecological risks associated with contaminated sediments include the following, 1) chemical transformation including abiotic or biological degradation or mineralization of organic compounds and redox transformation of heavy metals; 2) reduction in contaminant mobility or bioavailability via sorption or precipitation; 3) physical isolation through deposition; and 4) chemical dispersion through resuspension and transport of contaminated sediments or dissolution of dissolved contaminants (Magar et al., 2009; USEPA, 2005).

MNR has been applied in several locations that pose relatively low risk, such as at the Sangamo-Weston/Twelve mile Creek/Lake Harwell Superfund sites (Brenner et al. 2004) and in Sydney Harbour, Nova Scotia (Walker et al., 2013). More MNR cases has been summarized in a technical guide prepared by Magar et al. (2009)

Since MNR does not include an actual construction phase, it is commonly much less expensive than other remediation approaches like dredging and in-situ capping. As shown by the remediation site in Hamilton Harbor, the unit cost for natural bioremediation is only $\$0.78/m^3$ versus $\$65/m^3$ the in-situ capping (Perelo, 2010).

2.2.2 Dredging

Dredging is the process of removing the contaminated sediment from the water body with subsequent treatment or disposal. It is the most common approach for contaminated sediment remediation (Reible, 2014) and has continuously represented a major proportion (69 over 100) of EPA's sediment remediation decisions (Mohan et al., 2016). The effectiveness of dredging approach has also been studied by the National Academy of Science (NRC, 2007) who were unable to document as to whether dredging reduced risks at sites, primarily due to the failure to conduct the monitoring necessary to support such a finding. Many of the details, such as the design and implantation approaches, have been summarized in technical guidelines and documents prepared by U.S. Army Corps of Engineers and EPA (Bridges et al. 2008; USACE 2004, 2008; USEPA, 2005).

Dredging has led to three major concerns, the potential short-term adverse environmental impacts from the sediment resuspension during the dredging process,

residual contamination that is not removed by dredging, and the high expense of removal, transport, dewatering and disposal of the contaminated sediment.

Manap et al. (2016) summarizes the adverse environmental impacts from dredging processes. Though there is not a generalized negative perception of dredging, the short-term rise of the surficial contaminant concentrations and ecosystem equilibrium disturbance has been recorded in various cases. For example, Thibodeaux and Duckworth (2001) evaluated the dredging performance at three sites contaminated with PCBs and concluded that dredging provides a practical means for the removal of large volumes of contaminants but also pointed out that the dredging only reduced the surficial-sediment concentration 25% to 50% and its short-term impacts on fish were always negative.

In addition to concerns about the environmental impacts associated, dredging is very expensive. Mohan et al. (2016) lists the range of the cost of each process in the dredging. The average total costs for environmental dredging in three cases were estimated at $\$1395/m^3$, $\$382/m^3$, and $\$336/m^3$ depending upon the volume of dredging conducted. The cost per unit volume decreases as the remediation volume increased.

2.2.3 In-situ Remediation

In-situ remediation such as capping or in-situ treatment are potentially more cost effective than dredging and often involve little disturbance of the sediment contaminants and can effective isolate or reduce the bioavailability of the sediment contaminants. In-situ remediation involves placement of a clean substrate to isolate contaminants (capping) or mixing amendments, typically sorbents such as activated carbon, into the sediment to reduce contaminant availability and mobility.

The first subaqueous capping project in the U.S. was conducted by USACE for a dredged material project in Providence, Rhode Island in 1967. In this project, a layer of cleaner dredged material was placed on the top of the contaminated dredged material in order to prevent the release of the contaminants to the overlying aquatic environment. In the following decade, capping was mostly used for containing the solid wastes that are unsuitable for direct disposal in open bodies of water (Palermo and Reible,2012). Truitt in (1987a) summarized these capping efforts and pointed out that the earliest in-situ capping project for sediment remediation was conducted in Japan. Starting from early 1990s, the capping technology has been applied widely in sediment remediation guided by a series of technical notes/documents published by USACE and EPA (Palermo et al., 1998; USEPA, 2005).

The conventional capping approaches commonly uses clean sediment or sands as the containment material to physically separate the contaminated sediment and the overlying water body. However, due to the permeable nature of the porous media capping layer, a conventional sand/sediment cap might not be enough to protect the overlying water. Over time, the contaminants may "breakthrough" the cap and increase risk to the benthic environment, particularly when there is continuous groundwater movement into the water (i.e. upwelling of groundwater). To handle such cases, sorptive materials have been proposed for addition into the capping layer. The sorptive materials have been applied in pilot experiments and include apatites (Reible et al., 2006), zeolites (Jacobs and Forstner, 1999; Jacobs and Waite, 2004), organophilic clay (Parrett and Blishke, 2005; Reible et

al., 2005), AquaBlok^{TM} clay (Hull et al., 1998), a permeability control agent, and activated carbon (McDounough et al., 2008; Rakowska et al., 2012)

As stated previously, one of the major benefits from in-situ remediation is its lower cost. Perelo et al. (2010) compares the cost of the dredging processes and in-situ remediation at various locations (Zarull et al. 1999; USEPA, 1994). The cost for the in-situ capping remediation ranges from \$43.2/m^3 to \$667/m^3 at four sites. In comparison, the cost for dredging construction ranges from \$132/m^3 to \$1750/m^3 at nine sites. The costs reported here are consistent with the average cost summarized in Mohan et al. (2016).

A major concern about the in-situ remediation is the possible breach of the containment layer caused by the transport of the contaminants or the erosion of capping layer. The transport process could be accelerated by the subaqueous ground water discharge or wave pumping (Eek, 2008). To evaluate the effectiveness of in-situ remediation designs, it is critical to predict behavior of contaminants in the sediment and the containment layer.

2.3 MODELS FOR IN-SITU REMEDIATION

In an early document, Truitt (1987) defined the design principles for in-situ capping remediation as a combination of the isolation performance of the underlying contaminants and the erosion rate of the capping layer. The conventional capping layer is treated as a single component with one design parameter thickness and the model focuses more on the transport of the capping materials per se rather than the transport of contaminants through the capping layer.

Palermo et al. (1998) suggested to use a conservative 'layer approach', which considered the capping system as a one-dimensional system with layered functional components. From the benthic surface to the cap-sediment surface, the cap is separated into an armoring component, bioturbation component, chemical isolation component and sand-sediment mixing component. These components are treated as porous media and the transport of the contaminants through the components are modeled by the classic one-dimensional fate and transport model. This design approach is widely accepted and recommended by EPA (EPA, 2005).

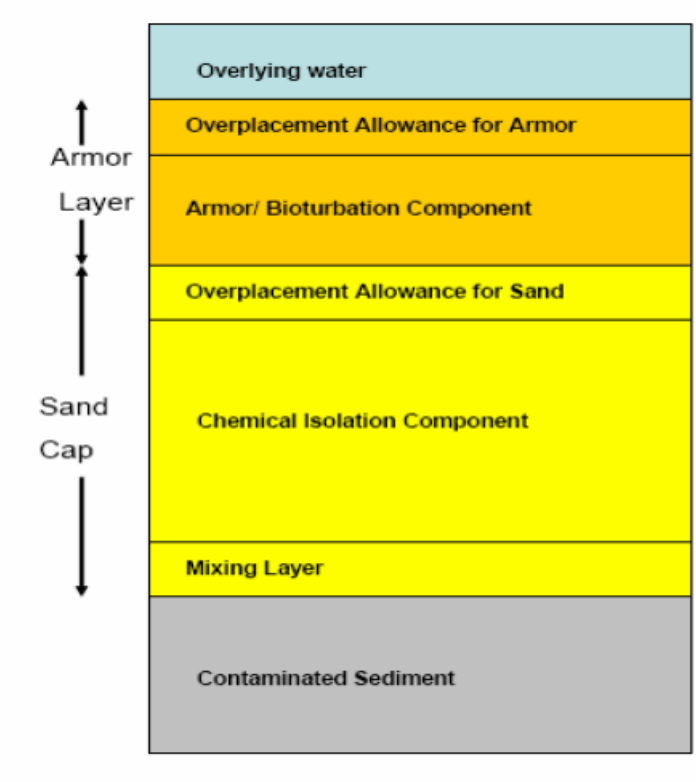

Figure 2.2: Illustration of cap components of a conventional armored sand cap (Palermo and Reible, 2007)

The chemical migration model in porous media (Bear, 1972) describes the behavior of the contaminants in the cap containment system. The transport in solid containment layers has been solved with various layer properties and boundary conditions (Rowe and Booker, 1985; Rubin and Rabideau, 2000; Malusis and Shackelford, 2002). The sediment capping system differs from the classic layered porous media system in several important aspects. Within the top a few centimeters from the benthic surface of the sediments, the activities of benthic organism lead to the formation of the bioturbation layer, where the physical and chemical characteristics, such as organic carbon content and redox conditions are significantly different than in the underlying ambient sediment. Furthermore, the burrowing and dredging activities of these organisms may accelerate the local transport process by mixing both the porewater and the solid materials. Besides bioturbation, the thickness of the cap may increase due to the deposition or decrease due to erosion. Finally, the turbulent motions in the overlying water may influence the mass transport across the sediment-water interface. Regarding these specific processes in sediments, several specific models have been developed. Thoma et al. (1993) presented several models for evaluating the effects of sediment capping on contaminant concentrations and fluxes. Palermo et al. (1998) provided guidance for modeling of contaminant transport in sediments. Lampert et al. (2009) presented an analytical modeling approach for the assessment of the concentration within the chemical isolation layer of a cap and the potential exposure in the biologically active zone after contaminant penetration of the chemical isolation layer. Lampert also laid the foundation for numerical modeling of the system (Lampert, 2010). Some aspects of this modeling are

reported in Go et al. (2009). The Corps of Engineers also developed a numerical model (Recovery) that has been used to model capping.

2.3.1 Sorption

The mass of the contaminant associated with the solid phase at equilibrium is commonly much higher than the mass in pore space (Karickhoff et al., 1979). Thus, the fate and transport of most contaminants in sediments and capping materials are highly controlled by their sorptive behavior.

2.3.1.1 Equilibrium Sorption isotherms

The sorption isotherms, which describe the explicit relationship between the solid phase concentration q and porewater concentration C at equilibrium, are commonly determined by batch sorption experiments.

Linear isotherm

The linear sorption isotherm (2.1) expresses the ratio of the mass of a contaminant between particulate matter and the neighboring water through a linear relationship with partitioning coefficients K_d. It is the simplest choice for modeling the sorption of a contaminant in a solid with complex chemical composition, such as sediments and some capping materials (Reible, 2014). However, the linear water-solid participation coefficient K_d is specific for a given solute contaminant and solid paired system, which can only be derived by batch equilibrium experiments.

$$q = K_d C \tag{2.1}$$

The efforts for developing more practical models to predict the sorption of HOC in sediments and sorbents have been made by a series of studies through decades. Goring (1962) initially revealed that the organic matter in soils and sediments was primarily responsible for the accumulation of organic compounds. Lambert (1966, 1967, and 1968) demonstrated that the sorption of neutral organic pesticides was well correlated with the organic matter content of the solid. Based on the previous evidence, Karickhoff et al. (1979) developed a widely accepted isotherm for sorption of HOCs onto sediments and soils. The model normalized the linear partitioning coefficients K_d to the solid material organic carbon fractions (f_{OC}) and derive compound-specified organic carbon partitioning coefficients (K_{OC}).

$$q = f_{OC} K_{OC} C \tag{2.2}$$

Karickhoff et al. (1979) also suggested to correlate K_{OC} to the octanol-water partition coefficient K_{OW}, a well characterized parameter available for most HOCs including PCBs (Hawker and Connell, 1998) and PAHs (Mackay, 2006). In the following 2 decades, more than 200 relationships between K_{OC} and other measurable properties, such as water solubility, RP-HPLC retention time and topological indices, have been developed (Gawlik, 1997). Seth et al. (1999) reviewed the previous correlation approaches and supports to use the correlation between K_{OC} and K_{OW} for its versatility in handling wide variation of K_{OC}. A broadly applicable correlation is given by Baker et al. (1997).

$$\log K_{OC} = 0.903 \log K_{OW} + 0.09 \tag{2.3}$$

Schwarzenbach et al. (2003) present a summary of K_{OC} - K_{OW} correlations for various classes of organic compounds. The correlation for PAH and PCBs are listed here.

$$\text{PAH:} \quad \log K_{OC} = 0.98 \log K_{OW} - 0.32 \tag{2.4}$$

$$\text{PCB:} \quad \log K_{OC} = 0.89 \log K_{OW} - 0.15 \tag{2.5}$$

Freundlich isotherm

The Freundlich isotherm (2.6) is the most widely applied sorption isotherm. This isotherm was initially developed to describe the concave-shape relationship between the porewater and solid concentrations from experimental results (Bemmelen, 1888; Freundlich, 1909). The isotherm is frequently applied in modeling the sorption onto strong sorbents, such as activated carbons.

$$q = K_{AC} C^{N_{AC}} \tag{2.6}$$

The sorption coefficients K_F and N_F are almost always determined by batch equilibrium experiments. A summary of the previous literature containing the Freundlich isotherm coefficients for HOCs in various organic sorbents (e.g. activated carbon) is shown in Table 2.1.

Weber et al. (1991) suggested using the Freundlich isotherm to describe the sorption behavior of 'hard' organic carbon, which is referred to as 'black carbon'(BC) in most literature. This is crystalline carbon most often originating in high temperature combustion processes as opposed to amorphous carbon originating from the diagenesis of natural organic matter. Koelmans (2006) summarizes the origination, properties and the

existence of black carbon and emphasized its important role in the sorption of HOC in some sediments.

Literature	Contaminants	Sorbents
El-Dim and Badawy(1978)	4 PAHs	GAC (Filtrasorb 400)
Water and Luthy(1984)	11 PAHs	GAC (Filtrasorb 400)
Jonker and Koelmans(2002)	6 PAHs/12PCBs	Soot-like sorbents/AC(Sigma-Aldrich)
McDonough et al. (2008)	9 PCBs	TOG AC
Brandli et al.(2008)	15 PAHs	GAC(Aquacarb208)/PAC(Norit SAE Super)
Azhar (2015)	3 PCBs /3 PAHs	TOG AC/Filtrasorb 400

Table 2.1: A summary of literatures that reported experimentally measured Freundlich isotherm coefficients for HOCs sorption in activated carbon

Table 2.2 shows a list of the selected literature containing the Freundlich isotherm coefficients for HOCs in black carbon.

$$q = f_{OC}K_{OC}C + f_{BC}K_{BC}C^{N_{BC}} \quad (2.7)$$

Literature	Contaminants	Sediments
Accardi-Dey et al. (2002)	1 PAH	Boston Harbor
Accardi-Dey et al. (2003)	17 PAHs	Boston Harbor
Cornelissen and Gustafsson (2005)	3 PAHs/2PCBs	Ketelmeer/Hoytiainen
Lohmann et al. (2005)	3 PAHs/3PCBs/3PCDDs	Boston/New York
Moremond et al. (2005)	14 PAHs/16PCBs	River Rhine (NED)
Hawthorne et al.(2007)	114 Compounds	New York/ NC
Brandli et al.(2008)	15 PAHs	Drammen, Norway

Table 2.2: A summary of literatures that reported experimentally measured Freundlich isotherm coefficients for HOCs sorption in black carbon

Langmuir isotherm

The inorganic compounds and ions are usually more selective on the adsorption sites of the sorbents surface. For example, the sorption of phosphate in sediment and soils has been related to the oxalate extractable fraction of Fe and Al (Beek and Van Riemsdijk, 1979; Beek et al., 1980; Van der Zee and Van Riemsdijk, 1986, Van der Zee et al., 1987). The sorption of mercury in the environment has been considered to primarily link to the sulfide minerals (Barnett et al. 2001).

For such sorption behavior that involves a clearer adsorption site, the Langmuir isotherm (Langmuir, 1918) is commonly applied. The Langmuir isotherm is based on surface reaction hypothesis. The solid surface is assumed to have a finite number of adsorption sites and a maximum solid concentration q_{max} is defined when all these sites are occupied by solute chemicals. The sorption rate is assumed to be a function dependent on the concentration of the solute chemical in the water and the concentration of vacant sites on the solid phase. The desorption rate is a function of the concentration of occupied sites.

$$q = q_{max} bC/(1 + bC) \tag{2.8}$$

The distribution coefficients q_{max} and b usually depends on the pH and salinity of the water as well as the number and type of available sites on solid surface, and hence requires site-specific measurements.

2.3.1.2 Sorption kinetics

The previous section introduces various types of equilibrium sorption isotherms, although non-equilibrium behavior may also observed. For example, the non-equilibrium sorption of HOC in activated carbon has been discussed by Ahn et al., 2005. Such results suggest that the assumption of fast equilibrium in sediments and sorbing materials, which has been applied frequently in previous fate and transport models, may not be fulfilled.

A number of kinetic sorption models have been developed in predicting the transient mass-exchange behavior between liquid-solid interphase. One of the oldest models was a pseudo-first-order model developed by Langergren (1898), who suggested to link the sorption rate to the difference between the current solid phase concentration and the equilibrium solid phase concentration.

The kinetic model suggested by Langmuir (1899) is probably the most well-known theoretical kinetic model and introduced the vacancy of solid phase sorption site as another variable. The sorption rate of a solute in the Langmuir model is proportional to the fluid phase concentration of the solute and the vacancy of the total sorption sites on the solid. The desorption rate is proportional to the occupied sites by the solute. At infinite time, the Langmuir kinetic model is simplified to the equilibrium isotherm, which has been introduced in the previous section.

Though Langmuir model has been recognized as the classic theoretical kinetic model, it has been not frequently used in modeling HOCs in sediment. Instead, the commonly used models are a one-compartment kinetic model, the multi-compartment model and the intraparticle diffusion model.

The one-compartment model simply assumes the kinetics of the sorption process is controlled by the concentration difference between the sorbent concentration and the solution. Analytical solutions of the one-dimensional fate and transport equation with one-compartment kinetic sorption model have been developed (Lapidus and Amundson, 1952)

However, the one compartment model has been found to not work well for fitting some experimental data. Sorption in some experiments have shown a faster rate initially that slowed upon approaching equilibrium (Wu and Gschwend, 1986). The multi-compartment model has been introduced and is widely used in modeling the kinetic sorption in sediments (Chai et al. 2006; Johnson et al. 2001; Rakowska et al, 2014) as well as in activated carbon (Lesage et al., 2010; Valderama et al., 2007, Rakowska et al., 2014). In the multi-compartment model, the sorbent is assumed to have multiple compartments with various kinetic behavior. One major limitation of this model, as pointed out by Wu and Gschwend (1986), is the number of coefficients introduced, which largely limits the generalization of the model. Even for a two-compartment model, three parameters (fast/slow sorption rate coefficients and the fraction of the fast/slow compartment) need to be fitted by experimental data.

The intraparticle diffusion model, which has been developed from the classic reaction model, was applied to modeling the kinetic sorption behavior of HOCs in sediments and soils by Wu and Gschwend (1986). The soil and sediment particle is described as a radial diffusive permeable sphere with a retardation factor reflecting microscale partitioning of the solute between the intraparticle liquid and the immobile

solid matrix. The model suggested defining the sorption kinetics using an effective diffusion coefficient that was predicted from water diffusivity, octanol-water partition coefficient and solid material properties.

2.3.2 Bioturbation

Bioturbation describes the activities of benthic organisms that mix sediment particles and porewater near the sediment-water surface (Wheatcroft et al., 1990). These activities not only change the structure, composition and other sedimentary properties (Rhoads, 1974; Berner, 1980; Aller, 1982), but also often dominate the mixing processes near the sediment-water interface and affect the fate and transport of solute chemicals. (Bosworth and Thibodeaux, 1990) The long-time average bioturbation impact is usually modeled as a diffusive process within a given depth, with the transport flux proportional to the local concentration gradient (Berner, 1980; Boudreau, 1986).

$$F_{bio} = -D_{bio}\nabla C \tag{2.9}$$

Bioturbation tends to lead to a shallow depth that is well mixed (Guinasso and Schink, 1975). Boudreau (1994) calculated a global mixed depth of bioturbation as $9.7 \pm 4.5\text{cm}$. Thoms et al. (1995) summarized literature values from 200 sites and derived an arithmetic mean mixed depth to be 5.5 cm for freshwater and 12.8 cm for estuarine systems. The arithmetic mean biodiffusion coefficients are $1.23 \times 10^{-7}\text{cm}^2/\text{s}$ for fresh water and $0.395 \times 10^{-5}\text{cm}^2/\text{s}$ for estuarine systems.

Roche et al. (2016) conducted a lab experiment using time-lapse imagery to study bioturbation's impact on sediment mixing. They made a thin layer of tracer labeled

particles on the top of an 8cm sediment and recorded the particle distribution using the fluorescence intensity as indicators. They applied both the traditional advection-dispersion model (ADE) and an innovative random-walk model to fit the observed particle density distribution over 15 days. Based on the model fitting results, they suggested to use the random-walk model as a more powerful tool in describing the sediment mixing process by bioturbation.

The potential impact of bioturbation on in-situ remediation is complicated. In most cases, bioturbation will lead to an increase in the surface flux by accelerating the mixing process near the surface (Boudreau, 1997). However, it can also mix solids or sorbents (Lin et al., 2014)

2.3.3 Hydrodynamic dispersion

Hydrodynamic dispersion is a mixing process due to the heterogeneity of the sediment. The microscopic local flow paths of sediments and caps have different lengths and orientations, and groundwater flow path may vary as the flow encounters heterogeneities. This process is analogous to the mass transfer in a turbulent flow, which is also impacted by both the uniform velocity on the macroscopic scale and random velocity on the microscopic scale. Similarly to the transport model in turbulent flow, the dispersion flux $F_{disp,n,i}$ is also modeled as a function of local concentration gradient.

$$F_{disp} = -\alpha_i U \frac{\partial C_n}{\partial z} \tag{2.10}$$

The dispersion coefficient is often expressed as the product of the corrected Darcy advection velocity U and a hydrodynamic dispersion coefficient α that is indicative of the heterogeneity of the medium:

Because dispersion is the result of the averaging on a macroscopic scale of the microscopic variations in the media, α_i is often claimed to be dependent on the length scale of the problem. In general, the value of α_i must be determined empirically through a tracer study. For a uniform material such as sand, the flow may be close to ideal and the dispersion coefficient may be similar in magnitude to the particle diameter. In the absence of site specific information, generally conservative estimates would apply, perhaps to scale the dispersion coefficient with the cap thickness e.g. 10 % of the cap thickness. (Clarke et al., 1993)

2.3.4 Tortuosity

It is currently well-known that the diffusion process in a porous media is slower than in an equivalent volume of pure water due to the finite void fraction and the convoluted path generated by the random structure of solid particles. The latter phenomena is termed tortuosity and commonly modeled by introducing an extra correction coefficient to the effective diffusivity. Millington (1959) developed a widely accepted theoretically based model that used the 4/3 power of the local porosity ε as the tortuosity correction coefficient. The model has been verified in granular media (sand media sand) by Penman (1940) and Taylor (1950), Reible and Shair (1981). This model is

$$D_{eff} = D_w \varepsilon^{\frac{4}{3}} \tag{2.11}$$

Boudreau (1996) summarized the tortuosity models including Archie's model (Lerman, 1979), Burger-Frieke equation (Low, 1981) and modified Weissberg relation (Weissberg, 1963). He compared the performance of these models in predicting the tortuosity-porosity relationship for a sediment system and derived an empirical tortuosity model that provided a better description for consolidated sediments.

$$D_{eff} = D_w \frac{\varepsilon}{1-\ln(\varepsilon^2)} \tag{2.12}$$

2.3.5 1-D fate and transport models in porous media

A sediment cap can be considered a layered porous media with different transport properties in the bioturbation, armoring, capping and sediment layers. Assuming lateral homogeneity, the transport could be modeled as second-order advection-diffusion partial differential equations (2.13) in each layer i.

$$R_i \frac{\partial C_i}{\partial t} = D_i \frac{\partial^2 C_i}{\partial z^2} - U \frac{\partial C_i}{\partial z} - \varepsilon_i \lambda_i C_i \tag{2.13}$$

The basic form of the governing equation includes a first-order time derivative term representing the accumulation/sorption/participation, a second-order space derivative term representing the diffusion/dispersion and a first-order spatial derivative term representing the advection and an optional terms representing reactions and decay. The boundary conditions introduced include three classic types (Dirichlet, Neumann and

Robin). The model could include multiple layers with layer-specified parameters and coefficients as well as time-dependent boundary conditions or spatially-dependent initial conditions and the transport coefficients and parameters as time-dependent or spatial dependent functions.

Numerous solution approaches and examples are available for the advection-dispersion equations, including analytical solution using separation of variables, Laplace transform, integral transform techniques and numerical solutions using finite difference or finite element schemes.

2.3.6 Analytical models and solutions

An analytical solution is a 'closed-form' expression describing the relationship between the dependent variable (concentration) and independent variables (space and time). The solution form and the solution approach for a specific system are dependent on the layer conditions and boundary conditions. The common transient solution for the second-order PDE in a finite domain is the sum of a series self-adjunct eigenfunctions, which may consist of exponential functions, trigonometric functions, hyperbolic functions and hyperbolic functions and/or Bessel functions. Equation (2.13) is a typical solution for single layer advection-dispersion equation with fixed concentration at two boundaries (van Genutchen, 1982).

$$\mathrm{C(z,t)} = \mathrm{C_{ss}(z)} + \sum_{n=1}^{\infty} \frac{2}{n\pi} \exp\left(\frac{\mathrm{Dt}}{\mathrm{RH^2}}\left(n^2\pi^2 + \frac{U^2}{4D^2}\right)\right) \exp\left(\frac{Uz}{2D}\right) \sin\left(n\pi \frac{z}{H}\right) \qquad (2.14)$$

2.3.6.1 Single layer system

Lapidus and Amundson (1952) presented a solution for the transport of a solute in an infinite porous media with equilibrium and non-equilibrium sorption. The boundary conditions are homogenized by splitting the governing equation to two parts, which then allowed the application of the existing solution from Churchill (1944).

Cleary and Adrian (1974) considered a finite domain. They applied the integral transform technique to derive a solution involving a series of eigenfunctions, and solved the resulting non-linear eigenvalue equations.

Van Genutchen and Alves (1982) summarized 40 analytical solutions in both infinite and finite domains with various boundary conditions and reaction options. Additional solutions include systems with exponentially decay (Premlata, 2011); time or spatial-dependent coefficients, e.g. diffusivities or Darcy velocity (Kumar et al., 2009; Guerrero and Skaggs, 2010; Jaiswal and Kumar, 2011; Kumar et al. 2012) and time-dependent boundary condition (Chen and Liu, 2011; Guerrero et al., 2013)

2.3.6.2 Multi-layered system

Few analytical solutions exist, however, for conditions that include advection in bounded multilayered systems and typically numerical solutions are required. Three different analytical techniques have been proposed to solve solute transport in a bounded multilayered advective system. Self–adjoint solution techniques, which arise from separation of variables, was used by Genuchten and Alves (1982) dealing with the single–layer problem and then broadened by Li and Cleall (2011) to multilayered problems. The lack of consideration of hyperbolic eigenfunctions, however, limits the Li

and Cleall solution to two layers with very limited property variations between layers (shown later). A general integral transform method (GITT), initially developed by Liu and Ball (1998, 2000), has been expanded to multiple–layer problems with multi–species, time–variable and spatially variable coefficients (Liu and Si 2008; Guerrero et al. 2009; Guerrero and Skaggs 2010). Despite its versatility, the GITT method is relatively complex and leads to solutions that require coefficient determination in fully populated matrices, effectively requiring significant numerical computation despite being an analytical solution in principle. Efforts have been made to improve the convergence of the GITT method by combining it with Laplace transform or by focusing on diffusive dominated conditions (Chen et al. 2012; Guerrero et al. 2009). The classical integral transform method (CITT) was applied by Guerrero et al. (2013) to bounded multilayer advection diffusion problems, but the as developed in their paper, encounters a problem similar to that of Li and Cleall (2011), limiting the solution to a similarly limited range of parameters and numbers of layers. Guerrero et al. (2013) reports are able to address a broad range of problems, but modifications of their solution are required to do so.

2.4 MONITORING PERFORMANCE OF CAPPING

Traditional approaches to risk assessment in sediments have related the risk to the bulk solid concentration of contaminants in the sediments. This is not particularly useful for in-situ treatment in which amendments such as activated carbon are added to sediments or for capping in that neither changes the bulk solid concentration appreciably. Instead, these approaches will change the flux of contaminants to the overlying water or

the interstitial concentration in the water. Thus evaluation of the performance of these in situ remedial approaches requires monitoring of interstitial water concentration or fluxes.

Recognition of the inadequacy of solid concentrations to assess risk in such conditions encouraged the development of better methods of sediment risk assessment (Burton, 1991). Di Toro et al. (1991) noted that contaminant accumulation in benthic organism was related to sediment pore water concentrations. This link was further evaluated by other studies (Kraaij et al., 2003, Lu et al., 2003, Lu et al., 2004a, Lu et al., 2004b, Lu et al., 2006). However, the porewater concentrations has historically been difficult to measure due to typically very low concentration sand sampling artifacts such as association with colloidal materials (Lu et al. 2003)

Huckins et al. (1990) explored the idea of passive sampling as an alternative method to measure the porewater concentrations in sediment with the minimum interference to the benthic environment. The authors used low density polyethylene tubing containing thi films of model lipids to simulate the bioconcentration of non-polar organic contaminants by aquatic organisms. More recently, various passive sampling approaches have been tested for estimating the in-situ pore water concentrations, including semi-permeable membrane devices or SPMDs (Huckins et al., 2006), and polyethylene (PE) sheets (Booij et al., 2003; Adams et al., 2007), Polyoxymethylene (POM) solid-phase extraction (Jonker and Koelmans, 2001; Cornelissen et al., 2008; Hawthorne et al., 2009; Hawthorne et al., 2011), and polydimethylsiloxane (PDMS) coated glass fibers (Mayer et al., 2000). For each of these methods, the sampler is placed in situ followed by a

contaminant uptake period within the device. The porewater concentration is then back-calculated from a pre-established equilibrium relationship.

Ideally, the sampling devices should be placed in the sediment until equilibrium is achieved, so the ambient contaminant levels can be directly derived by calibrating the sampling concentration with the equilibrium partitioning coefficients. However, some previous studies have revealed that the equilibrium can take a significant amount of time (Booji et al. 2003; Adams et al., 2007; Cornelissen et al., 2008). To overcome this difficulty, the correlations between the concentrations in the passive sampling device and environment are modeled by non-equilibrium uptake, which have rates calibrated using performance reference compounds (PRCs) method (Huckins et al., 1993; Huckins et al., 2002). PRCs are analytically non-interfering chemicals that are pre-loaded in the passive sampler, that are not present in the sediment to be sampled and deplete to the environment during the sampler deployment. If sorption and desorption are reversible, the depletion rate of a PRC reflects the uptake rates of a target analyte with equivalent sorption properties. .

The rates of the PRC release and target analytes uptake have been modeled by first-order kinetic mass exchanges, where the rate constant of a specific compound is inversely proportional to its sorbent-water partitioning coefficients (Tomaszewski and Luthy, 2008). Fernandez et al. 2009 presented a one-dimensional sorption-diffusion model to predict the fate and transport of PRCs and target compounds in both the passive sampler and the surrounding sediment system. Lampert et al. (2015) further discussed the internal and external resistance in the 1-D transport model and presented a practical analytical

approach using PRC data to derive the site-specific effective diffusion/dispersion coefficient assuming external mass transfer resistances control. This assumption is typically valid for PDMS as a passive sampler given geometries commonly in use. Choi et al. (2016) compared the performance of two non-equilibrium models for sorption onto PE and concluded that the transport model with both internal and external resistances describe the experimental data better.

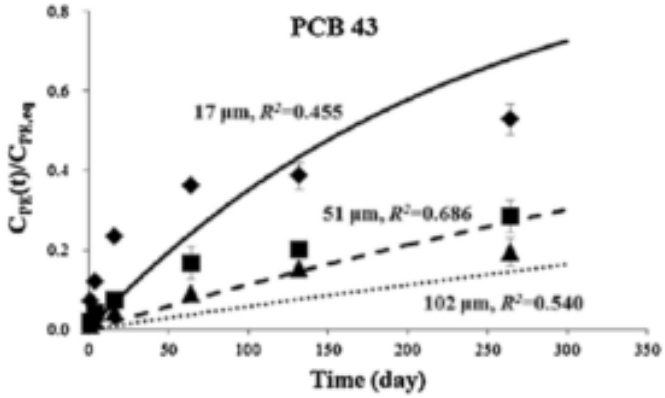

(a) 1st order model

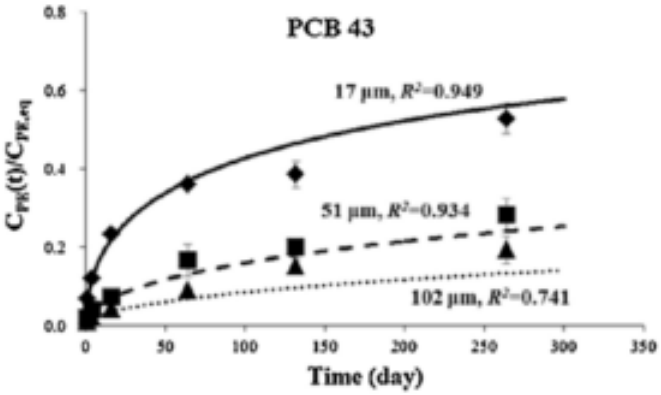

(b) 1-D diffusion model with external resistance for PCB uptake kinetics

Figure 2.3: Comparison of experimental data and simulation results using (a) 1st order model and (b) 1-D diffusion model with external resistance for PCB uptake kinetics of PE in quiescent sediment. The values are shown as the PE concentration at each contact time relative to the equilibrium PE concentration determined in the slurry phase experiments (CPE(t)/CPE,eq). The experimental data are shown as means (symbols) with standard deviations (bars). (Choi et al., 2016)

2.5 SUMMARY

This chapter discussed the occurrence of contaminated sediment, the assessment and three remediation approaches for the contaminated sediment. A summary of the current remediation approaches were presented with an emphasis on the in-situ remediation. The previous models for in-situ remediation are summarized as well as the existing solutions for some of the models (e.g. one dimensional fate and transport model). Passive sampling, a technique for assessment and remediation of contaminated sediments is also introduced here. There is a need for the analytical model that deals with the full multi-layer problem that represents a cap system with various properties in individual layers and a numerical model that incorporates the processes important in a cap and can simulate multiple reactions, bioturbation and deposition etc. Passive sampling is needed to monitor the performance of a cap and its accuracy is dependent upon the analysis of performance reference compounds and improvements are needed in the analysis of their behavior and the evaluation of the extent of equilibration of the passive sampler.

2.6 REFERENCE

Accardi-Dey, A. and P. M. Gschwend (2002). "Assessing the combined roles of natural organic matter and black carbon as sorbents in sediments." Environmental Science & Technology 36(1): 21-29.

Accardi-Dey, A. and P. M. Gschwend (2003). "Reinterpreting literature sorption data considering both absorption into organic carbon and adsorption onto black carbon." Environmental Science & Technology 37(1): 99-106.

Adams, R. G., R. Lohmann, L. A. Fernandez, J. K. MacFarlane and P. M. Gschwend (2007). "Polyethylene devices: Passive samplers for measuring dissolved

hydrophobic organic compounds in aquatic environments." Environmental Science & Technology 41(4): 1317-1323.

Ahn, S., D. Werner, H. K. Karapanagioti, D. R. McGlothlin, R. N. Zare and R. G. Luthy (2005). "Phenanthrene and pyrene sorption and intraparticle diffusion in polyoxymethylene, coke, and activated carbon." Environmental science & technology 39(17): 6516-6526.

Aller, R. C. (1982). The effects of macrobenthos on chemical properties of marine sediment and overlying water. Animal-sediment relations, Springer: 53-102.

Andelman, J. B. and M. J. Suess (1970). "Polynuclear aromatic hydrocarbons in the water environment." Bulletin of the World Health Organization 43(3): 479.

Barnett, M. O., R. R. Turner and P. C. Singer (2001). "Oxidative dissolution of metacinnabar (β-HgS) by dissolved oxygen." Applied Geochemistry 16(13): 1499-1512.

Bear, J. (1972). "Dynamics of fluids in porous materials." Society of Petroleum Engineers.

Bedard, D. L., R. E. Wagner, M. J. Brennan, M. L. Haberl and J. Brown (1987). "Extensive degradation of Aroclors and environmentally transformed polychlorinated biphenyls by Alcaligenes eutrophus H850." Applied and Environmental Microbiology 53(5): 1094-1102.

Beek, J. and W. Van Riemsdijk (1979). "Interaction of orthophosphate ions with soil." Developments in Soil Science 5: 259-284.

Beek, J., W. Van Riemsdijk and K. Koenders (1980). "Aluminium and ion fractions affecting phosphate bonding in a sandy soil treated with sewage water." Agrochemicals in Soils. Pergamon Press, Oxford: 369-379.

Berner, R. A. (1980). Early diagenesis: A theoretical approach, Princeton University Press.

Bessinger, B. A., Vlassopoulos, D., Serrano, S., & O'Day, P. A. (2012). Reactive transport modeling of subaqueous sediment caps and implications for the long-term fate of arsenic, mercury, and methylmercury. Aquatic geochemistry, 18(4), 297-326.

Booij, K., H. E. Hofmans, C. V. Fischer and E. M. Van Weerlee (2003). "Temperature-dependent uptake rates of nonpolar organic compounds by semipermeable

membrane devices and low-density polyethylene membranes." Environmental Science & Technology 37(2): 361-366.

Bosworth, W. S. and L. J. Thibodeaux (1990). "Bioturbation: A facilitator of contaminant transport in bed sediment." Environmental Progress 9(4): 211-217.

Boudreau, B. P. (1986). "Mathematics of tracer mixing in sediments; II, Nonlocal mixing and biological conveyor-belt phenomena." American Journal of Science 286(3): 199-238.

Boudreau, B. P. (1994). "Is burial velocity a master parameter for bioturbation?" Geochimica et Cosmochimica Acta 58(4): 1243-1249.

Boudreau, B. P. (1996). "The diffusive tortuosity of fine-grained unlithified sediments." Geochimica et Cosmochimica Acta 60(16): 3139-3142.

Boudreau, B. P. (1997). Diagenetic models and their implementation, Springer Berlin.

Brändli, R. C., T. Hartnik, T. Henriksen and G. Cornelissen (2008). "Sorption of native polyaromatic hydrocarbons (PAH) to black carbon and amended activated carbon in soil." Chemosphere 73(11): 1805-1810.

Brenner, R. C., V. S. Magar, J. A. Ickes, E. A. Foote, J. E. Abbott, L. S. Bingler and E. A. Crecelius (2004). "Long-term recovery of PCB-contaminated surface sediments at the Sangamo-Weston/Twelvemile Creek/Lake Hartwell Superfund site." Environmental science & technology 38(8): 2328-2337.

Bridges, T. S., S. Ells, D. Hayes, D. Mount, S. C. Nadeau, M. R. Palermo, C. Patmont and P. Schroeder (2008). the four rs of Environmental dredging: resuspension, release, residual, and risk, DTIC Document.

Burton, G. A. (1991). "Assessing the toxicity of freshwater sediments." Environmental Toxicology and Chemistry 10(12): 1585-1627.

Chai, Y., A. Kochetkov and D. D. Reible (2006). "Modeling biphasic sorption and desorption of hydrophobic organic contaminants in sediments." Environmental toxicology and chemistry 25(12): 3133-3140.

Chen, J.-S. and C.-W. Liu (2011). "Generalized analytical solution for advection-dispersion equation in finite spatial domain with arbitrary time-dependent inlet boundary condition." Hydrology and Earth System Sciences 15(8): 2471.

Choi, Y., Y. Wu, R. G. Luthy and S. Kang (2016). "Non-equilibrium passive sampling of hydrophobic organic contaminants in sediment pore-water: PCB exchange kinetics." Journal of Hazardous Materials 318: 579-586.

Churchill, R. V. (1944). "Modern operational mathematics in engineering."

Clarke, J., D. D. Reible and R. Mutch (1993). "Contaminant transport and behavior in the subsurface." Hazardous Waste Soil Remediation: Theory and Application of Innovative Technologies. Marcel-Dekker, New York, NY, USA: 1-49.

Clarkson, T. W. (1998). "Human toxicology of mercury." The Journal of trace elements in experimental medicine 11(2-3): 303-317.

Cleary, R. W. and D. D. Adrian (1973). "Analytical solution of the convective-dispersive equation for cation adsorption in soils." Soil Science Society of America Journal 37(2): 197-199.

Cornelissen, G. and Ö. Gustafsson (2005). "Prediction of large variation in biota to sediment accumulation factors due to concentration-dependent black carbon adsorption of planar hydrophobic organic compounds." Environmental toxicology and chemistry 24(3): 495-498.

Cornelissen, G., A. Pettersen, D. Broman, P. Mayer and G. D. Breedveld (2008). "Field testing of equilibrium passive samplers to determine freely dissolved native polycyclic aromatic hydrocarbon concentrations." Environmental Toxicology and Chemistry 27(3): 499-508.

Di Toro, D. M., C. S. Zarba, D. J. Hansen, W. J. Berry, R. C. Swartz, C. E. Cowan, S. P. Pavlou, H. E. Allen, N. A. Thomas and P. R. Paquin (1991). "Technical basis for establishing sediment quality criteria for nonionic organic chemicals using equilibrium partitioning." Environmental toxicology and chemistry 10(12): 1541-1583.

Eek, E., Cornelissen, G., Kibsgaard, A., & Breedveld, G. D. (2008). Diffusion of PAH and PCB from contaminated sediments with and without mineral capping; measurement and modelling. Chemosphere, 71(9), 1629-1638.

El-Dib, M. A. and M. I. Badawy (1979). "Adsorption of soluble aromatic hydrocarbons on granular activated carbon." Water Research 13(3): 255-258.

Fitzgerald, W. F., D. R. Engstrom, R. P. Mason and E. A. Nater (1998). "The case for atmospheric mercury contamination in remote areas." Environmental Science & Technology 32(1): 1-7.

Freundlich, H. (1909). "Kolloidchemie." Akademischer Verlagsgeselschaft, Leipzig.

Gawlik, B., N. Sotiriou, E. Feicht, S. Schulte-Hostede and A. Kettrup (1997). "Alternatives for the determination of the soil adsorption coefficient, KOC, of non-ionicorganic compounds—a review." Chemosphere 34(12): 2525-2551.

Goring, C. A. (1962). "Control of Nitrification by 2-chloro-6-(trichloro-methyl) pyridine." Soil Science 93(3): 211-218.

Guerrero, J. P., E. Pontedeiro, M. T. van Genuchten and T. Skaggs (2013). "Analytical solutions of the one-dimensional advection–dispersion solute transport equation subject to time-dependent boundary conditions." Chemical Engineering Journal 221: 487-491.

Guerrero, J. P. and T. Skaggs (2010). "Analytical solution for one-dimensional advection–dispersion transport equation with distance-dependent coefficients." Journal of Hydrology 390(1): 57-65.

Guerrero, J. S. P., T. H. Skaggs and M. T. van Genuchten (2009). "Analytical solution for multi-species contaminant transport subject to sequential first-order decay reactions in finite media." Transport in Porous Media 80(2): 373-387.

Guinasso, N. and D. Schink (1975). "Quantitative estimates of biological mixing rates in abyssal sediments." Journal of Geophysical Research 80(21): 3032-3043.

Hawker, D. W. and D. W. Connell (1988). "Octanol-water partition coefficients of polychlorinated biphenyl congeners." Environmental Science & Technology 22(4): 382-387.

Hawthorne, S. B., C. B. Grabanski and D. J. Miller (2007). "Measured partition coefficients for parent and alkyl polycyclic aromatic hydrocarbons in 114 historically contaminated sediments: Part 2. Testing the KOCKBC two carbon–type model." Environmental toxicology and chemistry 26(12): 2505-2516.

Hawthorne, S. B., M. T. Jonker, S. A. van der Heijden, C. B. Grabanski, N. A. Azzolina and D. J. Miller (2011). "Measuring picogram per liter concentrations of freely dissolved parent and alkyl PAHs (PAH-34), using passive sampling with polyoxymethylene." Analytical chemistry 83(17): 6754-6761.

Hawthorne, S. B., D. J. Miller and C. B. Grabanski (2009). "Measuring low picogram per liter concentrations of freely dissolved polychlorinated biphenyls in sediment pore water using passive sampling with polyoxymethylene." Analytical Chemistry 81(22): 9472-9480.

Howsam, M. and K. C. Jones (1998). Sources of PAHs in the environment. PAHs and related compounds, Springer: 137-174.

Huckins, J. N., G. K. Manuweera, J. D. Petty, D. Mackay and J. A. Lebo (1993). "Lipid-containing semipermeable membrane devices for monitoring organic contaminants in water." Environmental science & technology 27(12): 2489-2496.

Huckins, J. N., J. D. Petty, J. A. Lebo, F. V. Almeida, K. Booij, D. A. Alvarez, W. L. Cranor, R. C. Clark and B. B. Mogensen (2002). "Development of the permeability/performance reference compound approach for in situ calibration of semipermeable membrane devices." Environmental science & technology 36(1): 85-91.

Huckins, J. N., M. W. Tubergen and G. K. Manuweera (1990). "Semipermeable membrane devices containing model lipid: A new approach to monitoring the bioavaiiability of lipophilic contaminants and estimating their bioconcentration potential." Chemosphere 20(5): 533-552.

Hull, J. H., J. M. Jersak and B. J. McDonald (1998). "Examination of a New Remedial Technology for Capping Contaminated Sediments: Large-Scale Laboratory Evaluation of Sediment Mixing and Cap Resistance to Erosive Forces." Remediation Journal 8(3): 37-58.

Jacobs, P. and T. Waite (2004). "The role of aqueous iron (II) and manganese (II) in sub-aqueous active barrier systems containing natural clinoptilolite." Chemosphere 54(3): 313-324.

Jacobs, P. H. and U. Förstner (1999). "Concept of subaqueous capping of contaminated sediments with active barrier systems (ABS) using natural and modified zeolites." Water Research 33(9): 2083-2087.

Jaiswal, D. and A. Kumar (2011). "Analytical solutions of time and spatially dependent one-dimensional advection-diffusion equation." Elixir Poll 32: 2078-2083.

Jensen, S. (1972). "The PCB story." Ambio: 123-131.

Johnson, M. D., T. M. Keinath and W. J. Weber (2001). "A distributed reactivity model for sorption by soils and sediments. 14. Characterization and modeling of phenanthrene desorption rates." Environmental Science & Technology 35(8): 1688-1695.

Jonker, M. T. and A. A. Koelmans (2001). "Polyoxymethylene solid phase extraction as a partitioning method for hydrophobic organic chemicals in sediment and soot." Environmental Science & Technology 35(18): 3742-3748.

Jonker, M. T. and A. A. Koelmans (2002). "Sorption of polycyclic aromatic hydrocarbons and polychlorinated biphenyls to soot and soot-like materials in the aqueous environment: mechanistic considerations." Environmental Science & Technology 36(17): 3725-3734.

Karcher, W., Fordham, R.J., Dubois, J.J., Glaude, P.G.J.M., & Ligthart, J.A.M. (1985). Spectral atlas of polycyclic aromatic compounds. United States: D. Reidel Publishing Co.,Hingham, MA.

Karickhoff, S. W., D. S. Brown and T. A. Scott (1979). "Sorption of hydrophobic pollutants on natural sediments." Water Research 13(3): 241-248.

Koelmans, A. A., M. T. Jonker, G. Cornelissen, T. D. Bucheli, P. C. Van Noort and Ö. Gustafsson (2006). "Black carbon: the reverse of its dark side." Chemosphere 63(3): 365-377.

Kraaij, R., P. Mayer, F. J. Busser, M. van Het Bolscher, W. Seinen, J. Tolls and A. C. Belfroid (2003). "Measured pore-water concentrations make equilibrium partitioning work a data analysis." Environmental Science & Technology 37(2): 268-274.

Kraepiel, A. M., K. Keller, H. B. Chin, E. G. Malcolm and F. M. Morel (2003). "Sources and variations of mercury in tuna." Environmental Science &Technology 37(24): 5551-5558.

Kudo, A. and S. Miyahara (1991). "A case history; Minamata mercury pollution in Japan–from loss of human lives to decontamination." Water Science and Technology 23(1-3): 283-290.

Kumar, A., D. K. Jaiswal and N. Kumar (2009). "Analytical solutions of one-dimensional advection-diffusion equation with variable coefficients in a finite domain." Journal of Earth System Science 118(5): 539-549.

Kumar, A., D. K. Jaiswal and N. Kumar (2010). "Analytical solutions to one-dimensional advection–diffusion equation with variable coefficients in semi-infinite media." Journal of Hydrology 380(3): 330-337.

Kumar, A., D. K. Jaiswal and N. Kumar (2012). "One-dimensional solute dispersion along unsteady flow through a heterogeneous medium, dispersion being proportional to the square of velocity." Hydrological Sciences Journal 57(6): 1223-1230.

Largegren, S. (1898). About the theory of so-called adsorption of soluble substances. Kungliga Suensk Vetenskapsakademiens Handlingar, 241(1).

Lambert, S. (1966). "The influence of soil-moisture content on herbicidal response." Weeds: 273-275.

Lambert, S. M. (1967). "Functional relation between sorption in soil and chemical structure." Journal of Agricultural and Food Chemistry 15(4): 572-576.

Lambert, S. M. (1968). "Omega (. OMEGA.), a useful index of soil sorption equilibria." Journal of Agricultural and Food Chemistry 16(2): 340-343.

Lampert, D., C. Thomas and D. Reible (2015). "Internal and external transport significance for predicting contaminant uptake rates in passive samplers." Chemosphere 119: 910-916.

Lampert, D. J. and D. Reible (2009). "An analytical modeling approach for evaluation of capping of contaminated sediments." Soil and Sediment Contamination 18(4): 470-488.

Langmuir, I. (1918). "The evaporation of small spheres." Physical review 12(5): 368.

Lapidus, L. and N. R. Amundson (1952). "Mathematics of adsorption in beds. VI. The effect of longitudinal diffusion in ion exchange and chromatographic columns." The Journal of Physical Chemistry 56(8): 984-988.

Lerman, A. (1979). Geochemical processes. Water and sediment environments, John Wiley and Sons, Inc.

Lesage, G., M. Sperandio and L. Tiruta-Barna (2010). "Analysis and modelling of non-equilibrium sorption of aromatic micro-pollutants on GAC with a multi-compartment dynamic model." Chemical Engineering Journal 160(2): 457-465.

Li, Y. C. and P. J. Cleall (2011). "Analytical solutions for advective–dispersive solute transport in double-layered finite porous media." International Journal for Numerical and Analytical Methods in Geomechanics 35(4): 438-460.

Lin, D., Y.-M. Cho, D. Werner and R. G. Luthy (2014). "Bioturbation delays attenuation of DDT by clean sediment cap but promotes sequestration by thin-layered activated carbon." Environmental Science & Technology 48(2): 1175-1183.

Liu, C., W. P. Ball and J. H. Ellis (1998). "An analytical solution to the one-dimensional solute advection-dispersion equation in multi-layer porous media." Transport in Porous Media 30(1): 25-43.

Liu, C., J. E. Szecsody, J. M. Zachara and W. P. Ball (2000). "Use of the generalized integral transform method for solving equations of solute transport in porous media." Advances in Water Resources 23(5): 483-492.

Lohmann, R., J. MacFarlane and P. Gschwend (2005). "Importance of black carbon to sorption of native PAHs, PCBs, and PCDDs in Boston and New York harbor sediments." Environmental Science & Technology 39(1): 141-148.

Low, P. F. (1981). "Principles of ion diffusion in clays." Chemistry in the Soil Environment(chemistryinthes): 31-45.

Lu, X., D. D. Reible and J. W. Fleeger (2004). "Bioavailability and assimilation of sediment-associated benzo [a] pyrene by Ilyodrilus templetoni (oligochaeta)." Environmental Toxicology and Chemistry 23(1): 57-64.

Lu, X., D. D. Reible and J. W. Fleeger (2004). "Relative importance of ingested sediment versus pore water as uptake routes for PAHs to the deposit-feeding oligochaete Ilyodrilus templetoni." Archives of Environmental Contamination and Toxicology 47(2): 207-214.

Lu, X., D. D. Reible and J. W. Fleeger (2006). "Bioavailability of polycyclic aromatic hydrocarbons in field-contaminated Anacostia River (Washington, DC) sediment." Environmental Toxicology and Chemistry 25(11): 2869-2874.

Lu, X., D. D. Reible, J. W. Fleeger and Y. Chai (2003). "Bioavailability of desorption-resistant phenanthrene to the oligochaete Ilyodrilus templetoni." Environmental Toxicology and Chemistry 22(1): 153-160.

Mackay, D., W. Y. Shiu and K.-C. Ma (1997). Illustrated handbook of physical-chemical properties of environmental fate for organic chemicals, CRC press.

Mackay, D., W.-Y. Shiu, K.-C. Ma and S. C. Lee (2006). Handbook of physical-chemical properties and environmental fate for organic chemicals, CRC press.

Magar, V. S., D. B. Chadwick, T. S. Bridges, P. C. Fuchsman, J. M. Conder, T. J. Dekker, J. A. Steevens, K. E. Gustavson and M. A. Mills (2009). Monitored natural recovery at contaminated sediment sites, DTIC Document.

Malusis, M. A. and C. D. Shackelford (2002). "Theory for reactive solute transport through clay membrane barriers." Journal of Contaminant Hydrology 59(3): 291-316.

Manap, N. and N. Voulvoulis (2016). "Data analysis for environmental impact of dredging." Journal of Cleaner Production 137: 394-404.

Manes, M. and L. J. Hofer (1969). "Application of the Polanyi adsorption potential theory to adsorption from solution on activated carbon." The Journal of Physical Chemistry 73(3): 584-590.

Mayer, P., W. H. Vaes and J. L. Hermens (2000). "Absorption of hydrophobic compounds into the poly (dimethylsiloxane) coating of solid-phase microextraction fibers: High partition coefficients and fluorescence microscopy images." Analytical Chemistry 72(3): 459-464.

McDonough, K. M., J. L. Fairey and G. V. Lowry (2008). "Adsorption of polychlorinated biphenyls to activated carbon: Equilibrium isotherms and a preliminary assessment of the effect of dissolved organic matter and biofilm loadings." Water Research 42(3): 575-584.

Millington, R. and J. Quirk (1961). "Permeability of porous solids." Transactions of the Faraday Society 57: 1200-1207.

Moermond, C. T., J. J. Zwolsman and A. A. Koelmans (2005). "Black carbon and ecological factors affect in situ biota to sediment accumulation factors for hydrophobic organic compounds in flood plain lakes." Environmental Science & Technology 39(9): 3101-3109.

Mohan, R., J. P. Doody, C. Patmont, R. Gardner and A. Shellenberger (2016). "REVIEW OF ENVIRONMENTAL DREDGING IN NORTH AMERICA: CURRENT PRACTICE AND LESSONS LEARNED." Journal of Dredging 15(2): 29.

Morel, F. M., A. M. Kraepiel and M. Amyot (1998). "The chemical cycle and bioaccumulation of mercury." Annual Review of Ecology and Systematics 29(1): 543-566.

NRC (National Research Council). (1997). Contaminated Sediments in Ports and Waterways: Cleanup Strategies and Technologies. National Academies Press, Washington, DC, USA.

Palermo, M. and D. Reible. 2007. The Evolution of Cap Design. Proceedings, World Dredging Congress WODCON XVIII, Orlando, FL, May 27-June1, 2007.

Palermo, M. R. (1998). "Design considerations for in-situ capping of contaminated sediments." Water Science and Technology 37(6-7): 315-321.

Parrett, K. and H. Blishke (2005). "23 Acre Multilayer Sediment Cap in Dynamic Riverine Environment Using organoclay an adsorptive Capping Material." SETAC Presentation.

Penman, H. (1940). "Gas and vapour movements in the soil: I. The diffusion of vapours through porous solids." The Journal of Agricultural Science 30(03): 437-462.

Penman, H. (1940). "Gas and vapour movements in the soil: I. The diffusion of vapours through porous solids." The Journal of Agricultural Science 30(03): 437-462.

Perelo, L. W. (2010). "Review: in situ and bioremediation of organic pollutants in aquatic sediments." Journal of Hazardous Materials 177(1): 81-89.

Premlata, S. (2011). "One dimensional solute transport originating from a exponentially decay type point source along unsteady flow through heterogeneous medium." Journal of Water Resource and Protection 2011.

Rakowska, M., D. Kupryianchyk, J. Harmsen, T. Grotenhuis and A. Koelmans (2012). "In situ remediation of contaminated sediments using carbonaceous materials." Environmental Toxicology and Chemistry 31(4): 693-704.

Reible, D., D. Lampert, D. Constant, R. D. Mutch Jr and Y. Zhu (2006). "Active capping demonstration in the Anacostia River, Washington, DC." Remediation Journal 17(1): 39-53.

Reible, D. D., F. H. Shair and E. Kauper (1981). "Plume dispersion and bifurcation in directional shear flows associated with complex terrain." Atmospheric Environment (1967) 15(7): 1165-1172.

Rhoads, D. (1974). "Organism-sediment relations on the muddy sea floor. Oceanogr." Mar. Biol. Ann. Rev. 12: 263-300.

Roche, K. R., A. F. Aubeneau, M. Xie, T. Aquino, D. Bolster and A. I. Packman (2016). "An integrated experimental and modeling approach to predict sediment mixing from benthic burrowing behavior." Environmental Science & Technology 50(18): 10047-10054.

Rowe, R. K. and J. R. Booker (1985). "1-D pollutant migration in soils of finite depth." Journal of Geotechnical Engineering 111(4): 479-499.

Rubin, H. and A. J. Rabideau (2000). "Approximate evaluation of contaminant transport through vertical barriers." Journal of Contaminant Hydrology 40(4): 311-333.

Schwarzenbach, R. P., P. M. Gschwend and D. M. Imboden (2003). Transformation Processes, Wiley Online Library.

Seth, R., D. Mackay and J. Muncke (1999). "Estimating the organic carbon partition coefficient and its variability for hydrophobic chemicals." Environmental Science & Technology 33(14): 2390-2394.

Shiaris, M. P. and G. S. Sayler (1982). "Biotransformation of PCB by natural assemblages of freshwater microorganisms." Environ. Sci. Technol.;(United States) 16(6).

Sims, R. C. and M. Overcash (1983). Fate of polynuclear aromatic compounds (PNAs) in soil-plant systems. Residue Reviews, Springer: 1-68.

Taylor, S. A. (1950). "Oxygen diffusion in porous media as a measure of soil aeration." Proceedings. Soil Science Society of America, 1949 14: 55-61.

Thibodeaux, L. J. and K. T. Duckworth (2001). "The effectiveness of environmental dredging: A study of three sites." Remediation Journal 11(3): 5-33.

Thoma, G. J., D. RELBLE, K. T. Valsaraj and L. J. Thibodeaux (1993). "Efficiency of capping contaminated sediments in situ. II: Mathematics of diffusin-adsorption in the capping layer." Environmental Science & Technology 27(12): 2412-2419.

Thoms, S., G. Matisoff, P. L. McCall and X. Wang (1995). "Models for alteration of sediments by benthic organisms." Water Environment Research Foundation.

Tomaszewski, J. E. and R. G. Luthy (2008). "Field deployment of polyethylene devices to measure PCB concentrations in pore water of contaminated sediment." Environmental Science & Technology 42(16): 6086-6091.

Truitt, C. (1987). "Engineering Considerations for Capping Subaqueous Dredged Material Deposits: Design Concepts and Placement Techniques." Environmental Effects of Dredging Technical Note: 01-03.

Truitt, C. L. (1987). Engineering Considerations for Capping Subaqueous Dredged Material Deposits--Background and Preliminary Planing, DTIC Document.

USACE/USEPA (U.S. Environmental Protection Agency). 1998. (Updated 2004). Evaluation of Dredged Material Proposed for Discharge in Waters of the U.S. - Testing Manual (Inland Testing Manual). EPA-823-B-98-004. USEPA and USACE, Washington, DC, USA. http://www.epa.gov/ostwater/itm/index.html. November 17, 2012.

USACE/USEPA. 2004. Evaluating Environmental Effects of Dredged Material Management Alternatives - A Technical Framework. EPA842-B-92-008. USEPA and USACE, Washington, DC, USA.

http://el.erdc.usace.army.mil/dots/pdfs/epa/tech-frame-rev04.pdf. November 17, 2012.

USEPA. 1994. Remediation Guidance Document. EPA 905-B94-003. Assessment and Remediation of Contaminated Sediments Program, USEPA Great Lakes National Program Office, Chicago, IL, USA. http://www.epa.gov/greatlakes/arcs/EPA-905-B94-003/B94-003.ch7.html. Accessed November 17, 2012.

USEPA. 1998. National Conference on Management and Treatment of Contaminated Sediments. EPA-625-R-98-001. USEPA, Cincinnati, OH, USA.

USEPA. 2005a. Contaminated Sediment Remediation Guidance for Hazardous Waste Sites. EPA-540-R-05-012. USEPA Office of Solid Waste and Emergency Response, Washington, DC, USA. http://www.epa.gov/superfund/health/conmedia/sediment/guidance.htm. Accessed March 12, 2012.

Valderrama, C., X. Gamisans, X. De las Heras, A. Farran and J. Cortina (2008). "Sorption kinetics of polycyclic aromatic hydrocarbons removal using granular activated carbon: intraparticle diffusion coefficients." Journal of Hazardous Materials 157(2): 386-396.

van Bemmelen, J. M. (1888). Die Absorptinsverbindungen und das Absorptionsvermögen der Ackererde, publisher not identified.

Van der Zee, S., v. d. Fokkink, LGJ and W. Van Riemsdijk (1987). "A new technique for assessment of reversibly adsorbed phosphate." Soil Science Society of America Journal 51(3): 599-604.

Van der Zee, S. and W. Van Riemsdijk (1986). "Sorption kinetics and transport of phosphate in sandy soil." Geoderma 38(1-4): 293-309.

Van Genuchten, M. T. and W. Alves (1982). Analytical solutions of the one-dimensional convective-dispersive solute transport equation, United States Department of Agriculture, Economic Research Service.

Walker, T. R., D. MacAskill, T. Rushton, A. Thalheimer and P. Weaver (2013). "Monitoring effects of remediation on natural sediment recovery in Sydney Harbour, Nova Scotia." Environmental Monitoring and Assessment 185(10): 8089-8107.

Weber, W. J., P. M. McGinley and L. E. Katz (1991). "Sorption phenomena in subsurface systems: concepts, models and effects on contaminant fate and transport." Water Research 25(5): 499-528.

Weissberg, H. L. (1963). "Effective diffusion coefficient in porous media." Journal of Applied Physics 34(9): 2636-2639.

Wheatcroft, R., P. Jumars, C. Smith and A. Nowell (1990). "A mechanistic view of the particulate biodiffusion coefficient: step lengths, rest periods and transport directions." Journal of Marine Research 48(1): 177-207.

Wu, S. C. and P. M. Gschwend (1986). "Sorption kinetics of hydrophobic organic compounds to natural sediments and soils." Environmental Science & Technology 20(7): 717-725.

Zarull, M. A., J. H. Hartig and L. Maynard (1999). "Ecological benefits of contaminated sediment remediation in the Great Lakes basin."

Chapter 3 An analytical solution for one–dimensional advective–dispersive solute equation in multilayered finite porous media[1]

3.0 ABSTRACT

A general analytical solution for the one-dimensional advective–dispersive–reactive solute transport equation in multilayered porous media is presented. The separation of variables technique was employed to derive the analytical solution. Hyperbolic eigenfunctions, as well as traditional trigonometric eigenfunctions, were found to contribute an important part to the series solution and were not included in some existing solutions. The closed-form analytical solution was verified against a numerical solution from a finite difference-based approach and an existing solution derived from general integral transform technique (GITT). The solution has several important advantages over the GITT technique and other existing solutions. The limitations of existing solutions and the ability of the current solution to address those limitations are identified. Among other applications, the current analytical solution will be useful for modeling the transport of contaminants in sediments and, particularly for the design of layered caps as a remedial approach. The analytical solution also has significant advantages over numerical solutions for sensitivity analyses and the solution of inverse problems.

[1] Published as: Shen, X., & Reible, D. (2015). An analytical solution for one-dimensional advective–dispersive solute equation in multilayered finite porous media. Transport in Porous Media, 107(3), 657-666. Reprinted here with the permission of the co-author.

3.1 INTRODUCTION

Advective–diffusive transport is often encountered in multilayered porous media. Examples include stratified soils and sediments subject to groundwater movement and multilayered confining layers surrounding landfills or in contaminated sediments caps. The layered soil or sediment systems are usually modeled using the generalized advection–dispersion reaction equation with potentially different physical and chemical properties in each layer. Analytical solutions in an infinite domain system with specific property variations have been developed by applying Laplace transforms (Leij and Genuchten 1995; Kumar et al. 2010; Kumar et al. 2010, 2012). Few analytical solutions exist, however, for conditions that include advection in bounded multilayered systems and typically numerical solutions are required. Three different analytical techniques have been proposed to solve solute transport in a bounded multilayered advective system. Self–adjoint solution techniques, which arise from separation of variables, was used by Genuchten and Alves (1982) dealing with the single–layer problem and then broadened by Li and Cleall (2011) to multilayered problems. The lack of consideration of hyperbolic eigenfunctions, however, limits the Li and Cleall solution to two layers with very limited property variations between layers (shown later). A general integral transform method (GITT), initially developed by Liu and Ball (1998, 2000), has been expanded to multiple–layer problems with multi–species, time–variable and spatially variable coefficients (Liu and Si 2008; Guerrero et al. 2009; Guerrero and Skaggs 2010). Despite its versatility, the GITT method is relatively complex and leads to solutions that require coefficient determination in fully populated matrices, effectively requiring significant numerical

computation despite being an analytical solution in principle. Efforts have been made to improve the convergence of the GITT method by combining it with Laplace transform or by focusing on diffusive dominated conditions (Chen et al. 2012; Guerrero et al. 2009). The classical integral transform method (CITT) was applied by Guerrero et al. (2013) to bounded multilayer advection diffusion problems, but as developed in their paper, encounters a problem similar to that of Li and Cleall (2011), limiting the solution to a similarly limited range of parameters and numbers of layers. Guerrero et al. (2013) reports are able to address a broad range of problems, but modifications of their solution are required to do so.

This chapter presents an analytical solution for one–dimensional advective–dispersive–reactive solute transport equation in multiple–layered porous media with an arbitrary number of layers, arbitrary parameter values and initial concentration distributions, and requiring only a simple eigenvalue determination. Each layer is assumed to possess constant physical properties (e.g., porosity, diffusivity), linear sorption and reaction, and steady state flow. Several examples of the application of the solution are shown. In addition, the comparison of the solution with the existing solutions (Li and Cleall 2011; Liu et al. 1998 and Guerrero et al. 2013) is discussed, illustrating the limitations of the existing solutions.

3.2 PROBLEM STATEMENT

Considered here is a porous media system with constant–flow and first–order reaction consisting of multiple individual internal homogeneous layers with arbitrary but

fixed thickness (Fig. 1). The coordinate system (z) is chosen to be in the same direction of the flow, characterized by the Darcy velocity, U, so the inlet and exit boundaries bounding the multilayered system are defined as $z = 0$ and H respectively. The subscript i represents the layer number, with $i = 1$ corresponding to the inlet layer and $i = l$ to the outlet layer. The thickness of layer i is h_i , and the total thickness H is the sum of the h_i ($H = \sum_{i=1}^{l} h_i$). The ratio of thickness at the interfacial boundary between layer i and $i + 1$ to total thickness is defined as: $r_{i,i+1} = \sum_{j=1}^{i} h_j/H$. Transport in the i th layer in the system is governed by

$$R_i \frac{\partial C_i}{\partial t} = D_i \frac{\partial^2 C_i}{\partial z^2} - U \frac{\partial C_i}{\partial z} - \varepsilon_i \lambda_i C_i \tag{3.1}$$

The retardation factor R_i reflects the accumulation of solute on the immobile solid phase in the porous media and is given by the ratio of the total concentration in an elementary volume of solid and pore fluid to the concentration of the solute in the pore fluid. If linear sorption and local equilibrium is assumed between the solid and pore fluid, the retardation factor is defined as $R_i = \varepsilon_i + K_{d,i}\rho_i$, where $K_{d,i}$ is the linear partition coefficient between the solid and adjacent water phases ; ε_i and ρ_i are the porosity and dry bulk density of the sorptive material, respectively. The effective diffusivity D_i is defined as the molecular diffusivity in the pore fluid (water), D_w, corrected by the void fraction (porosity) since diffusion is occurring only through the fluid and a tortuosity factor T_i which is the ratio of the effective diffusion path to the straight line (z) path as

$D_i = \varepsilon_i * D_w/T_i$. As written above, the first–order decay process with rate coefficient λ_i is assumed to occur only in the pore fluid.

Three boundary conditions are considered for the inlet and outlet boundaries (Table 3.1). The combined conditions are assumed from which concentration specified and flux specified conditions can be defined.

	Inlet Boundary ($z = 0$)	Outlet Boundary ($z = H$)
Concentration	$C_1(0,t) = C_0$	$C_l(H,t) = C_H$
Diffusive Flux	$-D_1 \frac{\partial C_1}{\partial z}(0,t) = F_0$	$-D_l \frac{\partial C_l}{\partial z}(H,t) = F_H$
Combined	$-D_1 \frac{\partial C_1}{\partial z}(0,t) + UC_1(0,t) = F_0$	$-D_l \frac{\partial C_l}{\partial z}(H,t) + UC_l(H,t) = F_H$

Table 3.1: The three types of boundary conditions applied in the problem

C_0 and C_H are characteristic concentrations outside of the inlet and outlet boundary, applied at the surface for concentration conditions. F_0 and F_H are characteristic fluxes at the inlet and outlet boundary in the bulk fluid for flux and combined conditions. Interfacial boundary conditions between layers are based on continuity of concentration and flux at the interfacial boundary between layer i and i+1:

$$C_i(r_{i,i+1}, t) = C_{i+1}(r_{i,i+1}, t) \tag{3.2}$$

$$-D_i \frac{\partial C_i(r_{i,i+1},t)}{\partial z} + UC_i(r_{i,i+1}, t) = -D_{i+1} \frac{\partial C_{i+1}(r_{i,i+1},t)}{\partial z} + UC_{i+1}(r_{i,i+1}, t) \tag{3.3}$$

Interfacial boundary condition (3.3) can also be simplified with constant velocity between layers and (3.2):

$$D_i \frac{\partial C_i(r_{i,i+1},t)}{\partial z} = D_{i+1} \frac{\partial C_{i+1}(r_{i,i+1},t)}{\partial z} \tag{3.4}$$

Note that the solute concentration in the pore fluids is continuous across a boundary between two porous layers, while the total concentration (solid plus fluid) is, in general, discontinuous. Arbitrary initial conditions in each layer are defined as follows:

$$C_i(z, t = 0) = C_{i,init}(z) \tag{3.5}$$

where $C_{i,init}(z)$ is an arbitrary function for the initial concentration distribution in the i th layer.

3.3 ANALYTICAL SOLUTION

3.3.1 Non–dimensionalization and homogenization

The total thickness of sediment layers H and total diffusive characteristic time t_0 are chosen to be the characteristic length and time scale, respectively. The characteristic concentration C_R is chosen from the nonzero inlet or outlet characteristic concentrations C_0 or C_H. Three non–dimensional variables are defined using these scales:

$$\eta = \frac{z}{H} \quad ; \quad C^* = \frac{C}{C_R} \; ; \quad \tau = \frac{t}{t_0} \tag{3.6}$$

The total diffusive characteristic time is the sum of diffusive times in each layer as defined below:

$$t_0 = \sum_{i=1}^{l} t_i \quad ; \quad t_i = \frac{R_i {h_i}^2}{D_i} \tag{3.7}$$

Combining diffusivity D_i, Darcy velocity U, first–order decay rate λ_i, general mass transfer coefficient k and characteristic length H, two dimensionless numbers are introduced:

$$\text{Peclet Number} \quad Pe_i = \frac{UH}{D_i} \quad ; \quad \text{Damköhler Number} \quad Da_i = \frac{\lambda_i H^2}{D_i} \tag{3.8}$$

The governing equations and boundary conditions are homogenized by separating the full solution to a steady–state term that fulfills the inhomogeneous boundary conditions and the temporal–spatial transient solution that fulfills the homogeneous boundary conditions (3.9). The dimensionless and homogenized governing equation is shown in (3.10) and the corresponding inhomogeneous boundary conditions are given in Table 3.2. The homogenous boundary can be easily derived by subtracting the inhomogeneous boundary conditions from the dimensionless boundary conditions.

$$C_i^* = C_{i,ss}^*(\eta) + C_{i,t}^*(\tau, \eta) \tag{3.9}$$

$$0 = \frac{\partial^2 C_{i,ss}^*}{\partial \eta^2} - Pe_i \frac{\partial C_{i,ss}^*}{\partial \eta} - \varepsilon_i Da_i C_{i,ss}^* \tag{3.10}$$

$$\frac{R_i H^2}{D_i t_o} \frac{\partial C_{i,t}^*}{\partial \tau} = \frac{\partial^2 C_{i,t}^*}{\partial \eta^2} - Pe_i \frac{\partial C_{i,t}^*}{\partial \eta} - \varepsilon_i Da_i C_{i,t}^* \tag{3.11}$$

	Inlet ($\eta = 0$)	Interface ($\eta = r_{i,i+1}$)	Outlet ($\eta = 1$)
Concentration	$C_{1,ss}{}^{*} = \frac{C_0}{C_R}$	$C_{i,ss}{}^{*} = C_{i+1,ss}{}^{*}$	$C_{l,ss}{}^{*} = \frac{C_H}{C_R}$
Flux	$-\frac{\partial C_{1,ss}{}^{*}}{\partial \eta} = \frac{F_0 H}{D_1 C_R}$	$D_i \frac{\partial C_{i,ss}{}^{*}}{\partial \eta} = D_{i+1} \frac{\partial C_{i+1,ss}{}^{*}}{\partial \eta}$	$-\frac{\partial C_{l,ss}{}^{*}}{\partial \eta} = \frac{F_H H}{D_l C_R}$
Combined	$-\frac{\partial C_{1,ss}{}^{*}}{\partial \eta} + Pe_1 C_{1,ss}{}^{*} = \frac{F_0 H}{D_1 C_R}$		$-\frac{\partial C_{l,ss}{}^{*}}{\partial \eta} + Pe_l C_{l,ss}{}^{*} = \frac{F_H H}{D_l C_R}$

Table 3.2: Dimensionless inhomogeneous boundary conditions

3.3.2 Steady–state and transient solution

The general solution form for the ordinary differential equation (3.10) is given in (3.12):

$$C_{i,ss}{}^{*} = \exp\left(\frac{Pe_i}{2}\eta\right)\left(\alpha_{i,ss}\cosh\left(\sqrt{\gamma_i}\eta\right) + \sigma_{i,ss}\sinh\left(\sqrt{\gamma_i}\eta\right)\right) \tag{3.12}$$

where $\gamma_i = \varepsilon_i D\alpha_i + \frac{{Pe_i}^2}{4}$, and coefficient $\alpha_{i,ss}$ and $\sigma_{i,ss}$ can be solved by the linear system (3.13)

$$\begin{bmatrix} p_0 & q_0 & 0 & 0 & 0 & 0 & \dots & 0 & 0 \\ p_1(r_{12}) & q_1(r_{12}) & -p_2(r_{12}) & -q_2(r_{12}) & 0 & 0 & \dots & 0 & 0 \\ p_1'(r_{12}) & q_1'(r_{12}) & -p_2'(r_{12}) & -q_2'(r_{12}) & 0 & 0 & \dots & 0 & 0 \\ 0 & 0 & p_2(r_{23}) & q_2(r_{23}) & -p_3(r_{23}) & -q_3(r_{23}) & \dots & 0 & 0 \\ 0 & 0 & p_2'(r_{23}) & q_2'(r_{23}) & -p_3'(r_{23}) & -q_3'(r_{23}) & \dots & 0 & 0 \\ \vdots & \vdots & \vdots & \vdots & \vdots & \vdots & \vdots & \vdots & \vdots \\ \vdots & \vdots & \vdots & 0 & 0 & p_{l-1}(r_{l-1,l}) & q_{l-1}(r_{l-1,l}) & -p_l(r_{l-1,l}) & -q_l(r_{l-1,l}) \\ 0 & 0 & 0 & 0 & 0 & p_{l-1}'(r_{l-1,l}) & q_{l-1}'(r_{l-1,l}) & -p_l'(r_{l-1,l}) & -q_l'(r_{l-1,l}) \\ 0 & 0 & 0 & 0 & 0 & 0 & \dots & p_{l+1} & q_{l+1} \end{bmatrix} * \begin{bmatrix} \alpha_{1,ss} \\ \sigma_{1,ss} \\ \alpha_{2,ss} \\ \sigma_{2,ss} \\ \vdots \\ \alpha_{l-1,ss} \\ \sigma_{l-1,ss} \\ \alpha_{l,ss} \\ \sigma_{l,ss} \end{bmatrix} = \begin{bmatrix} b_0 \\ 0 \\ 0 \\ 0 \\ \vdots \\ 0 \\ 0 \\ 0 \\ b_l \end{bmatrix} \tag{3.13}$$

The elements in the linear system, p and q are derived by applying Table 3.2 boundary conditions

For $i = 1$ to l:

$$p_i(\eta) = \exp(\frac{Pe_i}{2}\eta)\cosh(\sqrt{\gamma_i}\eta)\ ; \quad q_i(\eta) = \exp(\frac{Pe_i}{2}\eta)\sinh(\sqrt{\gamma_i}\eta) \tag{3.14}$$

$$p_i'(\eta) = D_i\sqrt{\gamma_i}\exp(\frac{Pe_i}{2}\eta)\sinh(\sqrt{\gamma_i}\eta); \quad q_i'(\eta) = D_i\sqrt{\gamma_i}\exp(\frac{Pe_i}{2}\eta)\cosh(\sqrt{\gamma_i}\eta) \tag{3.15}$$

	p_0	q_0	p_{l+1}	q_{l+1}	b_0	b_l
Dirichlet	1	0	$\exp(\frac{Pe_l}{2})\cosh(\sqrt{\gamma_l})$	$\exp(\frac{Pe_l}{2})\sinh(\sqrt{\gamma_l})$	$\frac{C_0}{C_R}$	$\frac{C_H}{C_R}$
Neumann	$-\frac{Pe_1}{2}$	$-\sqrt{\gamma_1}$	$-\exp\left(\frac{Pe_l}{2}\right)\left(\frac{Pe_l}{2}\cosh(\sqrt{\gamma_l}) + \sqrt{\gamma_l}\sinh(\sqrt{\gamma_l})\right)$	$-\exp\left(\frac{Pe_l}{2}\right)\left(\frac{Pe_l}{2}\sinh(\sqrt{\gamma_l}) + \sqrt{\gamma_l}\cosh(\sqrt{\gamma_l})\right)$	$\frac{F_0H}{D_1C_R}$	$\frac{F_HH}{D_lC_R}$
Robin	$\frac{Pe_1}{2}$	$-\sqrt{\gamma_1}$	$\exp\left(\frac{Pe_l}{2}\right)\left(\frac{Pe_l}{2}\cosh(\sqrt{\gamma_l}) - \sqrt{\gamma_l}\sinh(\sqrt{\gamma_l})\right)$	$\exp\left(\frac{Pe_l}{2}\right)\left(\frac{Pe_l}{2}\sinh(\sqrt{\gamma_l}) - \sqrt{\gamma_l}\cosh(\sqrt{\gamma_l})\right)$	$\frac{F_0H}{D_1C_R}$	$\frac{F_HH}{D_lC_R}$

Table 3.3: Coefficients in elements of the linear system

The transient term in (3.9) can be defined as the product of a time–dependent function $G_n(\tau)$ times the spatially dependent function $F_{i,n}(\eta)$.

$$C_{i,t}{}^*(\tau,\eta) = \sum_{n=1}^{\infty} G_n(\tau)F_{i,n}(\eta) \tag{3.16}$$

The general solution equation (3.17) to (3.21) can be derived by applying separation of variables with coefficients $A_{i,n}$, β_n and $\alpha_{i,n}$, which are then evaluated by applying initial and homogeneous boundary conditions in equation (15).

$$\frac{R_iH^2}{D_it_o}\frac{\partial G_n}{\partial\tau} * \frac{1}{G_n} = -\beta_n{}^2\frac{R_iH^2}{D_it_o} = (\frac{\partial^2F_{i,n}}{\partial\eta^2} - Pe_i\frac{\partial F_{i,n}}{\partial\eta} - \varepsilon_iDa_iF_{i,n})\frac{1}{F_{i,n}} \tag{3.17}$$

$$G_n = e^{-\beta_n{}^2 \tau} \tag{3.18}$$

$$F_{i,n} = A_{i,n} e^{\frac{Pe_i}{2}\eta} \varphi_{i,n}(\eta) \tag{3.19}$$

$$\text{When } x_{i,n}{}^2 = \gamma_i - \beta_n{}^2 \frac{R_i H^2}{D_i t_o} \geq 0 ; \quad \varphi_{i,n}(\eta) = \left(\sinh\left(x_{i,n}\eta\right) + \alpha_{i,n} \cosh\left(x_{i,n}\eta\right)\right) \tag{3.20}$$

$$\text{When } y_{i,n}{}^2 = \beta_n{}^2 \frac{R_i H^2}{D_i t_o} - \gamma_i \geq 0 ; \quad \varphi_{i,n}(\eta) = \left(\sin\left(y_{i,n}\eta\right) + \alpha_{i,n} \cos\left(y_{i,n}\eta\right)\right) \tag{3.21}$$

Neither Li and Cleall (2011) or Guerrero et al. (2013) included the hyperbolic eigenfunctions from (3.20) or identify the existence of the equivalent imaginary eigenvalues. This severely limits the usefulness of their solutions. The hyperbolic eigenfunctions corresponds to the smallest eigenvalues β_n, which indicates that it dominates behavior of the transient profile at long times in the general multilayer problem. The solutions of Li and Cleall (2011) and Guerrero et al. (2013) are valid under a single–layer or multiple–layer problems with severely restricted parameter values. This is explored further in the discussion section.

The eigenvalues β_n and the eigenfunction coefficients are $\alpha_{i,n}$ derived by solving the nonlinear system (3.22) containing $i + 1$ equations and unknowns. The 'sign–count' method (Wittrick and Williams 1971; Milkhailov and Vulchanov, 1983) is used here for finding nonlinear roots.

$$\left(\frac{D_i\frac{\partial\varphi_{i,n}}{\partial\eta}}{\varphi_{i,n}} = \frac{D_{i+1}\frac{\partial\varphi_{i+1,n}}{\partial\eta}}{\varphi_{i+1,n}}\right)\Bigg|_{\eta=r_{i,i+1}} \quad \text{for } i = 1 \text{ to } l-1 \tag{3.22}$$

	$\alpha_{1,n}$	$\alpha_{l,n}$
Concentration	0	$-\tanh(x_{l,n})$ or $-\tan(y_{l,n})$
Flux	$-\frac{2x_{1,n}}{Pe_1}$ or $-\frac{2y_{1,n}}{Pe_1}$	$\frac{-\frac{Pe_l}{2}\tanh(x_{l,n}) - x_{l,n}}{\frac{Pe_l}{2} + x_{l,n}\tanh(x_{l,n})}$ or $\frac{\frac{Pe_l}{2}\tan(y_{l,n}) + y_{l,n}}{y_{l,n}\tan(y_{l,n}) - \frac{Pe_l}{2}}$
Combined	$\frac{2x_{1,n}}{Pe_1}$ or $\frac{2y_{1,n}}{Pe_1}$	$\frac{\frac{Pe_l}{2}\tanh(x_{ln}) - x_{l,n}}{x_{l,n}\tanh(x_{ln}) - \frac{Pe_l}{2}}$ or $\frac{y_{l,n} - \frac{Pe_l}{2}\tan(y_{l,n})}{y_{l,n}\tan(y_{l,n}) + \frac{Pe_l}{2}}$

Table 3.4: Coefficients in eigenfunctions of various boundary conditions

The coefficients $A_{i,n}$, which determine the magnitude of the contribution from nth order eigenfunction to the total concentration, are derived by introducing the initial conditions. The eigenfunctions $\varphi_{i,n}(\eta)$ follow the orthogonal relation (3.24) and the coefficients $A_{i,n}$ can be calculated by (3.25) and (3.26). These reduce to simple forms if $C_{i,init}(\eta)$ is constant within a particular layer as illustrated in the Appendix A.

$$\text{at } \tau = 0; \quad {C_{i,t}}^*(\tau = 0, \eta) = \frac{C_{i,init}(\eta)}{C_H} - {C_{i,ss}}^*(\eta) \tag{3.23}$$

$$\sum_{i=1}^{l}\int_{r_{i-1,i}}^{r_{i,i+1}} \varphi_{i,n}\varphi_{i,m}\, d\eta * A_{i,n}A_{i,m}e^{\left(\sum_{j=2}^{i} Pe_j r_{j-1,j} + \sum_{j=i}^{l-1} Pe_j r_{j,j+1}\right)}R_i$$

$$= \begin{cases} \sum_{i=1}^{l} \int_{r_{i-1,i}}^{r_{i,i+1}} \varphi_{i,n}{}^2 \, d\eta * A_{i,n}{}^2 e^{\left(\sum_{j=2}^{i} Pe_j r_{j-1,j} + \sum_{j=i}^{l-1} Pe_j r_{j,j+1}\right)} R_i & \text{when } n = m \\ 0 & \text{when } n \neq m \end{cases} \quad (3.24)$$

$$\sum_{i=1}^{l} \int_{r_{i-1,i}}^{r_{i,i+1}} \varphi_{i,n} \left(\frac{C_{i,init}}{C_b} - c_{i,ss}{}^* \right) e^{-\frac{Pe_i}{2}\eta} \, d\eta * A_{i,n} e^{\left(\sum_{j=2}^{i} Pe_j r_{j-1,j} + \sum_{j=i}^{l-1} Pe_j r_{j,j+1}\right)} R_i$$
$$= \sum_{i=1}^{l} \int_{r_{i-1,i}}^{r_{i,i+1}} \varphi_{i,n}{}^2 \, d\eta * A_{i,n}{}^2 e^{\left(\sum_{j=2}^{i} Pe_j r_{j-1,j} + \sum_{j=i}^{l-1} Pe_j r_{j,j+1}\right)} R_i \quad (3.25)$$

$$A_{i,n} \varphi_{i,n}(r_{i,i+1}) e^{\frac{Pe_i}{2} r_{i,i+1}} = A_{i+1,n} \varphi_{i+1,n}(r_{i,i+1}) e^{\frac{Pe_{i+1}}{2} r_{i,i+1}} \quad (3.26)$$

The general form of solution can be expressed as:

$$C_i{}^*(\eta, \tau) = e^{\frac{Pe_i}{2}\eta} \left(\alpha_{i,ss} \cosh(\sqrt{\gamma_i}\eta) + \sigma_{i,ss} \sinh(\sqrt{\gamma_i}\eta) + \sum_{n=1}^{\infty} A_{i,n} e^{-\beta_n{}^2 \tau} \varphi_{i,n}(\eta) \right) \quad (3.27)$$

3.4 VERIFICATION

The analytical solution was compared to the GITT solution five–layer example given in Liu et al. (1998). The concentration distributions are in full agreement with those obtained in Liu et al.'s paper (Figure 3.1). Note that the parameter values in this example vary little between layers. Although the same solution is found, the solutions here converge more quickly and with significantly less computational effort due to the generally full matrices that must be solved for the GITT method versus the banded matrices in the current solution. The faster convergence of the current method compared with the GITT is illustrated in the session 3.5.2 with equivalent results shown with 60 terms ($n = 60$) versus 20 terms in the present analytical solution ($n = 20$). Moreover, the total number of operations required to solve the GITT method for this case by direct

evaluation is of order $O(n^3) = O(60^3)$ compared with $O(n) = O(20)$ for the current method. (Moler and Van Loan, 2003)

This example compares the results from analytical solution to those from Liu et al (1998). A five-layer system is considered in this case and the parameter data for the sand-clay-sand-clay-sand media is given in Table 3.5. The combined boundary condition and flux specified boundary conditions are used for inlet and outlet, respectively. The concentration distributions (lines) shown in Figure 3.1 are in full agreement with those obtained in Liu et al.'s paper (solid dots).

Layer	h_i(cm)	ε_i	R_i	D_i(cm^2/d)	$C_{i,init}$(μg/L)	λ_i(/yr)	ρ_i (kg/L)	U(cm/yr)
1	10	0.4	1.7	2.8	0	0	1	4
2	2	0.5	7	9	0	0	1	4
3	8	0.4	1.7	2.8	0	0	1	4
4	2	0.5	7	9	0	0	1	4
5	8	0.4	1.7	2.8	0	0	1	4

Table 3.5: Layer properties in the example of five-layer sand-clay-sand-clay-sand system

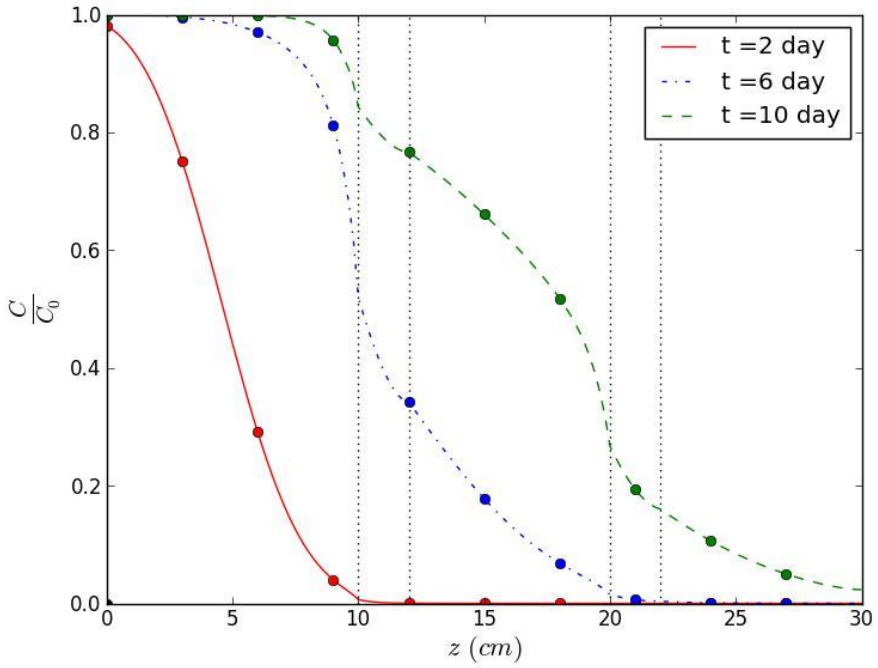

Figure 3.1: Concentration as a function of distance at various times in a five layer case (results coincide with the results of Liu, 1998)

The analytical solution was also used to compare two layered containment systems as shown in Figure 3.2. Both systems have the same total thickness and sorption capacity but in one case the sorbing component is confined to a thin 1 cm layer and, in the other, mixed uniformly over a 10 cm layer. The separated layer case might be an example of a strong sorbent (such as granular activated carbon, GAC) placed in a thin reactive core mat (RCM®, CETCO, Illinois, USA), while the mixed layer case would represent the same mass of sorbent mixed uniformly within a thicker layer of inert sand. The sorbing component is considered to be 1000 times more sorbing than the media in the other

layers. The layer properties are summarized in Table 3. The characteristic concentration at inlet boundary C_0 is fixed at 1ug/L. The plots of concentration profiles versus time (Fig. 2) show agreement between the analytical solution (solid and dashed lines) and a numerical solution (circles, triangles and crosses) solved by a finite difference method from Reible and Lampert (2014). As shown in the Table 3.8, the accuracy of the analytical solution is better than the numerical solution for this example with similar computational expense. The migration of contaminant to the exit boundary of the containment layer (20 cm) is less in the mixed layer case despite having the same overall thickness and sorbent mass as the thin layer sorbent case.

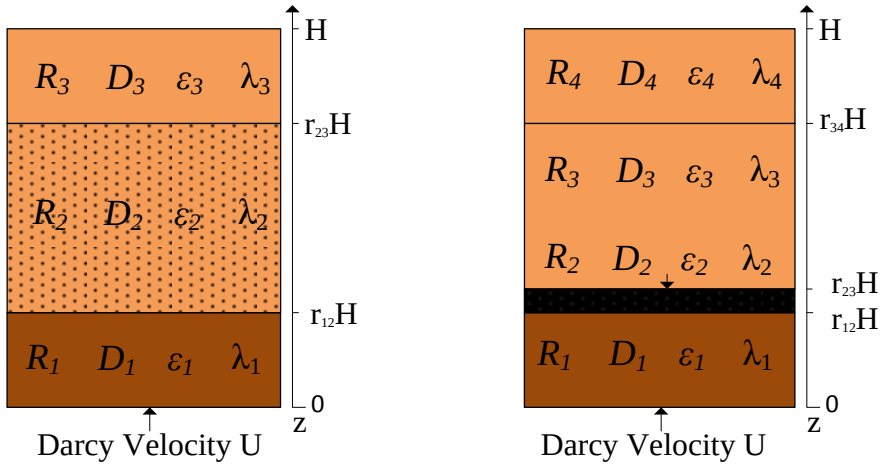

Figure 3.2: Porous media systems consisting of multiple individual homogeneous layers:
(1) contaminated sediment capped with separated sand and sorbent layers;
(2) contaminated sediment capped with mixing sand and sorbent layer

Layer	h_i(cm)	ε_i	$K_{d,i}$(L/kg)	$C_{i,init}$(μg/L)	λ_i(/yr)	ρ_i (kg/L)	U(cm/yr)
4	5	0.5	10	0	5	1	20
3	9	0.5	10	0	0	1	20
2	1	0.5	10000	0	0	1	20
1	5	0.5	100	1	0	1	20

(a) Capping with separated thin sorbent layers

Layer	h_i(cm)	ε_i	$K_{d,i}$(L/kg)	$C_{i,init}$(μg/L)	λ_i(/yr)	ρ_i (kg/L)	U(cm/yr)
3	5	0.5	10	0	5	1	20
2	10	0.5	1009	0	0	1	20
1	5	0.5	100	1	0	1	20

(b) Capping with mixing sorbent layer

Table 3.6: Layer properties in the example comparing a mixed and thin layer sorbent layer

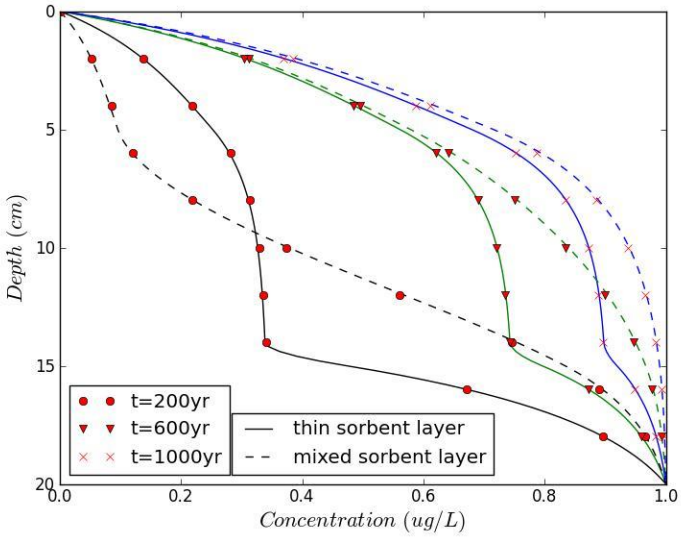

(a) Concentration inlet – Concentration outlet

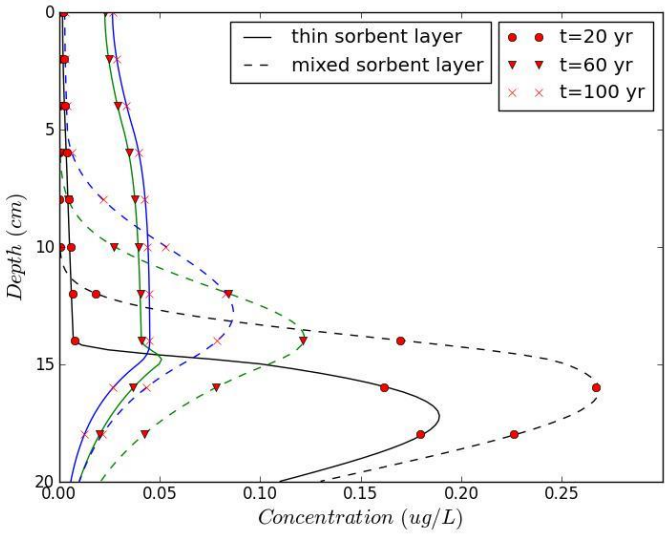

(b) Combined inlet – Flux outlet

Figure 3.3: Comparison of the solute concentration profiles with mixing sorbent layers or separated thin sorbent layers. Analytical solution (solid and dashed lines) and the numerical solution (circles, triangles and crosses) solved by the numerical method from Reible and Lampert (2014).

3.5 DISCUSSION

3.5.1 Existence of hyperbolic eigenfunctions

The general solution of multiple layers with arbitrary parameter values requires consideration of the hyperbolic eigenfunctions. Shown in criterion (3.20) and (3.21), the hyperbolic eigenfunctions corresponds to the smallest eigenvalues, which dominate the transient behavior at large times. The hyperbolic eigenfunction arise in cases of strong advection or large physical property variation between layers.

The existence of hyperbolic eigenfunctions is dependent on the parameter values of the system. In a typical two-layered system with fixed concentration at both the inlet and outlet boundary, three types of eigenvectors could be involved in the transient solution: hyperbolic-hyperbolic eigenvectors $\begin{pmatrix}\sinh(x_{1,n}\eta)+\alpha_{1,n}\cosh(x_{1,n}\eta)\\ \sinh(x_{2,n}\eta)+\alpha_{2,n}\cosh(x_{2,n}\eta)\end{pmatrix}$, hyperbolic-trigonometric eigenvectors: $\begin{pmatrix}\sinh(x_{1,n}\eta)+\alpha_{1,n}\cosh(x_{1,n}\eta)\\ \sin(y_{2,n}\eta)+\alpha_{2,n}\cos(y_{2,n}\eta)\end{pmatrix}$ or $\begin{pmatrix}\sin(y_{1,n}\eta)+\alpha_{1,n}\cos(y_{1,n}\eta)\\ \sinh(x_{2,n}\eta)+\alpha_{2,n}\cosh(x_{2,n}\eta)\end{pmatrix}$ and the trigonometric-trigonometric eigenvectors $\begin{pmatrix}\sin(y_{1,n}\eta)+\alpha_{1,n}\cos(y_{1,n}\eta)\\ \sin(y_{2,n}\eta)+\alpha_{2,n}\cos(y_{2,n}\eta)\end{pmatrix}$. Fig.S1 illustrates that the presence of these types of eigenvectors is dependent on the eigenvalues β_n. No hyperbolic-hyperbolic eigenvector should be included in the solution as they are incompatible with the boundary conditions in this problem. On the contrary, trigonometric-trigonometric eigenvectors, the "regular" eigenvectors which always arise in eigenvalue problems and contribute to most of the terms in the infinite solution series, have already been studied in the solution given in Li and Cleall (2011). Under general parameter conditions, however, the hyperbolic-trigonometric eigenvectors arise and these

were not considered in the solution of Li and Cleall (2011) and Guerrero et al. (2013). Failure to consider these solutions leads to invalid solutions with even modest variations in parameter values between layers, particularly when the number of layers is large.

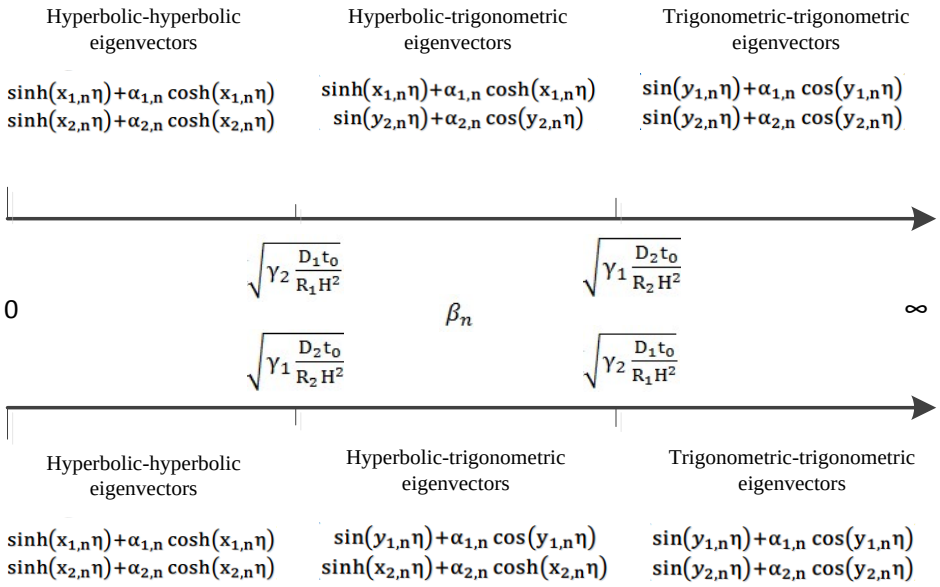

Figure 3.4: Three types of eigenvectors and their correspondent eigenvalue range

Considering a two-layer system with r_{12} representing the ratio of the thickness of the top layer to the total thickness, two interfacial boundary functions $f_1(\beta)$ (when $\gamma_1 - \gamma_2\frac{R_1D_2}{R_2D_1} > 0$) and $f_2(\beta)$ (when $\gamma_2 - \gamma_1\frac{R_2D_1}{R_1D_2} > 0$) are defined by replacing coefficients $\alpha_{1,n}$ and $\alpha_{2,n}$ with Dirichlet boundary conditions in Table 3.4. A necessary and sufficient requirement for the existence of hyperbolic-trigonometric eigenvectors is that equation $f_1(\beta) = 0$ or $f_2(\beta) = 0$ have non-negative roots $\beta = \beta_n$.

$$f_1(\beta) = D_1x_1\frac{1}{\tanh(x_1r_{12})} - D_2y_2\frac{1}{\tan(y_2(r_{12}-1))} \tag{3.28}$$

Where $x_1 = \sqrt{\gamma_1 - \beta^2 \frac{R_1 H^2}{D_1 t_o}}$; $y_2 = \sqrt{\beta^2 \frac{R_2 H^2}{D_2 t_o} - \gamma_2}$

$$f_2(\beta) = D_1 x_1 \frac{1}{\tan(y_1 r_{12})} - D_2 x_2 \frac{1}{\tanh(x_2(r_{12}-1))} \tag{3.29}$$

Where $x_2 = \sqrt{\gamma_2 - \beta^2 \frac{R_2 H^2}{D_2 t_o}}$; $y_1 = \sqrt{\beta^2 \frac{R_1 H^2}{D_1 t_o} - \gamma_1}$

The interfacial boundary functions $f_1$and f_2 meet periodic singular points ${\beta^s}_n$, which divide the positive β-axis to intervals where both functions are monotonically decreasing with β. (Figure 3.5). The interval $[\sqrt{\gamma_2 \frac{D_1 t_o}{R_1 H^2}}, \sqrt{\gamma_1 \frac{D_2 t_o}{R_2 H^2}}]$ in $f_1(\beta)$ or $[\sqrt{\gamma_1 \frac{D_2 t_o}{R_2 H^2}}, \sqrt{\gamma_2 \frac{D_1 t_o}{R_1 H^2}}]$ in $f_2(\beta)$ (dashed-dotted lines) defines the range of independent variable β. ${f_1}^0$and ${f_2}^0$, the values of the function at the lower β value, $\sqrt{\gamma_2 \frac{D_1 t_o}{R_1 H^2}}$ or $\sqrt{\gamma_1 \frac{D_2 t_o}{R_2 H^2}}$, are positive.

$$f_1(\beta): \quad {\beta^s}_n = \sqrt{\frac{D_2 t_o}{R_2 H^2}\left(\gamma_2 + {y^s}_{2,n}{}^2\right)} \quad \text{where } {y^s}_{2,n} = \frac{n\pi}{1-r_{12}} \tag{3.30}$$

$$f_2(\beta): \quad {\beta^s}_n = \sqrt{\frac{D_2 t_o}{R_2 H^2}\left(\gamma_1 + {y^s}_{1,n}{}^2\right)} \quad \text{where } {y^s}_{1,n} = \frac{n\pi}{r_{12}} \tag{3.31}$$

The necessary and sufficient condition for existence of hyperbolic-trigonometric vectors is that the greater β value, $\sqrt{\gamma_1 \frac{D_1 t_o}{R_1 H^2}}$ or $\sqrt{\gamma_2 \frac{D_2 t_o}{R_2 H^2}}$, is larger than the critical value β_c which is the smallest root for equation $f_1(\beta^c) = 0$ or $f_2(\beta^c) = 0$. The function value ${f_1}^\delta$ or ${f_2}^\delta$ corresponding to the maximum β value can be determined as equation (3.32) or

(3.33). The critical case $\sqrt{\gamma_1 \frac{D_1 t_o}{R_1 H^2}} = \beta^c$ or $\sqrt{\gamma_2 \frac{D_2 t_o}{R_2 H^2}} = \beta^c$ is evaluated by equating the functions ${f_1}^{\delta}(\delta_1)$ or ${f_2}^{\delta}(\delta_2)$to 0 (Equation (3.23) and (3.24)). ${\delta_1}^c$ and ${\delta_2}^c$ are the critical parameter values and systems with δ_1 or δ_2 larger than ${\delta_1}^c$ or ${\delta_2}^c$s will consist of at least one hyperbolic-trigonometric eigenvector. Three system parameters variables, r_{12}, $Bi_m + \frac{Pe_1}{2}$ and $\frac{D_1}{D_2}$, impact the bounding parameter values ${\delta_1}^c$ and ${\delta_2}^c$ through equation (3.34) and (3.35). The presence or absence of hyperbolic-trigonometric eigenvectors is summarized in Figure 3.6.

$${f_1}^{\delta}\left(\delta_1, r_{12}, \frac{D_1}{D_2}\right) = D_1 \frac{1}{r_{12}} - D_2 \delta_1 \frac{1}{\tan(\delta_1(r_{12}-1))} \tag{3.32}$$

$${f_2}^{\delta}\left(\delta_2, r_{12}, \frac{D_1}{D_2}\right) = D_1 \delta_2 \frac{1}{\tan(\delta_2 r_{12})} - D_2 \frac{1}{r_{12}-1} \tag{3.33}$$

Where $\delta_1 = \sqrt{\frac{D_1 R_2}{D_2 R_1}\gamma_1 - \gamma_2}$ and $\delta_2 = \sqrt{\frac{D_2 R_1}{D_1 R_2}\gamma_2 - \gamma_1}$

$${f_1}^{\delta}({\delta_1}^c) = 0 \quad : \quad {\delta_1}^c \cot\left({\delta_1}^c(r_{12}-1)\right) = \frac{D_1}{D_2}\frac{1}{r_{12}} \tag{3.34}$$

$${f_2}^{\delta}({\delta_2}^c) = 0 \quad : \quad {\delta_2}^c \cot({\delta_1}^c r_{12}) = \frac{D_2}{D_1}\frac{1}{1-r_{12}} \tag{3.35}$$

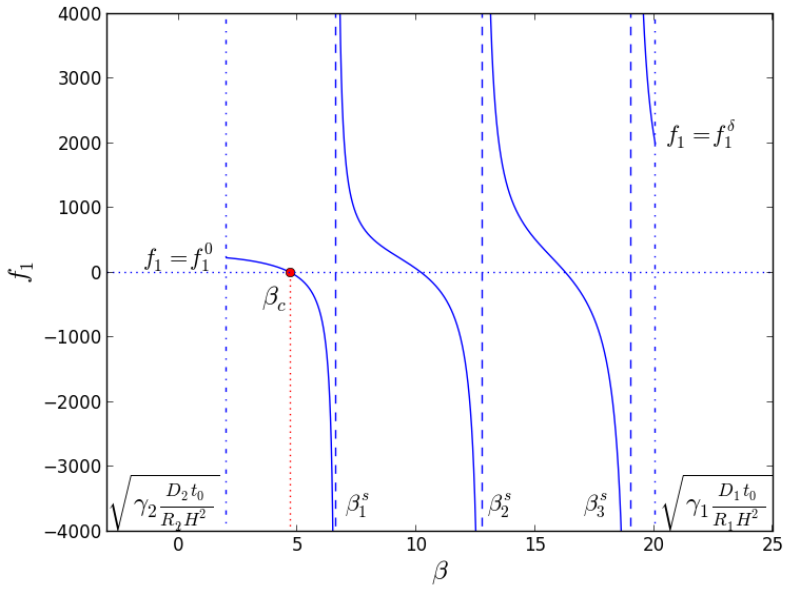

(a)

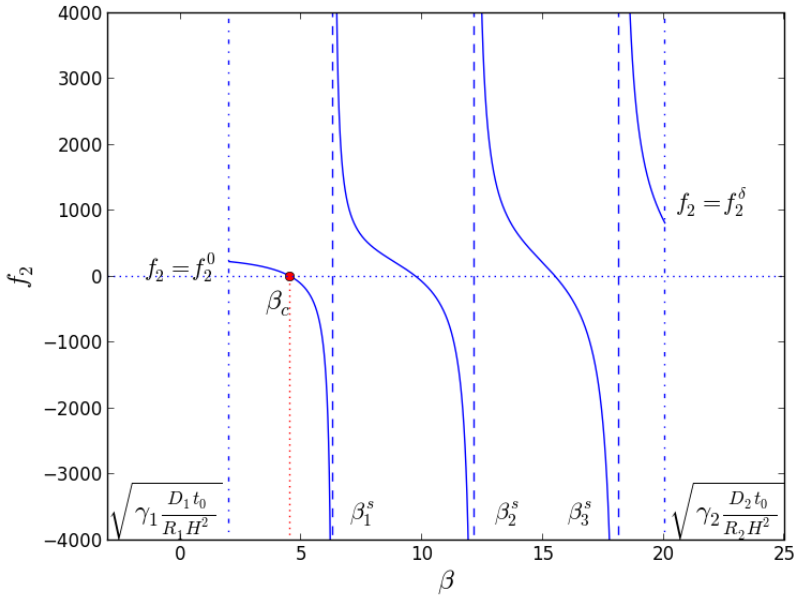

(b)

Figure 3.5: The boundary function f_1 and f_2 versus eigenvalue β shown in equation (20)

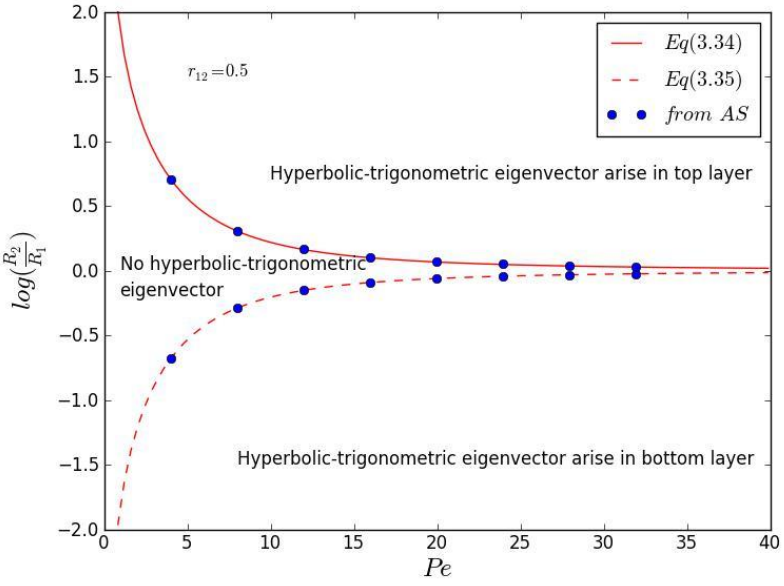

(a) r_{12} =0.5

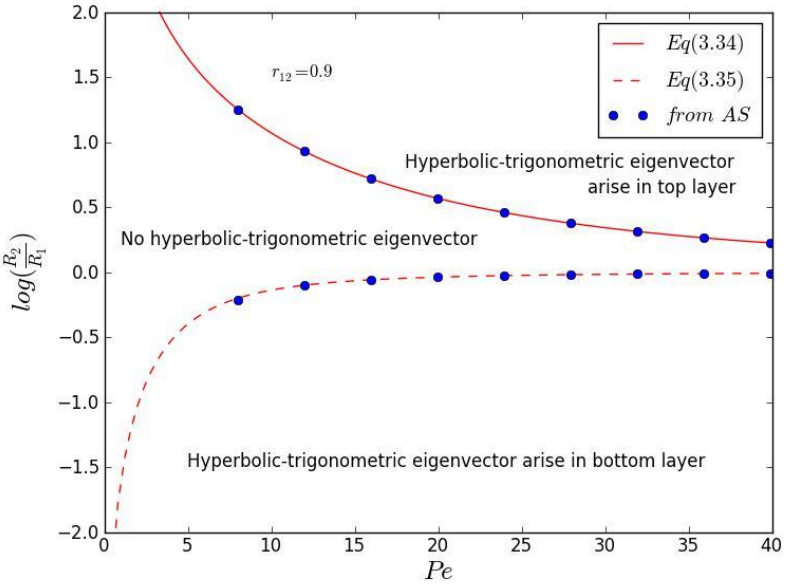

(b) r_{12} =0.9

Figure 3.6: Bounding Peclet number and ratio of retardation factors for existence of hyperbolic eigenfunctions in a two layer problem

Figure 3.6 illustrates the existence of hyperbolic-trigonometric eigenvectors in the series solution for a two-layer non-reactive system with uniform diffusivities ($\frac{D_1}{D_2} = 1$). The solid and dashed curves represent the solution of equation (3.34) and (3.35) with layer thickness ratio r_{12} and the solid dots are results derived by direct tests on systems with various parameters through analytical solution (3.28). The x-axis and y-axis variables are Peclet number and ratio of retardation factors respectively, which contributes to the critical parameter values ${\delta_1}^c$ and ${\delta_2}^c$ as: ${\delta_1}^c = \frac{Pe}{2}\sqrt{\frac{R_2}{R_1} - 1}$ and ${\delta_2}^c = \frac{Pe}{2}\sqrt{\frac{R_1}{R_2} - 1}$. The left-middle region corresponds to the systems that can be solved without consideration of hyperbolic-trigonometric eigenvectors and it is this region that the solution of Li and Cleall (2011) is limited (Figure 3.7(a)). The top right and below right regions correspond to systems exhibiting hyperbolic functions in top or bottom layer respectively. A general trend here is that a larger advective velocity or difference in retardation factors between two layers will tend to lead to hyperbolic-trigonometric eigenvectors.

Figure 3.7(a) shows the existence conditions for the hyperbolic functions for the two–layer system illustrated in Li and Cleall (2011). For the parameters employed in the paper, no hyperbolic eigenfunction arise and Li and Cleall's solution is valid. For other parameter values, for example, somewhat larger retardation (sorption) differences between layers, even small advection will cause Li and Cleall (2011) solution to fail.

Figure 3.7(b) shows the failure of Li's solution with the relatively modest change in retardation by a factor of 10 between layers.

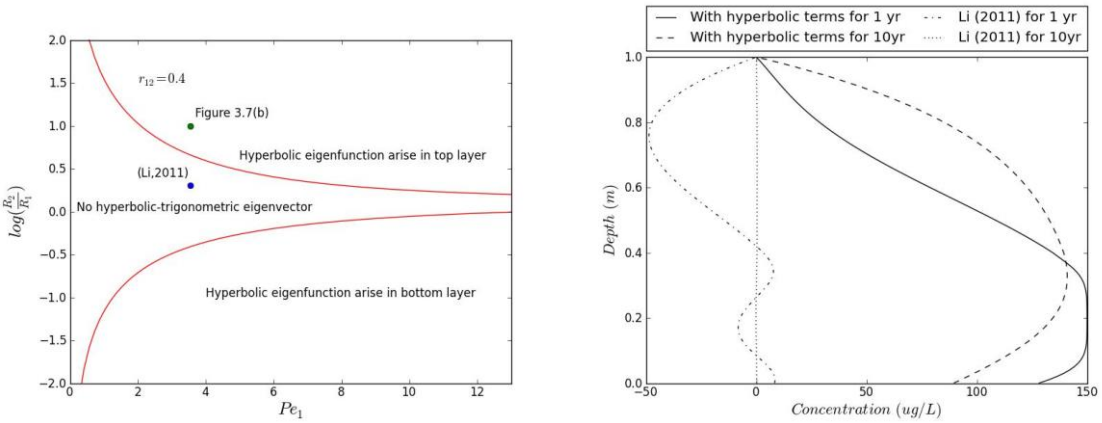

(a) (b)

Figure 3.7: Existence condition for hyperbolic–trigonometric eigenvectors with parameters given by Li and Cleall (2011)

3.5.2 Comparison with the existing analytical solution and numerical solution

Table 3.7 compares the results got from our analytical solution to the results derived by GITT methods (Liu 1998) and numerical Laplace inversion method (Leij and Genuchten 1995). LT is from the inverse Laplace transform method; GITT is the solution from GITT with first 60 terms and AS is the solution present here with first 20 terms in the series solution given by equation (3.28). Root mean square differences (RMSD) are equivalent between the methods as compared to the inverse Laplace transform method. Note that the GITT method would require approximately $O(60)^3$ operations by direct

elimination whereas the banded matrices in the analytical solution presented here would require of order O(20) operations.

Table 3.8 compares the results of Figure 3.3 got from the analytical solution to the results derived by numerical method (Lampert and Reible, 2014). Root mean square differences (RMSD) are derived by comparing results from the 20-term analytical solution presented herein (AS) to the numerical solution with an equivalent computational expense (NME). The reference in both cases is to a small timestep, high resolution numerical simulation with high computational expense (Ref). The computational expenses for simulation results are estimated based on the average CPU time for 20 runs.

$U = 10\text{cm/d}$; $D_1 = 20\text{cm}^2/\text{d}$; $D_2 = 5\text{cm}^2/\text{d}$; $\varepsilon_1 = 0.4$; $\varepsilon_2 = 0.25$; $R_1 = 0.4$; $R_2 = 0.25$												
	$t = 0.2\text{d}$			$t = 0.4\text{ d}$			$t = 0.6\text{d}$			$t = 0.8\text{d}$		
x(cm)	Ref	GITT	AS	Ref	GITT	AS	Ref	GITT	AS	Ref	GITT	AS
0	0.884	0.884	0.884	0.963	0.963	0.963	0.987	0.987	0.987	0.995	0.995	0.995
2	0.742	0.742	0.742	0.915	0.915	0.915	0.969	0.969	0.969	0.988	0.988	0.988
4	0.561	0.561	0.561	0.841	0.841	0.841	0.940	0.940	0.940	0.977	0.977	0.977
6	0.374	0.374	0.374	0.746	0.746	0.746	0.901	0.901	0.901	0.962	0.962	0.962
8	0.222	0.222	0.222	0.645	0.644	0.645	0.858	0.858	0.858	0.945	0.945	0.945
10	0.142	0.144	0.142	0.579	0.582	0.579	0.829	0.830	0.829	0.933	0.934	0.933
12	0.063	0.064	0.063	0.480	0.481	0.480	0.781	0.782	0.781	0.914	0.914	0.914
14	0.021	0.02	0.021	0.372	0.372	0.372	0.722	0.722	0.722	0.889	0.889	0.889
16	0.005	0.005	0.005	0.265	0.265	0.264	0.651	0.651	0.651	0.858	0.858	0.858
18	0.001	0.001	0.001	0.169	0.169	0.168	0.567	0.567	0.567	0.819	0.819	0.819
20	0.000	0.000	0.000	0.094	0.094	0.094	0.473	0.473	0.473	0.770	0.770	0.770
RMSD	-	7×10^{-4}	3×10^{-4}	-	1×10^{-3}	4×10^{-4}	-	4×10^{-4}	$<3\times10^{-4}$	-	3×10^{-4}	$<3\times10^{-4}$

(a)

(Table 3.7 continued next page)

$U = 10cm/d$; $D_1 = 8cm^2/d$; $D_2 = 10cm^2/d$; $\varepsilon_1 = 0.4$; $\varepsilon_2 = 0.25$; $R_1 = 0.4$; $R_2 = 0.25$												
	t = 0.2d			t = 0.4 d			t = 0.6d			t = 0.8d		
x(cm)	Ref	GITT	AS	Ref	GITT	AS	Ref	GITT	AS	Ref	GITT	AS
0	0.978	0.977	0.978	0.998	0.998	0.998	1.000	1.000	1.000	1.000	1.000	1.000
2	0.868	0.867	0.868	0.984	0.984	0.984	0.998	0.998	0.998	1.000	1.000	1.000
4	0.634	0.653	0.634	0.942	0.942	0.942	0.991	0.991	0.991	0.999	0.998	0.999
6	0.345	0.345	0.345	0.849	0.848	0.849	0.972	0.972	0.972	0.995	0.995	0.995
8	0.131	0.131	0.131	0.693	0.693	0.693	0.930	0.929	0.930	0.986	0.986	0.986
10	0.033	0.033	0.033	0.496	0.496	0.496	0.853	0.853	0.853	0.966	0.966	0.966
12	0.011	0.011	0.011	0.370	0.370	0.370	0.784	0.783	0.784	0.944	0.944	0.944
14	0.003	0.003	0.003	0.257	0.258	0.257	0.699	0.698	0.699	0.913	0.913	0.913
16	0.001	0.001	0.001	0.166	0.166	0.166	0.601	0.601	0.601	0.871	0.871	0.871
18	0.000	0.000	0.000	0.098	0.099	0.098	0.498	0.498	0.498	0.817	0.817	0.817
20	0.000	0.000	0.000	0.054	0.054	0.054	0.395	0.395	0.395	0.751	0.750	0.751
RMSD	-	5×10^{-4}	$<3\times10^{-4}$	-	5×10^{-3}	$<3\times10^{-4}$	-	5×10^{-4}	$<3\times10^{-4}$	-	4×10^{-4}	$<3\times10^{-4}$

(b)

$U = 10cm/d$; $D_1 = 5cm^2/d$; $D_2 = 20cm^2/d$; $\varepsilon_1 = 0.25$; $\varepsilon_2 = 0.4$; $R_1 = 0.25$; $R_2 = 0.25$												
	t = 0.2d			t = 0.4 d			t = 0.6d			t = 0.8d		
x(cm)	Ref	GITT	AS	Ref	GITT	AS	Ref	GITT	AS	Ref	GITT	AS
0	0.999	0.999	0.999	1.000	1.000	1.000	1.000	1.000	1.000	1.000	1.000	1.000
2	0.988	0.987	0.988	1.000	1.000	1.000	1.000	1.000	1.000	1.000	1.000	1.000
4	0.928	0.928	0.928	0.999	0.999	0.999	1.000	1.000	1.000	1.000	1.000	1.000
6	0.764	0.763	0.764	0.995	0.996	0.995	1.000	1.000	1.000	1.000	1.000	1.000
8	0.496	0.495	0.496	0.976	0.977	0.976	0.998	0.999	0.998	0.999	1.000	0.999
10	0.152	0.152	0.152	0.780	0.779	0.780	0.939	0.94	0.940	0.979	0.979	0.979
12	0.049	0.05	0.049	0.600	0.600	0.600	0.870	0.871	0.870	0.952	0.953	0.952
14	0.013	0.013	0.013	0.417	0.418	0.418	0.773	0.773	0.773	0.911	0.911	0.911
16	0.003	0.003	0.003	0.262	0.262	0.262	0.653	0.653	0.653	0.851	0.852	0.851
18	0.000	0.000	0.000	0.148	0.148	0.148	0.522	0.522	0.522	0.774	0.774	0.774
20	0.000	0.000	0.000	0.075	0.075	0.075	0.393	0.393	0.393	0.681	0.681	0.681
RMSD	-	6×10^{-4}	$<3\times10^{-4}$	-	6×10^{-3}	3×10^{-4}	-	5×10^{-4}	3×10^{-4}	-	5×10^{-4}	$<3\times10^{-4}$

(c)

Table 3.7: Dimensionless solute concentration in a two-layer porous medium and mean differences with the reference (Ref) approach of numerical Laplace inversion approach of Leij and Genuchten (1995)

	t = 200yr			t = 600yr			t = 1000yr		
x(cm)	Ref	AS	NME	Ref	AS	NME	Ref	AS	NME
0	1.000	1.000	1.000	1.000	1.000	1.000	1.000	1.000	1.000
2	0.897	0.897	0.899	0.967	0.967	0.968	0.960	0.960	0.960
4	0.671	0.672	0.678	0.896	0.896	0.900	0.871	0.873	0.874
6	0.338	0.338	0.352	0.754	0.753	0.762	0.739	0.743	0.745
8	0.333	0.334	0.348	0.567	0.567	0.581	0.733	0.736	0.738
10	0.326	0.326	0.340	0.377	0.377	0.393	0.718	0.721	0.724
12	0.311	0.311	0.324	0.220	0.220	0.234	0.687	0.690	0.693
14	0.279	0.280	0.292	0.119	0.119	0.130	0.619	0.622	0.624
16	0.218	0.218	0.227	0.082	0.082	0.090	0.484	0.486	0.488
18	0.137	0.137	0.143	0.051	0.052	0.056	0.304	0.306	0.307
20	0.000	0.000	0.000	0.000	0.000	0.000	0.000	0.000	0.000
RMSD	-	4×10^{-4}	1×10^{-2}	-	2×10^{-4}	9×10^{-3}	-	2×10^{-3}	4×10^{-3}

(a) Capping with separated thin sorbent layers

	t = 200yr			t = 600yr			t = 1000yr		
x(cm)	Ref	AS	NME	Ref	AS	NME	Ref	AS	NME
0	1.000	1.000	1.000	1.000	1.000	1.000	1.000	1.000	1.000
2	0.994	0.994	0.994	0.984	0.984	0.984	0.998	0.998	0.998
4	0.979	0.979	0.980	0.948	0.950	0.950	0.994	0.994	0.994
6	0.950	0.950	0.951	0.895	0.898	0.897	0.985	0.985	0.985
8	0.904	0.904	0.906	0.887	0.890	0.890	0.968	0.968	0.969
10	0.840	0.839	0.843	0.871	0.873	0.873	0.940	0.940	0.941
12	0.756	0.756	0.760	0.834	0.836	0.836	0.890	0.889	0.891
14	0.648	0.647	0.653	0.751	0.753	0.753	0.795	0.794	0.796
16	0.501	0.501	0.505	0.587	0.588	0.589	0.620	0.619	0.621
18	0.315	0.315	0.318	0.369	0.370	0.370	0.390	0.390	0.391
20	0.000	0.000	0.000	0.000	0.000	0.000	0.000	0.000	0.000
RMSD	-	2×10^{-4}	3×10^{-3}	-	2×10^{-3}	2×10^{-3}	-	2×10^{-4}	6×10^{-4}

(b) Capping with mixing sorbent layer

Table 3.8: Comparison of solute concentration with separated thin sorbent layers (a) and mixed sorbent layers (b) by the analytical solution and numerical solution with equivalent computation expense (NME). Both are referenced to a high spatial and time resolution numerical simulation with high computational expense (Ref, Lampert and Reible [2014])

3.5.3 Solution limits

The proposed analytical solution has no limitations associated with the number of layers or the properties of those layers. It is difficult to determine eigenvalues with the proposed analytical solution at very high Pe (of O(100) or greater) due to their proximity

but this is not a fundamental flaw but instead associated with the limitations of finite precision arithmetic in any computational scheme. Some convenient tools for analysis of the analytical solution (e.g. Excel) have fixed precision which may limit the magnitude of Pe for which accurate results can be obtained.

3.5.4 CapAn

A spreadsheet model CapAn was developed based on the presented innovative analytical solution (Appendix B). The current version of CapAn is available in Microsoft Excel spreadsheet with a programmed macro written in Visual Basic for Applications (VBA). The input parameters and output results are also generated by a VBA macro. CapAn is also available in python version for accuracy and computational speed.

3.6 CONCLUSIONS

A closed–form analytical solution for one–dimensional advective–dispersive solute equation with first–order reaction and linear sorption in multilayered finite porous media was developed. An arbitrary number of layers and transport parameter values in each layer can be addressed by the analytical solution. The analytical solution was verified by comparing the results with numerical solutions based on a finite difference method as well as an existing solution developed by the slower converging GITT method.

The solution presented in this paper overcomes the severe limitations of Li and Cleall (2011) by introducing the hyperbolic eigenfunctions. The solution also converges more quickly and requires a simpler coefficient determination than the GITT method.

3.7 REFERENCES

Chen, J. S., Lai, K. H., Liu, C. W., & Ni, C. F.: A novel method for analytically solving multi–species advective–dispersive transport equations sequentially coupled with first–order decay reactions. Journal of Hydrology, 420, 191–204 (2012)

Guerrero, J. P., Pimentel, L. C. G., Skaggs, T. H., van Genuchten, M. T.: Analytical solution of the advection–diffusion transport equation using a change–of–variable and integral transform technique. International Journal of Heat and Mass Transfer, 52(13), 3297–3304 (2009)

Guerrero, J. P., Skaggs, T. H.: Analytical solution for one–dimensional advection–dispersion transport equation with distance–dependent coefficients. Journal of hydrology, 390(1), 57–65 (2010)

Guerrero, J. P., Pimentel, L. C. G., Skaggs, T. H.: Analytical solution for the advection–dispersion transport equation in layered media. International Journal of Heat and Mass Transfer, 56(1–2), 274–282 (2013)

Kumar, A., Jaiswal, D. K., & Kumar, N.: Analytical solutions to one–dimensional advection–diffusion equation with variable coefficients in semi–infinite media. Journal of Hydrology, 380(3), 330–337 (2010)

Kumar, A., Jaiswal, D. K., & Kumar, N.: One–dimensional solute dispersion along unsteady flow through a heterogeneous medium, dispersion being proportional to the square of velocity. Hydrological Sciences Journal, 57(6), 1223–1230 (2012)

Li, Y. C., Cleall, P. J.: Analytical solutions for advective–dispersive solute transport in double-layered finite porous media. International Journal for Numerical and Analytical Methods in Geomechanics, 35(4), 438–460 (2011)

Liu, C., Ball, W. P., Ellis, J. H.: An analytical solution to the one–dimensional solute advection–dispersion equation in multilayer porous media. Transport in porous media, 30(1), 25–43 (1998)

Liu, G., Si, B. C.: Analytical modeling of one–dimensional diffusion in layered systems with position–dependent diffusion coefficients. Advances in Water Resources, 31(2), 251–268 (2008)

Leij, F. J., Van Genuchten, M. T.: Approximate analytical solutions for solute transport in two–layer porous media. Transport in Porous Media, 18(1), 65–85 (1995)

Milkhailov, M. D. and N. L. Vulchanov."Computational procedure for Sturm–Liouville problems." Journal of Computational Physics 50(3): 323–336. (1983)

Moler, C. and C. Van Loan. "Nineteen dubious ways to compute the exponential of a matrix, twenty–five years later." SIAM review 45(1): 3–49. (2003)

Reible, D. D., and Lampert, D.J., Capping for Remediation of Contaminated Sediments, Chapter 12 in., Processes, Assessment and Remediation of Contaminated Sediments, D.D. Reible, Ed., Springer. (2014)

Van Genuchten, M. T., Alves, W. J.: Analytical solutions of the one–dimensional convective–dispersive solute transport equation. United States. Dept. of Agriculture. Technical bulletin (1982)

Wittrick, W. H. and F. Williams. "A general algorithm for computing natural frequencies of elastic structures." The Quarterly Journal of Mechanics and Applied Mathematics 24(3): 263–284. (1971)

Chapter 4 CapSim – a numerical modeling tool for evaluation of capping of contaminated sediment and sediment remedial design

4.1 INTRODUCTION

Aquatic sediment is solid matter that accumulates on the bottom of a water body. The high carbon content sediment performs a strong sorption capability to the environmental emerging contaminants, particularly hydrophobic organic compounds (HOC) and heavy metals (U.S.EPA, 1998). Since the removal of original contaminant sources, the sediments that once served as sinks now become a primary source of the contaminants to the water body and the benthic ecosystem.

For the remediation of contaminated sediments, one of the few economic alternatives with proven records of success is in-situ management, which includes monitored natural recovery (MNR), in-situ treatment, typically with sorbents, and in-situ capping. MNR is a remedy that uses known naturally occurring processes to contain, eliminate or reduce the bioavailability and toxicity of contaminants in sediment. In-situ capping refers to the placement of a subaqueous covering capping layer of clean material over contaminated sediment that remains in place. The capping layer is constructed of clean sediment, sand or gravels (Wang et al., 1991; Thoma et al., 1993) and active materials such as organoclay or activated carbon to handle sediment with more serious contamination (McDonough et al., 2007; Zimmerman, 2004; Murphy et al., 2006; Reible

et al., 2006; Jacobs et al., 1999). In-situ treatment employs these active materials as a direct amendment to the sediment without a capping layer.

The evaluation and the design of remediation approaches need a model to predict the behavior of contaminants in the sediment system and connect the remediation performance to the design parameters. The behavior of the contaminants in the sediment or in a capped sediment are essentially described by the chemical migration model in porous media (Bear, 1972), then expanded further to numerous studies solving the transport in solid containment layers with various layer properties and boundary conditions (Rowe and Booker, 1985; Rubin and Rabideau, 2000; Malusis and Shackelford, 2002; Lampert and Reible, 2009). The analytical models for such containment system with multiple layers with various properties are also available (van Genuchten, 1982, Liu et al. 1998; van Genuchten, 2003; Li and Cleall, 2011; Shen and Reible 2015).

The sediment system differs from the classic layered porous media system in several important aspects. Within the top a few centimeters from the benthic surface of the sediments, the activities of benthic organism leads to the formation of the bioturbation layer, where the physical and chemical characteristics, such as organic carbon content and redox conditions are significantly different from the underlying sediment. Furthermore, the burrowing and dredging activities of these organisms may accelerate the local transport process by mixing both the porewater and the solid materials. Besides bioturbation, the sediment may increase due to deposition of additional sediment or decrease due to the erosion. Finally, the mass transport across the sediment-water

interface requires more comprehensive boundary conditions than the classic boundary condition types due to the presence of turbulent motions in the overlying water bodies and the potential for mixing and dilution by the overlying water. Regarding these specific processes in sediments, several specific models are developed. Thoma et al. (1993) presented several models for evaluating the effects of sediment capping on contaminant concentrations and fluxes. Palermo et al. (1998) provided guidance for modeling of contaminant transport in sediments. In the most recent study, Lampert et al. (2009) presented an analytical modeling approach for the assessment of the concentration within a surface layer (e.g., a cap layer) and a deeper layer of sediment. However, none of these models provides a full picture of the impacts from the dynamic sorption/desorption, redox reactions, bioturbation, oscillated advection and deposition to the fate and transport of contaminants.

This chapter presents an innovative numerical model (CapSim 3), which focuses on simulating the contaminant processes in sediment environment for design and predicting performance of in-situ remediation. The model includes the dynamics of multiple chemical species with linked linear or nonlinear reactions and dynamic sorption/desorption between the solute chemical and the sediments and amendment materials. Sorption and reaction dynamics are not meant to be predicted on the basis of first principles but instead employs empirical rate constants (e.g. first order sorption rates) to describe the kinetic processes in an advective/diffusive environment. The model also includes the impacts of the bioturbation and deposition. The model provides a reliable prediction of the contaminant behavior and can be used as a reference in in-situ

sediment remediation design including natural recovery, capping and in-situ treatment with sorbents.

The goal of the modeling effort is not a predictive model but a simulation tool that can be routinely used for design and estimation of long-term fate and transport behavior using largely empirical estimates of key processes. The model is designed to simulate behavior at the sediment-water interface with a relatively simple interface and with minimal overhead to make it easier for practitioners to employ the model. General purpose commercial modeling packages (e.g. Comsol Multiphysics) could be used to solve the equations describing the sediment-water interface but require far more user knowledge and expertise to tailor the modeling to the specific conditions of the sediment-water interface.

4.2 MODELING APPROACH

4.2.1 Conceptual model

The sediment and any potential cap or treatment layers are considered as a one-dimensional system consists of multiple vertical layers that have various physical and chemical properties. The top and the bottom of the stratified system are in contact with the overlying water body and the underlying sediment, respectively. Each layer is considered as a 1-D porous media system with porewater as the mobile phase and the solid particles as the immobile frame except a bioturbation layer near the surface in which both solid particles and porewater can move. Dissolved organic carbon (DOC), which is large organic molecules or small particles, is treated as a third phase besides the water and the sediment solids – it can associate with hydrophobic organics and contribute

to the total porewater burden of these contaminants. The contaminants distribute to all three phases and transport within the layer and across the interface between layers.

The local distribution of the chemicals in the porewater, DOC, and solid matrices is described by either the thermodynamic equilibrium isotherms or kinetic sorption/desorption models. The equilibrium isotherms, which assumes the solid/DOC concentration as an explicit function of the porewater concentrations (4.1), is used to model fast sorption/desorption processes between the chemicals and solids. For slow sorption/desorption processes that are kinetically limited, the kinetic sorption/desorption models are applied as shown in (4.2). The concentrations in porewater and the solid are independent and controlled by the coupled sorption/desorption process.

$$\text{Fast equilibrium partitioning:} \quad q = f_{equi}(C) \tag{4.1}$$

$$\text{Transient sorption:} \quad \frac{dq}{dt} = f_{sorp}(C, q);\ \frac{dC}{dt} = f_{desorp}(C, q) \tag{4.2}$$

The transport processes within and across layers include advection, diffusion, hydrodynamic dispersion, and bioturbation. Diffusion comes from the random molecular motions, which is sensitive to the molecular weight of the compound. The diffusion rate of DOC and the DOC associated contaminants are neglected due to its high molecular weight comparing to the free molecules contaminants. The advection together with the hydrodynamic dispersion describes the transport of contaminants forced externally by the groundwater flow. The advection term describes the transport by the average

macroscopic scale flow and the hydrodynamic dispersion term represents the mixing process caused by the random microscopic scale flows, which comes from the heterogeneity of the local flow paths in sediments and caps. The macroscopic groundwater upwelling flow is impacted by consolidation of the sediments as well as periodic flow associated with tides or storms. Bioturbation, comes from the activities of the benthic organisms near the benthic surface (5-15cm), causing mixing of both the porewater and the solids.

Transport process	Dissolved	DOC associated	Solid Associated
Diffusion	✓	✗	✗
Hydrodynamic dispersion	✓	✓	✗
Advection	✓	✓	✗
Bioturbation	✓	✓	✓
Reaction	✓	✗	✗

Table 4.1: Summary of fate and transport processes for various forms of contaminants

Reactions between solute chemicals are usually included for the redox-sensitive contaminants that could interact with the ambient redox species. Such chemicals include mercury, arsenic and other possible heavy metal ions or complexes. The discovered long-term decay process of some organic contaminant can be modeled as first-order decay reactions.

Deposition is the process in which the solid particles in the overlying water added to the top of the existing sediment or capping layers. The deposition layer normally consists of clean sediment and serves as a ‘natural’ capping layer – it separates the

overlying water body from the contaminated sediments and reduces the transport rate of contaminants to the overlying water body. Meanwhile, the downward transport of oxygen is reduced and the bioturbation dominate mixing zone as well as anaerobic zone may show a shift up. In systems where a strong bioturbation force presents, the deposited sediment might be mixed with the top layer materials within the bioturbation zone and further affect the chemical behavior.

4.2.2 Mass conservative equations and auxiliary conditions

4.2.2.1 Mass conservative equations

Equation (4.3) is the mass conservation equation for a one-dimensional multi-layered multi-species porous media system combining all the fate and transport processes discussed.

$$\sum_m \left(\varepsilon_m \frac{\partial \phi_m C_n}{\partial t} + \varepsilon_m \frac{\partial \phi_m \rho_{DOC,i} q_{DOC,n}}{\partial t} + \rho_{b,m} \frac{\partial \phi_m q_{m,n}}{\partial t}\right) = -\frac{\partial F_{n,i}}{\partial z} + \varepsilon_i \sum_l a_{l,n} rxn_{l,i} \quad (4.3)$$

$$F_{n,i} = -D_{n,i} \frac{\partial C_n}{\partial z} - \alpha_i U \frac{\partial (C_n + \rho_{DOC,i} q_{DOC,n})}{\partial z} + U\left(C_n + \rho_{DOC,i} q_{DOC,n}\right) + F_{bio,n} \quad (4.4)$$

$$F_{bio,n} = -D_{bio,p} \sum_m \rho_{b,m} \frac{\partial \phi_m q_{m,n}}{\partial z} - D_{bio,pw} \frac{\partial (C_n + \rho_{DOC,i} q_{DOC,n})}{\partial z} \quad (4.5)$$

$$\frac{\partial \phi_m}{\partial t} = D_{bio,p} \frac{\partial^2 \phi_m}{\partial z^2} \quad (4.6)$$

The four subscripts here, i, n, m and l, indicate the indices of layers, the solute chemicals, the solid materials and the reaction, respectively. C_n, $q_{m,n}$, $q_{DOC,n}$ are the n-th contaminant concentrations in porewater, m-th solid matrix material and DOC. ϕ_m is the volumetric fraction of m-th solid material. $D_{n,i}$, α_i, $D_{bio,pw}$, $D_{bio,p}$ and U are effective

molecular diffusion coefficients, hydrodynamic dispersion coefficients, porewater biodiffusion coefficients, solid particle biodiffusion coefficients and the upwelling groundwater Darcy velocity, respectively. The sum $\sum_l a_{l,n} rxn_{l,i}$ represents the total mass or moles of the n-th chemical generated or consumed by reactions. $rxn_{l,i}$ is the reaction rate of the l-th reaction in the i-th layer and $a_{l,n}$ is the stoichiometric coefficient of the n-th chemical in the l-th reaction. ε_m and $\rho_{b,m}$ are the porosities and bulk density of the m-th material. The properties of solid mixtures in the system are assumed to be the sums of the individual solid components properties by their volumetric fractions. This assumption is valid when the particles sizes of the mixture components are similar. The competition between sorption processes is neglected here and the total solid mass is the sum of the contaminant mass in various material components.

The correlation between the individual solid and DOC concentrations $q_{m,n}$ and $q_{DOC,n}$ are explained by equilibrium isotherms or the kinetic constitutional differential equations. In sediment, the time scale of transport process is normally much longer than the time required for the local reversible sorption/desorption reactions. A local equilibrium could be assumed to be achieved at all time and the solid phase concentrations of n-th chemical in m-th solid material $q_{m,n}$ can be expressed as an explicit function of pore water concentrations C_n using appropriate sorption isotherms in Table 4.2.

However, a series of studies suggests that the sorption/desorption of some organic compounds, such as HOCs could be slow and the local equilibrium assumption is not

valid (Wu, 1986; Brusseau, 1991; Pignatello, 1995; Lick, 1996). The one-compartment model with a sorption kinetic coefficient $k_{sorp,m,n}$, is employed here to take advantage of typical empirically-based design approaches. The data to support the sorption kinetic coefficients for a pure material comes from simple kinetic measurements from the half-equilibrium time $t_{0.5}$ from the batch sorption experiments. $t_{0.5}$ is defined as the time when the porewater concentration in the experiment drops to the half way between the initial concentration and the equilibrium concentration. Though not provided directly, the popular multi-compartment sorption model can be simulated by separating a solid material to a mixture of various compartments consisting various kinetic sorption properties.

$$k_{sorp} = \frac{0.693}{t_{0.5}\left(1+\frac{\varepsilon}{\rho_b K_d}\right)} \tag{4.7}$$

In porous media, the water diffusion coefficients in sediment need to be corrected for the tortuosity and porosity of the diffusion pathway. CapSim includes two models of tortuosity. Millington and Quirk (1961) suggest a combined correction factor of the porosity to the four-thirds power and Boudreau (1997) proposes an alternative correction that may be more applicable to fine-grained sediments.

Hydrodynamic dispersion is a result of the averaging on a macroscopic scale of the microscopic variations in the media, the hydrodynamic dispersion coefficient α_i is often claimed to be dependent on the length scale of the system. In general, the value of α_i shall be determined empirically through a tracer study. For a uniform material such as sand, the flow may be close to ideal and dispersion coefficient may be similar in

magnitude to the particle diameter. In the absence of site-specific information, a conservative estimate would be to scale the dispersion coefficient with the cap thickness, such as 10 % of the cap thickness. (Clarke et al., 1993)

Sorption process	Equilibrium ($q_{m,n}$)	Kinetic sorption ($\rho_{b,m}\frac{\partial \phi_m q_{m,n}}{\partial t}$)
Linear	$K_{d.m,n}C_n$	$\phi_m \varepsilon_m k_{sorp,m,n}(C_n - \frac{1}{K_{d,m,n}} q_{m,n})$
Langmuir	$\frac{q_{max.m,n} b_{m,n} C_n}{1+b_{m,n}C_n}$	$\phi_m k_{sorp,m,n}\left(C_n(q_{max,m,n} - q_{m,n}) - \frac{1}{b_{m,n}} q_{m,n}\right)$
Freundlich	$K_{F,m,n}C_n^{N_{F,m,n}}$	$\phi_m \varepsilon_{i,m} k_{sorp,m,n}\left(C_n - \left(\frac{1}{K_{F,m,n}} q_{m,n}\right)^{\frac{1}{N_{F,m,n}}}\right)$

(a) The equilibrium/transient sorption/desorption model

	Millington and Quirk	Boudreau
Effective diffusivity	$D_{n,i} = \varepsilon_i^{4/3} D_{w,n}$	$D_{n,i} = \frac{\varepsilon_i D_w}{1-\ln(\varepsilon_i^2)}$

(b) The effective diffusion coefficient using two tortuosity correction models

Table 4.2: Constitutional equations for the parameters and coefficients in the conservation equation

The bioturbation, the mixing process from benthic organism activities, is commonly characterized as an expected depth and mixing intensity. One common modeling approach is to assume the mixing process is random and the bioturbation flux is a Fickian diffusion process for both the free molecular and the solid-associated contaminant. The bioturbation coefficients and the depth either can be derived using traditional approaches (Thoms et al., 1995) or estimated by comparing the simulated solid fraction distributions to the field measurement. Beyond the traditional approaches, a depth-dependent Gaussian function correction is provided to model the biodiffusion coefficient (4.8). σ is the Gaussian RMS width that represents the depth where the

bioturbation strength drops to 60% of maximum. With such correction, the bioturbation in model is forced to weaken with distance from the benthic interface and should be more representative to the natural environment.

$$D_{bio,p} = D_{bio,p,0} * \exp\left(-\frac{z^2}{2\sigma^2}\right);\ D_{bio,pw} = D_{bio,pw,0} * \exp\left(-\frac{z^2}{2\sigma^2}\right) \quad (4.8)$$

The corrected Darcy velocity U describes the advection terms in the sediment system, which combines the flows forced by the upwelling groundwater, consolidation, and other periodically discharging flow, such as tides or storms. Consolidation is a process by which sediment decrease in volume in response to the pressure from the overlying cap placement. The degree of potential consolidation should be evaluated based on consolidation testing procedures. The thickness of the contaminated sediment layer and the physical properties of the sediment underlying this layer need to be determined to assess potential consolidation of the sediment due to the cap loading. For simplicity, the consolidation impact is modeled as an extra groundwater upwelling flow with the flow rate decreases exponentially versus time. The 'decay rate coefficient' k_{con} can be calculated by the 90% consolidation time t_{90}, which indicates the time required for the consolidation velocity to drop to 10% of the initial value $V_{con,0}$. Periodic groundwater flow velocity is modeled as a sinusoid function versus time. V_{max} is the maximum velocity and t_c is the period for a full tidal cycle or other periodic flow (Moore, 1999; Moore et al., 2002; Taniguchi, 2002).

$$U = V_{Darcy} + V_{con,0}e^{-k_{con}t} + V_{oscillation} * \sin(2\pi\, t/t_c) \quad (4.9)$$

4.2.2.2 Boundary conditions

At the interface of two layers, the porewater concentrations C_n and the fluxes $F_{n,i}$ are matched for the mass continuity. The solid material fractions ϕ_m and the contaminant solid concentrations $q_{m,n,i}$ are discontinuous for the immobility of solid particles except in the cases with bioturbation, where the benthic organism activities mix the solid materials as well as porewater. In such cases, the matching flux will involve in the solid transport term (4.5) along with the regular terms in Equation (4.4).

$$C_n\,|_{z=h_{i,i+1}+} = C_n\,|_{z=h_{i,i+1}-} \tag{4.10}$$

$$\left(F_{diff,n} + F_{disp,n} + F_{bio,n} + F_{adv,n}\right)\big|_{z=h_{I,i+1}+} = \left(F_{diff,n} + F_{disp,n} + F_{bio,n} + F_{adv,n}\right)\big|_{z=h_{i,i+1}-} \tag{4.11}$$

The top boundary between the system and the overlying water body are described by the boundary layer theory that the flux across the boundary is a function of the difference between the surface porewater concentration and the overlying water concentration (Boudreau and Jorgensen 2001).

$$k_{bl,n}\left(C_{0,n} - C_{w,n}\right) = \left(D_{n,1} + \left(E_{n,1} + D_{bio,pw}\right)\left(1 + \rho_{DOC,1}K_{DOC,n}\right) + D_{bio,p}\sum_{m=1}^{M}\rho_{b,m,i}\phi_{m,i}K_{d,m,n}\right)\frac{\partial C_{0,n}}{\partial z} \tag{4.12}$$

The benthic mass transfer coefficient $k_{bl,n}$ is estimated using various empirical correlations for rivers and lakes (Thibodeaux, 1996).

$$k_{bl,n} = \frac{0.114\, v_{river} * {D_{w,n}}^{2/3}}{{\mu_n}^{2/3}} \tag{4.13}$$

Where v_{river} is the river velocity, μ is the viscosity of the water at given temperature and $D_{w,n}$ is the water diffusivity of chemical n.

$$k_{bl,n} = \frac{18.9 * C_D * (\rho_{air}/\rho_{water}) * v_{air}{}^2 * h^2}{l * MW_n{}^{1/2}} \quad (4.14)$$

Where v_{air} is the wind speed, ρ_{air} is the density of the air, ρ_{water} is the density of the water, MW is the molecular weight of the chemical, h is the depth of the lake, and l is the fetch of the lake. C_D, represent the drag coefficient is 0.00166 for wind speed smaller than 6 m/s and 0.00237 for wind speed larger than 6 m/s.

One particular case for the flux-matching boundary conditions at the benthic surface is fixed concentration boundary. When the turbulence in the overlying water is intense, the large mass transfer coefficient $k_{bl,n}$ reduces the concentration difference between the sediment pore water and the overlying water $(C_{0,n} - C_{w,n})$. In this case, the $C_{n,0}$ can be assumed to be the same as $C_{w,n}$.

$$C_{0,n} = C_{w,n} \quad (4.15)$$

The overlying water concentration $C_{w,n}$ may not be kept at a constant zero level when the release rate of the contaminant from the sediment overwhelms its self-cleaning rate in the water body. The contaminants may accumulate in the water body until the removal rate balances the inlet rate. The respond time of the overlying body is assumed much smaller than the time scale of the sediment, so the water concentration $C_{w,n}$ can be an explicit function of the benthic surface concentration $C_{0,n}$ by the pseudo-steady-state continuous-stirred-tank-reactor model (4.16). The resident time τ_n in the overlying water body is calculated from the inflow rate Q_{in}, water evaporation rate Q_{evap}, water body

volume V, average depth H_w, compound water-air mass transfer rate coefficient $k_{evap,n}$, compound deposition rate coeffcient $k_{dep,n}$, and water decay rate coefficient $k_{decay,n}$.

$$\frac{k_{bl,n}}{H_w}\left(C_{0,n} - C_{w,n}\right) + \frac{U}{H_w}C_{0,n}\left(1 + \rho_{DOC,1}K_{DOC,n}\right) = \frac{1}{\tau_n}C_{w,n} \tag{4.16}$$

$$\frac{1}{\tau_n} = \left(\frac{Q_{in}}{V} - \frac{Q_{evap}}{V} + \frac{U}{H_w}\right)\left(1 + \rho_{DOC,w}K_{DOC,n}\right) + \frac{k_{dep,n}}{H_w}\left(\varepsilon_{dep} + \rho_{b,dep}\frac{\partial q_{dep,n}}{\partial C_{w,n}}\right) + \frac{k_{evap,n}}{H_w} + k_{decay,n} \tag{4.17}$$

Comparing to the benthic surface boundary, the bottom boundary condition is commonly less clear due to the lack of information about the underlying structure and composition of the sediment. The depth of the bottom boundary and the physicochemical phenomena occurring on this boundary might be variant from sites to sites, and the investigation work faces a not difficulties. Three types of boundary conditions, fixed concentration, zero gradient condition and flux-matching are available to circumvent the uncertainty of bottom boundary.

$$\text{Fixed concentration: } C_n|_{z=h_{l,l+1}} = C_{b,n} \tag{4.18}$$

$$\text{Zero gradient: } \left.\frac{\partial C_n}{\partial z}\right|_{z=h_{l,l+1}} = 0 \tag{4.19}$$

$$\text{Flux-matching: } F_n|_{z=h_{l,l+1}} = UC_{f,n} \tag{4.20}$$

The fixed concentration condition describes the release of contaminants from a heavy loaded sediment that can be treated as a continuous source. This boundary is frequently used in designing a cap for contaminated sediment with unknown thickness or

loading since it tends to make a safer capping layer design since it maximizes the contaminant loading. The zero gradient condition is applied to model the sediment system with a semi-infinite thickness. Different from the fixed concentration, it involves the impacts from depletion of contaminants in the top sediment. The flux-matching condition is applied to model the well-studied sediment layers with known mass loading and thickness. By fixing the bottom flux to zero, the contaminated sediment is defined as a finite source of a given initial mass loading. The depletion of contaminants in contaminated sediments is fully modeled.

4.2.2.3 Initial conditions

The initial distribution of contaminants is assumed to be uniform or linear in each layer. For contaminants and solids that do not perform equilibrium partitioning, the initial solid concentrations $q_{init,m,n,i}$ are also required by the system.

$$C_{n,i}\big|_{t=0} = C_{init,n,i}\ ;\ q_{m,n,i}\big|_{t=0} = q_{init,m,n,i} \tag{4.21}$$

For systems that consists a spatial variation of initial concentrations, CapSim includes a linear initial boundary condition shown:

$$C_{n,i}\big|_{t=0} = \frac{z-H_i}{H_i}\left(C_{init,top,n,i} - C_{init,bot,n,i}\right) + C_{init,top,n,i} \tag{4.22}$$

4.2.3 Numerical solutions

Finite difference method (FDM) is used here to solve the governing equations and auxiliary conditions. The standard procedure of the FDM involves three steps; establish a discrete domain from the continuous domain; derivation of finite difference equations

based on the discrete domain, simulation. The constitutive equations with non-linear terms such as Freundlich sorption isotherm or higher order kinetic reactions are solved at each time step by Newton's method. The oscillation in the results from the periodical sediment processes, such as tidal advection and deposition, are offered to be attenuated by averaging the simulated results over the span of the cycling period.

4.2.3.1 Discretization

The discretization is a process of transferring continuous variables and functions to a discrete domain with finite space and time points. To solve the transient fate and transport model in a multi-layer sediment system, the time step size is a uniform constant Δt and the grid sizes needs to be a group of layer-specified constants Δz_i to handle the variation of layer properties. The total number of time steps W, the number of grids in the i-th layer J_i , and the total number of grids J_{total} are defined based on the .

$$W = t_{final}/\Delta t \tag{4.23}$$

$$J_i = H_i/\Delta z_i \tag{4.24}$$

$$J_{total} = \sum_{i=1}^{I} J_i \tag{4.25}$$

The choice of the time step size Δt and the layer grid size Δz_i needs to meet the stability and convergence criteria, which requires the grid Peclet number $Pe_{g,n,i}$ to be smaller than 2 for controlling the numerical diffusion from the implicit method.

$$Pe_{g,n,i} = \Delta z_i * U/D_{n,i} < 2 \tag{4.26}$$

The grid and time step sizes are determined by the Courant-Levy-Friedrich Law (Courant et al. 1967) for linear problems.

$$\Delta t < \frac{R_{n,i} 2\Delta z_i}{2D_{n,i}} \tag{4.27}$$

The concentration profile of the n-th chemical $C_n(z,t)$ is transferred into a two-dimensional $W \times (J_{total} + 1)$ space $\mathbf{C_n}$. The elements in the discretized concentration array $\mathbf{C_n}$ are labeled by the lower case w and j_i, which ranges from 1 to W and 1 to J_i, respectively. The w-th row of the concentration array is denoted by $\mathbf{C_n}^{\boldsymbol{w}}$ that represent the spatial concentration profile at the time step ($t = w\Delta t$).

$$(C_n)_{j_i}^{w} = C_n(z,t) \quad \text{at } z = h_{i-1,i} + j_i\, \Delta z_i \text{ and } t = w\Delta t \tag{4.28}$$

4.2.3.2 Finite difference equation

The differential terms of the porewater and solid concentrations in the governing equations are then discretized to the discrete domain built in the previous session. The second-order terms are discretized by the three-point central difference scheme, and first-order differential terms are discretized by the four-point upwind difference scheme to minimize the oscillation problem brought from the numerical dispersion. Crank-Nicolson discrete method (Crank and Nicolson, 1948) is applied for problems with strong advection for its lack of numerical dispersion and a fully implicit method (Smith, 1985) is applied for systems with less advection but stronger non-linear sorption and reactions for its better stability.

$$\frac{\partial^2 C_{n,i}}{\partial z^2} = \frac{(C_{n,i})^{w}_{j_i-1} - 2(C_{n,i})^{w}_{j_i} + (C_{n,i})^{w}_{j_i+1}}{\Delta z^2} \tag{4.29}$$

$$\frac{\partial C_{n,i}}{\partial z} = \frac{\frac{1}{3}(C_{n,i})^{w}_{j_i-1} - \frac{1}{2}(C_{n,i})^{w}_{j_i} + (C_{n,i})^{w}_{j_i+1} - \frac{1}{6}(C_{n,i})^{w}_{j_i+2}}{\Delta z} \tag{4.30}$$

Following the above finite difference approximations, the governing equations and the boundary conditions are transferred to a functions space, $\mathbf{F_n} : \mathbf{R}^{J_{total}+1} \rightarrow \mathbf{R}^{J_{total}+1}$, which contains $(J_{total} - I)$ governing equations and $(I + 1)$ boundary equations.

$$\mathbf{F_n}\left(\mathbf{C_n}^{w},\ \mathbf{C_n}^{w-1}\right) = 0 \tag{4.31}$$

4.2.3.3 Deposition and oscillated advection

The deposition of sediment on the top is modeled by a special layer with growing number of grids to imitate the accumulation of solid materials. To avoid the discontinuity of the top layer concentration and fluxes brought from the jump of the deposition grid and keep the continuity, the simulated results are averaged over the time span of the deposition grid deposition. For example, the concentration results at all time points between t_1 and t_2 are averaged to be an average value $C_{avg,1,2}$ at the time point $(t_1 + t_2)/2$. The output concentration results at the time point between $(t_1 + t_2)/2$ and $(t_2 + t_3)/2$ are then calculated by using linear interpolation with the average concentrations $C_{avg,1,2}$ and $C_{avg,2,3}$. This average approach can also be applied for

systems with fast changing oscillation advection term to avoid the possible bias from output sampling points.

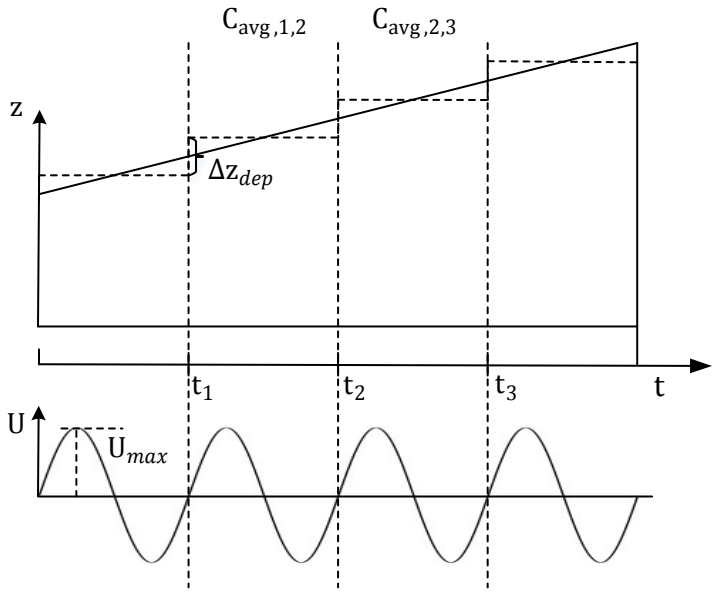

Figure 4.1: Averaging output results in given time period in cases with a growing deposition layer or oscillated advection flow

4.2.4 Model structure

The closed-form CapSim model was coded by Python programming language. The developed executive program obtains the system parameters and properties, transport and reaction coefficients and numerical simulation setups, by a series of visualized input windows. A database including the information of common environmental emerging contaminants and remediation solid materials from literatures (Mackay, 2006; Hawker,1988; Walters and Luthy, 1984; Azhar, 2015; and McDonough et al., 2008) is

provided. The coefficients and properties in the database file can be further edited and updated by users for specific needs. An alternative input method is to use the batch file function, which enables CapSim model to read and run a series of systems sequentially from a user-defined .csv file. This is especially useful for sensitivity analysis of key design parameters for the cap. The simulation cases with input information are stored in input files and can be reloaded back to the system or shared to other users. The simulated results, including porewater concentrations/fluxes/solid concentrations/pore space concentrations/water concentrations, are available in the form of the temporal or spatial plots or in .csv spreadsheets.

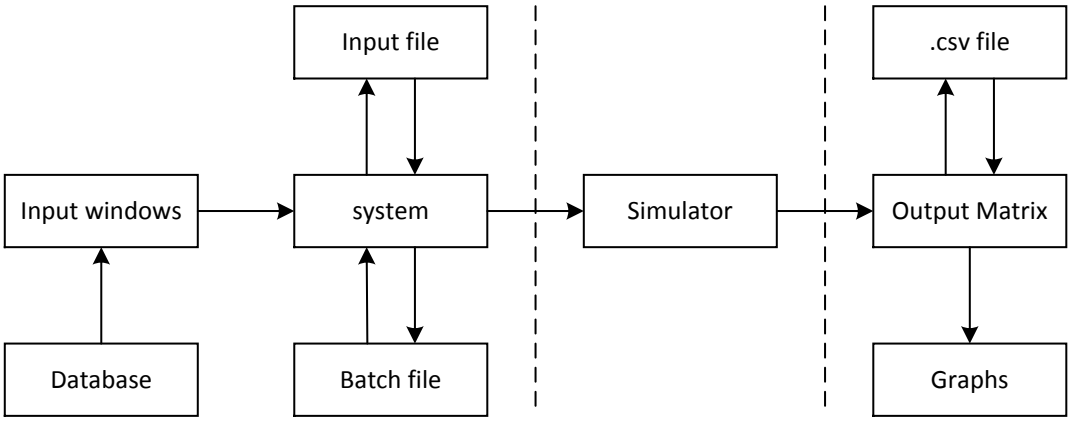

Figure 4.2: Programming Structure of the CapSim 3 model

4.3 MODEL VERIFICATION AND APPLICATION

The CapSim 3 model was performed for several case studies to verify its computational validity and to highlight its capability and utility. Two redox-sensitive

inorganic contaminants mercury and methylmercury and a common organic contaminant phenanthrene are presented as examples here. The cases were focused on simulating the performance of in-situ capping in particular sceanarios and performing sensitivity analyses on the impacts from advection, kinetic sorption/desorption, bioturbation and deposition. The baseline simulation results from CapSim were also compared with the commercial multiphysics model Comsol (AB Comsol, 2012) as a check of numerical accuracy.

4.3.1 Mercury and methylmercury

Mercury (Hg) and methylmercury (MeHg) are typical redox-sensitive contaminants in the sediment environment. MeHg is the major toxic form of Hg that accumulates in fish and lead to exposure to humans through the food chain. (Morel et al. 1998; Kraepiel et al. 2003; Kudo and Miyahara, 1991) The transformation between Hg and MeHg is commonly considered as a pair of first order reactions, which reaction coefficients are specified according to the local redox conditions. The redox profile in the following case is simplified to two extreme regions, an aerobic zone near the benthic surface and an anaerobic zone underlying. The methylation is assumed to only occur in the anaerobic sediment layer and the demethylation occurs uniformly in the sediment. The demethylation rate coefficient is $0.005\ \mathrm{yr}^{-1}$ from (Huntelman, 2000) and the methylation rate coefficient is evaluated to be $0.4\ \mathrm{yr}^{-1}$from mesocosm experiments (Vrtlar et al., 2017). In the following case, a 30 cm sediment with initial Hg concentration 3mg/kg has

been capped by a 2 cm activated carbon layer and 15 cm sand layer. The top 5 cm of the sand layer is assumed to be affected by bioturbation of a uniform strength at ($D_{bio,pw,0} = 50 cm^2/yr$ and $D_{bio,p,0} = 1 cm^2/yr$).

The MeHg concentrations simulated by CapSim were verified with the Comsol results (Figure 4.3). The activated carbon-sand capping layers slowed down the upward transport of MeHg generated in the deeper layer transports. The potential impact from a daily tidal groundwater discharge is shown in Figure 4.4. The release rate of the MeHg to the overlying water increased to 10 times large as the baseline top flux with a strong tidal groundwater ($\pm 2000 cm/yr$).

Material	ρ_m (kg/L)	ε_m	f_{oc}	$K_{d,Hg}$(L/kg)	$K_{d,MeHg}$(L/kg)
Sand	1	0.5	0.001	2	0.2
Activated Carbon	0.4	0.5		20000	2000
Sediment	1.25	0.5	0.01	3000	400

(a) Solid material properties and sorption coefficients

Layer	h_i(cm)	Material	Tortuosity	α_i(cm)
1	15	Sand	Millington and Quirk	1.5
2	2	Activated carbon	Millington and Quirk	0.2
3	30	Sediment	Boudreau	3

(b) Layer properties

Table 4.3: Summary of the properties in the mercury and phenanthrene example

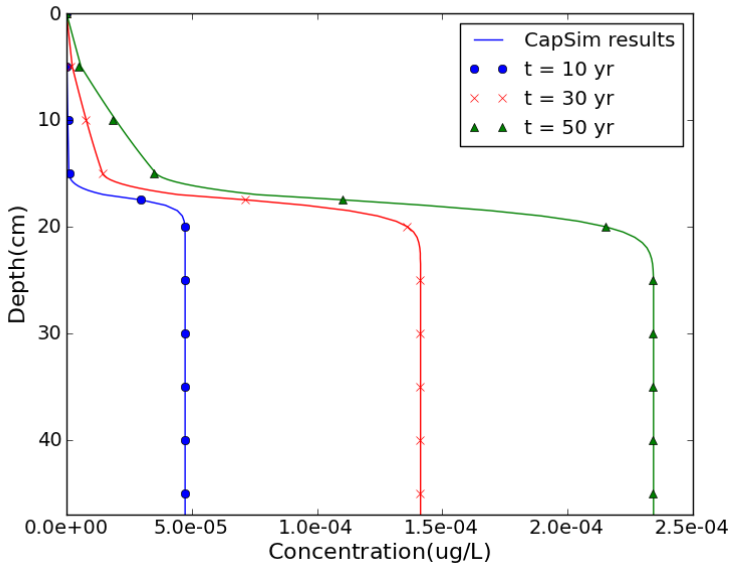

Figure 4.3: Comparison of porewater concentration depth profiles of MeHg simulated by CapSim(solid lines) and Comsol (dots, crosses and triangles)

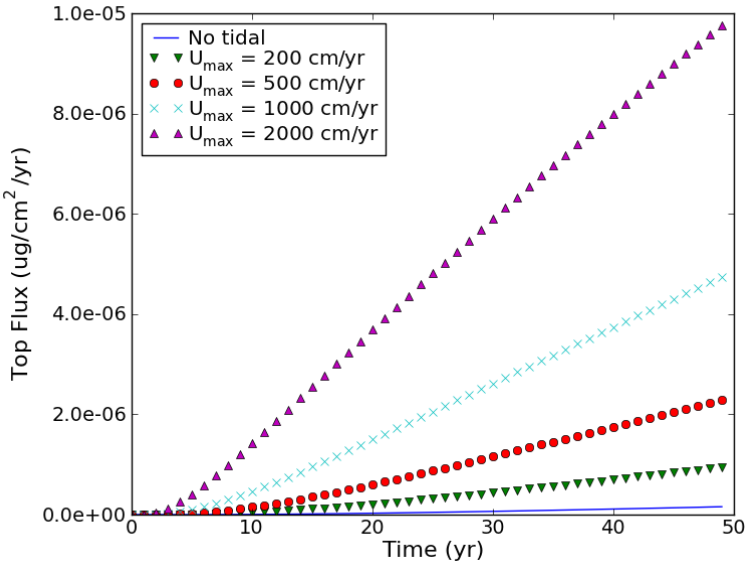

Figure 4.4: Sensitivity analysis on the impacts of the tidal advection flow with various maximum Darcy velocity to the flux of the methylmercury at the top of the capping layer

4.3.2 Phenanthrene

Phenanthrene is a hydrophobic contaminant that performs a strong sorption process in high carbon content materials. The phenanthrene sorption in sand and sediments were calibrated by their organic carbon fractions with a $\log K_{oc} = 4.57$ and its sorption in activated carbon was modeled by Freundlich isotherm $q = 1.03 \times 10^{7} \times C^{0.44}$ (Walter and Luthy, 1988). The sediment system of the baseline or the activated carbon-sand case was similar to the mercury example except the layer 2 was made of pure sand or a 0.1%wt activated carbon-sand mixture. The phenanthrene porewater concentrations in the sediment layer and at the bottom were fixed at 100ug/kg to circumvent the unclear phenanthrene loading. The overlying water was assumed a well-mixed lake with a benthic transfer coefficient $k_{bl} = 0.00273 cm/yr$ estimated by empirical correlation (4.14). The fate and transport of phenanthrene in the sediment and the capping layer were simulated over 50 years. The baseline result (Figure 4.6) was verified with the analytical solution (Shen and Reible, 2015). Figure 4.6a shows the impacts from a sediment deposition layer to the benthic surface concentrations, the top surface concentration drops to 0 with the 0.1cm/yr deposition layer.

Figure 4.6b shows the possible impacts from the kinetic sorption of activated carbon in the 2 cm activated carbon-sand layer to the top benthic flux to the overlying water. Initially, the sorption process is controlled by kinetics and top fluxes in all kinetic cases behave like the no activated carbon case. With an increase in time, the partitioning of

phenanthrene in porewater and activated carbon moves forward to equilibrium and the top flux converges to the equilibrium case flux.

Figure 4.6c shows the impact from the depth-dependent bioturbation to the top surface flux. A porewater bio-irritation ($D_{bio,pw,0} = 50 cm^2/yr$) is applied to all six scenarios and a $1 cm^2/yr$ solid particle bioturbation ($D_{bio,p,0} = 1 cm^2/yr$) is applied to the later three scenarios labeled as 'solid'. σ, the Gaussian RMS width in (4.8) is selected to be 7cm, 10cm and 15cm to represent the various bioturbation strength in natural environment. When the bioturbation is limited in the top surface ($\sigma = 7 cm$), the top fluxes of both the porewater and the solid bioturbation case show slightly increases from the baseline. As soon as the bioturbation starts reaching the activated carbon cap, the solid bioturbation case flux meets a sudden rise for the transporting the highly sorptive material - activated carbon.

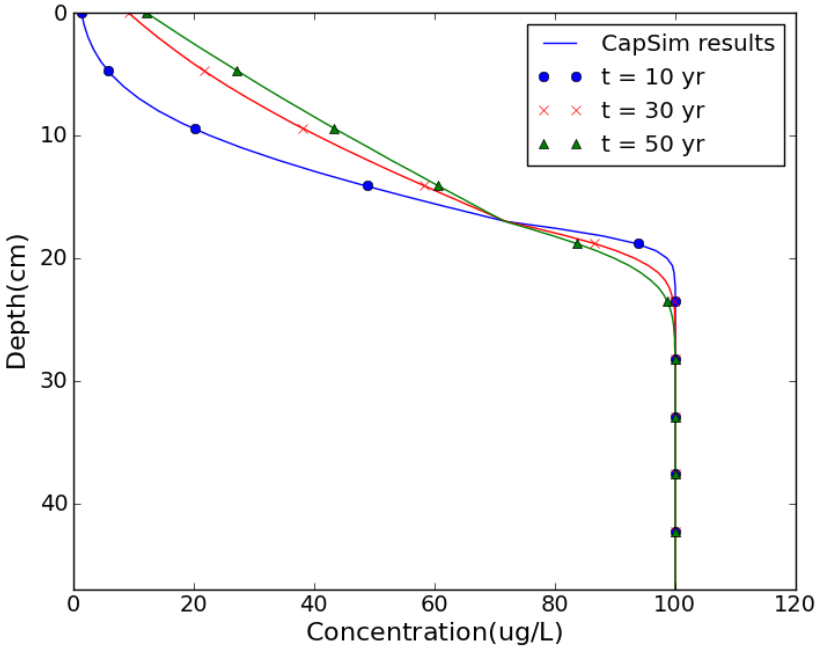

Figure 4.5: Comparison of porewater concentration depth profiles of phenanthrene simulated by CapSim (solid lines) and Comsol (dots, crosses and triangles)

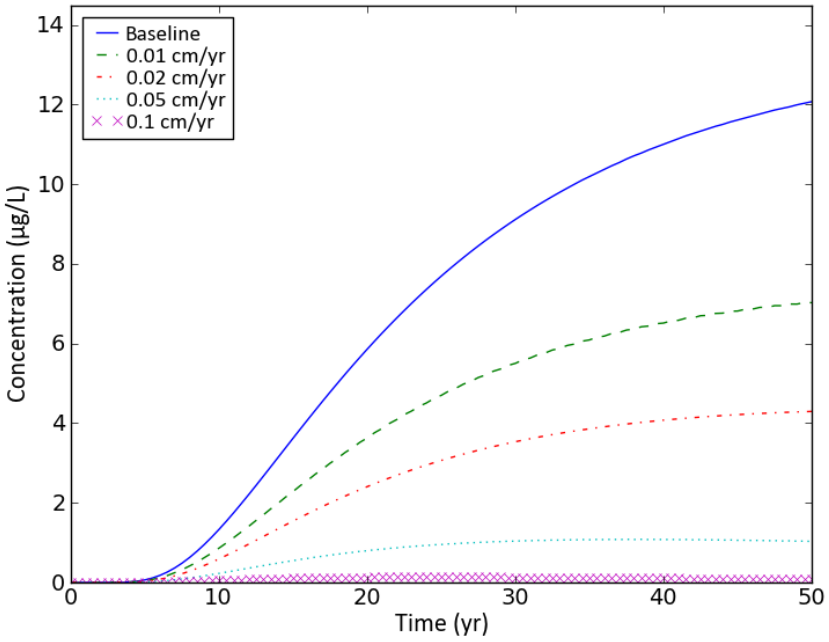

(a)

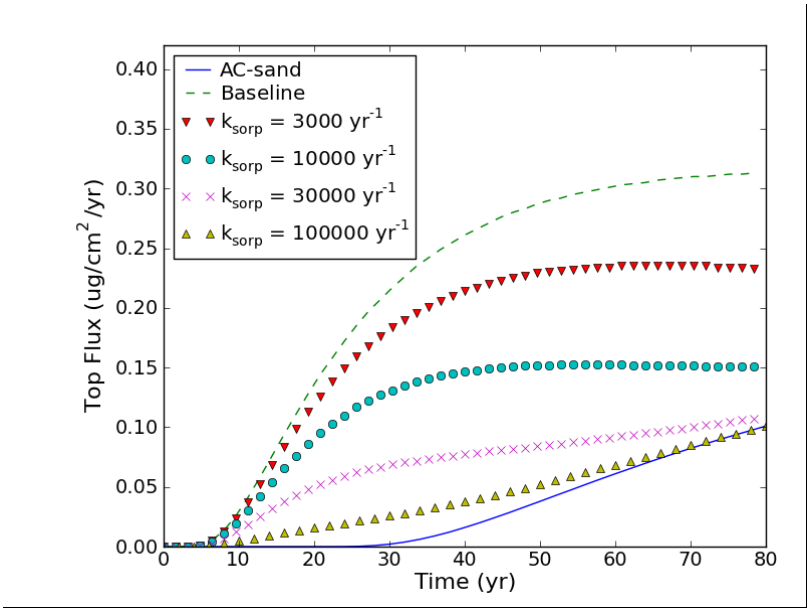

(b)

(Figure 4.6 continued next page)

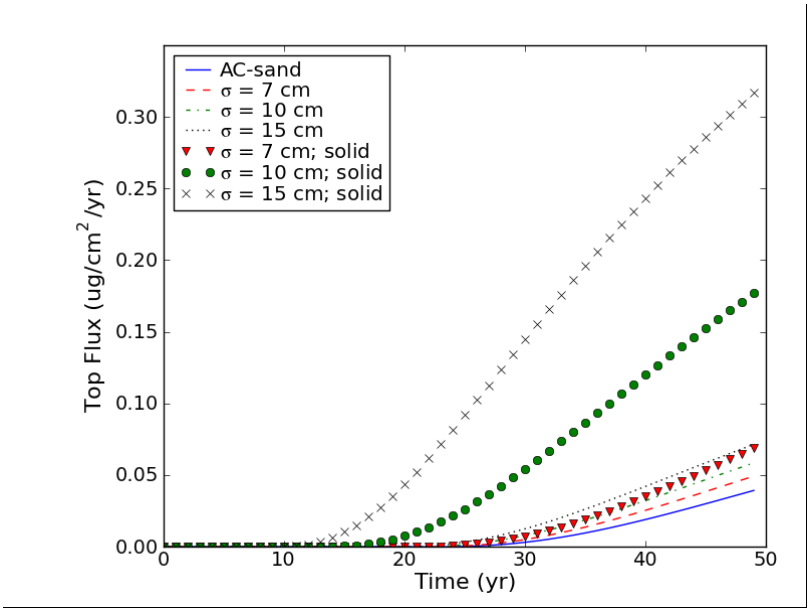

(c)

Figure 4.6: Sensitivity analysis on the impacts of (a) the deposition rate, (b) the kinetic sorption rate and (c) the bioturbation layer thickness, to the flux of the methylmercury at the top of the capping layer

4.4 DISCUSSION

4.4.1 Modeling activated carbon rework by bioturbation

Bioturbation is a general process describing the activities of benthic organisms near the sediment-water interface. It is accounted to the dominant transport process near the sediment-water interface for not only irritating the exchange rates of the porewater but also mix the solids of the sediment and potential remediation sorbents. The potential impact of bioturbation on in-situ remediation includes leading to an increase in the surface flux by accelerating the mixing process near the surface (Boudreau, 1997) and mix solids or sorbents (Lin et al., 2014)

Roche et al. (2016) conducted a lab experiment using time-lapse imagery to study bioturbation's impact on sediment mixing. They made a 0.08 mm thin layer of tracer-labeled particles on the top of an 8 cm sediment and recorded the particle distribution using the fluorescence intensity as indicators. They applied both the advection-dispersion model (ADE) and an innovative random-walk model to fit the observed particle density distribution over 15 days. Here we applied the biodiffusion model in CapSim with a depth-dependent biodiffusion coefficient to fit their experimental results. The simulation results provide a reasonable description of the average particle migration with a particle biodiffusion coefficient $D_{bio,p} = 8 \times 10^{-8} cm^2/s$ and a Gaussian model coefficient $\sigma = 0.9$. The simulation does not attempt to capture the stochastic nature of the observed behavior but only the general mixing characteristics over time.

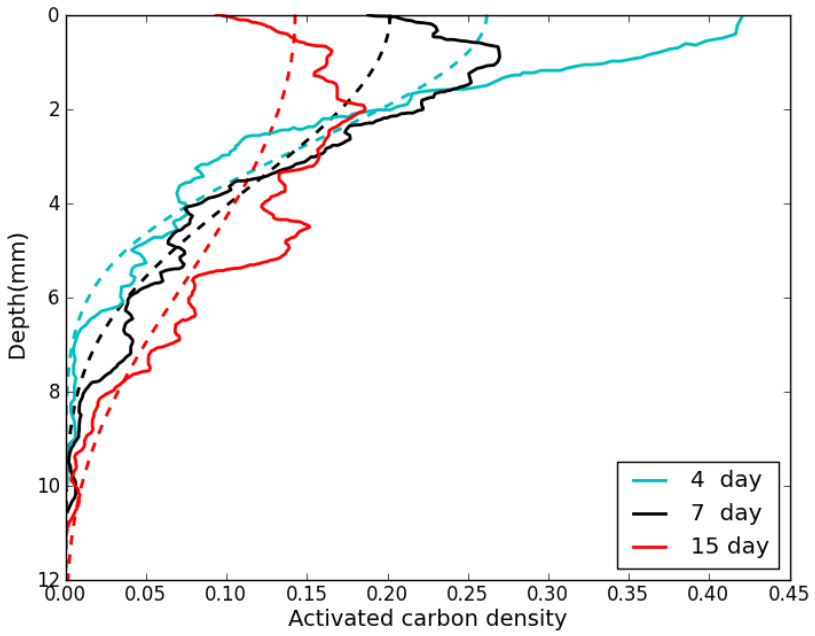

Figure 4.7: The tracer-particle density profiles simulated by CapSim with the solid particle biodiffusion coefficient fitted to the observation from Roche et al. (2016)

Lin et al. (2014) conducted research on the impacts from the sediment-sorbent mixing by bioturbation to the availability of dichloro-diphenyl-trichloroethane (DDT) in the underlying sediment. The results showed that the downward migration of activated carbon from a thin capping layer enhanced the sequestration of the porewater DDT in the top 2 cm of the sediment system.

The simulated activated carbon fractions are lower than the experimental measurements for keeping the mass of activated carbon to be conserved as the initial loading of a 0.3cm layer. The solid particle biodiffusion coefficient $D_{bio,p}$ in (4.8) is calibrated to be $5.07 \times 10^{-8} \mathrm{cm}^2/\mathrm{s}$ by using the activated carbon fraction measurements

at 28 days. The calibrated biodiffusion coefficient is then applied in modeling impacts from the downward migration of activated carbon.

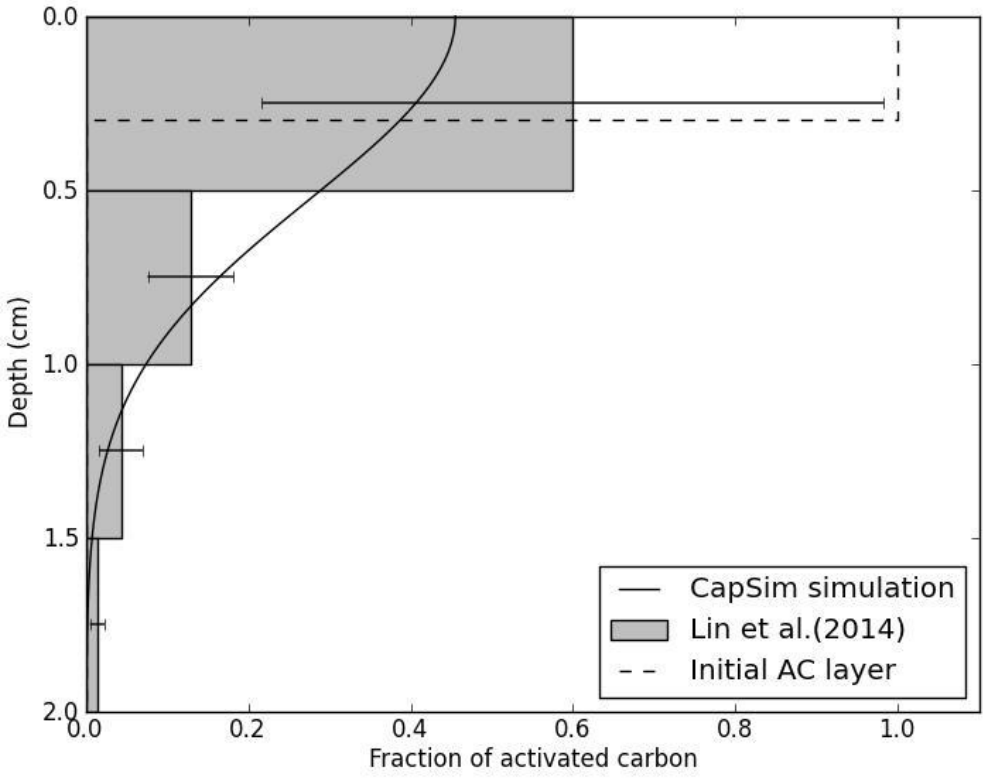

Figure 4.8: The activated carbon fraction distribution profile simulated by CapSim with the solid particle biodiffusion coefficient fitted to the measurements from Lin et al. (2014)

Figure 4.9 illustrates the CapSim simulation results of porewater concentrations in the cases with or without bioturbation impacts. The DDT transported into the activated carbon layer (top 3mm) was fully sequestrated by activated carbon. In the case with bioturbation present, the porewater concentration near the cap-sediment interface also

meets a significant drop due to the adsorption of the migrated activated carbon. During 28 days, the activated carbon-sediment mixing region expanded to approximately 1.5 cm depth, which agrees with the experimental observation of the mixed region by Lin et al (2014).

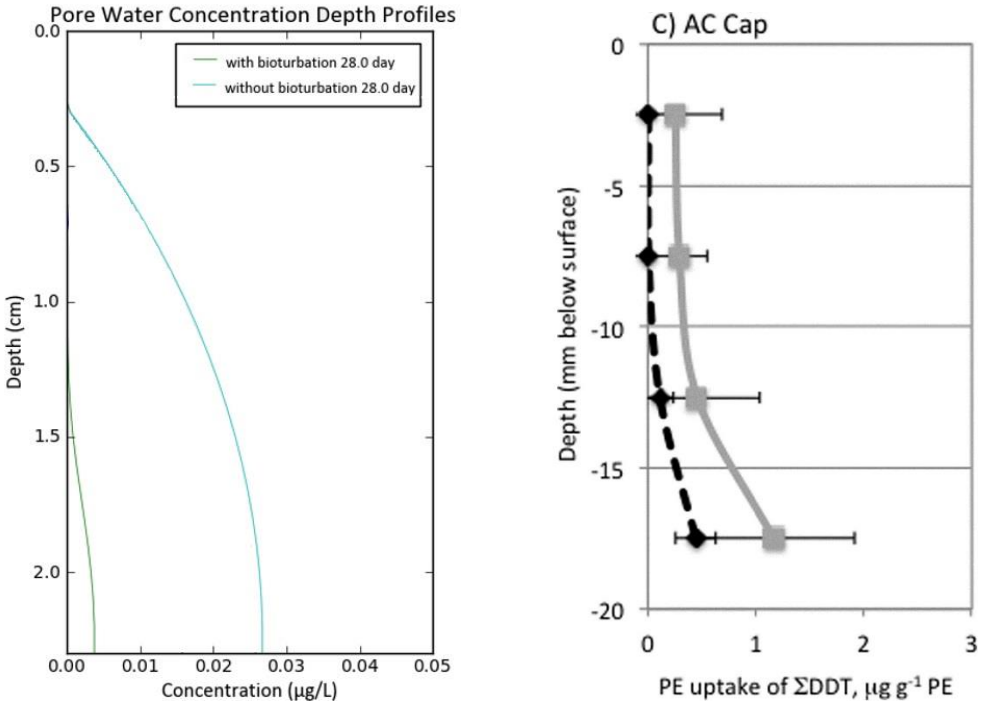

(a) (b)

Figure 4.9: Illustration of the impacts from the bioturbation-caused migration of activated carbon to the behavior of DDT in the underlying sediment: (a) porewater concentration depth profile simulated by CapSim for activated carbon capping system without or with bioturbation case; (b) PE uptake concentration for non-bioturbation case (solid line) and bioturbation case (broken line) from Lin et al (2014)

4.4.2 Modeling multi-compartment kinetic sorptions

The multi-compartment kinetic sorption model is developed for modeling the observed variation of kinetic sorption rates at different stages in sorption process. It is now widely accepted in modeling the kinetic sorption in various sorbents including sediments (Chai et al. 2006; Johnson et al. 2001; Rakowska et al., 2014) and activated carbons (Lesage et al., 2010; Valderama et al., 2007, Rakowska et al., 2014). In the multi-compartment model, the sorbent is assumed to have multiple compartments with various kinetic behavior. Though CapSim only includes the one-compartment sorption kinetic models, it can circumvent the problem by treating the sorbent as a mixture of multiple materials, which perform the same property but different sorption kinetic rates.

Wu and Gschwend (1986) studied the sorption kinetics of HOCs in sediment and soils by applying various types of sorption model to the batch sorption experiment. Though the authors ultimately recommended a mechanistic intra-particle diffusion model, they also show that the experimental data could be described by a two-compartment empirical model. Figure 4.10 illustrates the example of 1,2,3,4-tetrachlorobenze sorption in Charles River sediments shown in Wu and Gschwend (1986) and the capability of CapSim to handle a two-compartment sorption model using a sorbent mixture. In the case, the sorbent was assumed to be a 50:50 mixture of the fast sorption sediment with a kinetic rate coefficient of $0.212\ min^{-1}$ and the slow sorption sediment with a kinetic rate coefficient of $0.00316\ min^{-1}$. The rate coefficients here were re-calibrated by the

fraction of the solids compartment in the mixture. The simulation results here fit the data presented by Wu and Gschwend(1986).

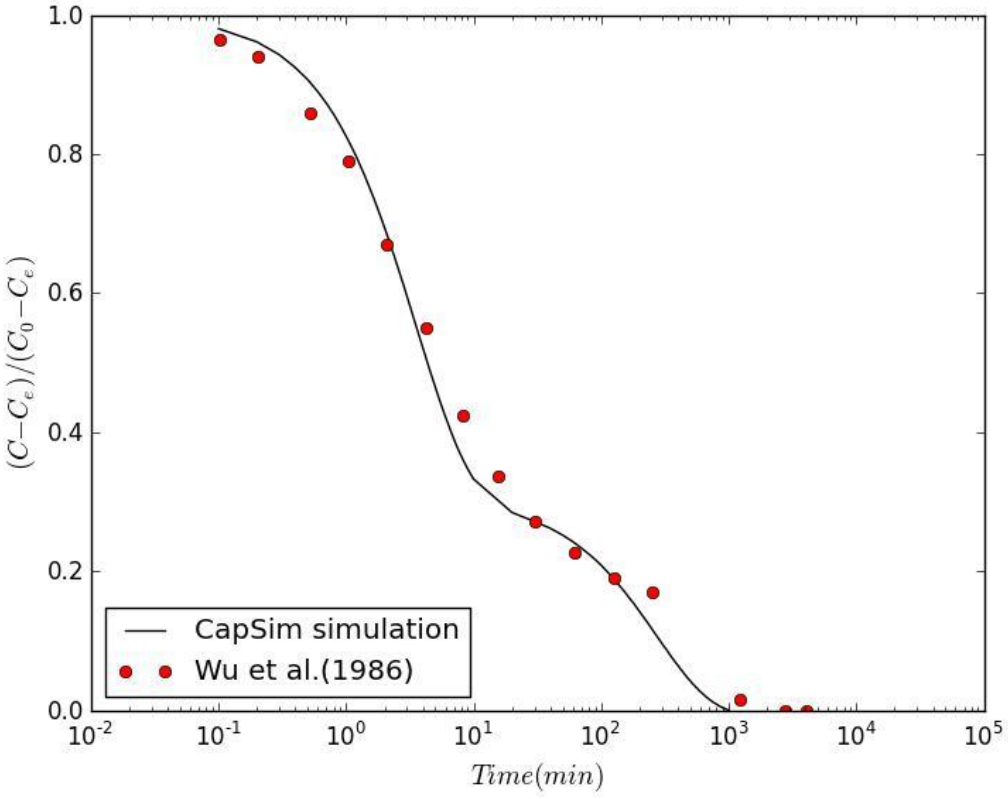

Figure 4.10: The 1,2,3,4-tetrachlorobenze concentration profile simulated by CapSim with the kinetic coefficients fitted to the batch sorption experimental results from Wu and Gschwend (1986).

4.4.3 Modeling the breakthrough of in-situ remediation

The breakthrough time is a key parameter to evaluate the effectiveness of a remediation capping layer to the specific sediment. Lampert and Reible (2009) developed

a conservative estimate of the penetration time through a layer of thickness H. Because the processes of advection and diffusion are parallel, the overall time for penetration is the harmonic mean of the diffusion characteristic time t_{diff} and the advection characteristic time t_{adv},

$$\tau_{adv/diff} = \frac{1}{\frac{1}{t_{adv}}+\frac{1}{t_{diff}}} = \frac{RH^2}{16D+UH} \quad (4.32)$$

Where D is the effective diffusivity in the system and R is the retardation factor defined as $R = \varepsilon + \rho_b K_d$ for system with linear sorption isotherm. ε is the layer porosity, ρ_b is the bulk density of the layer and K_d is the sediment-porewater partition coefficient. U is the Darcy velocity.

In the absence of equilibrium partitioning, the characteristic transport or residence time τ_{res} through the porewater in the layer is given by (4.33).

$$\tau_{res} = \frac{1}{\frac{1}{\tau_{adv}}+\frac{1}{\tau_{diff}}} = \frac{H^2}{16D+UH} \quad (4.33)$$

This can be compared to other porewater processes such as kinetic sorption. Assuming these are first order with a rate constant given by k_{sorp}, there is a characteristic time $\tau_{sorp} = 1/k_{sorp}$ and a half-life $\tau_{0.5}$ is given by (4.34), which is commonly simplified to $0.693/\tau_{0.5}$ in cases where K_d is large.

$$\tau_{sorp} = \frac{0.693}{\tau_{0.5}\left(1+\frac{\varepsilon}{\rho_b K_d}\right)} \sim \frac{0.693}{\tau_{0.5}} \quad (4.34)$$

The non-equilibrium sorption will significantly increase migration through the layer when $\tau_{sorp}/\tau_{res} > 0.2$. This criterion is based upon less than a 10% difference from the

equilibrium condition for sorption and from assuming no reactivity for reactions. The figure below portrays the effect of sorption kinetics on time to "breakthrough" a layer. The y axis is time relative to equilibrium sorption and the x axis is τ_{sorp}/τ_{res}. At τ_{sorp}/τ_{res} ~1, the time to achieve breakthrough is approximately twice as fast as when equilibrium sorption can be assumed and when $\tau_{sorp}/\tau_{res} < 0.2$, there is less than a 10% difference from the migration time through a layer than the time required assuming equilibrium sorption.

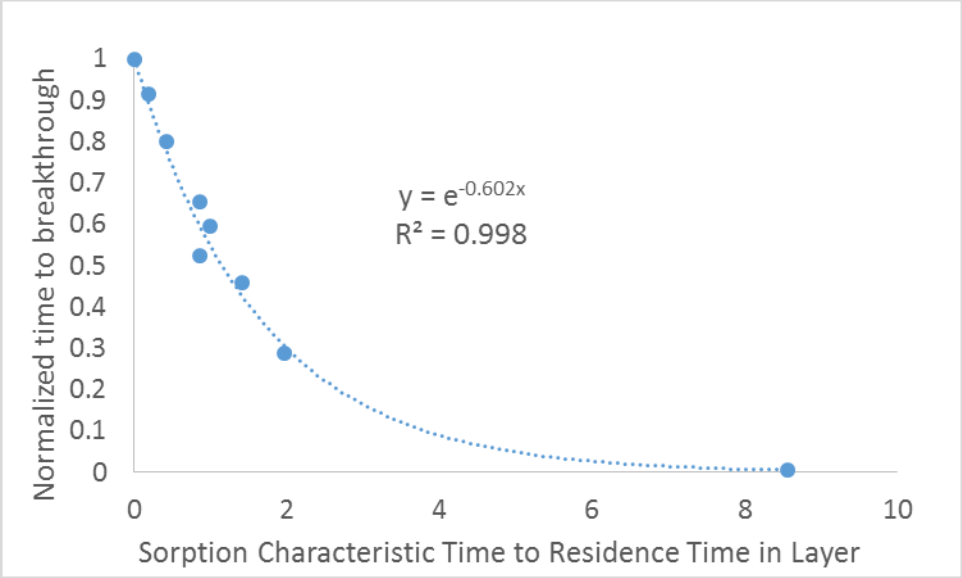

Figure 4.11: The relationship between sorption characteristic time to porewater residence time in a layer to contaminant migration time relative to the assumption of equilibrium sorption (0 sorption time)

4.5 CONCLUSIONS

This chapter presents an innovative numerical model CapSim 3 developed for predicting the contaminants behavior in sediment and optimizing the in-situ remediation design. The model has greatly expanded capabilities over the existing model in handling several essential physical and chemical processes in sediments. Firstly, the model can handle systems with an arbitrary number of layers and chemical species with linked linear or nonlinear reactions. Secondly, the kinetic sorption/desorption processes are included in the model to get more accurate results for problems with slow sorption/desorption processes. Thirdly, the impacts from the important sediment processes, such as bioturbation, deposition, consolidation are included. The model has been verified with the existing analytical model and commercial numerical model, its application in modeling the bioturbation, the multi-compartment sorption and the breakthrough of a remediation cap has been included here.

4.6 REFERENCES

Azhar, W. (2015). Evaluation of sorbing amendments for in-situ remediation of contaminated sediments (Order No. 10035640). Available from ProQuest Dissertations & Theses Global. (1773635522). Retrieved from https://search.proquest.com/docview/1773635522?accountid=7098

Bear, J. (1972). "Dynamics of fluids in porous materials." Society of Petroleum Engineers.

Boudreau, B. P. (1997). Diagenetic models and their implementation, Springer Berlin.

Boudreau, B. P. and B. B. Jorgensen (2001). The benthic boundary layer: Transport processes and biogeochemistry, Oxford University Press.

Chai, Y., A. Kochetkov and D. D. Reible (2006). "Modeling biphasic sorption and desorption of hydrophobic organic contaminants in sediments." Environmental Toxicology and Chemistry 25(12): 3133-3140.

Clarke, J., D. D. Reible and R. Mutch (1993). "Contaminant transport and behavior in the subsurface." Hazardous Waste Soil Remediation: Theory and Application of Innovative Technologies. Marcel-Dekker, New York, NY, USA: 1-49.

Courant, R., K. Friedrichs and H. Lewy (1967). "On the partial difference equations of mathematical physics." IBM journal of Research and Development 11(2): 215-234.

Crank, J. and P. Nicolson (1947). A practical method for numerical evaluation of solutions of partial differential equations of the heat-conduction type. Mathematical Proceedings of the Cambridge Philosophical Society, Cambridge Univ Press.

EPA, U. (1998). "EPA's Contaminated Sediment Management Strategy."

Hawker, D. W. and D. W. Connell (1988). "Octanol-water partition coefficients of polychlorinated biphenyl congeners." Environmental Science & Technology 22(4): 382-387.

Jacobs, P. H. and U. Förstner (1999). "Concept of subaqueous capping of contaminated sediments with active barrier systems (ABS) using natural and modified zeolites." Water Research 33(9): 2083-2087.

Johnson, M. D., T. M. Keinath and W. J. Weber (2001). "A distributed reactivity model for sorption by soils and sediments. 14. Characterization and modeling of phenanthrene desorption rates." Environmental Science & Technology 35(8): 1688-1695.

Kraepiel, A. M., K. Keller, H. B. Chin, E. G. Malcolm and F. M. Morel (2003). "Sources and variations of mercury in tuna." Environmental Science & Technology 37(24): 5551-5558.

Kudo, A. and S. Miyahara (1991). "A case history; Minamata mercury pollution in Japan–from loss of human lives to decontamination." Water Science and Technology 23(1-3): 283-290.

Lampert, D. J. and D. Reible (2009). "An analytical modeling approach for evaluation of capping of contaminated sediments." Soil and Sediment Contamination 18(4): 470-488.

Lesage, G., M. Sperandio and L. Tiruta-Barna (2010). "Analysis and modelling of non-equilibrium sorption of aromatic micro-pollutants on GAC with a multi-compartment dynamic model." Chemical Engineering Journal 160(2): 457-465.

Li, Y. C. and P. J. Cleall (2011). "Analytical solutions for advective‐dispersive solute transport in double‐layered finite porous media." International Journal for Numerical and Analytical Methods in Geomechanics 35(4): 438-460.

Lick, W. and V. Rapaka (1996). "A quantitative analysis of the dynamics of the sorption of hydrophobic organic chemicals to suspended sediments." Environmental Toxicology and Chemistry 15(7): 1038-1048.

Lin, D., Y.-M. Cho, D. Werner and R. G. Luthy (2014). "Bioturbation delays attenuation of DDT by clean sediment cap but promotes sequestration by thin-layered activated carbon." Environmental Science & Technology 48(2): 1175-1183.

Liu, C., W. P. Ball and J. H. Ellis (1998). "An analytical solution to the one-dimensional solute advection-dispersion equation in multi-layer porous media." Transport in porous media 30(1): 25-43.

Mackay, D., W.-Y. Shiu, K.-C. Ma and S. C. Lee (2006). Handbook of physical-chemical properties and environmental fate for organic chemicals, CRC press.

Malusis, M. A. and C. D. Shackelford (2002). "Theory for reactive solute transport through clay membrane barriers." Journal of Contaminant Hydrology 59(3): 291-316.

McDonough, K. M., J. L. Fairey and G. V. Lowry (2008). "Adsorption of polychlorinated biphenyls to activated carbon: Equilibrium isotherms and a preliminary assessment of the effect of dissolved organic matter and biofilm loadings." Water Research 42(3): 575-584.

McDonough, K. M., P. Murphy, J. Olsta, Y. Zhu, D. Reible and G. V. Lowry (2007). "Development and placement of a sorbent-amended thin layer sediment cap in the Anacostia River." Soil and Sediment Contamination: An International Journal 16(3): 313-322.

Millington, R. and J. Quirk (1961). "Permeability of porous solids." Transactions of the Faraday Society 57: 1200-1207.

Moore, W. S. (1999). "The subterranean estuary: a reaction zone of ground water and sea water." Marine Chemistry 65(1): 111-125.

Moore, W. S., J. Krest, G. Taylor, E. Roggenstein, S. Joye and R. Lee (2002). "Thermal evidence of water exchange through a coastal aquifer: Implications for nutrient fluxes." Geophysical Research Letters 29(14).

Morel, F. M., A. M. Kraepiel and M. Amyot (1998). "The chemical cycle and bioaccumulation of mercury." Annual review of ecology and systematics 29(1): 543-566.

Multiphysics, C. (2012). "COMSOL multiphysics user guide (Version 4.3 a)." COMSOL, AB: 39-40.

Murphy, P., A. Marquette, D. Reible and G. V. Lowry (2006). "Predicting the performance of activated carbon-, coke-, and soil-amended thin layer sediment caps." Journal of Environmental Engineering 132(7): 787-794.

Palermo, M. R. (1998). "Design considerations for in-situ capping of contaminated sediments." Water Science and Technology 37(6-7): 315-321.

Pignatello, J. J. and B. Xing (1995). "Mechanisms of slow sorption of organic chemicals to natural particles." Environmental Science & Technology 30(1): 1-11.

Rakowska, M., D. Kupryianchyk, M. Smit, A. Koelmans, J. Grotenhuis and H. Rijnaarts (2014). "Kinetics of hydrophobic organic contaminant extraction from sediment by granular activated carbon." Water Research 51: 86-95.

Rakowska, M. I., D. Kupryianchyk, A. A. Koelmans, T. Grotenhuis and H. H. Rijnaarts (2014). "Equilibrium and kinetic modeling of contaminant immobilization by activated carbon amended to sediments in the field." Water Research 67: 96-104.

Reible, D., D. Lampert, D. Constant, R. D. Mutch Jr and Y. Zhu (2006). "Active capping demonstration in the Anacostia River, Washington, DC." Remediation Journal 17(1): 39-53.

Roche, K. R., A. F. Aubeneau, M. Xie, T. Aquino, D. Bolster and A. I. Packman (2016). "An integrated experimental and modeling approach to predict sediment mixing from benthic burrowing behavior." Environmental Science & Technology 50(18): 10047-10054.

Rowe, R. K. and J. R. Booker (1985). "1-D pollutant migration in soils of finite depth." Journal of Geotechnical Engineering 111(4): 479-499.

Rubin, H. and A. J. Rabideau (2000). "Approximate evaluation of contaminant transport through vertical barriers." Journal of Contaminant Hydrology 40(4): 311-333.

Shen, X. and D. Reible (2015). "An analytical solution for one-dimensional advective–dispersive solute equation in multilayered finite porous media." Transport in Porous Media 107(3): 657-666.

Smith, G. D. (1985). Numerical solution of partial differential equations: finite difference methods, Oxford university press.

Taniguchi, M. (2002). "Tidal effects on submarine groundwater discharge into the ocean." Geophysical Research Letters 29(12).

Thibodeaux, L. J. (1996). Environmental chemodynamics: Movement of chemicals in air, water, and soil, John Wiley & Sons.

Thoma, G. J., D. RELBLE, K. T. Valsaraj and L. J. Thibodeaux (1993). "Efficiency of capping contaminated sediments in situ. II: Mathematics of diffusin-adsorption in the capping layer." Environmental Science & Technology 27(12): 2412-2419.

Thoms, S., G. Matisoff, P. L. McCall and X. Wang (1995). "Models for alteration of sediments by benthic organisms." Water Environment Research Foundation.

Valderrama, C., X. Gamisans, X. De las Heras, A. Farran and J. Cortina (2008). "Sorption kinetics of polycyclic aromatic hydrocarbons removal using granular activated carbon: intraparticle diffusion coefficients." Journal of Hazardous Materials 157(2): 386-396.

Van Genuchten, M. T. and W. Alves (1982). Analytical solutions of the one-dimensional convective-dispersive solute transport equation, United States Department of Agriculture, Economic Research Service.

Van Genuchten, M. T., F. J. Leij, T. H. Skaggs, N. Toride, S. A. Bradford and E. M. Pontedeiro (2013). "Exact analytical solutions for contaminant transport in rivers 2. Transient storage and decay chain solutions." Journal of Hydrology and Hydromechanics 61(3): 250-259.

Vrtlar, T. (2016) Field sampling and laboratory evaluation of reactive capping/in situ treatment of mercury contaminated solids using DGT devices, presented at 7th Setac World Congress, Orlando, 2016, FL

Walters, R. W. and R. G. Luthy (1984). "Equilibrium adsorption of polycyclic aromatic hydrocarbons from water onto activated carbon." Environmental science & technology 18(6): 395-403.

Wang, X., L. Thibodeaux, K. Valsaraj and D. Reible (1991). "Efficiency of capping contaminated bed sediments in situ. 1. Laboratory-scale experiments on diffusion-

adsorption in the capping layer." Environmental Science & Technology 25(9): 1578-1584.

Wu, S. C. and P. M. Gschwend (1986). "Sorption kinetics of hydrophobic organic compounds to natural sediments and soils." Environmental Science & Technology 20(7): 717-725.

Zimmerman, J. R., U. Ghosh, R. N. Millward, T. S. Bridges and R. G. Luthy (2004). "Addition of carbon sorbents to reduce PCB and PAH bioavailability in marine sediments: Physicochemical tests." Environmental Science & Technology 38(20): 5458-5464.

Chapter 5 An Analytical Model for the Fate and Transport of Compounds in a Cylindrical PDMS Passive Samplers

5.1 INTRODUCTION

Sediment that serves as a sink for hydrophobic organic contaminants (HOCs) such as polycyclic aromatic hydrocarbons (PAHs) and polychlorinated biphenyls (PCBs) presents continuous environmental risks to the benthic ecosystems and human beings through the food chain (EPA 2005). The management and remediation of such contaminated sediments require a comprehensive risk assessment.

Traditionally, the solid concentrations of contaminants in the sediments have frequently been used to assess sediment contamination level because of its relative simplicity in measurement. Beginning in the 1990s, widespread recognition of the poor representation of solid concentrations for bioavailability has heightened regulatory and research activities into better ways for sediment risk assessment (Burton, 1991). Di Tori et al. (1991) correlated organism accumulation with sediment pore water concentrations, which is then demonstrated to be linked to the bioaccumulation by a series studies (Kraaij et al., 2003, Lu et al., 2003, Lu et al., 2004a, Lu et al., 2004b, Lu et al., 2006). However, the porewater concentrations are often difficult to measure due to the low concentrations and other measurement difficulties.

Huckins et al. (1990) explored the idea of passive sampling as an alternative method to measure the porewater concentrations in sediment with the minimum interference to

the benthic environment. The authors used low-density polyethylene tubing containing this films of model lipids to simulate the bioconcentration of non-polar organic contaminants by aquatic organisms with a more consistent and less costly approach. Following the above paper, various passive sampling approaches have been tested for estimating the in-situ pore water concentrations, including semi-permeable membrane devices or SPMDs (Huckins et al., 2006), and polyethylene (PE) sheets (Booij et al., 2003; Adams et al., 2007,), Polyoxymethylene (POM) solid-phase extraction (Jonker and Koelmans, 2001; Cornelissen et al., 2008; Hawthorne et al., 2009; Hawthorne et al., 2011), and polydimethylsiloxane (PDMS) coated glass fibers (Mayer et al., 2000). For each of these methods, the samplers are placed in situ followed by a contaminant uptake period within the device. The porewater concentration is then back-calculated from a pre-established relationship.

Ideally, the sampling devices should be placed in the sediment until the equilibrium is achieved, so the ambient contaminant levels can be directly derived by calibrating the sampling concentration with the equilibrium partitioning coefficients. However, some previous studies have revealed that the equilibrium can take a significant amount of time (Booji et al. 2003; Adams et al., 2007; Cornelissen et al., 2008). To overcome this difficulty, the correlations between the concentrations in the passive sampling device and environment are modeled by non-equilibrium uptake, which rates are calibrated using performance reference compounds (PRCs) (Huckins et al., 1993; Huckins et al., 2002) or Multiple Thickness Method (Lampert et al. 2015; Choi et al., 2016). PRCs are analytically non-interfering chemicals that are pre-loaded in the passive sampler and

deplete to the environment during the sampler deployment. The depletion rate of a PRC reflects the uptake rates of a target analyte if sorption and desorption are reversible. The transport and the sorption properties of the PRCs used might be different from the target contaminant compounds, so the release rates need to be calibrated using fate and transport models.

The initial model used for calibrating PRC release rate is the first-order kinetic mass exchange model, which assumes the release/uptake rate constant of a specific compound is inversely proportional to its sorbent-water partitioning coefficients (Tomaszewski and Luthy, 2008). This model majorly focuses on the fate and transport behavior on passive sampler side since it assumes the ambient concentrations to be constant in the whole progress. Fernandez et al. (2009) presented a one-dimensional sorption-diffusion model to predict the fate and transport of PRCs and target compounds in both the passive sampler and the surrounding sediment system. Lampert et al. (2015) further discussed the internal and external resistance in the 1-D transport model and presented a practical analytical approach using PRC data to derive the site-specific effective diffusion/dispersion coefficient on sediment side. Choi et al. (2016) compared the performance of the two non-equilibrium models with the experimental data and concluded that the transport model with both parameters acquire approaches describes the experimental data better.

However, the existing 1-D transport models have important limits. It is based on the rectangular coordinate transport equations that only meet the circumstance of the PE or POM flat sheet passive sampler. The application of the model in cylindrical shape PDMS

fiber passive sampler may cause an underestimation of the release rates of target compounds that are less hydrophobic than the PRCs.

This chapter presented a cylindrical fate and transport model for describing and predicting the behavior of PRCs and the target compounds in the sediment. The model is closed by an innovative analytical solution developed using Laplace transform and asymptotic approximation. The closed-form analytical model is verified with the results from numerical model CapSim. The results of the cylindrical model are compared with the rectangular model.

5.2 MODELING APPROACHES

5.2.1 Existing 1-D rectangular model

The one-dimensional two-layer rectangular model presented by Fernandez et al. (2009) and Lampert et al. (2015) is briefly outlined here. The modeling domain includes a thin flat sheet of passive sampling material with thickness L and a semi-infinite thick sediment layer (Figure 5.1a). The concentration of the compound in the passive sampler C_p is described by the classic Fick's second equation (3.1), with the diffusivity of the compound in the sampling material as D_p. The transport in the sediment layer may include molecular diffusion, hydrodynamic dispersion, and bioturbation, which are motivated by random motions of molecules, random microscopic groundwater flow caused by heterogeneity of sediments, and random mixing process by benthic organism activities, respectively. The randomness of these transport processes allows us to model them using one combined gradient transport term with site-specific effective diffusivity

D. The total mass in an elementary sediment volume is defined as the sum of the mass in porewater and the mass associated with solids. ε is the local porosity of the sediment and ρ_b is the bulk density of the solid particles. Assuming the sorption process is in equilibrium, the solid phase concentrations q is a linear function of the porewater concentration C with either the water-sediment partitioning coefficient K_d , or the organic carbon partitioning coefficient K_{oc} and organic carbon fraction f_{oc}.

$$\frac{\partial C_p}{\partial t} = D_p \frac{\partial^2 C_p}{\partial z^2} \tag{5.1}$$

$$\frac{\partial}{\partial t}(\varepsilon C + \rho_b q) = D\frac{\partial^2 C}{\partial z^2} \tag{5.2}$$

$$R\frac{\partial C}{\partial t} = D\frac{\partial^2 C}{\partial z^2} \tag{5.3}$$

$$R = \varepsilon + \rho_b K_d = \varepsilon + \rho_b K_{oc} f_{oc} \tag{5.4}$$

The flux of the contaminant at the bottom surface is fixed at 0. At the sampler-sediment interface (x = L), the polymer concentration C_p and the porewater concentrations are assumed to remain in equilibrium. The porewater concentration of the compound at the infinite distance from the sampler is kept at the ambient porewater concentrations C_0. The initial concentration in the polymer and the sediment porewater are $C_{p,0}$ and C_0, respectively.

$$@x = 0,\ \frac{\partial C_p}{\partial x} = 0 \tag{5.5}$$

$$@x\ = L,\ D_p \frac{\partial C_p}{\partial x} = D \frac{\partial C}{\partial x} \text{ and } C_p = K_{pw} C \tag{5.6}$$

$$@x = \infty, C = C_0 \tag{5.7}$$

$$@t = 0,\ C_p = C_{p,0},\ \ C = C_0 \tag{5.8}$$

The analytical solution of the solute transport in two-layer rectangular porous media has been developed using Laplace transform with numerical inversion (Leij and Van Genuchten, 1995; Fernandez et al., 2009). The results are finalized to the fraction of steady-state (fss), which is parameter easily derived from experimental measurements. It is the polymer mass M_T normalized by the equilibrium mass $M_{T,ss}$ for the target compounds and polymer mass M_{PRC} normalized by the initial mass $M_{PRC,0}$ for PRC.

$$f_{ss} = \frac{M_T}{M_{T,ss}} = 1 - \frac{M_{PRC}}{M_{PRC,0}} = L^{-1}\{\frac{1}{s} - \frac{\sqrt{D/D_p}}{s^{0.5}(K_{pw} + \sqrt{D/D_p}\coth(\sqrt{s}))}\} \tag{5.9}$$

A simplified approximate analytical solution by neglecting the transport resistance in either passive sampling layer (internal) or the sediment layer (external) is given by Lampert et al. (2015). The relative importance of the internal and external resistance is derived by comparing the transport characteristic time of the two layers. For hydrophobic contaminants such as PAHs and PCBs in sediments, the external resistance dominates the transport process Lampert et al. (2015). The equation (5.10) has been used for calibrating

the fss of target compounds from the of the PRCs in for various sites (Apell and Gschwend, 2016; Choi et al. 2016; Belles et al., 2016).

$$f_{ss} = 1 - \exp\left(\frac{RDt}{L^2 {K_{pw}}^2}\right) \mathrm{erfc}\left(\frac{\sqrt{RDt}}{LK_{pw}}\right) \tag{5.10}$$

$$f_{ss} = 1 - \frac{8}{\pi^2} \sum_{n=0}^{\infty} \frac{1}{(2n+1)^2} \exp\left(-(2n+1)^2 \frac{\pi^2 \tau}{4}\right) \tag{5.11}$$

$$\frac{t_{external}}{t_{internal}} = \frac{36.1 {K_{pw}}^2 D_p}{RD} \tag{5.12}$$

5.2.2 1-D cylindrical model

Different from the PE and POM, PDMS and some other polymers (e.g., polyacrylate) have often been deployed as a coating on a thin SPME glass fiber (Ghosh et al., 2014). Lampert et al. (2015) suggested applying the above rectangular solution model to the cylindrical PDMS sampler with a thin coat as a close approximation. However, this assumption might fail on the external side (sediment side) when the compound transports a distance much further than the fiber thickness (Figure 5.1b). The characteristic length of diffusion for a common HOC is approximated using the correlation (5.13). During 30 days sampling time, a typical hydrophobic contaminant with sorption coefficient $K_d = 10^6 L/kg$ and molecular diffusivity $D = 5 \times 10^{-6} cm^2/s$ will diffuse approximate 0.5 mm in the sediment, which is roughly the same scale as the fiber outer radius. The characteristic lengths of various HOCs with specific compounds properties in a sediment

with organic carbon fraction $f_{oc} = 0.01$ are shown in Table 5.1. This traveling distance could be further increased by possible mixing processes like hydrodynamic dispersion or benthic organism bioturbation.

Compound	$\log(K_{ow})$	$D(10^{-6}cm^2/s)$	$\log(K_{oc})$	$r_{30}(mm)$
Naphthalene	3.17	2.98	2.79	117500
Dibenzo(a,h)pyrene	7.85	2.01	7.37	2.22
PCB2	4.65	2.43	3.99	6450
PCB28	5.67	2.22	4.90	735
PCB52	5.84	2.13	5.05	499
PCB180	7.36	1.94	5.53	159
PCB209	8.18	1.79	6.40	20.1

Table 5.1: Characteristic length (30 days) of selected PAH and PCBs in a given sediment

Thus, the application of the rectangular model and solutions on a cylindrical shape PDMS fiber might introduce additional errors in estimating the effective diffusivities and the fss for target contaminant.

$$r = \sqrt{\frac{4Dt}{R}} \tag{5.13}$$

The mass conservation equations for the two-layer porous cylindrical system are corrected by using cylindrical coordinates. The inner and outer radius of the fiber is labeled as L_i and L_o.

$$\text{Sampler layer } (L_i < r < L_o): \frac{\partial C_p}{\partial t} = D_p \frac{1}{r}\frac{\partial}{\partial r}\left(r\frac{\partial C_p}{\partial r}\right) \tag{5.14}$$

$$\text{Sediment layer}(r > L_o): R\frac{\partial C}{\partial t} = D\frac{1}{r}\frac{\partial}{\partial r}\left(r\frac{\partial C}{\partial r}\right) \tag{5.15}$$

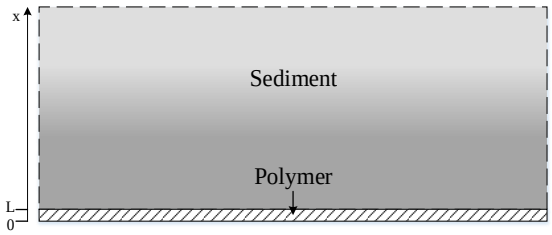

(a) Flat sheet passive sampler

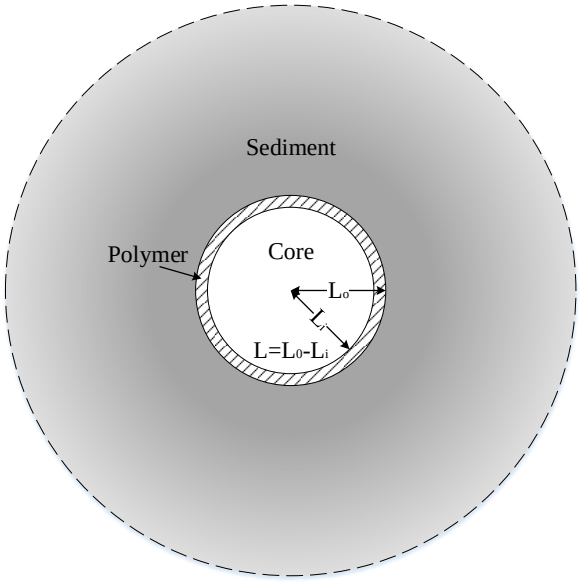

(b) Cylindrical fiber passive sampler

Figure 5.1: Sketch of the cross-section of passive sampler in sediment system

The thin fiber layer meets the semi steady-state transport assumption and the inner layer mass conservation equation (5.14) is replaced with a finite volume boundary condition described by Wilson (1948) and Crank (1948).

$$@\ r = R_o:\ \ K_{pw}A\frac{\partial C}{\partial t} = -D\frac{\partial C}{\partial r} * 2\pi L_o \tag{5.16}$$

The constant A in equation (5.16) is cross-section area of the thin polymer layer $A = \pi({L_o}^2 - {L_i}^2)$. The analytical solution for the cylindrical coordinate transport equation system at short time is given below. Defining a new integral variable M as the mass of the target compounds in the sediment side and transforming the governing equation (5.15) to the mass form by integrating both hand sides gives the following equations:

$$M = 2\pi \int_r^{\infty} r'C(t, r')dr' \tag{5.17}$$

$$(\varepsilon + \rho_b K_d)\frac{\partial M}{\partial t} = Dr\frac{\partial}{\partial r}(\frac{1}{r}\frac{\partial M}{\partial r}) \tag{5.18}$$

$$@r = L_o \quad (\varepsilon + \rho_b K_d)M - K_{pw}A\frac{1}{2\pi L_o}\frac{\partial M}{\partial r} = K_{pw}AC_0 \tag{5.19}$$

The analytical solution for a cylindrical coordinate system with infinite boundary condition was derived by Wilson (1948) and Crank (1948). They studied the adsorption of the dye into a semi-infinite cylinder from a finite dye batch. Using the Laplace transform suggested by these previous paper, the governing equation and boundary conditions is transformed to a typical Bessel differential equations with the solution (5.23).

$$\eta^2\frac{\partial^2 \bar{M}}{\partial \eta^2} - \eta\frac{\partial \bar{M}}{\partial \eta} - \eta^2 s\bar{M} = 0 \tag{5.20}$$

$$@\eta = \infty \quad \bar{M} = 0 \tag{5.21}$$

$$@\eta = 1 \quad \bar{M} - \frac{K_{pw}A}{2\pi L^2 R}\frac{\partial \bar{M}}{\partial \eta} = \frac{1}{s} \tag{5.22}$$

$$\bar{M} = \frac{1}{s\left(1+\xi\frac{\sqrt{s}K_0(\sqrt{s})}{2\,K_1(\sqrt{s})}\right)} \tag{5.23}$$

$\frac{K_0(\sqrt{s})}{K_1(\sqrt{s})}$ was further simplified by taking the asymptotic expansion at $s = \infty$ and the innovative inversed solution was derived in (5.25).

$$\frac{K_0(\sqrt{s})}{K_1(\sqrt{s})} \sim \frac{\sqrt{s}}{\sqrt{s}+1/2} \tag{5.24}$$

$$f_{ss} = 1 - \frac{1}{2\omega}\left(\left(\frac{1}{\xi}+\omega\right)e^{\left(\frac{1}{\xi}+\omega\right)^2\frac{\tau}{4}}\text{erfc}\left(\left(\frac{1}{\xi}+\omega\right)\frac{\sqrt{\tau}}{2}\right) - \left(\frac{1}{\xi}-\omega\right)e^{\left(\frac{1}{\xi}-\omega\right)^2\frac{\tau}{4}}\text{erfc}\left(\left(\frac{1}{\xi}-\omega\right)\frac{\sqrt{\tau}}{2}\right)\right) \tag{5.25}$$

Where $\xi = \frac{K_{pw}({L_o}^2-{L_i}^2)}{R{L_o}^2}$; $\omega = \frac{\sqrt{1-\xi}}{\xi}$ or $\frac{\sqrt{\xi-1}}{\xi}$j; $\tau = \frac{4Dt}{R{L_o}^2}$

The sorption ratio coefficient ξ represents the ratio of the equilibrium mass loading in thin polymer layer ($K_{pw}A$) versus an imaginary equilibrium mass loading by replacing the whole fiber (polymer layer and inert core) with sediments ($R\pi{L_o}^2$). In other words, it indicates the sorption capability of the polymer and the sediment to the given compound. In the cases that the sorption in the sediment is much stronger than in the polymer, the compound released from the fiber are adsorbed nearly simultaneously by the sediment and its transport would be limited to a short distance, which invalids the thin film assumption. In such cases, the coefficient ξ approaches to 0 and the cylindrical solution at the limit $\xi = 0$ is equivalent to the rectangular solution (5.26).

The dimensionless time τ can be explained as the ratio of the characteristic length of diffusion ($\sqrt{4Dt/R}$) versus the polymer layer thickness L_o. With the sampling time

grows, the PRC or target compounds travel to a further distance (characteristic length of diffusion). The thin layer assumption is, and the rectangular solution diverts away from the cylindrical solution.

5.3 RESULTS AND DISCUSSIONS

5.3.1 Solution verification

The results from the asymptotic analytical solution (5.25) were compared with the simulated results from the numerical model CapSim 3 in Figure 5.3. It is expected that the short time limit of $s = 0$ in Laplace domain would be limited with the increase of the time τ, which then lead a growth of the error of the asymptotic solution. Since the coefficient ξ determines the significance of the asymptotic approximate term $\frac{K_0(\sqrt{s})}{K_1(\sqrt{s})}$ in the Laplace domain solution, the increase of ξ values is also expected to contribute to a larger error for the analytical solution. Figure 5.2 illustrates the relative errors of fss derived by the analytical solution comparing to the numerical results from CapSim. As expected in theory, the absolute errors from asymptotic approximation increase with the growth of time and the coefficients ξ. The relative errors initially increase and then turn smaller as the absolute value of f_{ss} increases to large. Within the range of ξ and τ for HOCs in a typical passive sampling system, the relative error of the solution is controlled to be under 20%.

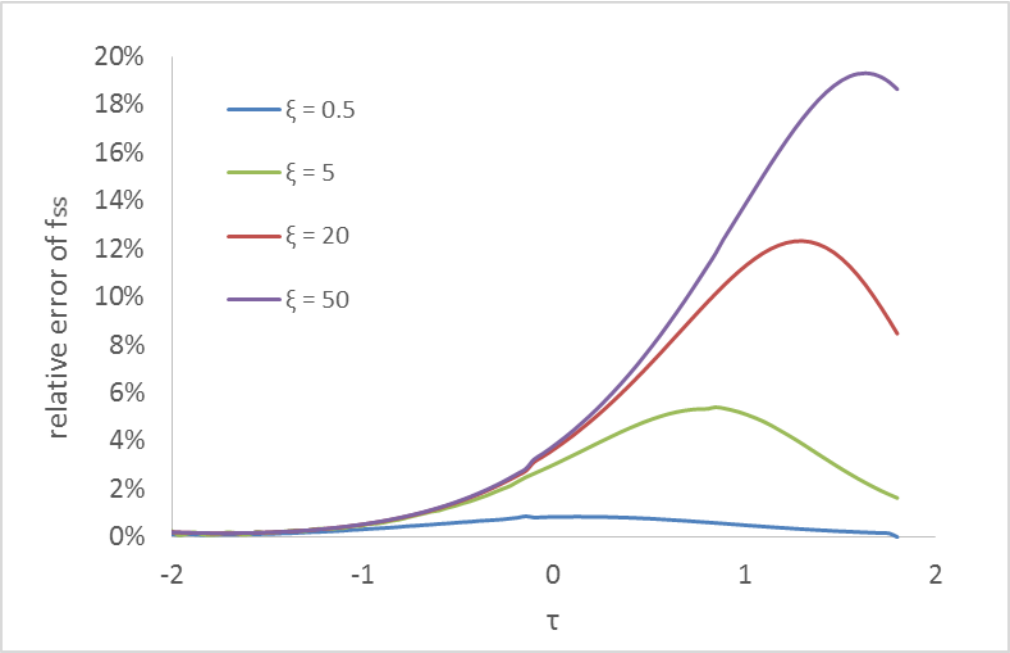

Figure 5.2: Illustration of the relative errors of fss calculated by the asymptotic approximate analytical solution (5.25) comparing to the numerical results for system with various value of coefficient ξ

5.3.2 Comparing the cylindrical solution versus rectangular solution

The rectangular solution (5.10) is also rearranged to be in the form of the dimensionless time τ and sorption ratio coefficient ξ for a easier comparison to the cylindrical solution. The sheet thickness L is defined as the average thickness of the fiber as $L = (L_o^2 - L_i^2)/2L_o$.

$$f_{ss} = 1 - \exp\left(\frac{\tau}{\xi^2}\right) \operatorname{erfc}\left(\frac{\sqrt{\tau}}{\xi}\right) \tag{5.26}$$

Figure 5.3 shows the difference in fractions of steady-state calculated by the cylindrical and rectangular coordinate solutions with the given dimensionless coefficients ξ and time τ. The results were also verified with the numerical results from the modified

transport model CapSim., The prediction of fss from the rectangular and the cylindrical solution models were closed for a passive sampling system with small $\xi = 0.5$. For a system with higher ξ range (from 20 to 50) and large τ, the fss predicted by the rectangular solution could be twice as much as the fss predicted by the cylindrical solution.

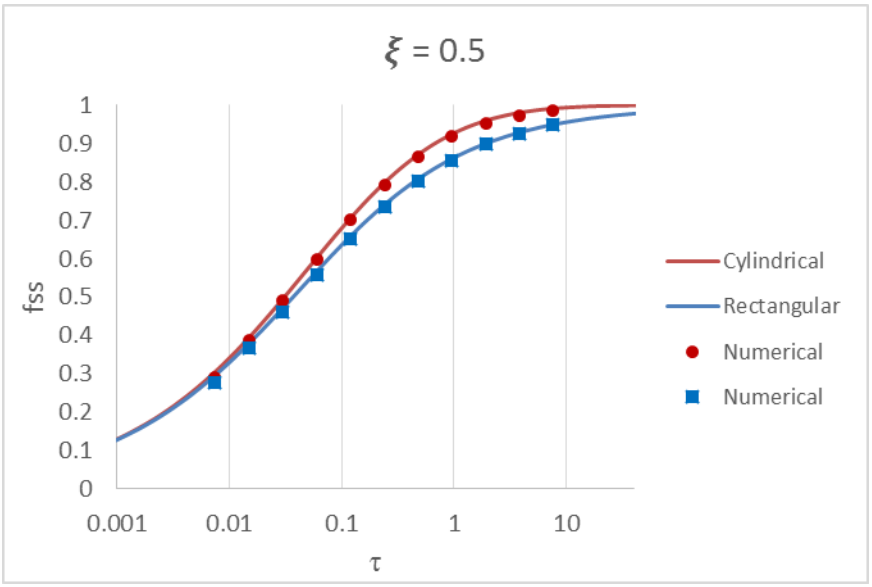

(a)

(Figure 5.3 continued next page)

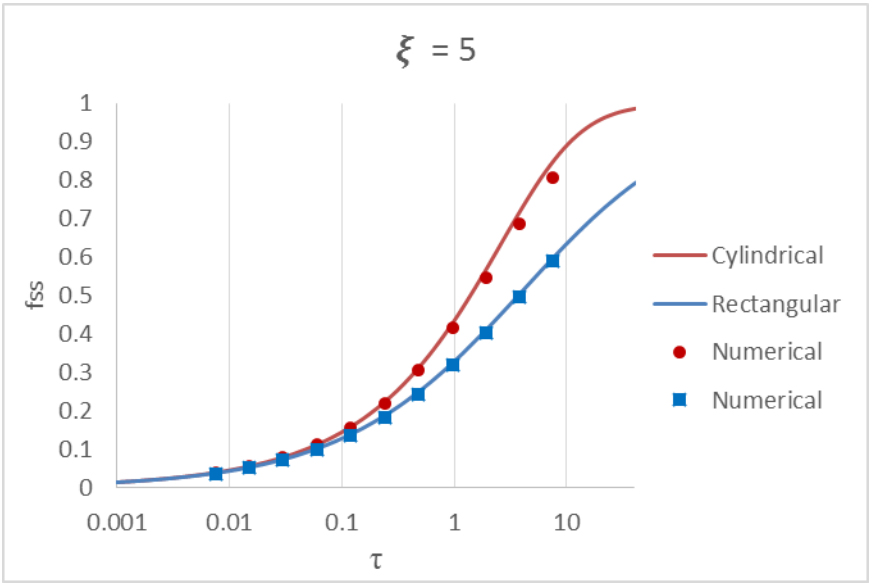

(b)

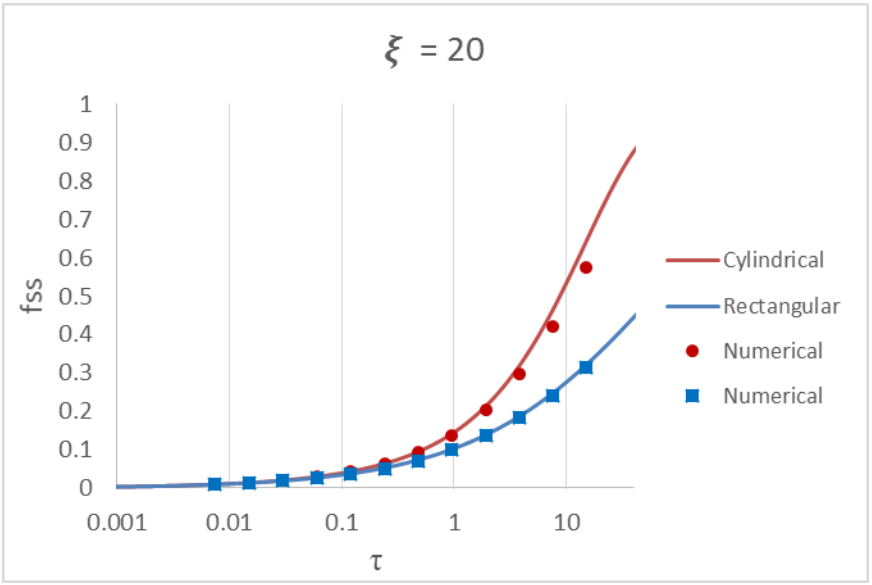

(c)

(Figure 5.3 continued next page)

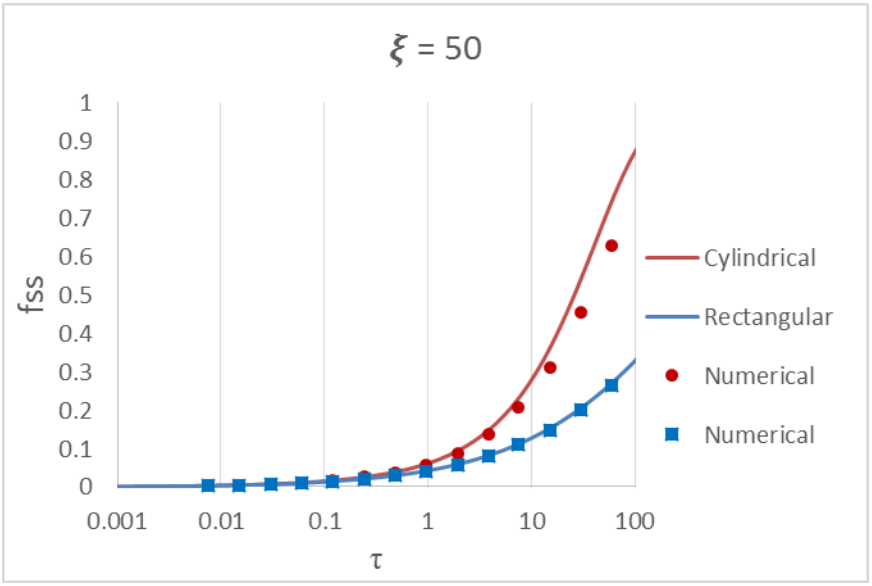

(d)

Figure 5.3: Comparison of fss calculated by analytical solution in rectangular coordinate (blue lines) and cylindrical coordinate (red lines), and simulated numerically by CapSim (dots) for a passive sampling system with various coefficient ξ

Table 5.2 shows the ξ and τ values for representative PAHs or PCBs released or uptake by a PDMS passive sampler device deployed in a natural sediment ($f_{OC} = 0.01$) over 28 days. The octanol-water partitioning coefficients K_{ow} are extracted from Hilal et al. (2004) for PAHs, and Hawker and Connell (1988) for PCBs. The PDMS-water partitioning coefficients K_P are calculated using the correlation (5.27) (Smedes et al. 2009; Ghosh et al., 2014) and the retardation factor R is calculated using the organic carbon fraction f_{OC} and the organic carbon partitioning coefficients K_{OC} that evaluated from correlation (2.4) and (2.5). The effective diffusion coefficients D here only include the tortuosity corrected water diffusivity. The effective diffusion coefficients measured

from the field measurements are commonly larger due to other mixing process such as hydrodynamic dispersion and benthic organism bioturbation.

$$\log(K_{pw}) = 0.947 \log(K_{ow}) - 0.017 \quad (5.27)$$

The calculated results show that the typical ξ values for HOCs ranges from 10.3 to 66.1 in various thickness PDMS fiber. The dimensionless time τ ranges widely from 0.007 to 32908 due to the range of the retardation factors. Both the coefficients ξ and the dimensionless time τ decreases with the increase of compound hydrophobicity or fiber polymer thickness.

		PDMS fibers		
Compound	$\log(K_{ow})$	$230/210\mu m$	$1060/1000\mu m$	$2100/2000\mu m$
Naphthalene	3.17	26.1	17.2	14.6
Dibenzo(a,h)pyrene	7.85	18.4	12.2	10.3
PCB2	4.65	23.5	15.5	13.1
PCB28	5.67	47.6	31.4	26.6
PCB52	5.84	48.6	32.2	27.2
PCB180	7.36	59.4	39.3	33.2
PCB209	8.18	66.1	43.7	36.9

(a) Dimensionless coefficient ξ

		PDMS fibers		
Compound	$D(10^{-6}cm^2/s)$	$230/210\mu m$	$1060/1000\mu m$	$2100/2000\mu m$
Naphthalene	2.98	32908	1549	395
Dibenzo(a,h)pyrene	2.01	0.622	0.029	0.007
PCB2	2.43	1807	85.1	21.7
PCB28	2.22	206	9.70	2.47
PCB52	2.13	140	6.58	1.68
PCB180	1.94	5.64	0.27	0.068
PCB209	1.79	0.97	0.046	0.012

(b) Dimensionless time τ for a 28 days sampling period (Lampert et al. 2013)

Table 5.2: The dimensionless coefficients ξ and time τ for selected PAH and PCBs in passive sampling system with various PDMS fibers

5.3.3 Calibration of PRCs

The previous results show that the rectangular model underestimates both the release and uptake rates in passive samplers of cylindrical geometry. The errors in calculating the uptake rates of target compounds might be offset by the calibrating the transport parameters R and D at the same transport condition.

Lampert et al. (2015) developed a calibration model by building a correlation between the octanol-water coefficients K_{ow} and the external transport parameters RD evaluated by the rectangular solution. The calibration model assumes the effective diffusion coefficient D is more dependent on the site-specific transport conditions rather than the properties of a compound. The RD values evaluated from release rates of PRCs shall be scaled with the octanol-water coefficients K_{ow} of a compound. In a sediment environment, the parameter RD should be a linear function of K_{ow} on a log scale. The calibration method had been verified using experimental data from various locations and performed a reliable prediction of the uptake rate of the target compound in the sediment (Lampert et al., 2015; Choi, 2016).

$$\log(RD) = a\log(K_{ow}) - b \tag{5.28}$$

The calibration equation (5.28) can be extended to dimensionless coefficients ξ and dimensionless time τ with a correction factor for the other hydrophobicity-related parameter K_p involved. The polymer-water partitioning coefficients K_{pw} in (5.27) are introduced in the modified calibration parameters a' and b'.

$$\log(\tau/\xi^2) = a' \log(K_{ow}) - b' \quad (5.29)$$

$$a' = a - 1.894;\ b' = b + 0.034 + 2\log(L) \quad (5.30)$$

A two-point PRC calibration is performed here to show the difference in target compounds f_{ss} predicted by the rectangular solution (5.26) and the cylindrical solution (5.25). In Figure 5.4, the fractions of steady-state (f_{ss}) calculated from both solutions for 5 PCBs in a $1060/1000\mu m$ PDMS fiber (Table 5.2) are plotted versus the dimensionless parameter τ/ξ^2. 2-point calibrations correlation between τ/ξ^2 and K_{ow} is generated from PRCs (PCB28 and 180, red dots) and then applied to calculate the τ/ξ^2 for the target compounds (PCB2, 101 and 209). The predicted f_{ss} for each target compound are read from the curves using the τ/ξ^2 calculated. The predicted f_{ss} in Table 5.3 summarized the parameters and results of the calibration calculation, the differences between the rectangular solution and the cylindrical solution are not significant for a maximum relative error of 8.5%. On the other hand, the system parameters $\log(\tau/\xi^2)$ and RD estimated from rectangular solutions are averaged one order larger than the value estimated by cylindrical. The results suggested that the rectangular model developed by Lampert et al. (2015) may still be a possible alternative in predicting the fss of target compounds for a cylindrical shape passive sampler system.

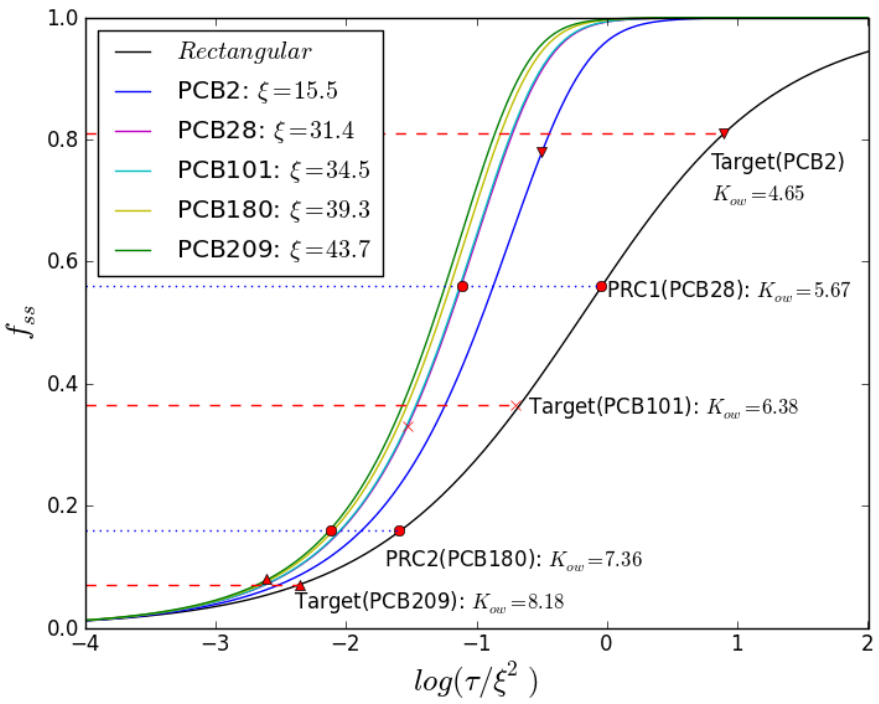

Figure 5.4: Illustration of predicting fss of target compounds, PCB2(upper triangles), PCB101(lower triangles) and PCB209(crosses) from the PRCs fss (red dots) using the rectangular solution or the cylindrical solutions.

			Rectangular		Cylindrical		
Compound	$\log(K_{ow})$	f_{ss}	$\log(\tau/\xi^2)$	log(RD)	ξ	$\log(\tau/\xi^2)$	log(RD)
PCB28	5.67	0.56	-0.046	-2.6	31.4	-1.11	-3.7
PCB180	7.36	0.16	-1.6	-2.6	39.3	-2.12	-3.1

(a) PRCs

		Rectangular			Cylindrical	
Compound	$\log(K_{ow})$	$\log(\tau/\xi^2)$	f_{ss}	$\boldsymbol{\xi}$	$\log(\tau/\xi^2)$	f_{ss}
PCB2	4.65	-0.70	0.07	15.5	-1.53	0.08
PCB52	5.84	-2.35	0.36	32.2	-2.61	0.33
PCB209	8.18	0.89	0.81	43.7	-0.50	0.78

(b) Target compound

Table 5.3: Comparison of the predicted fss using the rectangular and cylindrical solution with 2 PRCs

The difference of the calibration results using multiple PRCs is also shown here. The parameter RD is used here instead of τ/ξ^2 for its better performance in linear regression. The fss of six PRCs (PCB congeners 28, 52, 101, 138, 153 and 180) measured from experiments are applied to build calibration curves for predicting the RD and fss of 88 PCB contaminants. The calibration curves are derived by fitting the calculated logarithms of RD versus the logarithms of octanol-water partitioning coefficients $\log(K_{ow})$ by linear regression (Lampert et al. 2015). For the rectangular solution, the RD values are calculated directly from the solution. For the cylindrical coordinate solution, the best-fit effective diffusivity D and retardation factor R need to be determined (Appendix C). In this case, a variety of effective diffusivities D, ranging from $1 \times 10^6 \mathrm{cm}^2$ to $2 \times 10^5 \mathrm{cm}^2$, are input into the cylindrical solution (5.15) as estimated values. The returned parameters log(RD) are then correlated with K_{ow} (Figure 5.5). The effective diffusivity D is

determined by minimizing the coefficients of determination from the linear regression of log(RD) vs log(K_{ow}).

The estimated parameters are consistent with the 2-point calibration results. The RD values from the rectangular solution are 1-2 log units greater than from the cylindrical solution.

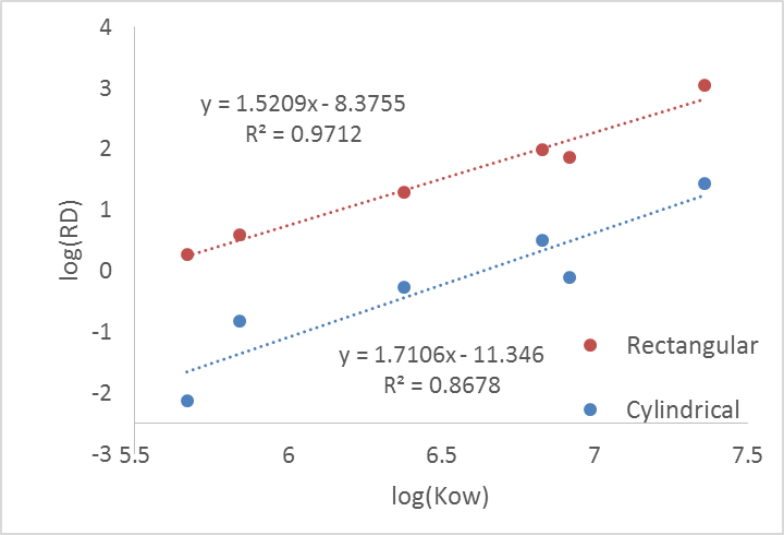

Figure 5.5: Estimated values of RDs for six PRCs from the rectangular and cylindrical solution

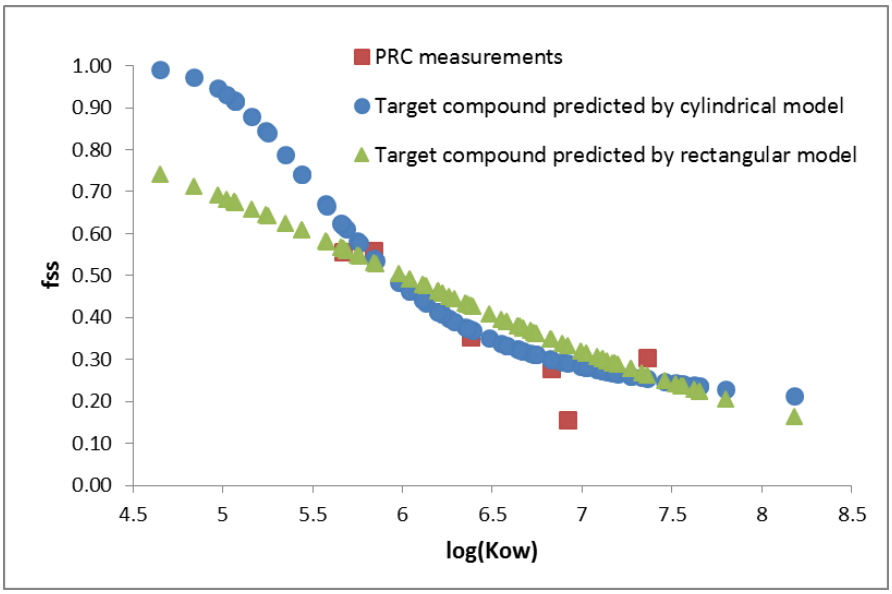

Figure 5.6: Comparison of 30-day fss of 88 target PCB congeners predicted by the rectangular and cylindrical solution using RD values estimated from calibration equation in Figure 5.5

5.4 CONCLUSIONS

This chapter discussed the limits of the application of existing 1-D rectangular model for a passive sampler in cylindrical geometry. A cylindrical analytical model for such systems was developed by applying the Laplace transform and asymptotic analysis. The prediction of fss from the cylindrical model and the rectangular model were compared in passive sampling systems with 1) given transport parameters and 2) transport parameters estimated from fss of PRCs. For the system with given transport parameters, the difference of the predicted fss depends on the transport distance of the compounds during the sampling period. For the system with parameters calibrated from PRCs, the predictions of f_{ss} from two solutions are similar, but the estimated system transport parameters (e.g., RD) can be orders different.

5.5 REFERENCES

Adams, R. G., R. Lohmann, L. A. Fernandez, J. K. MacFarlane and P. M. Gschwend (2007). "Polyethylene devices: Passive samplers for measuring dissolved hydrophobic organic compounds in aquatic environments." Environmental Science & Technology 41(4): 1317-1323.

Apell, J. N. and P. M. Gschwend (2016). "In situ passive sampling of sediments in the Lower Duwamish Waterway Superfund site: Replicability, comparison with ex situ measurements, and use of data." Environmental Pollution 218: 95-101.

Belles, A., C. Alary, J. Criquet and G. Billon (2016). "A new application of passive samplers as indicators of in-situ biodegradation processes." Chemosphere 164: 347-354.

Booij, K., H. E. Hofmans, C. V. Fischer and E. M. Van Weerlee (2003). "Temperature-dependent uptake rates of nonpolar organic compounds by semipermeable membrane devices and low-density polyethylene membranes." Environmental Science & Technology 37(2): 361-366.

Burton, G. A. (1991). "Assessing the toxicity of freshwater sediments." Environmental Toxicology and Chemistry 10(12): 1585-1627.

Choi, Y., Y. Wu, R. G. Luthy and S. Kang (2016). "Non-equilibrium passive sampling of hydrophobic organic contaminants in sediment pore-water: PCB exchange kinetics." Journal of Hazardous Materials 318: 579-586.

Cornelissen, G., A. Pettersen, D. Broman, P. Mayer and G. D. Breedveld (2008). "Field testing of equilibrium passive samplers to determine freely dissolved native polycyclic aromatic hydrocarbon concentrations." Environmental Toxicology and Chemistry 27(3): 499-508.

Crank, J. (1948). "XLV. A diffusion problem in which the amount of diffusing substance is finite.—IV. solutions for small values of the time." The London, Edinburgh, and Dublin Philosophical Magazine and Journal of Science 39(292): 362-376.

Di Toro, D. M., C. S. Zarba, D. J. Hansen, W. J. Berry, R. C. Swartz, C. E. Cowan, S. P. Pavlou, H. E. Allen, N. A. Thomas and P. R. Paquin (1991). "Technical basis for establishing sediment quality criteria for nonionic organic chemicals using equilibrium partitioning." Environmental Toxicology and Chemistry 10(12): 1541-1583.

Fernandez, L. A., C. F. Harvey and P. M. Gschwend (2009). "Using performance reference compounds in polyethylene passive samplers to deduce sediment porewater concentrations for numerous target chemicals." Environmental Science & Technology 43(23): 8888-8894.

Ghosh, U., S. Kane Driscoll, R. M. Burgess, M. T. Jonker, D. Reible, F. Gobas, Y. Choi, S. E. Apitz, K. A. Maruya and W. R. Gala (2014). "Passive sampling methods for contaminated sediments: Practical guidance for selection, calibration, and implementation." Integrated Environmental Assessment and Management 10(2): 210-223.

Hawker, D. W. and D. W. Connell (1988). "Octanol-water partition coefficients of polychlorinated biphenyl congeners." Environmental Science & Technology 22(4): 382-387.

Hawthorne, S. B., M. T. Jonker, S. A. van der Heijden, C. B. Grabanski, N. A. Azzolina and D. J. Miller (2011). "Measuring picogram per liter concentrations of freely dissolved parent and alkyl PAHs (PAH-34), using passive sampling with polyoxymethylene." Analytical Chemistry 83(17): 6754-6761.

Hawthorne, S. B., D. J. Miller and C. B. Grabanski (2009). "Measuring low picogram per liter concentrations of freely dissolved polychlorinated biphenyls in sediment pore water using passive sampling with polyoxymethylene." Analytical Chemistry 81(22): 9472-9480.

Hilal, S., S. Karickhoff and L. Carreira (2004). "Prediction of the solubility, activity coefficient and liquid/liquid partition coefficient of organic compounds." Molecular Informatics 23(9): 709-720.

Huckins, J. N., G. K. Manuweera, J. D. Petty, D. Mackay and J. A. Lebo (1993). "Lipid-containing semipermeable membrane devices for monitoring organic contaminants in water." Environmental Science & Technology 27(12): 2489-2496.

Huckins, J. N., J. D. Petty and K. Booij (2006). Monitors of organic chemicals in the environment: semipermeable membrane devices, Springer Science & Business Media.

Huckins, J. N., J. D. Petty, J. A. Lebo, F. V. Almeida, K. Booij, D. A. Alvarez, W. L. Cranor, R. C. Clark and B. B. Mogensen (2002). "Development of the permeability/performance reference compound approach for in situ calibration of semipermeable membrane devices." Environmental Science & Technology 36(1): 85-91.

Huckins, J. N., M. W. Tubergen and G. K. Manuweera (1990). "Semipermeable membrane devices containing model lipid: A new approach to monitoring the bioavaiiability of lipophilic contaminants and estimating their bioconcentration potential." Chemosphere 20(5): 533-552.

Jonker, M. T. and A. A. Koelmans (2001). "Polyoxymethylene solid phase extraction as a partitioning method for hydrophobic organic chemicals in sediment and soot." Environmental Science & Technology 35(18): 3742-3748.

Kraepiel, A. M., K. Keller, H. B. Chin, E. G. Malcolm and F. M. Morel (2003). "Sources and variations of mercury in tuna." Environmental Science & Technology 37(24): 5551-5558.

Lampert, D., C. Thomas and D. Reible (2015). "Internal and external transport significance for predicting contaminant uptake rates in passive samplers." Chemosphere 119: 910-916.

Leij, F. and M. T. Van Genuchten (1995). "Approximate analytical solutions for solute transport in two-layer porous media." Transport in Porous Media 18(1): 65-85.

Lu, X., D. D. Reible and J. W. Fleeger (2004). "Bioavailability and assimilation of sediment‐associated benzo [a] pyrene by Ilyodrilus templetoni (oligochaeta)." Environmental Toxicology and Chemistry 23(1): 57-64.

Lu, X., D. D. Reible and J. W. Fleeger (2004). "Relative importance of ingested sediment versus pore water as uptake routes for PAHs to the deposit-feeding oligochaete Ilyodrilus templetoni." Archives of Environmental Contamination and Toxicology 47(2): 207-214.

Lu, X., D. D. Reible and J. W. Fleeger (2006). "Bioavailability of polycyclic aromatic hydrocarbons in field‐contaminated Anacostia River (Washington, DC) sediment." Environmental Toxicology and Chemistry 25(11): 2869-2874.

Mayer, P., W. H. Vaes and J. L. Hermens (2000). "Absorption of hydrophobic compounds into the poly (dimethylsiloxane) coating of solid-phase microextraction fibers: High partition coefficients and fluorescence microscopy images." Analytical Chemistry 72(3): 459-464.

Smedes, F., R. W. Geertsma, T. v. d. Zande and K. Booij (2009). "Polymer− water partition coefficients of hydrophobic compounds for passive sampling: Application of cosolvent models for validation." Environmental Science & Technology 43(18): 7047-7054.

Tomaszewski, J. E. and R. G. Luthy (2008). "Field deployment of polyethylene devices to measure PCB concentrations in pore water of contaminated sediment." Environmental Science & Technology 42(16): 6086-6091.

Wilson, A. (1948). "V. A diffusion problem in which the amount of diffusing substance is finite: I." The London, Edinburgh, and Dublin Philosophical Magazine and Journal of Science 39(288): 48-58.

Chapter 6 Modeling the Impacts from Non-linear Sorption to the Behavior of PRCs and Target Compounds in Passive Sampler Systems

6.1 INTRODUCTION

As stated in the previous section, performance reference compounds (PRC) have been considered a reliable calibrating approach for estimating non-equilibrium uptake rates of target compounds during passive sampling. The initial model used for calibrating PRC release rate is the first-order kinetic mass exchange model, which assumes the release/uptake rate constant of a particular compound is inversely proportional to its sorbent-water partitioning coefficients (Tomaszewski and Luthy, 2008). This model mostly focuses on the fate and transport behavior on passive sampler side since it assumes the ambient concentrations to be constant during the whole sampling period. Fernandez et al. 2009 presented a one-dimensional sorption-diffusion model to predict the fate and transport of PRCs and target compounds in both the passive sampler and the surrounding sediment system. Lampert et al. (2015) further discussed the internal and external resistance in the 1-D transport model and presented a practical analytical approach to calibrating the site-specific target compound uptake rates using PRC measurements. Choi et al. (2016) compared the performance of the two non-equilibrium models with the experimental data and concluded that the transport model introduced by Lampert et al. (2015) describes the experimental data better.

The above non-equilibrium uptake models all assume that the partitioning of PRCs and target HOCs in sediment outside the passive sampler follows the linear sorption isotherm (5.3). However, for sediment sites that are remediated using active sorptive materials such as activated carbon (AC), the sorption process on the sediment/sorbent side might be dominated by the non-linear sorption behavior. Thus, the previous assumption of the symmetric behavior of PRCs and target compounds may fail. The release rate and uptake rate of a compound will not only be dependent on its properties but also on the concentration levels.

The non-symmetric behavior of the PRC and target compounds are reported by two papers with opposite conclusions. Choi et al. (2016) recognized a non-symmetric behavior of the PRC and target compounds. They discovered that the PRC released rates from a PE sheet passive sampler to the activated carbon amended sediment from Hunter's Pond were faster than the uptake rates of the target compounds. The RD values for target compounds estimated by (5.10) are half order smaller than the values for PRCs. They suggested this anisotropic phenomenon might be a result of sorption-desorption hysteresis from the aging and sequestration of the legacy contaminants in sediments.

In an earlier research by Bao et al. (2015), the release of the C-13 labeled PRCs are found to be slower than the uptake rates of the corresponding contaminant without a label. In this experiment, a group of contaminants with known concentrations are pre-spiked into the marine sediment from New Fields in Port Gamble (WA, USA). The porewater concentrations in the prepared sediments are measured using PDMS fibers within a sampling period varies from 82 to 168 days. For each scenario with various

thickness fibers and sorbents, at least six intermediate time points were measured to study the transient behavior of PRCs and target analytes. They observed hysteretic desorption of PRCs and adsorption of target compounds.

This chapter shows the application of the model CapSim to simulate the behavior of PRCs and target compounds in a passive sampling system deployed in activated carbon. The results indicate that the non-linear sorption will lead to non-symmetric phenomena between the release of PRCs and the uptake of target compounds. The results and conclusion can also be expanded to sediment remediation systems that have strong non-linear sorption characteristics, such as activated carbon amendment caps or in-situ treatments and sediments with nonlinear sorption (e.g. so-called "black carbon" such as soot).

6.2 MODEL DESCRIPTION

The details of passive sampling and the use of PRCs have been discussed in the previous chapter. Here we briefly summarize the fundamental equations and highlights the possible non-linear term in the system. The passive sampling device deploying in the sediment is treated as a two-layer rectangular or cylindrical system with a thin polymer layer and a semi-infinite sediment layer. The transport rate of the target analytes into the polymer is calibrated by measuring the release rate of the PRCs, which are a group of inert chemicals preloaded in the polymer layer with a known concentration. The percentage of PRCs loss and the percentage of target analytes to its equilibrium concentration are connected by the fraction of steady-state (fss) model. 1-D fate and

transport models were used in Chapter 5 to correlate the fss of target compounds from the PRC loss.

6.2.1 1-D fate and transport model in activated carbon amendment caps

The 1-D two-layer transport model with linear sorption isotherms in a rectangular coordinate or a cylindrical coordinate has been presented by Fernandez et al. (2009). A particular form of that transport model in an amendment cap made of activated carbon is shown as.

$$\frac{\partial C_p}{\partial t} = D_p \nabla^2 C_p \tag{6.1}$$

$$\frac{\partial}{\partial t}(\varepsilon C + \rho_{AC} q_{AC}) = D\nabla^2 C \tag{6.2}$$

The sorption of HOCs in activated carbon, are modeled by either the equilibrium Freundlich isotherm with coefficients K_{AC} and N_{AC} or a one-compartment kinetic model with rate constant k_{AC}. The sorption rate is defined as a first-order function of the difference between the present porewater concentration and the concentration in equilibrium with the solid phase.

$$q_{AC} = K_{AC} C^{N_{AC}} \tag{6.3}$$

$$\rho_{AC} \frac{\partial q_{AC}}{\partial t} = k_{AC} \left(C - \left(\frac{q_{AC}}{K_{AC}} \right)^{\frac{1}{N_{AC}}} \right) \tag{6.4}$$

The previous modeling efforts in PRC calibration and fss prediction have shown that the behavior of a compound in the external layer is dependent on its sorption activity in the solid material (Lampert et al., 2015; Choi et al., 2016). The current calibration models

assume that the partitioning/sorption of a compound in solid materials only depend on the chemical property of itself (e.g., hydrophobicity). However, in an amendment layer with activated carbon, the partitioning/sorption process that described by non-linear Freundlich isotherm are related to the local porewater concentration of the compound. In such cases, the assumption of non-concentration-dependent sorption may fail and the behavior of PRCs and target compounds may become non-symmetric when they present a different concentrations in the sediment.

6.2.2 Competitive sorption between PRC and target compounds

Sorption of HOCs in activated carbon may result in competition for the limited sorptive sites. Such competitive sorption behavior have been studied and modeled both theoretically and empirically (Xia and Ball, 1999; Sheindorf et al., 1981). The classic fate and transport models in activated carbon amendment cap or other non-linear sorptive remediation materials do not consider a separate competitive sorption term. The sorption competition effect is usually already included in the empirical sorption coefficients such as Freundlich isotherm coefficients. These coefficients are commonly measured in batch equilibrium experiments along with other same class of contaminants. Thus the coefficients should be roughly calibrated for competitive sorption before it is introduced to the system.

However, such assumptions would not fully cover the case of passive sampling, where the PRCs are only an isotope-labeled form of the contaminants that exist in the contaminants. The sorption characteristic of the isotope-labeled PRCs and the non-

labeled contaminants are the same (Ghosh et al., 2014). The Freundlich isotherm could be considered to apply to the total concentration instead of the individual isotopic compounds (6.5). The PRC concentration pre-loaded in the passive samplers are usually higher than the environmental concentrations of target compounds to ensure that detection. It potentially dominates the local sorption isotherm and affects the behavior of the target compound.

$$q_{AC,PRC} + q_{AC,Target} = K_{AC}(C_{PRC} + C_{Target})^{N_{AC}} \quad (6.5)$$

$$q_{AC,PRC}/q_{AC,Target} = C_{PRC}/C_{Target} \quad (6.6)$$

At equilibrium, one other criteria of the labeled/non-labeled compounds is that the abundance of the isotope should be the same in the solid phase and the porewater phase (6.6). Based on these two criteria, a first-order kinetic sorption model for PRC and the target compound was developed. The desorption term is derived by forcing the system to achieve the two requirements (6.5) and (6.6) at equilibrium ($\frac{\partial q_{AC,PRC}}{\partial t} = 0$).

$$\rho_{AC}\frac{\partial q_{AC,PRC}}{\partial t} = k_{AC}\left(C_{PRC} - \left(\frac{q_{AC,PRC}+q_{AC,Target}}{K_{AC}}\right)^{\frac{1}{N_{AC}}}\frac{q_{AC,PRC}}{q_{AC,PRC}+q_{AC,Target}}\right) \quad (6.7)$$

$$\rho_{AC}\frac{\partial q_{AC,Target}}{\partial t} = k_{AC}\left(C_{Target} - \left(\frac{q_{AC,PRC}+q_{AC,Target}}{K_{AC}}\right)^{\frac{1}{N_{AC}}}\frac{q_{AC,Target}}{q_{AC,PRC}+q_{AC,Target}}\right) \quad (6.8)$$

6.3 RESULTS AND DISCUSSION

6.3.1 Sorption model without competitive sorption

The compounds from the same chemical class are commonly applied as PRCs because they share similar properties as the target analytes. For example, in the lab experiment conducted by Choi et al. (2016) to predict the f_{ss} of target compounds PCBs 43, 101, 153 and 180, PCB congeners 29, 69, 103, 155, 192 were selected and pre-spiked in PE as PRCs. In this situation, the sorption of PRCs and target compounds are assumed to be independent.

To show the behavior in a more comparable way with no calibration for compound properties, the PRC and target compounds are assumed to share the same properties in the following examples. The Freundlich isotherm used here for activated carbon is from Azhar (2015) with coefficients $\log(K_f) = 6.91$ and $N = 0.416$ and the PRC and target compound sorption and desorption are independent of each other. Other system parameters and compound properties are summarized in Table 6.1. The initial porewater concentrations for PRCs here represent the water concentrations in equilibrium with the pre-spiked concentration in a fiber.

Figure 6.1 illustrates the fss values of PRCs and target compounds predicted by the 1-D transport model (6.1) and (6.2) with various initial concentrations. In the case of a low PRC porewater concentration the Freundlich isotherm suggests stronger sorption of the PRC than the target compounds. As a result, the estimated release rates of the PRC are faster than the uptake rates of the target compounds (i.e. scenario 1>scenario 2).

However, in cases of high PRC concentration, the release rates of the PRC is reduced and surpassed by the uptake rates of the target compounds (i.e. scenario 1 <scenario 3).

In field measurements, the PRCs are usually pre-spiked at a concentration higher than the target compound for the accuracy of the analysis. Within the range of loading concentrations, the fss for target compounds could be either higher or lower than the PRC fss (scenario 1 vs scenarios 4 and 5).

The rate of PRC release is also a function of the equilibrium sorption as shown in Figure 6.1c. Thus more sorbing compounds exhibit faster desorption rates, again potentially inconsistent with the desired target compounds.

Compound	$D_P(10^{-12}\text{cm/s})$	$\log K_P$
PRC	4.5	5.51
Target	4.5	5.51

(a) Chemical properties

Compound	Thickness(μm)	ε	ρ_b(kg/L)
Polymer	30	0	1
Sediment	∞	0.4	0.4

(b) Solid material parameters

		Equilibrium porewater concentration (μg/L)	
Scenarios	Compound	Polymer (C_p/K_p)	Activated carbon (C)
1	PRC	0.01	0
2	Target	0	0.01
3	Target	0	0.0001
4	Target	0	0.001
5	PRC	0.1	0
6	PRC	0.1	0.01
7	PRC	0.1	0.001
8	PRC	0.1	0.0001

(c) System parameters

Table 6.1: Summary of properties and parameters in the passive sampling system with activated carbon amendments

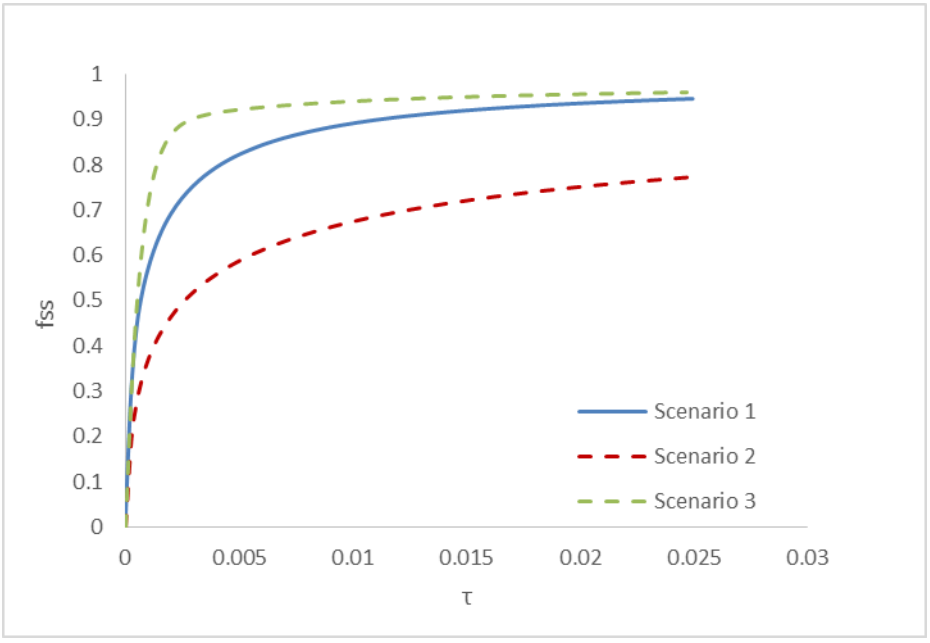

(a)

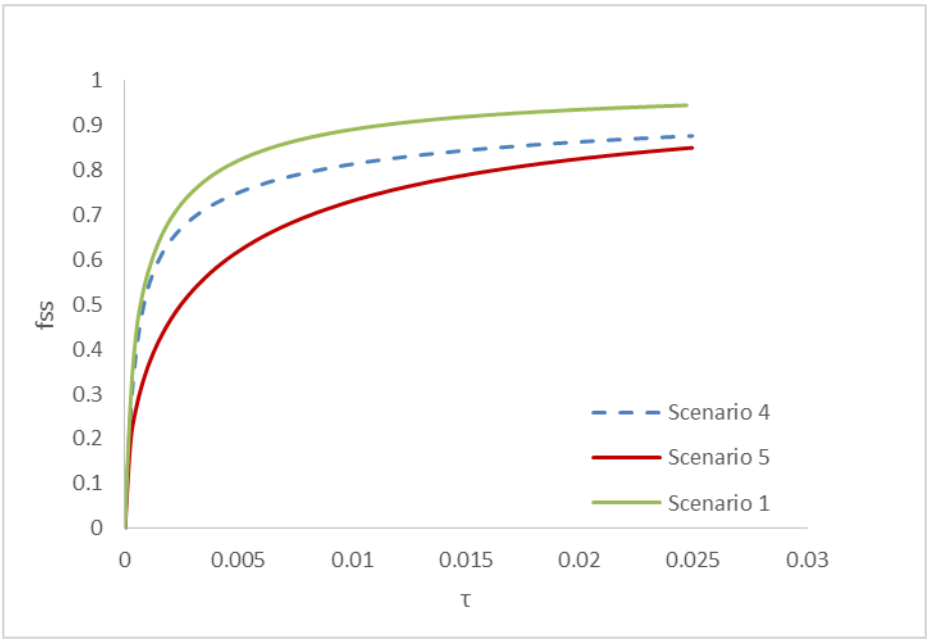

(b)

(Figure 6.1 continued next page)

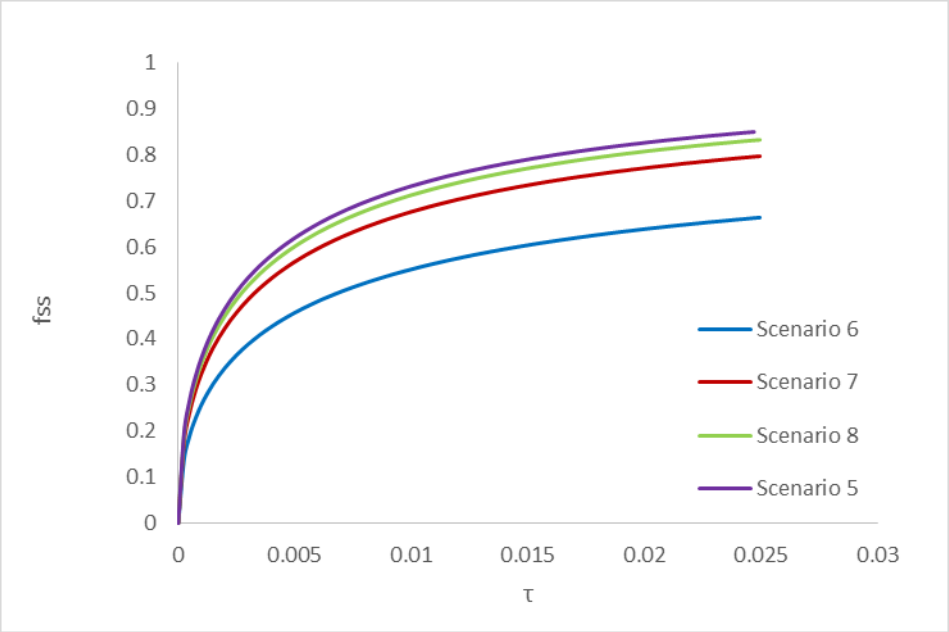

(c)

Figure 6.1: Comparison of the fss of PRCs and target compounds with various initial concentrations

The ratio of the PRC and target fss values are related to the concentration ratio (PRC/target) for different powers on the Freundlich isotherm in Figure 6.2. For the compounds with Freundlich isotherm coefficients $N_{AC} < 1$, PRCs overestimate fss for target compounds for low PRC concentration and underestimate at high PRC concentration. For the compounds with Freundlich isotherm coefficients $N_{AC} > 1$, PRCs underestimate fss for target compounds for low PRC concentration and overestimate at high PRC concentration. The simulation results suggested the PRC concentration should be spiked at roughly 10 times higher than the expected target

compound concentration to minimize the potential error of PRC methods in activated carbon.

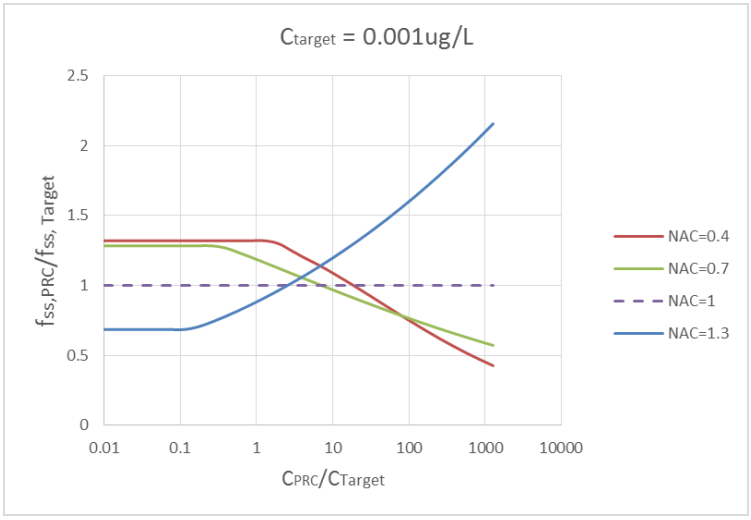

(a)

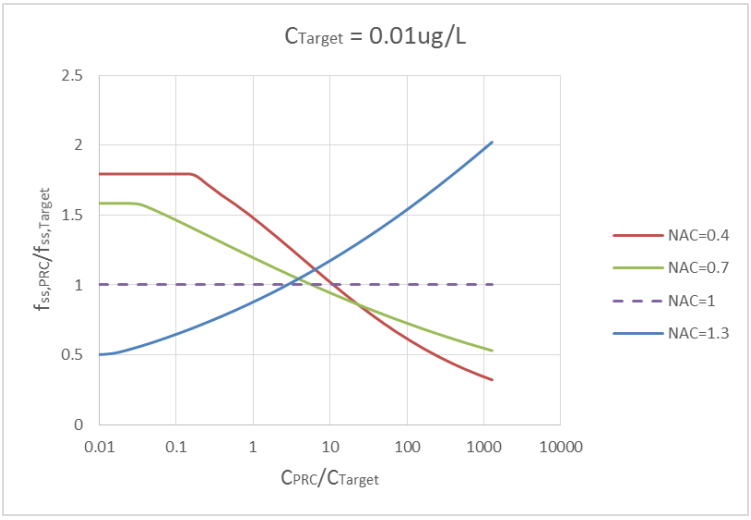

(b)

Figure 6.2: The dependency of the fss ratio on the initial concentration ratio between PRCs and target compounds with various sorption isotherm in activated carbon

6.3.2 Sorption model with competitive sorption

The isotope-labeled or the deuterated form of the compounds of interest has been suggested to be a good PRC because it behaves effectively identically to the target compound (Huckins et al., 2002; Fernandez et al., 2009). This is based on the assumption that isotope-labeled compounds and the native compounds do not interfere with each other in sediments. For sorption processes that show as a nonlinear dependency on the concentrations, such as in activated carbon, this assumption may be impacted.

Figure 6.3 shows the behavior of PRC and target analytes when they are the isotope-labeled form and non-labeled form of the same compound. The kinetic equations (6.7) and (6.8) are used to model the transient sorption of PRCs and target compounds in activated carbon with a kinetic rate constant k_{AC} of $100\ day^{-1}$. In the first three cases with various PRC and target concentrations, the release rates of PRCs are identical to the uptake rates of the target compounds. The fourth case, which presents the highest PRC concentration in four cases, shows that the target compound uptake rate is faster than the PRCs. The results suggested that the isotope labeled PRCs may be a reliable approach in predicting the f_{ss} of the same compound in activated carbon.

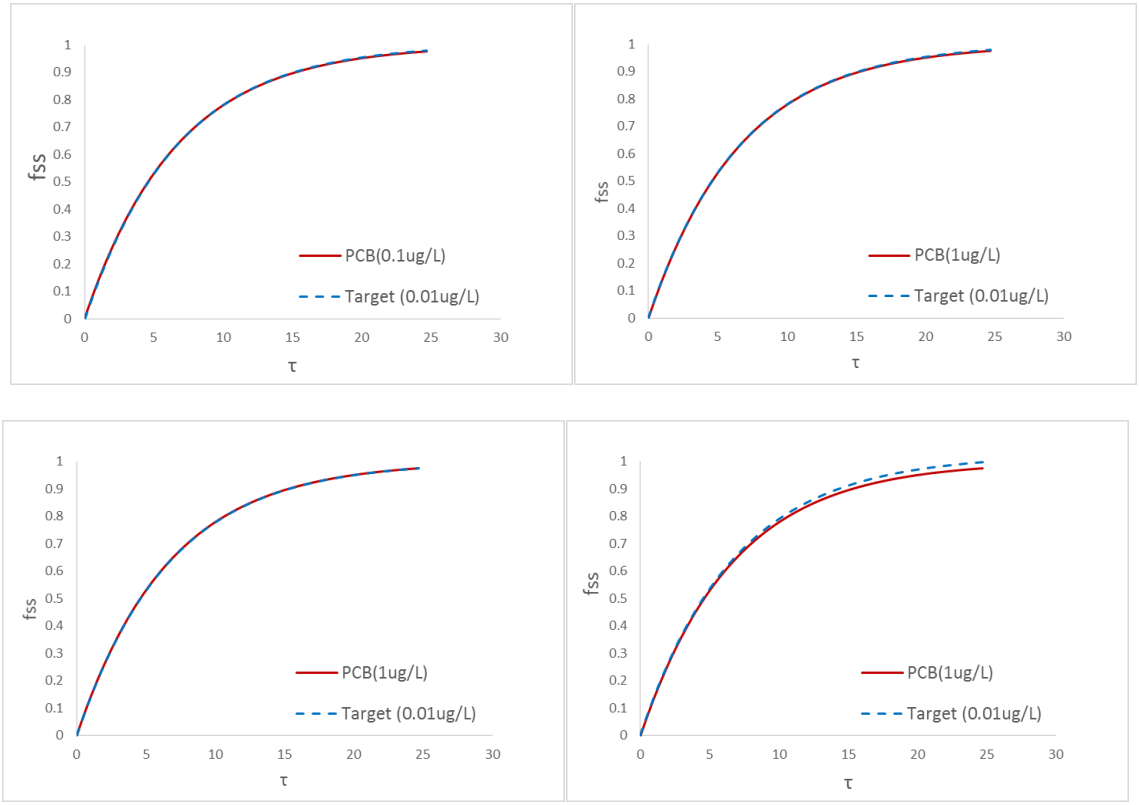

Figure 6.3: Comparison of the fss of isotope-labeled PRCs and target compounds with various initial concentrations

6.4 CONCLUSIONS

Previous literatures suggest that the behavior of PRCs and target compounds should be identical relative to their approach to steady state. However, two recent studies (Bao et al., 2015, Choi et al., 2016) observed non-symmetric behavior of PRCs and target compounds in activated carbon amended sediments. This chapter applied a numerical transport model CapSim to simulate the behavior of PRCs and target compounds in a strong non-linear sorptive sorbent - activated carbon. The potential competition between

a target compound and a PRC that is an isotopic form of the target compounds is also discussed here. The simulated results suggested that the non-linear sorption might be a potential cause of the observed non-symmetric behavior of the PRCs and target compounds. The simulation results also suggest that the isotope-labeled PRC might perform better in predicating the fss of target compounds in activated carbon rather than a common undetected compound.

6.5 REFERENCES

Azhar, W. (2015). Evaluation of sorbing amendments for in-situ remediation of contaminated sediments (Order No. 10035640). Available from ProQuest Dissertations & Theses Global. (1773635522). Retrieved from https://search.proquest.com/docview/1773635522?accountid=7098

Bao, L. J., X. Wu, F. Jia, E. Y. Zeng and J. Gan (2015). "Isotopic exchange on SPME fiber in sediment under stagnant conditions: Implications for field application of PRC calibration." Environmental Toxicology and Chemistry.

Choi, Y., Y. Wu, R. G. Luthy and S. Kang (2016). "Non-equilibrium passive sampling of hydrophobic organic contaminants in sediment pore-water: PCB exchange kinetics." Journal of Hazardous Materials 318: 579-586.

Fernandez, L. A., C. F. Harvey and P. M. Gschwend (2009). "Using performance reference compounds in polyethylene passive samplers to deduce sediment porewater concentrations for numerous target chemicals." Environmental Science & Technology 43(23): 8888-8894.

Ghosh, U., S. Kane Driscoll, R. M. Burgess, M. T. Jonker, D. Reible, F. Gobas, Y. Choi, S. E. Apitz, K. A. Maruya and W. R. Gala (2014). "Passive sampling methods for contaminated sediments: Practical guidance for selection, calibration, and implementation." Integrated Environmental Assessment and Management 10(2): 210-223.

Huckins, J. N., J. D. Petty, J. A. Lebo, F. V. Almeida, K. Booij, D. A. Alvarez, W. L. Cranor, R. C. Clark and B. B. Mogensen (2002). "Development of the permeability/performance reference compound approach for in situ calibration of

semipermeable membrane devices." Environmental Science & Technology 36(1): 85-91.

Lampert, D., C. Thomas and D. Reible (2015). "Internal and external transport significance for predicting contaminant uptake rates in passive samplers." Chemosphere 119: 910-916.

Sheindorf, C., M. Rebhun and M. Sheintuch (1981). "A Freundlich-type multicomponent isotherm." Journal of Colloid and Interface Science 79(1): 136-142.

Tomaszewski, J. E. and R. G. Luthy (2008). "Field deployment of polyethylene devices to measure PCB concentrations in pore water of contaminated sediment." Environmental Science & Technology 42(16): 6086-6091.

Xia, G. and W. P. Ball (1999). "Adsorption-partitioning uptake of nine low-polarity organic chemicals on a natural sorbent." Environmental Science & Technology 33(2): 262-269.

Chapter 7 Conclusions and Recommendations

7.1 RESEARCH OBJECTIVES

The goal of this research is to develop different modeling tools for the assessment and remediation of the contaminated sediments. This was achieved by focusing on the following main points.

- Developing an innovative analytical solution for 1-D transient advection-dispersion equation in multi-layered porous media.
- Developing an analytical model CapAn in spreadsheet based on the existing analytical solution.
- Developing a numerical model, CapSim, to model the transport and fate of solute chemicals under more general conditions. Several important processes in sediment environments, such as nonlinear and non-equilibrium sorption and reaction, bioturbation, consolidation and deposition, are incorporated in the model.
- Developing an analytical solution for predicting the release of performance reference compounds and uptake of target compounds in cylindrical passive sampling system.
- Applying the fate and transport model CapSim to simulate the behavior of PRCs and target compounds in a passive sampling system with activated carbon. The impacts from the non-linear sorption of the compounds in

activated carbon as well as the competitive sorption behavior between the isotope-labeled PRC and the non-labeled compound are discussed.

These objectives were achieved. The product tools, CapAn and CapSim are provided to the public as modeling tools for in-situ remedial design and other area purposes.

7.2 RESEARCH CONCLUSIONS

7.2.1 Analytical solution and CapAn

A general analytical solution for the one–dimensional advective–dispersive–reactive solute transport equation in multilayered porous media is presented. The model allows an arbitrary number of layers, parameter values, and initial concentration distributions. The separation of variables technique was employed to derive the analytical solution. Hyperbolic eigenfunctions, as well as traditional trigonometric eigenfunctions, were found to contribute an important part to the series solution and were not included in some existing solutions. The closed–form analytical solution was verified against a numerical solution from a finite–difference based approach and an existing solution derived from general integral transform technique (GITT). The solution has several important advantages over the GITT technique and other existing solutions. The limitations of existing solutions and the ability of the current solution to address those limitations are identified. Among other applications, the present analytical solution will be useful for modeling the transport of contaminants in sediments and, particularly for the design of layered caps as a remedial approach. The analytical solution also has significant

advantages over numerical solutions for sensitivity analyses and the solution of inverse problems.

7.2.2 CapSim

An innovative numerical model CapSim 3 is developed for predicting the contaminants behavior in sediment and optimizing the in-situ remediation design. The model has greatly expanded capabilities over the existing model in handling several essential physical and chemical processes in sediments. Firstly, the model can handle systems with an arbitrary number of layers and chemical species with linked linear or nonlinear reactions. Secondly, kinetic sorption/desorption and reaction processes are included in the model to get more accurate results for problems with slow sorption/desorption processes. Thirdly, the impacts from the important sediment processes, such as bioturbation, deposition, consolidation are included. The model has been verified with the existing analytical model and commercial numerical model, its application in modeling the bioturbation and multi-compartment sorption has also been included here.

7.2.3 Analytical solution for cylindrical PDMS fiber

A model for kinetics of uptake on the PDMS for cylindrical geometry was develop and compared to a 1-D rectangular model passive sampler. The model was developed by applying the Laplace transform and asymptotic analysis. The prediction of fss from the cylindrical model and the rectangular model were compared in passive

sampling systems with 1) given transport parameters and 2) transport parameters estimated from fss of PRCs. For the system with given transport parameters, the difference of the predicted fss depends on the transport distance of the compounds during the sampling period. For the system with parameters calibrated from PRCs, the predictions of f_{ss} from two solutions are similar, but the estimated system transport parameters (e.g., RD) can be orders different.

7.2.4 Modeling the impacts from non-linear sorption to the symmetric behavior of PRCs and target compounds in Passive sampling system

Previous literatures suggest that the behavior of PRCs and target compounds should be symmetric after calibration to compound properties. However, two recent studies (Bao et al., 2015, Choi et al., 2016) observed non-symmetric behavior of PRCs and target compounds in activated carbon amended sediments. A numerical transport model, CapSim, was used to simulate the behavior of PRCs and target compounds in a strong non-linear sorptive sorbent - activated carbon. The potential competition between a target compound and a PRC that is an isotopic form of the target compounds is also discussed here. The simulated results suggested that the non-linear sorption might be a potential cause of the observed non-symmetric behavior of the PRCs and target compounds. The simulation results also suggest that the isotope-labeled PRC might perform better in predicating the fss of target compounds in activated carbon rather than a common undetected compound.

7.3 RECOMMENDATION FOR FUTURE WORK

In-situ remediation of contaminated sediments through containment or active sorptive layers is a relatively new technology to the traditional removal technology and there are many issues to address. The results of this study have significant implications in the future for contaminated sediment management. However, the following is a list of outstanding questions about capping and potential future research topics in this area:

- *Addressing the limit of the analytical solution* – the analytical solution presented for multi-layered 1-D advection-dispersion equation exhibits difficulty in determining the eigenvalues at very high Petlet number (O(100)). This difficulty comes from the singularity of the equation and may be circumvented by solutions that include the singular perturbation or other asymptotic analysis.
- *Expanding the CapSim to include equilibrium reaction processes* – The time scale for various diagenetic processes may vary from seconds to years. To avoid the stiffness associated with fast processes in the numerical solution, the equilibrium reactions may be incorporated into the model.
- *Exploring the model validity in the field* – The analytical model and numerical model has been verified with each other. They need to be further supported by experimental results and field observation.
- *Developing tools for calibrating and calculating fss in passive sampling system* – The developed cylindrical solution needs a trial and error approach in

calibrating field and experimental data. A simple and fast closed-form analytical model on Laplace domain might be helpful.

- *Further investigation of the non-symmetric behavior of PRCs*- The numerical simulation here suggested a possible explanation for the non-symmetric behavior observed. The validity of the explanation needs to be proved by future experiments.

Appendix A. Example of the eigenvalues and coefficients evaluation

An example procedure for the evaluation of eigenvalues β_n and corresponding coefficients $A_{i,n}$, $\alpha_{i,n}$, $\alpha_{i,ss}$ and $\sigma_{i,ss}$ in the general solution (3.27) is shown in this section. Considering a three layer problem with the Dirichlet condition for both inlet and outlet boundaries and constant initial concentrations in each layer, the series solution for the problem is shown as equation (A1).

$$C_i^*(\eta,\tau) = e^{\frac{Pe_i}{2}\eta}\left(\alpha_{i,ss}\cosh(\sqrt{\gamma_i}\eta) + \sigma_{i,ss}\sinh(\sqrt{\gamma_i}\eta) + \sum_{n=1}^{\infty} A_{i,n}e^{-\beta_n{}^2\tau}\varphi_{i,n}(\eta)\right);\quad i = 1, 2, 3 \tag{A1}$$

The coefficients for the inhomogeneous steady-state solution, $\alpha_{i,ss}$ and $\sigma_{i,ss}$ are proposed to be evaluated by applying the equation (9). In the three-layer example, a 6×6 matrix is generated with all its elements shown explicitly in equation table (A2b). The matrix has bandwidth of four, so the linear system can be efficiently solved by Gaussian elimination.

$$\begin{bmatrix} p_0 & q_0 & 0 & 0 & 0 & 0 \\ p_1(r_{12}) & q_1(r_{12}) & -p_2(r_{12}) & -q_2(r_{12}) & 0 & 0 \\ p_1'(r_{12}) & q_1'(r_{12}) & -p_2'(r_{12}) & -q_2'(r_{12}) & 0 & 0 \\ 0 & 0 & p_2(r_{23}) & q_2(r_{23}) & -p_3(r_{23}) & -q_3(r_{23}) \\ 0 & 0 & p_2'(r_{23}) & q_2'(r_{23}) & -p_3'(r_{23}) & -q_3'(r_{23}) \\ 0 & 0 & 0 & 0 & p_4 & q_4 \end{bmatrix} * \begin{bmatrix} \alpha_{1,ss} \\ \sigma_{1,ss} \\ \alpha_{2,ss} \\ \sigma_{2,ss} \\ \alpha_{3,ss} \\ \sigma_{3,ss} \end{bmatrix} = \begin{bmatrix} C_0/C_R \\ 0 \\ 0 \\ 0 \\ 0 \\ C_H/C_R \end{bmatrix} \tag{A2a}$$

i	$p_i(\eta)$	$q_i(\eta)$	$p_i'(\eta)$	$q_i'(\eta)$
0	1	0		
1	$e^{\frac{Pe_1}{2}\eta}\cosh(\sqrt{\gamma_1}\eta)$	$e^{\frac{Pe_1}{2}\eta}\sinh(\sqrt{\gamma_1}\eta)$	$D_1\sqrt{\gamma_i}e^{\frac{Pe_1}{2}\eta}\sinh(\sqrt{\gamma_1}\eta)$	$D_1\sqrt{\gamma_1}e^{\frac{Pe_1}{2}\eta}\sinh(\sqrt{\gamma_1}\eta)$
2	$e^{\frac{Pe_2}{2}\eta}\cosh(\sqrt{\gamma_2}\eta)$	$e^{\frac{Pe_2}{2}\eta}\sinh(\sqrt{\gamma_2}\eta)$	$D_2\sqrt{\gamma_2}e^{\frac{Pe_2}{2}\eta}\sinh(\sqrt{\gamma_2}\eta)$	$D_2\sqrt{\gamma_2}e^{\frac{Pe_2}{2}\eta}\sinh(\sqrt{\gamma_2}\eta)$
3	$e^{\frac{Pe_3}{2}\eta}\cosh(\sqrt{\gamma_3}\eta)$	$e^{\frac{Pe_3}{2}\eta}\sinh(\sqrt{\gamma_3}\eta)$	$D_3\sqrt{\gamma_3}e^{\frac{Pe_3}{2}\eta}\sinh(\sqrt{\gamma_3}\eta)$	$D_3\sqrt{\gamma_3}e^{\frac{Pe_3}{2}\eta}\sinh(\sqrt{\gamma_3}\eta)$
4	$e^{\frac{Pe_3}{2}}\cosh(\sqrt{\gamma_l})$	$e^{\frac{Pe_3}{2}}\sinh(\sqrt{\gamma_l})$		

(A2b)

The eigenvalues and corresponding eigenfunction coefficients are evaluated with (3.22). The explicit form for the non-linear system in the three-layer Dirichlet-Dirichlet problem is shown in (A3), which is then solved by the 'sign-count' method (Wittrick and Williams 1971; Milkhailov and Vulchanov, 1983).

$$\frac{D_1\frac{\partial\varphi_{1,n}(r_{12})}{\partial\eta}}{\varphi_{1,n}(r_{12})} = \frac{D_2\frac{\partial\varphi_{2,n}(r_{12})}{\partial\eta}}{\varphi_{2,n}(r_{12})} \tag{A3a}$$

$$\frac{D_2\frac{\partial\varphi_{2,n}(r_{23})}{\partial\eta}}{\varphi_{2,n}(r_{23})} = \frac{D_3\frac{\partial\varphi_{3,n}(r_{23})}{\partial\eta}}{\varphi_{3,n}(r_{23})} \tag{A3b}$$

Where

$$\frac{D_1\frac{\partial\varphi_{1,n}(\eta)}{\partial\eta}}{\varphi_{1,n}(\eta)} = \frac{D_1\left(\gamma_1-\beta_n{}^2\frac{R_1H^2}{D_1t_o}\right)}{\tanh\left(\left(\gamma_1-\beta_n{}^2\frac{R_1H^2}{D_1t_o}\right)\eta\right)} \quad or \quad \frac{D_1\left(\beta_n{}^2\frac{R_1H^2}{D_1t_o}-\gamma_1\right)}{\tan\left(\left(\beta_n{}^2\frac{R_1H^2}{D_1t_o}-\gamma_1\right)\eta\right)}$$

$$\frac{D_2\frac{\partial\varphi_{2,n}(\eta)}{\partial\eta}}{\varphi_{2,n}(\eta)} = D_2\left(\gamma_2-\beta_n{}^2\frac{R_2H^2}{D_2t_o}\right)\frac{1+\alpha_{2,n}\tanh\left(\left(\gamma_2-\beta_n{}^2\frac{R_2H^2}{D_2t_o}\right)\eta\right)}{\alpha_{2,n}+\tanh\left(\left(\gamma_2-\beta_n{}^2\frac{R_2H^2}{D_2t_o}\right)\eta\right)} \; or \; D_2\left(\beta_n{}^2\frac{R_2H^2}{D_2t_o}-\gamma_2\right)\frac{1-\alpha_{2,n}\tan\left(\left(\beta_n{}^2\frac{R_2H^2}{D_2t_o}-\gamma_2\right)\eta\right)}{\alpha_{2,n}+\tan\left(\left(\beta_n{}^2\frac{R_2H^2}{D_2t_o}-\gamma_2\right)\eta\right)}$$

$$\frac{D_3\frac{\partial\varphi_{3,n}(\eta)}{\partial\eta}}{\varphi_{3,n}(\eta)} = \frac{D_3\left(\gamma_3-\beta_n{}^2\frac{R_3H^2}{D_3t_o}\right)}{\tanh\left(\left(\gamma_3-\beta_n{}^2\frac{R_3H^2}{D_3t_o}\right)(\eta-1)\right)} \quad or \quad \frac{D_1\left(\beta_n{}^2\frac{R_3H^2}{D_3t_o}-\gamma_3\right)}{\tan\left(\left(\beta_n{}^2\frac{R_3H^2}{D_3t_o}-\gamma_3\right)(\eta-1)\right)}$$

To apply 'sign-count' method, the eigenfunctions (3.20) and (3.21) are rearranged to (A4a) and (A4b)

$$\varphi_{i,n}(\eta) = \exp\left(\frac{Pe_1}{2}(\eta - r_{i-1,i})\right)\frac{\sinh\left(x_{i,n}(r_{i,i+1}-\eta)\right)}{\sinh\left(x_{i,n}(r_{i,i+1}-r_{i-1,i})\right)}\varphi_{i-1,i,n} + \exp\left(\frac{Pe_i}{2}(\eta - r_{i,i+1})\right)\frac{\sinh\left(x_{i,n}(\eta-r_{i-1,i})\right)}{\sinh\left(x_{i,n}(r_{i,i+1}-r_{i-1,i})\right)}\varphi_{i,i+1,n} \quad (A4a)$$

$$\varphi_{i,n}(\eta) = \exp\left(\frac{Pe_i}{2}(\eta - r_{i-1,i})\right)\frac{\sin\left(y_{i,n}(r_{i,i+1}-\eta)\right)}{\sin\left(y_{i,n}(r_{i,i+1}-r_{i-1,i})\right)}\varphi_{i-1,i,n} + \exp\left(\frac{Pe_i}{2}(\eta - r_{i,i+1})\right)\frac{\sin\left(y_{i,n}(\eta-r_{i-1,i})\right)}{\sin\left(y_{i,n}(r_{i,i+1}-r_{i-1,i})\right)}\varphi_{i,i+1,n} \quad (A4b)$$

Where coefficients $\varphi_{i-1,i,n}$ and $\varphi_{i,i+1,n}$ are equivalent to the eigenfunction coefficients $\alpha_{i,n}$. The interfacial boundary conditions (A3a) and (A3b) can be rearranged to (A5a) and (A5b),

$$B_1\exp\left(\frac{Pe_1}{2}(r_{12}-0)\right)\varphi_{0,1} + (A_1+A_2)\varphi_{1,2} + B_2\exp\left(\frac{Pe_2}{2}(r_{12}-r_{23})\right)\varphi_{2,3} = 0 \quad (A5a)$$

$$B_2\exp\left(\frac{Pe_2}{2}(r_{23}-r_{12})\right)\varphi_{0,1} + (A_2+A_3)\varphi_{1,2} + B_3\exp\left(\frac{Pe_3}{2}(r_{23}-1)\right)\varphi_{2,3} = 0 \quad (A5b)$$

Where $A_i = D_i x_{i,n}/\tanh\left(x_{i,n}(r_{i,i+1}-r_{i-1,i})\right)$ or $D_i y_{i,n}/\tan\left(y_{i,n}(r_{i,i+1}-r_{i-1,i})\right)$

$$B_i = D_i x_{i,n}/\sinh\left(x_{i,n}(r_{i,i+1}-r_{i-1,i})\right) \quad \text{or} \quad D_i y_{i,n}/\sin\left(y_{i,n}(r_{i,i+1}-r_{i-1,i})\right)$$

The homogeneous equations for the determination of eigenvalues β_n and corresponding eigenfunctions are

$$[K(\beta_n)][\varphi(\beta_n)] = 0 \quad (A6)$$

Where

$$[K(\beta_n)] = \begin{bmatrix} 1 & 0 & 0 & 0 \\ \overline{B}_{1,2} & \overline{A}_1 & \overline{B}_{2,2} & 0 \\ 0 & \overline{B}_{2,3} & \overline{A}_2 & \overline{B}_{3,3} \\ 0 & 0 & 0 & 1 \end{bmatrix}$$

$$\overline{A}_i = A_i + A_{i+1}$$

$$\overline{B}_{i,i} = B_i \exp\left(Pe_i\left(r_{i-1,i} - r_{i,i+1}\right)\right) \; ; \; \overline{B}_{i,i+1} = B_i \exp\left(Pe_i\left(r_{i,i+1} - r_{i-1,i}\right)\right)$$

$$[\varphi(\beta_n)] = [\varphi_{0,1} \quad \varphi_{1,2} \quad \varphi_{2,3} \quad \varphi_{3,4}]^T$$

The infinite number of real roots of the transcendental equation (A6) are the eigenvalues of the system (A3). The computational algorithm for the roots is given in Milkhailov and Vulchanov (1983).

The coefficients $A_{i,n}$ are evaluated by integrating the self-adjoint eigenfunctions. An explicit form of the integrals in (3.26) with constant initial concentrations is shown in (A7) and (A8). Combining equation (A7) to (A8), the coefficients $A_{i,n}$ are derived explicitly and the solution is fully closed with all eigenvalues and coefficients known.

The normalization group can be written

$$\int_{r_{i-1,i}}^{r_{i,i+1}} {\varphi_{i,n}}^2 \, d\eta = \frac{({\alpha_{i,n}}^2 - 1)}{2}\eta + \frac{(1+{\alpha_{i,n}}^2)}{4x_{i,n}}\sinh(2x_{i,n}\eta) + \frac{\alpha_{i,n}}{2x_{i,n}}\cosh(2x_{i,n}\eta)\Big|_{r_{i-1,i}}^{r_{i,i+1}} \qquad \text{(A7a)}$$

$$\int_{r_{i-1,i}}^{r_{i,i+1}} {\varphi_{i,n}}^2 \, d\eta = \frac{(1+{\alpha_{i,n}}^2)}{2}\eta + \frac{({\alpha_{i,n}}^2 - 1)}{4y_{i,n}}\sin(2y_{i,n}\eta) - \frac{\alpha_{i,n}}{2y_{i,n}}\cos(2y_{i,n}\eta)\Big|_{r_{i-1,i}}^{r_{i,i+1}} \qquad \text{(A7b)}$$

The integration for uniform initial concentration $C_{i,init}$ distribution in each layer can be written

$$\int_{r_{i-1,i}}^{r_{i,i+1}} \varphi_{i,n}\left(\frac{C_{i,init}}{C_R} - {c_{i,ss}}^*\right) e^{-\frac{Pe_i}{2}\eta}\, d\eta =$$

$$\frac{\frac{C_{i,init}}{C_R}}{\frac{{Pe_i}^2}{4} - {x_{i,n}}^2} e^{-\frac{Pe_i}{2}\eta}\left(-x_{i,n}\left(\alpha_{i,n}\sinh\left(x_{i,n}\eta\right) + \cosh\left(x_{i,n}\eta\right)\right) - \frac{Pe_i}{2}\left(\alpha_{i,n}\cosh\left(x_{i,n}\eta\right) + \sinh\left(x_{i,n}\eta\right)\right)\right)\Bigg|_{r_{i-1,i}}^{r_{i,i+1}} +$$

$$\frac{A_{i,ss}}{{x_{i,n}}^2 - {\gamma_i}^2} x_{i,n}\left(\alpha_{i,n}\sinh\left(x_{i,n}\eta\right) + \cosh\left(x_{i,n}\eta\right)\right)\left(\alpha_{i,ss}\cosh\left(\gamma_i\eta\right) + \sigma_{i,ss}\sinh\left(\gamma_i\eta\right)\right)\Big|_{r_{i-1,i}}^{r_{i,i+1}} -$$

$$\frac{A_{i,ss}}{{x_{i,n}}^2 - {\gamma_i}^2} \gamma_i\left(\alpha_{i,n}\cosh\left(x_{i,n}\eta\right) + \sinh\left(x_{i,n}\eta\right)\right)\left(\alpha_{i,ss}\sinh\left(\gamma_i\eta\right) + \sigma_{i,ss}\cosh\left(\gamma_i\eta\right)\right)\Big|_{r_{i-1,i}}^{r_{i,i+1}}$$

(A8a)

$$\int_{r_{i-1,i}}^{r_{i,i+1}} \varphi_{i,n}\left(\frac{C_{i,init}}{C_R} - {c_{i,ss}}^*\right) e^{-\frac{Pe_i}{2}\eta}\, d\eta =$$

$$\frac{\frac{C_{i,init}}{C_R}}{{y_{i,n}}^2 + \frac{{Pe_i}^2}{4}} e^{-\frac{Pe_i}{2}\eta}\left(y_{i,n}\left(\alpha_{i,n}\sin\left(y_{i,n}\eta\right) - \cos\left(y_{i,n}\eta\right)\right) - \frac{Pe_i}{2}\left(\alpha_{i,n}\cos\left(y_{i,n}\eta\right) + \sin\left(y_{i,n}\eta\right)\right)\right)\Bigg|_{r_{i-1,i}}^{r_{i,i+1}} +$$

$$\frac{A_{i,ss}}{{y_{i,n}}^2 + {\gamma_i}^2} y_{i,n}\left(\alpha_{i,n}\sin\left(y_{i,n}\eta\right) - \cos\left(y_{i,n}\eta\right)\right)\left(\alpha_{i,ss}\cosh(\gamma_i\eta) + \sigma_{i,ss}\sinh(\gamma_i\eta)\right)\Big|_{r_{i-1,i}}^{r_{i,i+1}} -$$

$$\frac{A_{i,ss}}{{y_{i,n}}^2 + {\gamma_i}^2} \gamma_i\left(\alpha_{i,n}\cos\left(y_{i,n}\eta\right) + \sin\left(y_{i,n}\eta\right)\right)\left(\alpha_{i,ss}\sinh(\gamma_i\eta) + \sigma_{i,ss}\cosh(\gamma_i\eta)\right)\Big|_{r_{i-1,i}}^{r_{i,i+1}}$$

(A8b)

$$A_{1,n} =$$

$$\frac{\begin{pmatrix} R_1 \int_0^{r_{12}} \varphi_{1,n}\left(\frac{C_{1,init}}{C_b} - {c_{1,ss}}^*\right) e^{-\frac{Pe_1}{2}\eta}\, d\eta * e^{(Pe_1 r_{1,2} + Pe_2 r_{2,3})} + \\ R_2 \int_{r_{12}}^{r_{23}} \varphi_{2,n}\left(\frac{C_{2,init}}{C_b} - {c_{2,ss}}^*\right) e^{-\frac{Pe_2}{2}\eta}\, d\eta * e^{(Pe_2 r_{1,2} + Pe_2 r_{2,3})} * \frac{\varphi_{1,n}(r_{1,2})}{\varphi_{2,n}(r_{1,2})} * e^{\left(\frac{Pe_1}{2} - \frac{Pe_2}{2}\right) r_{1,2}} + \\ R_3 \int_{r_{23}}^{1} \varphi_{3,n}\left(\frac{C_{3,init}}{C_b} - {c_{3,ss}}^*\right) e^{-\frac{Pe_3}{2}\eta}\, d\eta * e^{(Pe_2 r_{1,2} + Pe_3 r_{2,3})} * \frac{\varphi_{1,n}(r_{1,2})\varphi_{2,n}(r_{2,3})}{\varphi_{2,n}(r_{1,2})\varphi_{3,n}(r_{2,3})} * e^{\left(\frac{Pe_1}{2} - \frac{Pe_2}{2}\right) r_{1,2} + \left(\frac{Pe_2}{2} - \frac{Pe_3}{2}\right) r_{2,3}} \end{pmatrix}}{\begin{pmatrix} R_1 \int_0^{r_{1,2}} {\varphi_{1,n}}^2\, d\eta * e^{(Pe_1 r_{12} + Pe_2 r_{23})} + \\ R_2 \int_{r_{12}}^{r_{23}} {\varphi_{2,n}}^2\, d\eta * e^{(Pe_2 r_{1,2} + Pe_2 r_{2,3})} * \left(\frac{\varphi_{1,n}(r_{1,2})}{\varphi_{2,n}(r_{1,2})}\right)^2 * e^{(Pe_1 - Pe_2) r_{1,2}} + \\ R_3 \int_{r_{23}}^{1} {\varphi_{3,n}}^2\, d\eta * e^{(Pe_2 r_{1,2} + Pe_3 r_{2,3})} * \left(\frac{\varphi_{1,n}(r_{1,2})\varphi_{2,n}(r_{2,3})}{\varphi_{2,n}(r_{1,2})\varphi_{3,n}(r_{2,3})}\right)^2 * e^{(Pe_1 - Pe_2) r_{1,2} + (Pe_2 - Pe_3) r_{2,3}} \end{pmatrix}} \tag{A9a}$$

$$A_{2,n} = \frac{\varphi_{1,n}(r_{1,2})}{\varphi_{2,n}(r_{1,2})} * e^{\left(\frac{Pe_1}{2} - \frac{Pe_2}{2}\right) r_{1,2}} A_{1,n} \tag{A9b}$$

$$A_{3,n} = \frac{\varphi_{1,n}(r_{1,2})}{\varphi_{2,n}(r_{1,2})} \frac{\varphi_{2,n}(r_{2,3})}{\varphi_{3,n}(r_{2,3})} * e^{\left(\left(\frac{Pe_1}{2} - \frac{Pe_2}{2}\right) r_{1,2} + \left(\frac{Pe_2}{2} - \frac{Pe_3}{2}\right) r_{2,3}\right)} A_{1,n} \tag{A9c}$$

Appendix B. VBA codes of CapAn

Module 1: 'Simulation'

```
Attribute VB_Name = "Module1"

Sub CapAn_Solver()

'Define all variables

Dim U As Double, layers As Integer                                          'System
properties
Dim h(), Dw(), epsilon(), Kd(), lambda(), Cinit(), rho() As Double          'Layer
properties
Dim toptype, bottomtype, toptyper, bottomtyper As String, Fo, Fh, Co, Ch, Cr, ko,
kh As Double  'Boundary properties
Dim D(), Rd(), Pe(), eDa(), hcap, r() As Double
'Dimensionless properties
Dim num As Integer, stepsize As Double
'Simulation parameters
Dim Nnum, snum As Integer
Dim layertype() As String

Dim beta(), betatype(), y(), Fi() As Double, ytype() As Integer
Dim betatemp, jtemp(), ytemp(), Fitemp() As Double, ytypetemp() As Integer
Dim numcount, j, temptype1, temptype2, k As Integer
Dim eq, aa, bb, eqb, stepb, betaorigin, JJ, betatempa, betaa As Double
Dim i As Integer
Dim gamma(), X(), b(), CT(), C1(), C2() As Double                'Steady-state
parameters


'Solution coefficients

Dim front, back As Integer
Dim Int_total, eigengroup_total, Int_term, eigengroup_term As Double
Dim A(), coef(), inte(), ra() As Double

'Read system properties

layers = Worksheets("CapAn").Cells(7, 2).Value
U = Worksheets("CapAn").Cells(8, 2).Value

'Read Layer properties


ReDim h(1 To layers)
ReDim epsilon(1 To layers)
ReDim Dw(1 To layers)
```

```
ReDim Kd(1 To layers)
ReDim lambda(1 To layers)
ReDim Cinit(1 To layers)
ReDim rho(1 To layers)

For layer = 1 To layers
          h(layer) = Worksheets("CapAn").Cells(12, layer + 1).Value
    epsilon(layer) = Worksheets("CapAn").Cells(13, layer + 1).Value
         Dw(layer) = Worksheets("CapAn").Cells(14, layer + 1).Value
         Kd(layer) = Worksheets("CapAn").Cells(15, layer + 1).Value
     lambda(layer) = Worksheets("CapAn").Cells(16, layer + 1).Value
      Cinit(layer) = Worksheets("CapAn").Cells(17, layer + 1).Value
        rho(layer) = Worksheets("CapAn").Cells(18, layer + 1).Value
Next layer

'Read boundary conditions
toptyper = Worksheets("CapAn").Cells(22, 2).Value
bottomtyper = Worksheets("CapAn").Cells(22, 7).Value

If toptyper = "Concentration" Or toptyper = "concentration" Or toptyper =
"CONCENTRATION" Then
    toptype = "Dirichlet"
ElseIf toptyper = "Mass Transfer" Or toptyper = "mass transfer" Or toptyper =
"Mass transfer" Or toptyper = "mass Transfer" Or toptyper = "MASS TRANSFER" Then
    toptype = "Benthic"
ElseIf toptyper = "Gradient" Or toptyper = "gradient" Or toptyper = "GRADIENT"
Then
    toptype = "Neumann"
ElseIf toptyper = "Flux" Or toptyper = "flux" Or toptyper = "FLUX" Then
    toptype = "Robin"
Else
    MsgBox ("Please define the correct top boundary type")
End If

If bottomtyper = "Concentration" Or bottomtyper = "concentration" Or bottomtyper =
"CONCENTRATION" Then
    bottomtype = "Dirichlet"
ElseIf bottomtyper = "Mass Transfer" Or bottomtyper = "mass transfer" Or
bottomtyper = "Mass transfer" Or bottomtyper = "mass Transfer" Or bottomtyper =
"MASS TRANSFER" Then
    bottomtype = "Benthic"
ElseIf bottomtyper = "Gradient" Or bottomtyper = "gradient" Or bottomtyper =
"GRADIENT" Then
    bottomtype = "Neumann"
ElseIf bottomtyper = "Flux" Or bottomtyper = "flux" Or bottomtyper = "FLUX" Then
    bottomtype = "Robin"
Else
    MsgBox ("Please define the correct bottom boundary type")
End If

If toptype = "Dirichlet" Then
    Co = Worksheets("CapAn").Cells(23, 2).Value
ElseIf toptype = "Benthic" Then
```

```
    Co = Worksheets("CapAn").Cells(23, 2).Value
    ko = Worksheets("CapAn").Cells(24, 2).Value
Else
    Fo = Worksheets("CapAn").Cells(23, 2).Value
End If

If bottomtype = "Dirichlet" Then
    Ch = Worksheets("CapAn").Cells(23, 7).Value
ElseIf bottomtype = "Benthic" Then
    Ch = Worksheets("CapAn").Cells(23, 7).Value
    kh = Worksheets("CapAn").Cells(24, 7).Value
Else
    Fh = Worksheets("CapAn").Cells(23, 7).Value
End If

'Generate dimensionless variables

ReDim D(1 To layers)
ReDim Rd(1 To layers)
ReDim Pe(1 To layers)
ReDim eDa(1 To layers)
ReDim r(1 To layers + 1)
ReDim gamma(1 To layers)
ReDim layertype(1 To layers)

hcap = 0
For layer = 1 To layers
    hcap = hcap + h(layer)
Next layer

For layer = 1 To layers
    D(layer) = Dw(layer) * 3600 * 24 * 365 * epsilon(layer)
    Rd(layer) = Kd(layer) * rho(layer) + epsilon(layer)
    Pe(layer) = U * hcap / D(layer)
    eDa(layer) = epsilon(layer) * lambda(layer) * hcap ^ 2 / D(layer)
    gamma(layer) = (Pe(layer) ^ 2 + 4 * eDa(layer)) ^ 0.5 / 2
Next layer

Bio = ko * hcap / D(1)
Bih = kh * hcap / D(layers)
For layer = 1 To layers
    If gamma(layer) = 0 Then
        layertype(layer) = "Diffusion"
    Else
        layertype(layer) = "Regular"
    End If
Next layer

Dim Depth As Double
Depth = 0
r(1) = 0

For layer = 1 To layers
```

```
    Depth = Depth + h(layer)
    r(layer + 1) = Depth / hcap
Next layer

'Evaluate Eigenvalues

num = Worksheets("CapAn").Range("B27").Value
ReDim beta(1 To num)
ReDim betatype(1 To num)
ReDim y(1 To layers, 1 To num)
ReDim ytype(1 To layers, 1 To num)
ReDim Fi(1 To layers + 1, 1 To num)
ReDim ytemp(1 To layers)
ReDim Fitemp(1 To layers + 1)
ReDim ytypetemp(1 To layers)
ReDim jtemp(1 To layers)

betatemp = 0
temptype2 = 1
numcount = 0
aa = 0
Nnum = 0

'Determine the step size as one tenth of the smallest natural frequency
stepsize = ((3.14 / (r(2) - r(1))) ^ 2 + Pe(1) ^ 2 / 4 + eDa(1)) / hcap ^ 2 * D(1)
/ Rd(1) / 10
For layer = 1 To layers
    If stepsize > ((3.14 / (r(layer + 1) - r(layer))) ^ 2 + Pe(layer) ^ 2 / 4 +
eDa(layer)) / hcap ^ 2 * D(layer) / Rd(layer) / 10 Then
        stepsize = ((3.14 / (r(layer + 1) - r(layer))) ^ 2 + Pe(layer) ^ 2 / 4 +
eDa(layer)) / hcap ^ 2 * D(layer) / Rd(layer) / 10
    End If
Next layer
Do While (numcount < num)
    betatemp = betatemp + stepsize

    For layer = 1 To layers
        If (betatemp * Rd(layer) / D(layer) * hcap ^ 2 - Pe(layer) ^ 2 / 4 -
eDa(layer)) >= 0 Then
            ytypetemp(layer) = 1
        Else
            ytypetemp(layer) = 0
        End If
    Next layer

    For layer = 1 To layers
        If ytypetemp(layer) = 1 Then
            ytemp(layer) = (betatemp * Rd(layer) / D(layer) * hcap ^ 2 - Pe(layer)
^ 2 / 4 - eDa(layer)) ^ 0.5
        Else
            ytemp(layer) = (-betatemp * Rd(layer) / D(layer) * hcap ^ 2 +
Pe(layer) ^ 2 / 4 + eDa(layer)) ^ 0.5
        End If
```

```
    Next layer

    'Find EigenValues using Sign-count method
    Dim betaupper As Double, betalower As Double
    Nnum = N_Evaluation(ytemp, ytypetemp, D, Pe, eDa, r, layers, Rd, toptype,
bottomtype, Bio, Bih)
    If Nnum > numcount Then
        betaupper = betatemp
        betalower = betatemp - stepsize
        Do While (betaupper - betalower) / (betaupper + betalower) >
0.000000000001 And (betaupper + betalower) > 0.000000000001
            betatemp = (betaupper + betalower) / 2
                For layer = 1 To layers
                    If (betatemp * Rd(layer) / D(layer) * hcap ^ 2 - Pe(layer) ^ 2
/ 4 - eDa(layer)) >= 0 Then
                        ytypetemp(layer) = 1
                    Else
                        ytypetemp(layer) = 0
                    End If
                Next layer
                For layer = 1 To layers
                    If ytypetemp(layer) = 1 Then
                        ytemp(layer) = (betatemp * Rd(layer) / D(layer) * hcap ^ 2
- Pe(layer) ^ 2 / 4 - eDa(layer)) ^ 0.5
                    Else
                        ytemp(layer) = (-betatemp * Rd(layer) / D(layer) * hcap ^
2 + Pe(layer) ^ 2 / 4 + eDa(layer)) ^ 0.5
                    End If
                Next layer
            Nnum = N_Evaluation(ytemp, ytypetemp, D, Pe, eDa, r, layers, Rd,
toptype, bottomtype, Bio, Bih)
            If Nnum > numcount Then
                betaupper = betatemp
            Else
                betalower = betatemp
            End If
        Loop
        betatemp = (betaupper + betalower) / 2

        'Make sure there is no pseudo EigenValues that come from the double roots
        If Nnum = numcount + 1 Then
            numcount = Nnum
        Else
            numcount = Nnum + 1
        End If

        For layer = 1 To layers
            If (betatemp * Rd(layer) / D(layer) * hcap ^ 2 - Pe(layer) ^ 2 / 4 -
eDa(layer)) >= 0 Then
                ytypetemp(layer) = 1
            Else
                ytypetemp(layer) = 0
            End If
```

```
        Next layer

        For layer = 1 To layers
            If ytypetemp(layer) = 1 Then
                ytemp(layer) = (betatemp * Rd(layer) / D(layer) * hcap ^ 2 -
Pe(layer) ^ 2 / 4 - eDa(layer)) ^ 0.5
            Else
                ytemp(layer) = (-betatemp * Rd(layer) / D(layer) * hcap ^ 2 +
Pe(layer) ^ 2 / 4 + eDa(layer)) ^ 0.5
            End If
        Next layer

        temptype1 = 0
        For layer = 1 To layers
            temptype1 = 10 ^ (layers - layer) * ytypetemp(layer) + temptype1
        Next layer

        Fitemp(2) = 1

        If toptype = "Dirichlet" Then
            Fitemp(1) = 0
        ElseIf toptype = "Neumann" Then
            If ytypetemp(1) = 1 Then
                Fitemp(1) = ytemp(1) * Exp(-Pe(1) / 2 * r(2)) / (ytemp(1) *
Cos(ytemp(1) * r(2)) - Pe(1) / 2 * Sin(ytemp(1) * r(2))) * Fitemp(2)
            ElseIf ytypetemp(1) = 0 Then
                If (ytemp(1) * WorksheetFunction.Cosh(ytemp(1) * r(2)) - Pe(1) / 2
* WorksheetFunction.Sinh(ytemp(1) * r(2))) = 0 Then
                    Fitemp(1) = Fitemp(2)
                Else
                    Fitemp(1) = ytemp(1) * Exp(-Pe(1) / 2 * r(2)) / (ytemp(1) *
WorksheetFunction.Cosh(ytemp(1) * r(2)) - Pe(1) / 2 *
WorksheetFunction.Sinh(ytemp(1) * r(2)))
                End If
            End If
        ElseIf toptype = "Robin" Then
            If ytypetemp(1) = 1 Then
                Fitemp(1) = ytemp(1) * Exp(-Pe(1) / 2 * r(2)) / (ytemp(1) *
Cos(ytemp(1) * r(2)) + Pe(1) / 2 * Sin(ytemp(1) * r(2))) * Fitemp(2)
            ElseIf ytypetemp(1) = 0 Then
                If (ytemp(1) * WorksheetFunction.Cosh(ytemp(1) * r(2)) + Pe(1) / 2
* WorksheetFunction.Sinh(ytemp(1) * r(2))) = 0 Then
                    Fitemp(1) = Fitemp(2)
                Else
                    Fitemp(1) = ytemp(1) * Exp(-Pe(1) / 2 * r(2)) / (ytemp(1) *
WorksheetFunction.Cosh(ytemp(1) * r(2)) + Pe(1) / 2 *
WorksheetFunction.Sinh(ytemp(1) * r(2)))
                End If
            End If
        ElseIf toptype = "Benthic" Then
            If ytypetemp(1) = 1 Then
                Fitemp(1) = ytemp(1) * Exp(-Pe(1) / 2 * r(2)) / (ytemp(1) *
Cos(ytemp(1) * r(2)) - (Pe(1) / 2 - Bio) * Sin(ytemp(1) * r(2))) * Fitemp(2)
```

```
            ElseIf ytypetemp(1) = 0 Then
                If (ytemp(1) * WorksheetFunction.Cosh(ytemp(1) * r(2)) + Pe(1) / 2
* WorksheetFunction.Sinh(ytemp(1) * r(2))) = 0 Then
                    Fitemp(1) = Fitemp(2)
                Else
                    Fitemp(1) = ytemp(1) * Exp(-Pe(1) / 2 * r(2)) / (ytemp(1) *
WorksheetFunction.Cosh(ytemp(1) * r(2)) - (Pe(1) / 2 - Bio) *
WorksheetFunction.Sinh(ytemp(1) * r(2)))
                End If
            End If

        End If
        For layer = 2 To layers
            Fitemp(layer + 1) = Fi_Evaluation(ytemp(layer - 1), ytemp(layer),
ytypetemp(layer - 1), ytypetemp(layer), Fitemp(layer - 1), Fitemp(layer), D(layer
- 1), D(layer), Pe(layer - 1), Pe(layer), r(layer - 1), r(layer), r(layer + 1))
        Next layer
        'Save all the eigenvalues derived above
        beta(numcount) = betatemp
        betatype(numcount) = temptype1
        For layer = 1 To layers
            y(layer, numcount) = ytemp(layer)
            ytype(layer, numcount) = ytypetemp(layer)
            Fi(layer, numcount) = Fitemp(layer)
        Next layer
        Fi(layers + 1, numcount) = Fitemp(layers + 1)

    End If
Loop

For n = 1 To num
    Worksheets("Coef_beta").Cells(11 + n, 1).Value = n
    Worksheets("Coef_beta").Cells(11 + n, 2).Value = betatype(n)
    Worksheets("Coef_beta").Cells(11 + n, 3).Value = beta(n)
Next n

'Solving for steady-state solution
'Define variables and matrix

ReDim X(1 To layers + 1, 1 To layers + 1)
ReDim CT(1 To layers + 1)
ReDim b(1 To layers + 1)


'Build the matrix with governing equations
For layer = 1 To layers - 1
    If layertype(layer) = "Regular" And layertype(layer + 1) = "Regular" Then
        X(layer + 1, layer) = -gamma(layer) * D(layer) * Exp(Pe(layer) / 2 *
(r(layer + 1) - r(layer))) / WorksheetFunction.Sinh(gamma(layer) * (r(layer + 1) -
r(layer)))
        X(layer + 1, layer + 1) = gamma(layer) * D(layer) /
WorksheetFunction.Tanh(gamma(layer) * (r(layer + 1) - r(layer))) + gamma(layer +
```

```
1) * D(layer + 1) / WorksheetFunction.Tanh(gamma(layer + 1) * (r(layer + 2) -
r(layer + 1)))
        X(layer + 1, layer + 2) = -gamma(layer + 1) * D(layer + 1) * Exp(Pe(layer
+ 1) / 2 * (r(layer + 1) - r(layer + 2))) / WorksheetFunction.Sinh(gamma(layer +
1) * (r(layer + 2) - r(layer + 1)))
    End If

    If layertype(layer) = "Diffusion" And layertype(layer + 1) = "Regular" Then
        X(layer + 1, layer) = -D(layer) / (r(layer + 1) - r(layer))
        X(layer + 1, layer + 1) = D(layer) / (r(layer + 1) - r(layer)) +
gamma(layer + 1) * D(layer + 1) / WorksheetFunction.Tanh(gamma(layer + 1) *
(r(layer + 2) - r(layer + 1)))
        X(layer + 1, layer + 2) = -gamma(layer + 1) * D(layer + 1) * Exp(Pe(layer
+ 1) / 2 * (r(layer + 1) - r(layer + 2))) / WorksheetFunction.Sinh(gamma(layer +
1) * (r(layer + 2) - r(layer + 1)))
    End If

    If layertype(layer) = "Regular" And layertype(layer + 1) = "Diffusion" Then
        X(layer + 1, layer) = -gamma(layer) * D(layer) * Exp(Pe(layer) / 2 *
(r(layer + 1) - r(layer))) / WorksheetFunction.Sinh(gamma(layer) * (r(layer + 1) -
r(layer)))
        X(layer + 1, layer + 1) = gamma(layer) * D(layer) /
WorksheetFunction.Tanh(gamma(layer) * (r(layer + 1) - r(layer))) + D(layer + 1) /
(r(layer + 2) - r(layer + 1))
        X(layer + 1, layer + 2) = -D(layer + 1) / (r(layer + 2) - r(layer + 1))
    End If

    If layertype(layer) = "Diffusion" And layertype(layer + 1) = "Diffusion" Then
        X(layer + 1, layer) = -D(layer) / (r(layer + 1) - r(layer))
        X(layer + 1, layer + 1) = D(layer) / (r(layer + 1) - r(layer)) + D(layer +
1) / (r(layer + 2) - r(layer + 1))
        X(layer + 1, layer + 2) = -D(layer + 1) / (r(layer + 2) - r(layer + 1))
    End If

Next layer

'Build the matrix with boundary conditions
'Top boundary
If layertype(1) = "Regular" Then
    If toptype = "Dirichlet" Then
        X(1, 1) = 1
        b(1) = Co
    ElseIf toptype = "Neumann" Then
        X(1, 1) = -Pe(1) / 2 + gamma(1) / WorksheetFunction.Tanh(gamma(1) * r(2))
        X(1, 2) = -gamma(1) * Exp(-Pe(1) / 2 * r(2)) /
WorksheetFunction.Sinh(gamma(1) * r(2))
        b(1) = Fo * hcap / D(1)
    ElseIf toptype = "Robin" Then
        X(1, 1) = Pe(1) / 2 + gamma(1) / WorksheetFunction.Tanh(gamma(1) * r(2))
        X(1, 2) = -gamma(1) * Exp(-Pe(1) / 2 * r(2)) /
WorksheetFunction.Sinh(gamma(1) * r(2))
        b(1) = Fo * hcap / D(1)
    ElseIf toptype = "Benthic" Then
```

```
        X(1, 1) = -Pe(1) / 2 + gamma(1) / WorksheetFunction.Tanh(gamma(1) * r(2))
+ Bio
        X(1, 2) = -gamma(1) * Exp(-Pe(1) / 2 * r(2)) /
WorksheetFunction.Sinh(gamma(1) * r(2))
        b(1) = Bio * Co
    End If
Else
    If toptype = "Dirichlet" Then
        X(1, 1) = 1
        b(1) = Co
    ElseIf toptype = "Neumann" Then
        X(1, 1) = D(1) / r(2)
        X(1, 2) = -D(1) / r(2)
        b(1) = Fo * hcap / D(1)
    ElseIf toptype = "Robin" Then
        X(1, 1) = D(1) / r(2)
        X(1, 2) = -D(1) / r(2)
        b(1) = Fo * hcap / D(1)
    ElseIf toptype = "Benthic" Then
        X(1, 1) = D(1) / r(2) + Bio * D(1)
        X(1, 2) = -D(1) / r(2)
        b(1) = Bio * Co * D(1)
    End If
End If

'Bottom Boundary
If layertype(layers) = "Regular" Then
    If bottomtype = "Dirichlet" Then
        X(layers + 1, layers + 1) = 1
        b(layers + 1) = Ch
    ElseIf bottomtype = "Neumann" Then
        X(layers + 1, layers) = gamma(layers) * Exp(Pe(layers) / 2 * (1 -
r(layers))) / WorksheetFunction.Sinh(gamma(layers) * (1 - r(layers)))
        X(layers + 1, layers + 1) = -Pe(layers) / 2 - gamma(layers) /
WorksheetFunction.Tanh(gamma(layers) * (1 - r(layers)))
        b(layers + 1) = Fo * hcap / D(layers)
    ElseIf bottomtype = "Robin" Then
        X(layers + 1, layers) = gamma(layers) * Exp(Pe(layers) / 2 * (1 -
r(layers))) / WorksheetFunction.Sinh(gamma(layers) * (1 - r(layers)))
        X(layers + 1, layers + 1) = Pe(layers) / 2 - gamma(layers) /
WorksheetFunction.Tanh(gamma(layers) * (1 - r(layers)))
        b(layers + 1) = Fo * hcap / D(layers)
    ElseIf bottomtype = "Benthic" Then
        X(layers + 1, layers) = gamma(layers) * Exp(Pe(layers) / 2 * (1 -
r(layers))) / WorksheetFunction.Sinh(gamma(layers) * (1 - r(layers)))
        X(layers + 1, layers + 1) = -Pe(layers) / 2 - gamma(layers) /
WorksheetFunction.Tanh(gamma(layers) * (1 - r(layers))) - Bih
        b(layers + 1) = -Bih * Ch
    End If
Else
    If bottomtype = "Dirichlet" Then
        X(layers + 1, layers + 1) = 1
        b(layers + 1) = Ch
```

```
    ElseIf bottomtype = "Neumann" Then
        X(layers + 1, layers) = D(layers) / (1 - r(layers))
        X(layers + 1, layers + 1) = -D(layers) / (1 - r(layers))
        b(layers + 1) = Fo * hcap / D(layers)
    ElseIf bottomtype = "Robin" Then
        X(layers + 1, layers) = D(layers) / (1 - r(layers))
        X(layers + 1, layers + 1) = -D(layers) / (1 - r(layers))
        b(layers + 1) = Fo * hcap / D(layers)
    ElseIf bottomtype = "Benthic" Then
        X(layers + 1, layers) = D(layers) / (1 - r(layers))
        X(layers + 1, layers + 1) = -D(layers) / (1 - r(layers)) - Bih * D(layers)
        b(layers + 1) = -Bih * D(layers) * Ch
    End If
End If

'Solve the steady-state matrix
'Determine the determinant of the matrix to see whether this matrix is singular
Dim singularmatrix As Integer, Xtest() As Double
ReDim Xtest(1 To layers + 1, 1 To layers + 1)

For i = 1 To layers + 1
    For j = 1 To layers + 1
        Xtest(i, j) = X(i, j)
    Next j
Next i

singularmatrix = 0
For i = 1 To layers
    If Xtest(i, i) <> 0 Then
        Xtest(i + 1, i + 1) = Xtest(i + 1, i + 1) - Xtest(i, i + 1) * Xtest(i + 1,
i) / Xtest(i, i)
    End If
Next i

For i = 1 To layers + 1
    If Xtest(i, i) = 0 Then
        singularmatrix = 1
    End If
Next i

If singularmatrix = 1 Then
    For i = 1 To layers + 1
        CT(i) = 0
    Next i
Else
    'Reformat the tridiagonal matrix to the diagonal matrix using Gauss
elimination
    Dim ratio1, ratio2 As Double

    For i = 1 To layers
        ratio1 = X(i + 1, i) / X(i, i)
        For j = 1 To layers + 1
            X(i + 1, j) = X(i + 1, j) - X(i, j) * ratio1
```

```
        Next j
        b(i + 1) = b(i + 1) - b(i) * ratio1
    Next i

    For i = 1 To layers
        ratio2 = X(layers + 1 - i, layers + 2 - i) / X(layers + 2 - i, layers + 2
- i)
        For j = 1 To layers + 1
            X(layers + 1 - i, j) = X(layers + 1 - i, j) - ratio2 * X(layers + 2 -
i, j)
        Next j
        b(layers + 1 - i) = b(layers + 1 - i) - b(layers + 2 - i) * ratio2
    Next i

    'Solve the coefficients
    For i = 1 To layers + 1
        CT(i) = b(i) / X(i, i)
    Next i
End If


'Solving the interfacial concentrations


'Solving for magnitude coefficient A

ReDim A(1 To num)
ReDim coef(1 To layers, 1 To num)
ReDim inte(1 To layers, 1 To num)
ReDim ra(1 To layers, 1 To num)

For n = 1 To num
    Int_total = 0
    eigengroup_total = 0
    ra(1, n) = 1
    For layer = 1 To layers
        coef(layer, n) = Int_eigengroup(ytype(layer, n), r(layer), r(layer + 1),
y(layer, n), Fi(layer, n), Fi(layer + 1, n), Pe(layer))
        inte(layer, n) = Int_Init(layertype(layer), ytype(layer, n), r(layer),
r(layer + 1), CT(layer), CT(layer + 1), y(layer, n), Pe(layer), Fi(layer, n),
Fi(layer + 1, n), Cinit(layer), gamma(layer))
    Next layer

    For layer = 1 To layers
        Int_term = inte(layer, n)
        eigengroup_term = coef(layer, n)


        If layer > 1 Then
            For front = 2 To layer
                Int_term = Int_term * Exp(Pe(front) * r(front))
                eigengroup_term = eigengroup_term * Exp(Pe(front) * r(front))
            Next front
```

```
        End If

        If (layers - layer) > 0 Then
            For back = 1 To (layers - layer)
                Int_term = Int_term * Exp(Pe(layer + back - 1) * r(layer + back))
                eigengroup_term = eigengroup_term * Exp(Pe(layer + back - 1) *
r(layer + back))
            Next back
        End If
        'MsgBox (Int_term)
        'MsgBox (eigengroup_term)

        Int_total = Int_total + Int_term * Rd(layer)
        eigengroup_total = eigengroup_total + eigengroup_term * Rd(layer)
    Next layer

    A(n) = Int_total / eigengroup_total
Next n
'Output intermediate coefficients

'Sheet "Coef_beta"
For i = 0 To 200
    For j = 0 To 20
        Worksheets("Coef_beta").Cells(12 + i, 1 + j).ClearContents
    Next j
    Worksheets("Coef_beta").Cells(4, 2 + i).ClearContents
    Worksheets("Coef_beta").Cells(5, 2 + i).ClearContents
    Worksheets("Coef_beta").Cells(6, 2 + i).ClearContents
    Worksheets("Coef_beta").Cells(13, 2 + i).ClearContents
    Worksheets("Coef_beta").Cells(14, 4 + i).ClearContents
Next i

For layer = 1 To layers
    Worksheets("Coef_beta").Cells(5, layer + 1).Value = r(layer)
    Worksheets("Coef_beta").Cells(6, layer + 1).Value = CT(layer)
    Worksheets("Coef_beta").Cells(8, layer + 1).Value = layer
    Worksheets("Coef_beta").Cells(9, layer + 1).Value = layertype(layer)

    Worksheets("Coef_beta").Cells(13, layer * 2 + 2).Value = layer
    Worksheets("Coef_beta").Cells(13, layer * 2 + 3).Value = layer
    Worksheets("Coef_beta").Cells(14, layer * 2 + 2).Value = "ytype"
    Worksheets("Coef_beta").Cells(14, layer * 2 + 3).Value = "y"
Next layer

Worksheets("Coef_beta").Cells(5, layers + 2).Value = r(layers + 1)
Worksheets("Coef_beta").Cells(6, layers + 2).Value = CT(layers + 1)

For n = 1 To num
    Worksheets("Coef_beta").Cells(14 + n, 1).Value = n
    Worksheets("Coef_beta").Cells(14 + n, 2).Value = betatype(n)
    Worksheets("Coef_beta").Cells(14 + n, 3).Value = beta(n)
    For layer = 1 To layers
```

```
        Worksheets("Coef_beta").Cells(14 + n, 2 + layer * 2).Value = ytype(layer,
n)
        Worksheets("Coef_beta").Cells(14 + n, 3 + layer * 2).Value = y(layer, n)
    Next layer
Next n

'Sheet "Coef_Fi"
For i = 0 To 200
    For j = 0 To 20
        Worksheets("Coef_Fi").Cells(4 + i, 1 + j).ClearContents
    Next j
    Worksheets("Coef_Fi").Cells(3, 1 + i).ClearContents
Next i

For layer = 1 To layers
    Worksheets("Coef_Fi").Cells(3, layer + 1).Value = r(layer)
Next layer
Worksheets("Coef_Fi").Cells(3, layers + 2).Value = r(layers + 1)

For n = 1 To num
    Worksheets("Coef_Fi").Cells(3 + n, 1).Value = n
    For layer = 1 To layers
        Worksheets("Coef_Fi").Cells(3 + n, 1 + layer).Value = Fi(layer, n)
    Next layer
    Worksheets("Coef_Fi").Cells(3 + n, 2 + layers).Value = Fi(layer, n)
Next n

'Sheet "Coef_A"
For i = 0 To 200
    For j = 0 To 20
        Worksheets("Coef_A").Cells(4 + i, 1 + j).ClearContents
    Next j
    Worksheets("Coef_A").Cells(3, 1 + i).ClearContents
Next i

For n = 1 To num
    Worksheets("Coef_A").Cells(3 + n, 1).Value = n
    Worksheets("Coef_A").Cells(3 + n, 2).Value = A(n)
Next n


End Sub

Function Int_Init(layertype, ytype As Integer, lb, hb, CTl, CTh, y, Pe, Fil, Fih,
Cinit, gamma) As Double

    If layertype = "Regular" Then

        C1 = CTl * Exp(-Pe / 2 * lb) / WorksheetFunction.Sinh(gamma * (hb - lb))
        C2 = CTh * Exp(-Pe / 2 * hb) / WorksheetFunction.Sinh(gamma * (hb - lb))
        If ytype = 0 Then
            alpha = Fil * Exp(-Pe / 2 * lb) / WorksheetFunction.Sinh(y * (hb -
lb))
```

```
            beta = Fih * Exp(-Pe / 2 * hb) / WorksheetFunction.Sinh(y * (hb - lb))
            Int_Init = Cinit / ((Pe / 2) ^ 2 - y ^ 2) * (Exp(-Pe / 2 * hb) * ((-Pe
/ 2) * beta * WorksheetFunction.Sinh(y * (hb - lb)) - y * (-alpha + beta *
WorksheetFunction.Cosh(y * (hb - lb)))) - _
                                                          Exp(-Pe / 2 * lb) * ((-Pe
/ 2) * alpha * WorksheetFunction.Sinh(y * (hb - lb)) - y * (-alpha *
WorksheetFunction.Cosh(y * (hb - lb)) + beta))) - _
                        1 / (gamma ^ 2 - y ^ 2) * (gamma * (-C1 + C2 *
WorksheetFunction.Cosh(gamma * (hb - lb))) * beta * WorksheetFunction.Sinh(y * (hb
- lb)) - _
                                                   gamma * (-C1 *
WorksheetFunction.Cosh(gamma * (hb - lb)) + C2) * alpha * WorksheetFunction.Sinh(y
* (hb - lb)) - _
                                                   y * C2 *
WorksheetFunction.Sinh(gamma * (hb - lb)) * (-alpha + beta *
WorksheetFunction.Cosh(y * (hb - lb))) + _
                                                   y * C1 *
WorksheetFunction.Sinh(gamma * (hb - lb)) * (-alpha * WorksheetFunction.Cosh(y *
(hb - lb)) + beta))

        End If
        If ytype = 1 Then
            alpha = Fil * Exp(-Pe / 2 * lb) / Sin(y * (hb - lb))
            beta = Fih * Exp(-Pe / 2 * hb) / Sin(y * (hb - lb))

            Int_Init = Cinit / ((Pe / 2) ^ 2 + y ^ 2) * (Exp(-Pe / 2 * hb) * ((-Pe
/ 2) * beta * Sin(y * (hb - lb)) - y * (-alpha + beta * Cos(y * (hb - lb)))) - _
                                                          Exp(-Pe / 2 * lb) * ((-Pe
/ 2) * alpha * Sin(y * (hb - lb)) - y * (-alpha * Cos(y * (hb - lb)) + beta))) - _
                        1 / (gamma ^ 2 + y ^ 2) * (gamma * (-C1 + C2 *
WorksheetFunction.Cosh(gamma * (hb - lb))) * beta * Sin(y * (hb - lb)) - _
                                                   gamma * (-C1 *
WorksheetFunction.Cosh(gamma * (hb - lb)) + C2) * alpha * Sin(y * (hb - lb)) - _
                                                   y * C2 *
WorksheetFunction.Sinh(gamma * (hb - lb)) * (-alpha + beta * Cos(y * (hb - lb))) +
_
                                                   y * C1 *
WorksheetFunction.Sinh(gamma * (hb - lb)) * (-alpha * Cos(y * (hb - lb)) + beta))

        End If
    Else
        C1 = (CTh - CTl) / (hb - lb)
        C2 = (CTl * hb - CTh * lb) / (hb - lb)
        alpha = Fil * Exp(-Pe / 2 * lb) / Sin(y * (hb - lb))
        beta = Fih * Exp(-Pe / 2 * hb) / Sin(y * (hb - lb))
        Int_Init = ((alpha - beta * Cos(y * (hb - lb))) * (Cinit - C1 * hb - C2) /
y - beta * Sin(y * (hb - lb)) * C1 / y ^ 2 - _
                   (alpha * Cos(y * (hb - lb)) - beta) * (Cinit - C1 * lb - C2) /
y + alpha * Sin(y * (hb - lb)) * C1 / y ^ 2)

    End If

End Function
```

```
Function Int_eigengroup(ytype As Integer, lb, hb, y, Fil, Fih, Pe) As Double
    Dim alpha, beta, L1, L2 As Double

    If ytype = 0 Then
        alpha = Fil * Exp(-Pe / 2 * lb) / WorksheetFunction.Sinh(y * (hb - lb))
        beta = Fih * Exp(-Pe / 2 * hb) / WorksheetFunction.Sinh(y * (hb - lb))
        L1 = alpha * WorksheetFunction.Sinh(y * hb) - beta *
WorksheetFunction.Sinh(y * lb)
        L2 = beta * WorksheetFunction.Cosh(y * lb) - alpha *
WorksheetFunction.Cosh(y * hb)
        Int_eigengroup = (L1 ^ 2 - L2 ^ 2) / 2 * (hb - lb) + (L1 ^ 2 + L2 ^ 2) / 4
/ y * (WorksheetFunction.Sinh(2 * y * hb) - WorksheetFunction.Sinh(2 * y * lb)) +
L1 * L2 / 2 / y * (WorksheetFunction.Cosh(2 * y * hb) - WorksheetFunction.Cosh(2 *
y * lb))
    End If

    If ytype = 1 Then
        alpha = Fil * Exp(-Pe / 2 * lb) / Sin(y * (hb - lb))
        beta = Fih * Exp(-Pe / 2 * hb) / Sin(y * (hb - lb))
        L1 = alpha * Sin(y * hb) - beta * Sin(y * lb)
        L2 = beta * Cos(y * lb) - alpha * Cos(y * hb)
        Int_eigengroup = (L1 ^ 2 + L2 ^ 2) / 2 * (hb - lb) + (L1 ^ 2 - L2 ^ 2) / 4
/ y * (Sin(2 * y * hb) - Sin(2 * y * lb)) - L1 * L2 / 2 / y * (Cos(2 * y * hb) -
Cos(2 * y * lb))
    End If

End Function

Function Fi_Evaluation(y1, y2, ytype1, ytype2, Fi01, Fi12, D1, D2, Pe1, Pe2, r01,
r12, r23) As Double

Dim Fi23, Ass1, Ass2, Bss1, Bss2 As Double
If ytype1 = 1 Then
    Ass1 = D1 * y1 * Exp(Pe1 / 2 * (r12 - r01)) / Sin(y1 * (r12 - r01))
    Bss1 = D1 * y1 / Tan(y1 * (r12 - r01))
Else
    Ass1 = D1 * y1 * Exp(Pe1 / 2 * (r12 - r01)) / WorksheetFunction.Sinh(y1 * (r12
- r01))
    Bss1 = D1 * y1 / WorksheetFunction.Tanh(y1 * (r12 - r01))
End If

If ytype2 = 1 Then
    Ass2 = D2 * y2 * Exp(Pe2 / 2 * (r12 - r23)) / Sin(y2 * (r23 - r12))
    Bss2 = D2 * y2 / Tan(y2 * (r23 - r12))
Else
    Ass2 = D2 * y2 * Exp(Pe2 / 2 * (r12 - r23)) / WorksheetFunction.Sinh(y2 * (r23
- r12))
    Bss2 = D2 * y2 / WorksheetFunction.Tanh(y2 * (r23 - r12))
End If

Fi23 = (-Ass1 * Fi01 + (Bss1 + Bss2) * Fi12) / Ass2
Fi_Evaluation = Fi23
```

```
End Function

Function N_Evaluation(y, ytype, D, Pe, eDa, r, layers, Rd, toptype, bottomtype,
Bio, Bih)

'Evaluation of Natural Frequencies
Dim No, s As Integer, Ass(), Bss(), Xss() As Double

No = 0
For layer = 1 To layers:
    If ytype(layer) = 1 Then
        No = No + Int(y(layer) * (r(layer + 1) - r(layer)) /
WorksheetFunction.Pi())
    End If
Next layer

'Evaluation the sign-count
ReDim Xss(1 To layers + 1, 1 To layers + 1)
ReDim Ass(1 To layers)
ReDim Bss(1 To layers)

For layer = 1 To layers
    If ytype(layer) = 1 Then
        Ass(layer) = D(layer) * y(layer) * Cos(y(layer) * (r(layer + 1) -
r(layer))) / Sin(y(layer) * (r(layer + 1) - r(layer)))
        Bss(layer) = D(layer) * y(layer) / Sin(y(layer) * (r(layer + 1) -
r(layer)))
    ElseIf ytype(layer) = 0 Then
        Ass(layer) = D(layer) * y(layer) * WorksheetFunction.Cosh(y(layer) *
(r(layer + 1) - r(layer))) / WorksheetFunction.Sinh(y(layer) * (r(layer + 1) -
r(layer)))
        Bss(layer) = D(layer) * y(layer) / WorksheetFunction.Sinh(y(layer) *
(r(layer + 1) - r(layer)))
    End If
Next layer

If toptype = "Dirichlet" Then
    Xss(1, 1) = 1
ElseIf toptype = "Neumann" Then
    Xss(1, 1) = Ass(1) - Pe(1) / 2 * D(1)
    Xss(1, 2) = -Bss(1) * Exp(Pe(1) / 2 * (0 - r(2)))
ElseIf toptype = "Robin" Then
    Xss(1, 1) = Ass(1) + Pe(1) / 2 * D(1)
    Xss(1, 2) = -Bss(1) * Exp(Pe(1) / 2 * (0 - r(2)))
ElseIf toptype = "Benthic" Then
    Xss(1, 1) = Ass(1) - Pe(1) / 2 * D(1) + Bio * D(1)
    Xss(1, 2) = -Bss(1) * Exp(Pe(1) / 2 * (0 - r(2)))
End If

If bottomtype = "Dirichlet" Then
    Xss(layers + 1, layers + 1) = 1
ElseIf bottomtype = "Neumann" Then
```

```
    Xss(layers + 1, layers) = -Bss(layers) * Exp(Pe(layers) / 2 * (1 - r(layers)))
    Xss(layers + 1, layers + 1) = Ass(layers) + Pe(layers) / 2 * D(layers)
ElseIf bottomtype = "Robin" Then
    Xss(layers + 1, layers) = -Bss(layers) * Exp(Pe(layers) / 2 * (1 - r(layers)))
    Xss(layers + 1, layers + 1) = Ass(layers) - Pe(layers) / 2 * D(layers)
ElseIf bottomtype = "Benthic" Then
    Xss(layers + 1, layers) = -Bss(layers) * Exp(Pe(layers) / 2 * (1 - r(layers)))
    Xss(layers + 1, layers + 1) = Ass(layers) + Pe(layers) / 2 * D(layers) + Bih *
D(layers)
End If

For layer = 1 To (layers - 1)
    Xss(layer + 1, layer) = -Bss(layer) * Exp(Pe(layer) / 2 * (r(layer + 1) -
r(layer)))
    Xss(layer + 1, layer + 1) = Ass(layer) + Ass(layer + 1)
    Xss(layer + 1, layer + 2) = -Bss(layer + 1) * Exp(Pe(layer + 1) / 2 * (r(layer
+ 1) - r(layer + 2)))
Next layer

For layer = 2 To layers + 1
    Xss(layer, layer) = Xss(layer, layer) - Xss(layer - 1, layer) * Xss(layer,
layer - 1) / Xss(layer - 1, layer - 1)
Next layer

s = 0
For layer = 1 To layers + 1
    If Xss(layer, layer) < 0 Then
        s = s + 1
    End If
Next layer

N_Evaluation = No + s
End Function
```

Module 2: 'Plot'

```
Attribute VB_Name = "Module2"
Sub CapAn_plot()
' Using the eigenvalues and coefficients calculated by CapAn_solver to plot graphs


' Read plotting parameters

p = 30 ' The baseline for the plotting section in CapAn sheet

Dim NDP, NTP, LD, LT As Integer, ND(), NT() As Double

NDP = Worksheets("CapAn").Cells(p + 1, 2).Value
NTP = Worksheets("CapAn").Cells(p + 5, 2).Value


ReDim ND(1 To NDP)
ReDim NT(1 To NTP)

For LD = 1 To NDP
    ND(LD) = Worksheets("CapAn").Cells(p + 2, 1 + LD).Value
Next LD

For LT = 1 To NTP
    NT(LT) = Worksheets("CapAn").Cells(p + 6, 1 + LT).Value
Next LT

' Read coefficients in analytical solution


Dim U As Double, layers As Integer                                      'System
properties
Dim h(), epsilon(), Dw(), Kd(), lambda(), Cinit(), rho() As Double    'Layer
properties
Dim toptype, bottomtype, toptyper, bottomtyper, layertype() As String, Fo, Fh, Co,
Ch, Cr As Double     'Boundary properties
Dim D(), Rd(), Pe(), eDa(), Bi, hcap, r() As Double
'Dimensionless properties
Dim beta(), y(), alpha(), A(), C1(), C2(), CT(), gamma() As Double, ytype(), num
As Integer     'Analytical solution coeffcients

' Read all properties and parameters

layers = Worksheets("CapAn").Cells(7, 2).Value
U = Worksheets("CapAn").Cells(8, 2).Value

ReDim h(1 To layers)
ReDim epsilon(1 To layers)
ReDim Dw(1 To layers)
ReDim Kd(1 To layers)
ReDim lambda(1 To layers)
```

```
ReDim Cinit(1 To layers)
ReDim rho(1 To layers)
ReDim layertype(1 To layers)

For layer = 1 To layers
          h(layer) = Worksheets("CapAn").Cells(12, layer + 1).Value
    epsilon(layer) = Worksheets("CapAn").Cells(13, layer + 1).Value
         Dw(layer) = Worksheets("CapAn").Cells(14, layer + 1).Value
         Kd(layer) = Worksheets("CapAn").Cells(15, layer + 1).Value
     lambda(layer) = Worksheets("CapAn").Cells(16, layer + 1).Value
      Cinit(layer) = Worksheets("CapAn").Cells(17, layer + 1).Value
        rho(layer) = Worksheets("CapAn").Cells(18, layer + 1).Value
Next layer

'Read boundary conditions
toptyper = Worksheets("CapAn").Cells(22, 2).Value
bottomtyper = Worksheets("CapAn").Cells(22, 7).Value

If toptyper = "Concentration" Or toptyper = "concentration" Or toptyper =
"CONCENTRATION" Then
    toptype = "Dirichlet"
ElseIf toptyper = "Mass Transfer" Or toptyper = "mass transfer" Or toptyper =
"Mass transfer" Or toptyper = "mass Transfer" Or toptyper = "MASS TRANSFER" Then
    toptype = "Benthic"
ElseIf toptyper = "Gradient" Or toptyper = "gradient" Or toptyper = "GRADIENT"
Then
    toptype = "Neumann"
ElseIf toptyper = "Flux" Or toptyper = "flux" Or toptyper = "FLUX" Then
    toptype = "Robin"
Else
    MsgBox ("Please define the correct top boundary type")
End If

If bottomtyper = "Concentration" Or bottomtyper = "concentration" Or bottomtyper =
"CONCENTRATION" Then
    bottomtype = "Dirichlet"
ElseIf bottomtyper = "Mass Transfer" Or bottomtyper = "mass transfer" Or
bottomtyper = "Mass transfer" Or bottomtyper = "mass Transfer" Or bottomtyper =
"MASS TRANSFER" Then
    bottomtype = "Benthic"
ElseIf bottomtyper = "Gradient" Or bottomtyper = "gradient" Or bottomtyper =
"GRADIENT" Then
    bottomtype = "Neumann"
ElseIf bottomtyper = "Flux" Or bottomtyper = "flux" Or bottomtyper = "FLUX" Then
    bottomtype = "Robin"
Else
    MsgBox ("Please define the correct bottom boundary type")
End If

If toptype = "Dirichlet" Then
    Co = Worksheets("CapAn").Cells(23, 2).Value
Else:
    Fo = Worksheets("CapAn").Cells(23, 2).Value
```

```
End If

If bottomtype = "Dirichlet" Then
    Ch = Worksheets("CapAn").Cells(23, 7).Value
Else:
    Fh = Worksheets("CapAn").Cells(23, 7).Value
End If

'Generate dimensionless variables
ReDim D(1 To layers)
ReDim Rd(1 To layers)
ReDim Pe(1 To layers)
ReDim eDa(1 To layers)
ReDim r(1 To layers + 1)

hcap = 0
For layer = 1 To layers
    hcap = hcap + h(layer)
Next layer

For layer = 1 To layers
    D(layer) = Dw(layer) * 3600 * 24 * 365 * epsilon(layer)
    Rd(layer) = Kd(layer) * rho(layer) + epsilon(layer)
    Pe(layer) = U * hcap / D(layer)
    eDa(layer) = epsilon(layer) * lambda(layer) * hcap ^ 2 / D(layer)
Next layer

Dim Depth As Double
Depth = 0
r(1) = 0

For layer = 1 To layers
    Depth = Depth + h(layer)
    r(layer + 1) = Depth / hcap
Next layer

Bi = kbl * hcap / D(1)

' Read all analytical coefficients

num = Worksheets("CapAn").Cells(27, 2).Value

ReDim beta(1 To num)
ReDim y(1 To layers, 1 To num)
ReDim ytype(1 To layers, 1 To num)
ReDim Fi(1 To layers + 1, 1 To num)
ReDim A(1 To num)
ReDim CT(layers + 1)
ReDim gamma(1 To layers)


For n = 1 To num
    beta(n) = Worksheets("Coef_beta").Cells(14 + n, 3).Value
```

```
    A(n) = Worksheets("Coef_A").Cells(3 + n, 2).Value
    For layer = 1 To layers
        ytype(layer, n) = Worksheets("Coef_beta").Cells(14 + n, 2 + layer *
2).Value
        y(layer, n) = Worksheets("Coef_beta").Cells(14 + n, 3 + layer * 2).Value
        Fi(layer, n) = Worksheets("Coef_Fi").Cells(3 + n, 1 + layer).Value
    Next layer
    Fi(layers + 1, n) = Worksheets("Coef_Fi").Cells(3 + n, 2 + layers).Value
Next n

For layer = 1 To layers
    gamma(layer) = (Pe(layer) ^ 2 + 4 * eDa(layer)) ^ 0.5 / 2
    layertype(layer) = Worksheets("Coef_beta").Cells(9, 1 + layer).Value
Next layer

For layer = 1 To layers + 1
    CT(layer) = Worksheets("Coef_beta").Cells(6, layer + 1).Value
Next layer

' Clear all old data
For i = 1 To 103
    For j = NDP To 5
        Worksheets("Conc vs Depth").Cells(1 + i, 1 + j).Value = ""
        Worksheets("Flux vs Depth").Cells(1 + i, 1 + j).Value = ""
    Next j
Next i

For i = 1 To 103
    For j = NTP To 5
        Worksheets("Conc vs Time").Cells(1 + i, 1 + j).Value = ""
        Worksheets("Flux vs Time").Cells(1 + i, 1 + j).Value = ""
    Next j
Next i

' Generate Depth profile
Dim t, z, conc, flux, Gridsize As Double, Gridnum As Integer

Gridnum = 100
Gridsize = hcap / Gridnum

ReDim z(Gridnum)
ReDim conc(1 To NDP, Gridnum)
ReDim flux(1 To NDP, Gridnum)

For j = 0 To Gridnum
    z(j) = j * Gridsize
Next j
For i = 1 To NDP
    t = ND(i)
    For j = 0 To Gridnum
        l = j / 100
        For layer = 1 To layers
            If l >= r(layer) And l <= r(layer + 1) Then
```

```
                If layertype(layer) = "Regular" Then
                    conc(i, j) = CT(layer) * Exp(Pe(layer) / 2 * (1 - r(layer))) *
WorksheetFunction.Sinh(gamma(layer) * (r(layer + 1) - l)) /
WorksheetFunction.Sinh(gamma(layer) * (r(layer + 1) - r(layer))) + _
                                CT(layer + 1) * Exp(Pe(layer) / 2 * (1 - r(layer
+ 1))) * WorksheetFunction.Sinh(gamma(layer) * (1 - r(layer))) /
WorksheetFunction.Sinh(gamma(layer) * (r(layer + 1) - r(layer)))
                    flux(i, j) = ((CT(layer) * Exp(Pe(layer) / 2 * (1 - r(layer)))
* WorksheetFunction.Sinh(gamma(layer) * (r(layer + 1) - l)) /
WorksheetFunction.Sinh(gamma(layer) * (r(layer + 1) - r(layer))) + _
                                CT(layer + 1) * Exp(Pe(layer) / 2 * (1 - r(layer
+ 1))) * WorksheetFunction.Sinh(gamma(layer) * (1 - r(layer))) /
WorksheetFunction.Sinh(gamma(layer) * (r(layer + 1) - r(layer)))) * Pe(layer) / 2
+ _
                                (-CT(layer) * Exp(Pe(layer) / 2 * (1 - r(layer)))
* WorksheetFunction.Cosh(gamma(layer) * (r(layer + 1) - l)) /
WorksheetFunction.Sinh(gamma(layer) * (r(layer + 1) - r(layer))) + _
                                CT(layer + 1) * Exp(Pe(layer) / 2 * (1 - r(layer
+ 1))) * WorksheetFunction.Cosh(gamma(layer) * (1 - r(layer))) /
WorksheetFunction.Sinh(gamma(layer) * (r(layer + 1) - r(layer)))) * (-
gamma(layer))) * D(layer)
                Else
                    conc(i, j) = CT(layer) * (r(layer + 1) - l) / (r(layer + 1) -
r(layer)) + CT(layer + 1) * (1 - r(layer)) / (r(layer + 1) - r(layer))
                    flux(i, j) = -(CT(layer + 1) - CT(layer)) / (r(layer + 1) -
r(layer)) * D(layer)
                End If

                For n = 1 To num
                    If ytype(layer, n) = 0 Then
                        conc(i, j) = conc(i, j) + Exp(-t * beta(n)) * A(n) *
(Fi(layer, n) * Exp(Pe(layer) / 2 * (1 - r(layer))) *
WorksheetFunction.Sinh(y(layer, n) * (r(layer + 1) - l)) /
WorksheetFunction.Sinh(y(layer, n) * (r(layer + 1) - r(layer))) + _

Fi(layer + 1, n) * Exp(Pe(layer) / 2 * (1 - r(layer + 1))) *
WorksheetFunction.Sinh(y(layer, n) * (1 - r(layer))) /
WorksheetFunction.Sinh(y(layer, n) * (r(layer + 1) - r(layer))))
                        flux(i, j) = flux(i, j) + Exp(-t * beta(n)) * A(n) *
(Pe(layer) / 2 * (Fi(layer, n) * Exp(Pe(layer) / 2 * (1 - r(layer))) *
WorksheetFunction.Sinh(y(layer, n) * (r(layer + 1) - l)) /
WorksheetFunction.Sinh(y(layer, n) * (r(layer + 1) - r(layer))) + _

Fi(layer + 1, n) * Exp(Pe(layer) / 2 * (1 - r(layer + 1))) *
WorksheetFunction.Sinh(y(layer, n) * (1 - r(layer))) /
WorksheetFunction.Sinh(y(layer, n) * (r(layer + 1) - r(layer)))) - _

y(layer, n) * (-Fi(layer, n) * Exp(Pe(layer) / 2 * (1 - r(layer))) *
WorksheetFunction.Cosh(y(layer, n) * (r(layer + 1) - l)) /
WorksheetFunction.Sinh(y(layer, n) * (r(layer + 1) - r(layer))) + _

Fi(layer + 1, n) * Exp(Pe(layer) / 2 * (1 - r(layer + 1))) *
```

```
WorksheetFunction.Cosh(y(layer, n) * (l - r(layer))) /
WorksheetFunction.Sinh(y(layer, n) * (r(layer + 1) - r(layer))))) * D(layer)
                    End If

                    If ytype(layer, n) = 1 Then
                        conc(i, j) = conc(i, j) + Exp(-t * beta(n)) * A(n) *
(Fi(layer, n) * Exp(Pe(layer) / 2 * (l - r(layer))) * Sin(y(layer, n) * (r(layer +
1) - l)) / Sin(y(layer, n) * (r(layer + 1) - r(layer))) + _

Fi(layer + 1, n) * Exp(Pe(layer) / 2 * (l - r(layer + 1))) * Sin(y(layer, n) * (l
- r(layer))) / Sin(y(layer, n) * (r(layer + 1) - r(layer))))
                        flux(i, j) = flux(i, j) + Exp(-t * beta(n)) * A(n) *
(Pe(layer) / 2 * (Fi(layer, n) * Exp(Pe(layer) / 2 * (l - r(layer))) *
Sin(y(layer, n) * (r(layer + 1) - l)) / Sin(y(layer, n) * (r(layer + 1) -
r(layer))) + _

Fi(layer + 1, n) * Exp(Pe(layer) / 2 * (l - r(layer + 1))) * Sin(y(layer, n) * (l
- r(layer))) / Sin(y(layer, n) * (r(layer + 1) - r(layer)))) - _

y(layer, n) * (-Fi(layer, n) * Exp(Pe(layer) / 2 * (l - r(layer))) * Cos(y(layer,
n) * (r(layer + 1) - l)) / Sin(y(layer, n) * (r(layer + 1) - r(layer))) + _

Fi(layer + 1, n) * Exp(Pe(layer) / 2 * (l - r(layer + 1))) * Cos(y(layer, n) * (l
- r(layer))) / Sin(y(layer, n) * (r(layer + 1) - r(layer))))) * D(layer)

                    End If
                Next n
            End If
        Next layer
        Worksheets("Conc vs Depth").Cells(3 + j, 1 + i).Value = conc(i, j)
        Worksheets("Conc vs Depth").Cells(3 + j, 1).Value = l * hcap
        Worksheets("Flux vs Depth").Cells(3 + j, 1 + i).Value = flux(i, j) / hcap
/ 1000
        Worksheets("Flux vs Depth").Cells(3 + j, 1).Value = l * hcap
    Next j
    Worksheets("Conc vs Depth").Cells(2, 1 + i).Value = t
    Worksheets("Flux vs Depth").Cells(2, 1 + i).Value = t
Next i

' Generate Time profile
Dim tt, zz, tconc, tflux, stepsize As Double, Stepnum As Integer

Stepnum = 100
stepsize = ND(NDP) / Gridnum

ReDim tt(Stepnum)
ReDim conc(1 To NTP, Stepnum)
ReDim flux(1 To NTP, Stepnum)

For i = 1 To NTP
    zz = NT(i) / hcap
    For j = 0 To Stepnum
        tt = j * stepsize
```

```
        For layer = 1 To layers
            If zz >= r(layer) And zz <= r(layer + 1) Then
                If layertype(layer) = "Regular" Then
                    conc(i, j) = CT(layer) * Exp(Pe(layer) / 2 * (zz - r(layer)))
* WorksheetFunction.Sinh(gamma(layer) * (r(layer + 1) - zz)) /
WorksheetFunction.Sinh(gamma(layer) * (r(layer + 1) - r(layer))) + _
                                  CT(layer + 1) * Exp(Pe(layer) / 2 * (zz - r(layer
+ 1))) * WorksheetFunction.Sinh(gamma(layer) * (zz - r(layer))) /
WorksheetFunction.Sinh(gamma(layer) * (r(layer + 1) - r(layer)))
                    flux(i, j) = ((CT(layer + 0) * Exp(Pe(layer) / 2 * (zz -
r(layer))) * WorksheetFunction.Sinh(gamma(layer) * (r(layer + 1) - zz)) /
WorksheetFunction.Sinh(gamma(layer) * (r(layer + 1) - r(layer))) + _
                                    CT(layer + 1) * Exp(Pe(layer) / 2 * (zz -
r(layer + 1))) * WorksheetFunction.Sinh(gamma(layer) * (zz - r(layer))) /
WorksheetFunction.Sinh(gamma(layer) * (r(layer + 1) - r(layer)))) * Pe(layer) / 2
+ _
                                  (-CT(layer) * Exp(Pe(layer) / 2 * (zz -
r(layer))) * WorksheetFunction.Cosh(gamma(layer) * (r(layer + 1) - zz)) /
WorksheetFunction.Sinh(gamma(layer) * (r(layer + 1) - r(layer))) + _
                                  CT(layer + 1) * Exp(Pe(layer) / 2 * (zz - r(layer
+ 1))) * WorksheetFunction.Cosh(gamma(layer) * (zz - r(layer))) /
WorksheetFunction.Sinh(gamma(layer) * (r(layer + 1) - r(layer)))) * (-
gamma(layer))) * D(layer)
                Else
                    conc(i, j) = CT(layer) * (r(layer + 1) - zz) / (r(layer + 1) -
r(layer)) + CT(layer + 1) * (zz - r(layer)) / (r(layer + 1) - r(layer))
                    flux(i, j) = -(CT(layer + 1) - CT(layer)) / (r(layer + 1) -
r(layer)) * D(layer)
                End If
                For n = 1 To num
                    If ytype(layer, n) = 0 Then
                        conc(i, j) = conc(i, j) + Exp(-tt * beta(n)) * A(n) *
(Fi(layer, n) * Exp(Pe(layer) / 2 * (zz - r(layer))) *
WorksheetFunction.Sinh(y(layer, n) * (r(layer + 1) - zz)) /
WorksheetFunction.Sinh(y(layer, n) * (r(layer + 1) - r(layer))) + _

Fi(layer + 1, n) * Exp(Pe(layer) / 2 * (zz - r(layer + 1))) *
WorksheetFunction.Sinh(y(layer, n) * (zz - r(layer))) /
WorksheetFunction.Sinh(y(layer, n) * (r(layer + 1) - r(layer))))
                        flux(i, j) = flux(i, j) + Exp(-tt * beta(n)) * A(n) *
(Pe(layer) / 2 * (Fi(layer, n) * Exp(Pe(layer) / 2 * (zz - r(layer))) *
WorksheetFunction.Sinh(y(layer, n) * (r(layer + 1) - zz)) /
WorksheetFunction.Sinh(y(layer, n) * (r(layer + 1) - r(layer))) + _

Fi(layer + 1, n) * Exp(Pe(layer) / 2 * (zz - r(layer + 1))) *
WorksheetFunction.Sinh(y(layer, n) * (zz - r(layer))) /
WorksheetFunction.Sinh(y(layer, n) * (r(layer + 1) - r(layer)))) - _

y(layer, n) * (-Fi(layer, n) * Exp(Pe(layer) / 2 * (zz - r(layer))) *
WorksheetFunction.Cosh(y(layer, n) * (r(layer + 1) - zz)) /
WorksheetFunction.Sinh(y(layer, n) * (r(layer + 1) - r(layer))) + _

Fi(layer + 1, n) * Exp(Pe(layer) / 2 * (zz - r(layer + 1))) *
```

```
WorksheetFunction.Cosh(y(layer, n) * (zz - r(layer))) /
WorksheetFunction.Sinh(y(layer, n) * (r(layer + 1) - r(layer))))) * D(layer)
                    End If
                    If ytype(layer, n) = 1 Then
                        conc(i, j) = conc(i, j) + Exp(-tt * beta(n)) * A(n) *
(Fi(layer, n) * Exp(Pe(layer) / 2 * (zz - r(layer))) * Sin(y(layer, n) * (r(layer
+ 1) - zz)) / Sin(y(layer, n) * (r(layer + 1) - r(layer))) + _

Fi(layer + 1, n) * Exp(Pe(layer) / 2 * (zz - r(layer + 1))) * Sin(y(layer, n) *
(zz - r(layer))) / Sin(y(layer, n) * (r(layer + 1) - r(layer))))
                        flux(i, j) = flux(i, j) + Exp(-tt * beta(n)) * A(n) *
(Pe(layer) / 2 * (Fi(layer, n) * Exp(Pe(layer) / 2 * (zz - r(layer))) *
Sin(y(layer, n) * (r(layer + 1) - zz)) / Sin(y(layer, n) * (r(layer + 1) -
r(layer))) + _

Fi(layer + 1, n) * Exp(Pe(layer) / 2 * (zz - r(layer + 1))) * Sin(y(layer, n) *
(zz - r(layer))) / Sin(y(layer, n) * (r(layer + 1) - r(layer)))) - _

y(layer, n) * (-Fi(layer, n) * Exp(Pe(layer) / 2 * (zz - r(layer))) * Cos(y(layer,
n) * (r(layer + 1) - zz)) / Sin(y(layer, n) * (r(layer + 1) - r(layer))) + _

Fi(layer + 1, n) * Exp(Pe(layer) / 2 * (zz - r(layer + 1))) * Cos(y(layer, n) *
(zz - r(layer))) / Sin(y(layer, n) * (r(layer + 1) - r(layer))))) * D(layer)

                    End If
                Next n
            End If
        Next layer
        Worksheets("Conc vs Time").Cells(3 + j, 1 + i).Value = conc(i, j)
        Worksheets("Conc vs Time").Cells(3 + j, 1).Value = tt
        Worksheets("Flux vs Time").Cells(3 + j, 1 + i).Value = flux(i, j) / hcap /
1000
        Worksheets("Flux vs Time").Cells(3 + j, 1).Value = tt
    Next j
    Worksheets("Conc vs Time").Cells(2, 1 + i).Value = zz * hcap
    Worksheets("Flux vs Time").Cells(2, 1 + i).Value = zz * hcap
Next i


End Sub
```

Appendix C. Matlab code for PRC calibration using the cylindrical solution

```
D_num_total = 20;


ro    = 0.02485;
L     = 0.02835;
Kp    = [5.35249  5.51348 6.02486 6.45101 6.53624 6.95292];
fss_PRC = [0.44  0.44   0.65    0.72    0.84    0.70];
foc = 0.01;

D     = zeros(1,D_num_total);
Koc   = zeros(1,1000);
Koc_PRC = zeros(D_num_total,6);

for j = 1 : 6


for j = 1:1000
    Koc(j) = 10-(j-1)*0.01;
end

for j = 1:D_num_total
    D(j) = (j * 1e-6)*86400;
end

fss = zeros(6,1000);

for D_num   = 1:D_num_total
    for PRC_num = 1:6
        for Koc_num = 1:1000
            R     = 10^Koc(Koc_num) * foc * 1.25 + 1;
            alpha = 10^Kp(PRC_num)*(L^2-ro^2)/R/(L^2);
            L_p   = (L^2-ro^2)/2/L;
            tau   = 28*D(D_num)/R/L^2;

            x = 1/alpha;

            if alpha > 1
                y = (1/alpha-1/alpha^2)^0.5;
                b = (1/alpha + y*j);
                c = (1/alpha - y*j);
                fss(PRC_num, Koc_num) = real(exp((1/alpha^2-
y^2)*tau)/2/y/1j*((cos(2*y/alpha*tau)*y+sin(2*y/alpha*tau)/alpha)*1j*(2
```

```
-erfz(b*tau^0.5)-erfz(c*tau^0.5))+(cos(2*y/alpha*tau)/alpha-
sin(2*y/alpha*tau)*y)*(0-erfz(b*tau^0.5)+erfz(c*tau^0.5))));
            else
                y = (1/alpha^2-1/alpha)^0.5;
                b = (1/alpha + y);
                c = (1/alpha - y);
                fss(PRC_num, Koc_num) =
1/2/y*(b*exp(b^2*tau)*erfc(b*tau^0.5)-c*exp(c^2*tau)*erfc(c*tau^0.5));
            end

            if Koc_num > 1
                if fss(PRC_num, Koc_num-1) < fss_PRC(PRC_num) &&
fss(PRC_num, Koc_num)> fss_PRC(PRC_num)
                    Koc_PRC(D_num, PRC_num) = Koc(Koc_num);
                end
            end
        end
    end
end
```

References

Accardi-Dey, A. and P. M. Gschwend (2002). "Assessing the combined roles of natural organic matter and black carbon as sorbents in sediments." Environmental Science & Technology 36(1): 21-29.

Accardi-Dey, A. and P. M. Gschwend (2003). "Reinterpreting literature sorption data considering both absorption into organic carbon and adsorption onto black carbon." Environmental Science & Technology 37(1): 99-106.

Adams, R. G., R. Lohmann, L. A. Fernandez, J. K. MacFarlane and P. M. Gschwend (2007). "Polyethylene devices: Passive samplers for measuring dissolved hydrophobic organic compounds in aquatic environments." Environmental Science & Technology 41(4): 1317-1323.

Ahn, S., D. Werner, H. K. Karapanagioti, D. R. McGlothlin, R. N. Zare and R. G. Luthy (2005). "Phenanthrene and pyrene sorption and intraparticle diffusion in polyoxymethylene, coke, and activated carbon." Environmental Science & Technology 39(17): 6516-6526.

Aller, R. C. (1982). The effects of macrobenthos on chemical properties of marine sediment and overlying water. Animal-sediment relations, Springer: 53-102.

Andelman, J. B. and M. J. Suess (1970). "Polynuclear aromatic hydrocarbons in the water environment." Bulletin of the World Health Organization 43(3): 479.

Apell, J. N. and P. M. Gschwend (2016). "In situ passive sampling of sediments in the Lower Duwamish Waterway Superfund site: Replicability, comparison with ex situ measurements, and use of data." Environmental Pollution 218: 95-101.

Azhar, W. (2015). Evaluation of sorbing amendments for in-situ remediation of contaminated sediments (Order No. 10035640). Available from ProQuest Dissertations & Theses Global. (1773635522). Retrieved from https://search.proquest.com/docview/1773635522?accountid=7098

Bao, L. J., X. Wu, F. Jia, E. Y. Zeng and J. Gan (2015). "Isotopic exchange on SPME fiber in sediment under stagnant conditions: Implications for field application of PRC calibration." Environmental Toxicology and Chemistry.

Barnett, M. O., R. R. Turner and P. C. Singer (2001). "Oxidative dissolution of metacinnabar (β-HgS) by dissolved oxygen." Applied Geochemistry 16(13): 1499-1512.

Bear, J. (1972). "Dynamics of fluids in porous materials." Society of Petroleum Engineers.

Bedard, D. L., R. E. Wagner, M. J. Brennan, M. L. Haberl and J. Brown (1987). "Extensive degradation of Aroclors and environmentally transformed polychlorinated biphenyls by Alcaligenes eutrophus H850." Applied and Environmental Microbiology 53(5): 1094-1102.

Beek, J. and W. Van Riemsdijk (1979). "Interaction of orthophosphate ions with soil." Developments in Soil Science 5: 259-284.

Beek, J., W. Van Riemsdijk and K. Koenders (1980). "Aluminium and ion fractions affecting phosphate bonding in a sandy soil treated with sewage water." Agrochemicals in Soils. Pergamon Press, Oxford: 369-379.

Belles, A., C. Alary, J. Criquet and G. Billon (2016). "A new application of passive samplers as indicators of in-situ biodegradation processes." Chemosphere 164: 347-354.

Berner, R. A. (1980). Early diagenesis: A theoretical approach, Princeton University Press.

Bessinger, B. A., Vlassopoulos, D., Serrano, S., & O'Day, P. A. (2012). Reactive transport modeling of subaqueous sediment caps and implications for the long-term fate of arsenic, mercury, and methylmercury. Aquatic geochemistry, 18(4), 297-326.

Booij, K., H. E. Hofmans, C. V. Fischer and E. M. Van Weerlee (2003). "Temperature-dependent uptake rates of nonpolar organic compounds by semipermeable membrane devices and low-density polyethylene membranes." Environmental Science & Technology 37(2): 361-366.

Bosworth, W. S. and L. J. Thibodeaux (1990). "Bioturbation: A facilitator of contaminant transport in bed sediment." Environmental Progress 9(4): 211-217.

Boudreau, B. P. (1986). "Mathematics of tracer mixing in sediments; II, Nonlocal mixing and biological conveyor-belt phenomena." American Journal of Science 286(3): 199-238.

Boudreau, B. P. (1994). "Is burial velocity a master parameter for bioturbation?" Geochimica et Cosmochimica Acta 58(4): 1243-1249.

Boudreau, B. P. (1996). "The diffusive tortuosity of fine-grained unlithified sediments." Geochimica et Cosmochimica Acta 60(16): 3139-3142.

Boudreau, B. P. (1997). Diagenetic models and their implementation, Springer Berlin.

Boudreau, B. P. and B. B. Jorgensen (2001). The benthic boundary layer: Transport processes and biogeochemistry, Oxford University Press.

Brändli, R. C., T. Hartnik, T. Henriksen and G. Cornelissen (2008). "Sorption of native polyaromatic hydrocarbons (PAH) to black carbon and amended activated carbon in soil." Chemosphere 73(11): 1805-1810.

Brenner, R. C., V. S. Magar, J. A. Ickes, E. A. Foote, J. E. Abbott, L. S. Bingler and E. A. Crecelius (2004). "Long-term recovery of PCB-contaminated surface sediments at the Sangamo-Weston/Twelvemile Creek/Lake Hartwell Superfund site." Environmental Science & Technology 38(8): 2328-2337.

Bridges, T. S., S. Ells, D. Hayes, D. Mount, S. C. Nadeau, M. R. Palermo, C. Patmont and P. Schroeder (2008). the four rs of Environmental dredging: resuspension, release, residual, and risk, DTIC Document.

Burton, G. A. (1991). "Assessing the toxicity of freshwater sediments." Environmental Toxicology and Chemistry 10(12): 1585-1627.

Chai, Y., A. Kochetkov and D. D. Reible (2006). "Modeling biphasic sorption and desorption of hydrophobic organic contaminants in sediments." Environmental Toxicology and Chemistry 25(12): 3133-3140.

Chen, J.-S. and C.-W. Liu (2011). "Generalized analytical solution for advection-dispersion equation in finite spatial domain with arbitrary time-dependent inlet boundary condition." Hydrology and Earth System Sciences 15(8): 2471.

Choi, Y., Y. Wu, R. G. Luthy and S. Kang (2016). "Non-equilibrium passive sampling of hydrophobic organic contaminants in sediment pore-water: PCB exchange kinetics." Journal of Hazardous Materials 318: 579-586.

Churchill, R. V. (1944). "Modern operational mathematics in engineering."

Clarke, J., D. D. Reible and R. Mutch (1993). "Contaminant transport and behavior in the subsurface." Hazardous Waste Soil Remediation: Theory and Application of Innovative Technologies. Marcel-Dekker, New York, NY, USA: 1-49.

Clarkson, T. W. (1998). "Human toxicology of mercury." The Journal of Trace Elements in Experimental Medicine 11(2-3): 303-317.

Cleary, R. W. and D. D. Adrian (1973). "Analytical solution of the convective-dispersive equation for cation adsorption in soils." Soil Science Society of America Journal 37(2): 197-199.

Cornelissen, G. and Ö. Gustafsson (2005). "Prediction of large variation in biota to sediment accumulation factors due to concentration‐dependent black carbon adsorption of planar hydrophobic organic compounds." Environmental Toxicology and Chemistry 24(3): 495-498.

Cornelissen, G., A. Pettersen, D. Broman, P. Mayer and G. D. Breedveld (2008). "Field testing of equilibrium passive samplers to determine freely dissolved native polycyclic aromatic hydrocarbon concentrations." Environmental Toxicology and Chemistry 27(3): 499-508.

Courant, R., K. Friedrichs and H. Lewy (1967). "On the partial difference equations of mathematical physics." IBM journal of Research and Development 11(2): 215-234.

Crank, J. (1948). "XLV. A diffusion problem in which the amount of diffusing substance is finite.—IV. solutions for small values of the time." The London, Edinburgh, and Dublin Philosophical Magazine and Journal of Science 39(292): 362-376.

Crank, J. and P. Nicolson (1947). A practical method for numerical evaluation of solutions of partial differential equations of the heat-conduction type. Mathematical Proceedings of the Cambridge Philosophical Society, Cambridge Univ Press.

Di Toro, D. M., C. S. Zarba, D. J. Hansen, W. J. Berry, R. C. Swartz, C. E. Cowan, S. P. Pavlou, H. E. Allen, N. A. Thomas and P. R. Paquin (1991). "Technical basis for establishing sediment quality criteria for nonionic organic chemicals using equilibrium partitioning." Environmental Toxicology and Chemistry 10(12): 1541-1583.

Eek, E., Cornelissen, G., Kibsgaard, A., & Breedveld, G. D. (2008). Diffusion of PAH and PCB from contaminated sediments with and without mineral capping; measurement and modelling. Chemosphere, 71(9), 1629-1638.

El-Dib, M. A. and M. I. Badawy (1979). "Adsorption of soluble aromatic hydrocarbons on granular activated carbon." Water Research 13(3): 255-258.

EPA, U. (1998). "EPA's Contaminated Sediment Management Strategy."

Fernandez, L. A., C. F. Harvey and P. M. Gschwend (2009). "Using performance reference compounds in polyethylene passive samplers to deduce sediment porewater concentrations for numerous target chemicals." Environmental Science & Technology 43(23): 8888-8894.

Fitzgerald, W. F., D. R. Engstrom, R. P. Mason and E. A. Nater (1998). "The case for atmospheric mercury contamination in remote areas." Environmental Science & Technology 32(1): 1-7.

Freundlich, H. (1909). "Kolloidchemie." Akademischer Verlagsgeselschaft, Leipzig.

Gawlik, B., N. Sotiriou, E. Feicht, S. Schulte-Hostede and A. Kettrup (1997). "Alternatives for the determination of the soil adsorption coefficient, KOC, of non-ionicorganic compounds—a review." Chemosphere 34(12): 2525-2551.

Ghosh, U., S. Kane Driscoll, R. M. Burgess, M. T. Jonker, D. Reible, F. Gobas, Y. Choi, S. E. Apitz, K. A. Maruya and W. R. Gala (2014). "Passive sampling methods for contaminated sediments: Practical guidance for selection, calibration, and implementation." Integrated Environmental Assessment and Management 10(2): 210-223.

Go, J., D. J. Lampert, J. A. Stegemann and D. D. Reible (2009). "Predicting contaminant fate and transport in sediment caps: mathematical modelling approaches." Applied Geochemistry 24(7): 1347-1353.

Goring, C. A. (1962). "Control of Nitrification by 2-chloro-6-(trichloro-methyl) pyridine." Soil Science 93(3): 211-218.

Guerrero, J. P., E. Pontedeiro, M. T. van Genuchten and T. Skaggs (2013). "Analytical solutions of the one-dimensional advection–dispersion solute transport equation subject to time-dependent boundary conditions." Chemical Engineering Journal 221: 487-491.

Guerrero, J. P. and T. Skaggs (2010). "Analytical solution for one-dimensional advection–dispersion transport equation with distance-dependent coefficients." Journal of Hydrology 390(1): 57-65.

Guerrero, J. S. P., T. H. Skaggs and M. T. van Genuchten (2009). "Analytical solution for multi-species contaminant transport subject to sequential first-order decay reactions in finite media." Transport in Porous Media 80(2): 373-387.

Guinasso, N. and D. Schink (1975). "Quantitative estimates of biological mixing rates in abyssal sediments." Journal of Geophysical Research 80(21): 3032-3043.

Hawker, D. W. and D. W. Connell (1988). "Octanol-water partition coefficients of polychlorinated biphenyl congeners." Environmental Science & Technology 22(4): 382-387.

Hawthorne, S. B., C. B. Grabanski and D. J. Miller (2007). "Measured partition coefficients for parent and alkyl polycyclic aromatic hydrocarbons in 114 historically contaminated sediments: Part 2. Testing the KOCKBC two carbon–type model." Environmental Toxicology and Chemistry 26(12): 2505-2516.

Hawthorne, S. B., M. T. Jonker, S. A. van der Heijden, C. B. Grabanski, N. A. Azzolina and D. J. Miller (2011). "Measuring picogram per liter concentrations of freely dissolved parent and alkyl PAHs (PAH-34), using passive sampling with polyoxymethylene." Analytical Chemistry 83(17): 6754-6761.

Hawthorne, S. B., D. J. Miller and C. B. Grabanski (2009). "Measuring low picogram per liter concentrations of freely dissolved polychlorinated biphenyls in sediment pore water using passive sampling with polyoxymethylene." Analytical Chemistry 81(22): 9472-9480.

Hilal, S., S. Karickhoff and L. Carreira (2004). "Prediction of the solubility, activity coefficient and liquid/liquid partition coefficient of organic compounds." Molecular Informatics 23(9): 709-720.

Howsam, M. and K. C. Jones (1998). Sources of PAHs in the environment. PAHs and related compounds, Springer: 137-174.

Huckins, J. N., G. K. Manuweera, J. D. Petty, D. Mackay and J. A. Lebo (1993). "Lipid-containing semipermeable membrane devices for monitoring organic contaminants in water." Environmental Science & Technology 27(12): 2489-2496.

Huckins, J. N., J. D. Petty and K. Booij (2006). Monitors of organic chemicals in the environment: semipermeable membrane devices, Springer Science & Business Media.

Huckins, J. N., J. D. Petty, J. A. Lebo, F. V. Almeida, K. Booij, D. A. Alvarez, W. L. Cranor, R. C. Clark and B. B. Mogensen (2002). "Development of the permeability/performance reference compound approach for in situ calibration of semipermeable membrane devices." Environmental Science & Technology 36(1): 85-91.

Huckins, J. N., M. W. Tubergen and G. K. Manuweera (1990). "Semipermeable membrane devices containing model lipid: A new approach to monitoring the bioavaiiability of lipophilic contaminants and estimating their bioconcentration potential." Chemosphere 20(5): 533-552.

Hull, J. H., J. M. Jersak and B. J. McDonald (1998). "Examination of a New Remedial Technology for Capping Contaminated Sediments: Large‐Scale Laboratory

Evaluation of Sediment Mixing and Cap Resistance to Erosive Forces." Remediation Journal 8(3): 37-58.

Jacobs, P. and T. Waite (2004). "The role of aqueous iron (II) and manganese (II) in sub-aqueous active barrier systems containing natural clinoptilolite." Chemosphere 54(3): 313-324.

Jacobs, P. H. and U. Förstner (1999). "Concept of subaqueous capping of contaminated sediments with active barrier systems (ABS) using natural and modified zeolites." Water Research 33(9): 2083-2087.

Jacobs, P. H. and U. Förstner (1999). "Concept of subaqueous capping of contaminated sediments with active barrier systems (ABS) using natural and modified zeolites." Water Research 33(9): 2083-2087.

Jaiswal, D. and A. Kumar (2011). "Analytical solutions of time and spatially dependent one-dimensional advection-diffusion equation." Elixir Poll 32: 2078-2083.

Jensen, S. (1972). "The PCB story." Ambio: 123-131.

Johnson, M. D., T. M. Keinath and W. J. Weber (2001). "A distributed reactivity model for sorption by soils and sediments. 14. Characterization and modeling of phenanthrene desorption rates." Environmental Science & Technology 35(8): 1688-1695.

Jonker, M. T. and A. A. Koelmans (2001). "Polyoxymethylene solid phase extraction as a partitioning method for hydrophobic organic chemicals in sediment and soot." Environmental Science & Technology 35(18): 3742-3748.

Jonker, M. T. and A. A. Koelmans (2001). "Polyoxymethylene solid phase extraction as a partitioning method for hydrophobic organic chemicals in sediment and soot." Environmental Science & Technology 35(18): 3742-3748.

Jonker, M. T. and A. A. Koelmans (2002). "Sorption of polycyclic aromatic hydrocarbons and polychlorinated biphenyls to soot and soot-like materials in the aqueous environment: mechanistic considerations." Environmental Science & Technology 36(17): 3725-3734.

Karcher, W., Fordham, R.J., Dubois, J.J., Glaude, P.G.J.M., & Ligthart, J.A.M. (1985). Spectral atlas of polycyclic aromatic compounds. United States: D. Reidel Publishing Co.,Hingham, MA.

Karickhoff, S. W., D. S. Brown and T. A. Scott (1979). "Sorption of hydrophobic pollutants on natural sediments." Water Research 13(3): 241-248.

Koelmans, A. A., M. T. Jonker, G. Cornelissen, T. D. Bucheli, P. C. Van Noort and Ö. Gustafsson (2006). "Black carbon: the reverse of its dark side." Chemosphere 63(3): 365-377.

Kraaij, R., P. Mayer, F. J. Busser, M. van Het Bolscher, W. Seinen, J. Tolls and A. C. Belfroid (2003). "Measured pore-water concentrations make equilibrium partitioning work a data analysis." Environmental Science & Technology 37(2): 268-274.

Kraepiel, A. M., K. Keller, H. B. Chin, E. G. Malcolm and F. M. Morel (2003). "Sources and variations of mercury in tuna." Environmental Science & Technology 37(24): 5551-5558.

Kudo, A. and S. Miyahara (1991). "A case history; Minamata mercury pollution in Japan–from loss of human lives to decontamination." Water Science and Technology 23(1-3): 283-290.

Kumar, A., D. K. Jaiswal and N. Kumar (2009). "Analytical solutions of one-dimensional advection-diffusion equation with variable coefficients in a finite domain." Journal of Earth System Science 118(5): 539-549.

Kumar, A., D. K. Jaiswal and N. Kumar (2010). "Analytical solutions to one-dimensional advection–diffusion equation with variable coefficients in semi-infinite media." Journal of Hydrology 380(3): 330-337.

Kumar, A., D. K. Jaiswal and N. Kumar (2012). "One-dimensional solute dispersion along unsteady flow through a heterogeneous medium, dispersion being proportional to the square of velocity." Hydrological Sciences Journal 57(6): 1223-1230.

Lagergren, S. (1898). "About the theory of so-called adsorption of soluble substances."

Lambert, S. (1966). "The influence of soil-moisture content on herbicidal response." Weeds: 273-275.

Lambert, S. M. (1967). "Functional relation between sorption in soil and chemical structure." Journal of Agricultural and Food Chemistry 15(4): 572-576.

Lambert, S. M. (1968). "Omega (. OMEGA.), a useful index of soil sorption equilibria." Journal of Agricultural and Food Chemistry 16(2): 340-343.

Lampert, D. (2010). An assessment of the design of in situ management approaches for contaminated sediments (Doctoral dissertation).

Lampert, D., C. Thomas and D. Reible (2015). "Internal and external transport significance for predicting contaminant uptake rates in passive samplers." Chemosphere 119: 910-916.

Lampert, D. J. and D. Reible (2009). "An analytical modeling approach for evaluation of capping of contaminated sediments." Soil and Sediment Contamination 18(4): 470-488.

Langmuir, I. (1918). "The evaporation of small spheres." Physical Review 12(5): 368.

Lapidus, L. and N. R. Amundson (1952). "Mathematics of adsorption in beds. VI. The effect of longitudinal diffusion in ion exchange and chromatographic columns." The Journal of Physical Chemistry 56(8): 984-988.

Leij, F. and M. T. Van Genuchten (1995). "Approximate analytical solutions for solute transport in two-layer porous media." Transport in Porous Media 18(1): 65-85.

Lerman, A. (1979). Geochemical processes. Water and sediment environments, John Wiley and Sons, Inc.

Lesage, G., M. Sperandio and L. Tiruta-Barna (2010). "Analysis and modelling of non-equilibrium sorption of aromatic micro-pollutants on GAC with a multi-compartment dynamic model." Chemical Engineering Journal 160(2): 457-465.

Li, Y. C. and P. J. Cleall (2011). "Analytical solutions for advective‐dispersive solute transport in double‐layered finite porous media." International Journal for Numerical and Analytical Methods in Geomechanics 35(4): 438-460.

Lick, W. and V. Rapaka (1996). "A quantitative analysis of the dynamics of the sorption of hydrophobic organic chemicals to suspended sediments." Environmental Toxicology and Chemistry 15(7): 1038-1048.

Lin, D., Y.-M. Cho, D. Werner and R. G. Luthy (2014). "Bioturbation delays attenuation of DDT by clean sediment cap but promotes sequestration by thin-layered activated carbon." Environmental Science & Technology 48(2): 1175-1183.

Liu, C., W. P. Ball and J. H. Ellis (1998). "An analytical solution to the one-dimensional solute advection-dispersion equation in multi-layer porous media." Transport in Porous Media 30(1): 25-43.

Liu, C., J. E. Szecsody, J. M. Zachara and W. P. Ball (2000). "Use of the generalized integral transform method for solving equations of solute transport in porous media." Advances in Water Resources 23(5): 483-492.

Lohmann, R., J. MacFarlane and P. Gschwend (2005). "Importance of black carbon to sorption of native PAHs, PCBs, and PCDDs in Boston and New York harbor sediments." Environmental Science & Technology 39(1): 141-148.

Low, P. F. (1981). "Principles of ion diffusion in clays." Chemistry in the Soil Environment(chemistryinthes): 31-45.

Lu, X., D. D. Reible and J. W. Fleeger (2004). "Bioavailability and assimilation of sediment‐associated benzo [a] pyrene by Ilyodrilus templetoni (oligochaeta)." Environmental Toxicology and Chemistry 23(1): 57-64.

Lu, X., D. D. Reible and J. W. Fleeger (2004). "Relative importance of ingested sediment versus pore water as uptake routes for PAHs to the deposit-feeding oligochaete Ilyodrilus templetoni." Archives of Environmental Contamination and Toxicology 47(2): 207-214.

Lu, X., D. D. Reible and J. W. Fleeger (2006). "Bioavailability of polycyclic aromatic hydrocarbons in field‐contaminated Anacostia River (Washington, DC) sediment." Environmental toxicology and chemistry 25(11): 2869-2874.

Lu, X., D. D. Reible, J. W. Fleeger and Y. Chai (2003). "Bioavailability of desorption‐resistant phenanthrene to the oligochaete Ilyodrilus templetoni." Environmental Toxicology and Chemistry 22(1): 153-160.

Mackay, D., W. Y. Shiu and K.-C. Ma (1997). Illustrated handbook of physical-chemical properties of environmental fate for organic chemicals, CRC press.

Mackay, D., W.-Y. Shiu, K.-C. Ma and S. C. Lee (2006). Handbook of physical-chemical properties and environmental fate for organic chemicals, CRC press.

Magar, V. S., D. B. Chadwick, T. S. Bridges, P. C. Fuchsman, J. M. Conder, T. J. Dekker, J. A. Steevens, K. E. Gustavson and M. A. Mills (2009). Monitored natural recovery at contaminated sediment sites, DTIC Document.

Malusis, M. A. and C. D. Shackelford (2002). "Theory for reactive solute transport through clay membrane barriers." Journal of Contaminant Hydrology 59(3): 291-316.

Manap, N. and N. Voulvoulis (2016). "Data analysis for environmental impact of dredging." Journal of Cleaner Production 137: 394-404.

Manes, M. and L. J. Hofer (1969). "Application of the Polanyi adsorption potential theory to adsorption from solution on activated carbon." The Journal of Physical Chemistry 73(3): 584-590.

Mayer, P., W. H. Vaes and J. L. Hermens (2000). "Absorption of hydrophobic compounds into the poly (dimethylsiloxane) coating of solid-phase microextraction fibers: High partition coefficients and fluorescence microscopy images." Analytical Chemistry 72(3): 459-464.

McDonough, K. M., J. L. Fairey and G. V. Lowry (2008). "Adsorption of polychlorinated biphenyls to activated carbon: Equilibrium isotherms and a preliminary assessment of the effect of dissolved organic matter and biofilm loadings." Water Research 42(3): 575-584.

McDonough, K. M., J. L. Fairey and G. V. Lowry (2008). "Adsorption of polychlorinated biphenyls to activated carbon: Equilibrium isotherms and a preliminary assessment of the effect of dissolved organic matter and biofilm loadings." Water Research 42(3): 575-584.

McDonough, K. M., P. Murphy, J. Olsta, Y. Zhu, D. Reible and G. V. Lowry (2007). "Development and placement of a sorbent-amended thin layer sediment cap in the Anacostia River." Soil and Sediment Contamination: An International Journal 16(3): 313-322.

Millington, R. and J. Quirk (1961). "Permeability of porous solids." Transactions of the Faraday Society 57: 1200-1207.

Moermond, C. T., J. J. Zwolsman and A. A. Koelmans (2005). "Black carbon and ecological factors affect in situ biota to sediment accumulation factors for hydrophobic organic compounds in flood plain lakes." Environmental Science & Technology 39(9): 3101-3109.

Mohan, R., J. P. Doody, C. Patmont, R. Gardner and A. Shellenberger (2016). "Review of Environmental Dredging in North America: Current Practice and Lessons Learned." Journal of Dredging 15(2): 29.

Moore, W. S. (1999). "The subterranean estuary: a reaction zone of ground water and sea water." Marine Chemistry 65(1): 111-125.

Moore, W. S., J. Krest, G. Taylor, E. Roggenstein, S. Joye and R. Lee (2002). "Thermal evidence of water exchange through a coastal aquifer: Implications for nutrient fluxes." Geophysical Research Letters 29(14).

Morel, F. M., A. M. Kraepiel and M. Amyot (1998). "The chemical cycle and bioaccumulation of mercury." Annual Review of Ecology and Systematics 29(1): 543-566.

Multiphysics, C. (2012). "COMSOL multiphysics user guide (Version 4.3 a)." COMSOL, AB: 39-40.

Murphy, P., A. Marquette, D. Reible and G. V. Lowry (2006). "Predicting the performance of activated carbon-, coke-, and soil-amended thin layer sediment caps." Journal of Environmental Engineering 132(7): 787-794.

Palermo, M. and D. Reible. 2007. The Evolution of Cap Design. Proceedings, World Dredging Congress WODCON XVIII, Orlando, FL, May 27-June1, 2007.

Palermo, M. R. (1998). "Design considerations for in-situ capping of contaminated sediments." Water Science and Technology 37(6-7): 315-321.

Parrett, K. and H. Blishke (2005). "23 Acre Multilayer Sediment Cap in Dynamic Riverine Environment Using organoclay an adsorptive Capping Material." SETAC Presentation.

Penman, H. (1940). "Gas and vapour movements in the soil: I. The diffusion of vapours through porous solids." The Journal of Agricultural Science 30(03): 437-462.

Penman, H. (1940). "Gas and vapour movements in the soil: I. The diffusion of vapours through porous solids." The Journal of Agricultural Science 30(03): 437-462.

Perelo, L. W. (2010). "Review: in situ and bioremediation of organic pollutants in aquatic sediments." Journal of Hazardous Materials 177(1): 81-89.

Pignatello, J. J. and B. Xing (1995). "Mechanisms of slow sorption of organic chemicals to natural particles." Environmental Science & Technology 30(1): 1-11.

Premlata, S. (2011). "One dimensional solute transport originating from a exponentially decay type point source along unsteady flow through heterogeneous medium." Journal of Water Resource and Protection 2011.

Rakowska, M., D. Kupryianchyk, J. Harmsen, T. Grotenhuis and A. Koelmans (2012). "In situ remediation of contaminated sediments using carbonaceous materials." Environmental Toxicology and Chemistry 31(4): 693-704.

Rakowska, M., D. Kupryianchyk, M. Smit, A. Koelmans, J. Grotenhuis and H. Rijnaarts (2014). "Kinetics of hydrophobic organic contaminant extraction from sediment by granular activated carbon." Water Research 51: 86-95.

Rakowska, M. I., D. Kupryianchyk, A. A. Koelmans, T. Grotenhuis and H. H. Rijnaarts (2014). "Equilibrium and kinetic modeling of contaminant immobilization by activated carbon amended to sediments in the field." Water Research 67: 96-104.

Reible, D., D. Lampert, D. Constant, R. D. Mutch Jr and Y. Zhu (2006). "Active capping demonstration in the Anacostia River, Washington, DC." Remediation Journal 17(1): 39-53.

Reible, D. D., F. H. Shair and E. Kauper (1981). "Plume dispersion and bifurcation in directional shear flows associated with complex terrain." Atmospheric Environment (1967) 15(7): 1165-1172.

Rhoads, D. (1974). "Organism-sediment relations on the muddy sea floor. Oceanogr." Mar. Biol. Ann. Rev. 12: 263-300.

Roche, K. R., A. F. Aubeneau, M. Xie, T. Aquino, D. Bolster and A. I. Packman (2016). "An integrated experimental and modeling approach to predict sediment mixing from benthic burrowing behavior." Environmental Science & Technology 50(18): 10047-10054.

Rowe, R. K. and J. R. Booker (1985). "1-D pollutant migration in soils of finite depth." Journal of Geotechnical Engineering 111(4): 479-499.

Rubin, H. and A. J. Rabideau (2000). "Approximate evaluation of contaminant transport through vertical barriers." Journal of Contaminant Hydrology 40(4): 311-333.

Schwarzenbach, R. P., P. M. Gschwend and D. M. Imboden (2003). Transformation Processes, Wiley Online Library.

Seth, R., D. Mackay and J. Muncke (1999). "Estimating the organic carbon partition coefficient and its variability for hydrophobic chemicals." Environmental Science & Technology 33(14): 2390-2394.

Sheindorf, C., M. Rebhun and M. Sheintuch (1981). "A Freundlich-type multicomponent isotherm." Journal of Colloid and Interface Science 79(1): 136-142.

Shen, X. and D. Reible (2015). "An analytical solution for one-dimensional advective–dispersive solute equation in multilayered finite porous media." Transport in Porous Media 107(3): 657-666.

Shiaris, M. P., & Sayler, G. S. (1982). Notes. Biotransformation of PCB by natural assemblages of freshwater microorganisms. Environmental Science Technology, 16, 367-369.

Sims, R. C. and M. Overcash (1983). Fate of polynuclear aromatic compounds (PNAs) in soil-plant systems. Residue reviews, Springer: 1-68.

Smedes, F., R. W. Geertsma, T. v. d. Zande and K. Booij (2009). "Polymer− water partition coefficients of hydrophobic compounds for passive sampling: Application of cosolvent models for validation." Environmental Science & Technology 43(18): 7047-7054.

Smith, G. D. (1985). Numerical solution of partial differential equations: finite difference methods, Oxford university press.

Taniguchi, M. (2002). "Tidal effects on submarine groundwater discharge into the ocean." Geophysical Research Letters 29(12).

Taylor, S. A. (1950). "Oxygen diffusion in porous media as a measure of soil aeration." Proceedings. Soil Science Society of America, 1949 14: 55-61.

Thibodeaux, L. J. (1996). Environmental chemodynamics: Movement of chemicals in air, water, and soil, John Wiley & Sons.

Thibodeaux, L. J. and K. T. Duckworth (2001). "The effectiveness of environmental dredging: A study of three sites." Remediation Journal 11(3): 5-33.

Thoma, G. J., D. RELBLE, K. T. Valsaraj and L. J. Thibodeaux (1993). "Efficiency of capping contaminated sediments in situ. II: Mathematics of diffusin-adsorption in the capping layer." Environmental Science & Technology 27(12): 2412-2419.

Thoma, G. J., D. RELBLE, K. T. Valsaraj and L. J. Thibodeaux (1993). "Efficiency of capping contaminated sediments in situ. II: Mathematics of diffusin-adsorption in the capping layer." Environmental Science & Technology 27(12): 2412-2419.

Thoms, S., G. Matisoff, P. L. McCall and X. Wang (1995). "Models for alteration of sediments by benthic organisms." Water Environment Research Foundation.

Tomaszewski, J. E. and R. G. Luthy (2008). "Field deployment of polyethylene devices to measure PCB concentrations in pore water of contaminated sediment." Environmental Science & Technology 42(16): 6086-6091.

Truitt, C. (1987). "Engineering Considerations for Capping Subaqueous Dredged Material Deposits: Design Concepts and Placement Techniques." Environmental Effects of Dredging Technical Note: 01-03.

Truitt, C. L. (1987). Engineering Considerations for Capping Subaqueous Dredged Material Deposits--Background and Preliminary Planing, DTIC Document.

USACE/USEPA (U.S. Environmental Protection Agency). 1998. (Updated 2004). Evaluation of Dredged Material Proposed for Discharge in Waters of the U.S. -

Testing Manual (Inland Testing Manual). EPA-823-B-98-004. USEPA and USACE, Washington, DC, USA. http://www.epa.gov/ostwater/itm/index.html. November 17, 2012.

USACE/USEPA. 2004. Evaluating Environmental Effects of Dredged Material Management Alternatives - A Technical Framework. EPA842-B-92-008. USEPA and USACE, Washington, DC, USA. http://el.erdc.usace.army.mil/dots/pdfs/epa/tech-frame-rev04.pdf. November 17, 2012.

USEPA. 1994. Remediation Guidance Document. EPA 905-B94-003. Assessment and Remediation of Contaminated Sediments Program, USEPA Great Lakes National Program Office, Chicago, IL, USA. http://www.epa.gov/greatlakes/arcs/EPA-905-B94-003/B94-003.ch7.html. Accessed November 17, 2012.

USEPA. 1998. National Conference on Management and Treatment of Contaminated Sediments. EPA-625-R-98-001. USEPA, Cincinnati, OH, USA.

USEPA. 2005a. Contaminated Sediment Remediation Guidance for Hazardous Waste Sites. EPA-540-R-05-012. USEPA Office of Solid Waste and Emergency Response, Washington, DC, USA. http://www.epa.gov/superfund/health/conmedia/sediment/guidance.htm. Accessed March 12, 2012.

Valderrama, C., X. Gamisans, X. De las Heras, A. Farran and J. Cortina (2008). "Sorption kinetics of polycyclic aromatic hydrocarbons removal using granular activated carbon: intraparticle diffusion coefficients." Journal of Hazardous Materials 157(2): 386-396.

van Bemmelen, J. M. (1888). Die Absorptinsverbindungen und das Absorptionsvermögen der Ackererde, publisher not identified.

Van der Zee, S., v. d. Fokkink, LGJ and W. Van Riemsdijk (1987). "A new technique for assessment of reversibly adsorbed phosphate." Soil Science Society of America Journal 51(3): 599-604.

Van der Zee, S. and W. Van Riemsdijk (1986). "Sorption kinetics and transport of phosphate in sandy soil." Geoderma 38(1-4): 293-309.

Van Genuchten, M. T. and W. Alves (1982). Analytical solutions of the one-dimensional convective-dispersive solute transport equation, United States Department of Agriculture, Economic Research Service.

Van Genuchten, M. T., F. J. Leij, T. H. Skaggs, N. Toride, S. A. Bradford and E. M. Pontedeiro (2013). "Exact analytical solutions for contaminant transport in rivers 2. Transient storage and decay chain solutions." Journal of Hydrology and Hydromechanics 61(3): 250-259.

Vrtlar, T. (2016) Field sampling and laboratory evaluation of reactive capping/in situ treatment of mercury contaminated solids using DGT devices, presented at 7th Setac World Congress, Orlando, 2016, FL

Walker, T. R., D. MacAskill, T. Rushton, A. Thalheimer and P. Weaver (2013). "Monitoring effects of remediation on natural sediment recovery in Sydney Harbour, Nova Scotia." Environmental Monitoring and Assessment 185(10): 8089-8107.

Walters, R. W. and R. G. Luthy (1984). "Equilibrium adsorption of polycyclic aromatic hydrocarbons from water onto activated carbon." Environmental Science & Technology 18(6): 395-403.

Wang, X., L. Thibodeaux, K. Valsaraj and D. Reible (1991). "Efficiency of capping contaminated bed sediments in situ. 1. Laboratory-scale experiments on diffusion-adsorption in the capping layer." Environmental Science & Technology 25(9): 1578-1584.

Weber, W. J., P. M. McGinley and L. E. Katz (1991). "Sorption phenomena in subsurface systems: concepts, models and effects on contaminant fate and transport." Water Research 25(5): 499-528.

Weissberg, H. L. (1963). "Effective diffusion coefficient in porous media." Journal of Applied Physics 34(9): 2636-2639.

Wheatcroft, R., P. Jumars, C. Smith and A. Nowell (1990). "A mechanistic view of the particulate biodiffusion coefficient: step lengths, rest periods and transport directions." Journal of Marine Research 48(1): 177-207.

Wilson, A. (1948). "V. A diffusion problem in which the amount of diffusing substance is finite: I." The London, Edinburgh, and Dublin Philosophical Magazine and Journal of Science 39(288): 48-58.

Wu, S. C. and P. M. Gschwend (1986). "Sorption kinetics of hydrophobic organic compounds to natural sediments and soils." Environmental Science & Technology 20(7): 717-725.

Wu, S. C. and P. M. Gschwend (1986). "Sorption kinetics of hydrophobic organic compounds to natural sediments and soils." Environmental Science & Technology 20(7): 717-725.

Xia, G. and W. P. Ball (1999). "Adsorption-partitioning uptake of nine low-polarity organic chemicals on a natural sorbent." Environmental Science & Technology 33(2): 262-269.

Zarull, M. A., J. H. Hartig and L. Maynard (1999). "Ecological benefits of contaminated sediment remediation in the Great Lakes basin."

Zimmerman, J. R., U. Ghosh, R. N. Millward, T. S. Bridges and R. G. Luthy (2004). "Addition of carbon sorbents to reduce PCB and PAH bioavailability in marine sediments: Physicochemical tests." Environmental Science & Technology 38(20): 5458-5464.